SCHOOL OF MEDICINE
Graduate Program in
Biomedical Sciences

Final Examination

To the Assistant Dean and/or Co-Director of the Graduate Program in Biomedical Sciences:

This is to certify that Francesca Edgington-Giordano (Student Name) ID 977009446 (Tulane ID number) has stood and passed the final examination, and the thesis/dissertation, Characterizing the Effect of Parental Low Protein Diet on Offspring Kidney Development and Function (Thesis Title)

has been approved by the committee. Therefore, he/she is recommended for the degree of

Check one: ■ Doctor of Philosophy ☐ Master of Science

in Biomedical Sciences to be conferred in the following semester:

☐ Spring _____ (Year) ☐ Summer _____ (Year) ■ Fall 2020 (Year)

12/03/2020
Date of Examination if applicable

Tamas Kozicz Dissertation Committee Member Name	Tamas Kozicz M.D., Ph.D. Digitally signed by Tamas Kozicz M.D., Ph.D. Date: 2021.02.01 10:50:28 -06'00' Signature
Samir El-Dahr, MD Dissertation Committee Member Name	Samir El-Dahr, MD Digitally signed by Samir El-Dahr, MD Date: 2021.02.03 10:33:53 -06'00' Signature
Kevin Zwezdaryk Dissertation Committee Member Name	Kevin Zwezdaryk Digitally signed by Kevin Zwezdaryk DN: cn=Kevin Zwezdaryk, o=Tulane University, ou=Microbiology and Immunology, email=kzwezdar@tulane.edu, c=US Date: 2021.02.03 13:07:32 -06'00' Signature
Sarah Lindsey Dissertation Committee Member Name	Date: 2021.02.04 14:45:00 -06'00' Signature
Prasad Katakam Dissertation Committee Member Name	Prasad Katakam Digitally signed by Prasad Katakam DN: cn=Prasad Katakam, o=Tulane University School of Medicine, ou=Department of Pharmacology, email=pkatakam@tulane.edu, c=US Date: 2021.02.06 10:33:04 -06'00' Signature
_____ Dissertation Committee Member Name	_____ Signature

1430 Tulane Ave., Mail Code 8656, New Orleans LA 70112-2699 *tel.* 504.988.5226 *fax* 504.988.3779
bms@tulane.edu

CHARACTERIZING THE EFFECT OF PARENTAL LOW PROTEIN DIET ON OFFSPRING KIDNEY DEVELOPMENT AND FUNCTION

By: Francesca Edgington-Giordano

Zubaida Saifudeen Lab

Tulane School of Medicine:

Biomedical Sciences Doctor of Philosophy

Abstract

The kidney develops from the intermediate mesoderm from E10 to P4 in mice and weeks 5 to 34 in humans. The development relies on the physical and signaling interactions between the nephron progenitor cells (NPCs), the stroma progenitor cells, and the ureteric branching tip cells (UBTCs). Kidney development relies on signals that vary based on location and temporally with NPC recruitment order determining the part of the nephron they will form. Kidney organogenesis and nephrogenesis relies on signals from BMPs, growth factors, Wnt, cytokines, and autonomous and exogenous cell proliferation and survival signals. These signals lead into or are regulated by cell metabolism, environmental signals, and chromatin modifications. IUGR is an environmental condition known to cause hypertension, chronic kidney disease, and kidney failure. We hypothesized that disruption of metabolic homeostasis in the nephron progenitor cells in the IUGR fetus impairs nephrogenesis and is the direct link between the maternal environment and nephron endowment leading to adult hypertension and chronic kidney disease (CDK). IUGR from low protein diet caused small pups, small kidneys, increased kidney/body weight ratio. The changes begin at E13.5 with a 30% decrease in ureteric tip count, disorganized/smaller cap mesenchyme (CM) (37.5% decrease in Six2+ NPCs), and smaller kidneys. P0 NPCs show dysregulation to growth factors, Wnt, cell metabolism, and autonomous and exogenous cell proliferation and survival signals shown by bulk RNA-seq and immunofluorescence. Changes from LPD IUGR persist with delayed postnatal growth of skin, hair, body, and kidneys. P21 and adult IUGR show damage to kidneys and increased risk of developing hypertension, and CDK. IUGR LPD is the first hit in the multi-hit disease causation of CDK. The P0 NPCs had dysregulated metabolism and chromatin; postnatal development continues to be dysregulated despite removal of LPD environment. The LPD IUGR model produces a new tool for the study of multi-hit kidney disease.

Acknowledgements

To start I want to thank my PhD advisor and mentor Dr. Zubaida Saifudeen, who like all advisors took a chance on a young, enthusiastic, and unskilled researcher. Dr. Saifudeen's lab was a place of growth from her leadership and in her selection of amazing lab mates. Jiao Liu, an astounding lab tech and researcher, I thank you for your support and hours of training. I would not be half the researcher I am today without these amazing women supporting me and laying the foundation, studs, and roof of my PhD work. The Saifudeen lab has grown and changed during my time but a constant has been a willingness to lend a hand and guide each other. Dr. Giovane Tortelote, Dr. Tingfeng Li, and Mariel Colon-Leyva all showed a willingness to help in conversations about my project, career plans, and the less glamorous day to day of mouse work. Special thanks to Catie Diepenbrock as an amazing undergraduate who was game to count glomerular for me. The Saifudeen lab is part of a hardworking and collaborative department in Pediatrics. Pediatric Nephrology research at Tulane is a community made up of thoughtful researchers that never hesitated to support anyone. Dr. Samir El-Dahr, Dr. Hongbing Liu, Dr. Yuwen Li, Dr. Sylvia Hillard, Dr. Renfang Song, and Dr. Chao-Hui Chen all contributed with daily advice, encouragement, and a weekly struggle in a darkened lab meeting. Pediatric nephrology created an environment that supported every researcher that entered the space sometimes with food, and other times explaining antibody conditions for the thirtieth time.

It is not just your lab that supports PhD work, but also the institution at which you are trained. Tulane University is filled with talented and helpful people. The Tulane Biomedical Sciences program supports its students and is staffed by people that want us to succeed I thank the Co-chairs of the program, Dr. Diane Blake and Dr. Robert Garry, for leading a program focused on the success of its students, and my cohort for silent and loud encouragement.

Thank you sincerely to my committee. My prospectus helped me refocus on what was feasible and interesting. Every meeting has reminded me of why research is collaborative. Dr. Lindsey: thank you for the assistance in blood pressure calculations, and Dr. Katakam: thank you for the help with the Seahorse machine.

The Tulane Department of Comparative Medicine has helped me from the moment I started my lab work. The staff at the DCM do not just do their jobs they are always willing to go above and beyond for students and the animals. Special thanks to Dr. Andrews, Dr. Dobek, and Lynell Dupepe for your time, expertise, and patience.

For assistance in sample preparation and analysis I thank Hugh Alan Tucker of the Flow Cytometry Core, Dina Gaupp of Histology, Alexander Castillo of Phenotyping Core at Tulane University, and the UAB/UCSD O'Brien Center Core (Grant DK079337). Centers and core facilities are common, but so often I found facilities that were responsive to questions, generous with advice and willing to go the extra mile to make sure precious samples provided every bit of data they could. Thank you especially Alan for staying late and talking through assays, I know Tulane graduate students have much to be grateful for.

I have luckily been supported my entire life by a family that always wanted me to succeed. My entire family has listened to years of biology lectures, mouse breeding ideas, troubleshooting, terrible jokes, and blind panic. I have no doubt their reminders to finish my thesis are more for their benefit than mine. Thank you, Mom, Frederika, Patrick, Lucinda, Alexandra, and Kellen for listening, checking in on me, and telling me to get some sleep. The most exciting part of my next adventure will be the hours I spend telling all of you about it.

Table of Contents

Chapter 1: Introduction

1.1 Kidney Development:

Mammalian kidney development is novel in organogenesis by forming three successive structures (pronephros, mesonephros, and metanephros) with each successive stage representing a more complex organ over the course of development. The tissue of origin for each of these structures is the intermediate mesoderm (IM), a germ layer between the paraxial and lateral plate mesoderm. The IM will give rise to the entire urogenital system including the kidneys, gonads, their respective duct systems, and the adrenal cortex (Kastu 2012, Barak 2005, Fluming 2013) [Figure 1]. The IM forms from patterning along the anterior-posterior axis of the embryo with distinct mesoderm types from Vg1/Nodal signaling maintaining dorsal/anterior identity and BMPs promoting ventral/posterior identity. The IM is marked first by the presence of Osr1, which is also present in the lateral plate anterior to the IM, and later by Pax2, Pax8, and Lhx1 (Katsu, K., Tokumori, D., Tatsumi, N., Suzuki, A., & Yokouchi, Y., 2012, Barak, H., Rosenfelder, L., Schultheiss, T. M., & Reshef, R., 2005, Fleming, B. M., Yelin, R., James, R. G., & Schultheiss, T. M., 2013) [Figure 1]. The IM will be further divided along the dorsal-ventral axis before kidney development begins. The

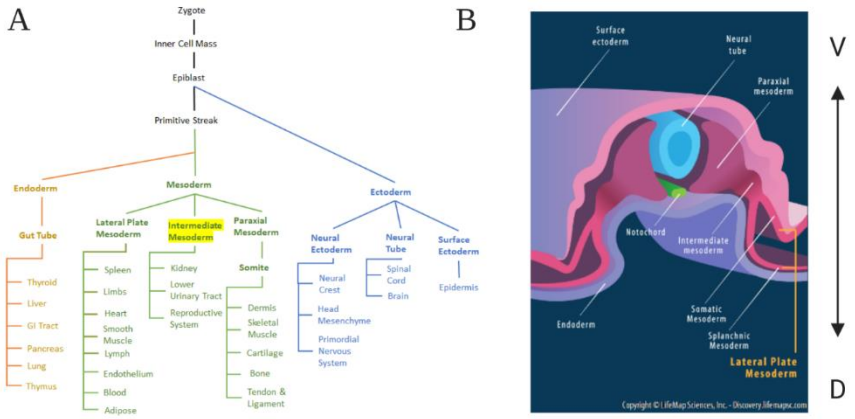

Figure 1: Early Germlayer differentiation
A) Following gastrulation into the germ layers ectoderm, mesoderm, and endoderm there are successive differentiations into increasingly differentiated stem cells and progenitors. The mesoderm will form into the paraxial, intermediate, and lateral mesoderm. B) The intermediate mesoderm forms between the somatic and paraxial mesoderm in early development regulated by patterned signaling of VG1/Nodal into BMPs. (Edgar, R., Mazor, Y., Rinon, A., Blumenthal, J., Golan, Y., Buzhor, E., Livnat, I., Ben-Ari, S., Lieder, I., Shitrit, A., Gilboa, Y., Ben-Yehudah, A., Edri, O., Shraga, N., Bogoch, Y., Leshansky, L., Aharoni, S., West, M. D., Warshawsky, D., & Shtrichman, R., 2013).

dorsal IM experiences increasing restriction in differential potential and forms the nephric duct while the ventral IM remains as undifferentiated mesenchyme of the nephric duct cord. A rostral to caudal wave of signal derived from the nephric duct induces the primitive renal tubules which will later form the pronephros and mesonephros. This represents a loss of differentiation potential in the rostral IM. [Figure 2] At the same time the caudal nephric duct cord forms a bean shaped and undifferentiated IM (Kopan, Chen, & Little 2014, Takasute, M., Little, M.H. 2015). [Figure 2 & Figure 3B]

In amphibian and zebrafish, the functional pronephros forms one single nephron that will filter and drain into the cloaca. The pronephros is not functional in mammals. In vertebrates the nonfunctional pronephros atrophies during development after the mesonephros has formed (Figure 2A & B).

The mesonephros forms on embryonic day 9.0 in mice and week 4 in humans. It branches from the nephric duct into a series of tubules that are induced by the lengthening of the nephric duct towards the tail. The nephric duct, formed from the intermediate mesoderm, connects the pronephros, the mesonephros, and the metanephros kidney to the cloaca. The formation of tubules involves the epithelization of the intermediate mesenchyme (Vize, Seufert, Carroll, Wallingford, 1997, Obara-Ishihara, Kuhlman, Niswander, & Herzlinger, 1999, Vainio, Lehtonen, Jalkanen, Bernfield, & Saxen, 1989, Kispert, Vainio, & McMahon, 1989). The mesonephros functions as a filter during early development. It contains structures similar to the nephrons of the metanephric kidney in the series of tubules off the nephric duct. A glomerulus forms with a bowman's capsule around capillaries off the aorta which is attached to the mesonephric duct that leads back to the posterior cardinal vein and drains into the nephric duct and then to the cloaca

(Zhou, Boucher, Bollig, Englert, & Hildebrandt, 2010, Vainio, Lehtonen, Jalkanen, Bernfield, & Saxen, 1989, Ganesh 2017) (Figure 2A & B).

The metanephros will form the adult mammalian kidney. The mammalian kidney is formed from 3 progenitor cell lineages: the ureteric branching cells of intermediate mesenchyme that forms off of the nephric duct, the nephron progenitor cells (NPCs), and the interstitial stroma cells that both form from the metanephric mesenchyme. Development of the metanephros kidney begins with the growth of the ureteric bud (UB) into the metanephric mesenchyme on embryonic day 10 of the mouse and in week 5 of human development. Kidney development ends in week 34 of human gestation and postnatal day 3 or 4 in the mouse. Thus, human kidney development is fully completed during gestation while mouse kidney development continues postnatally.

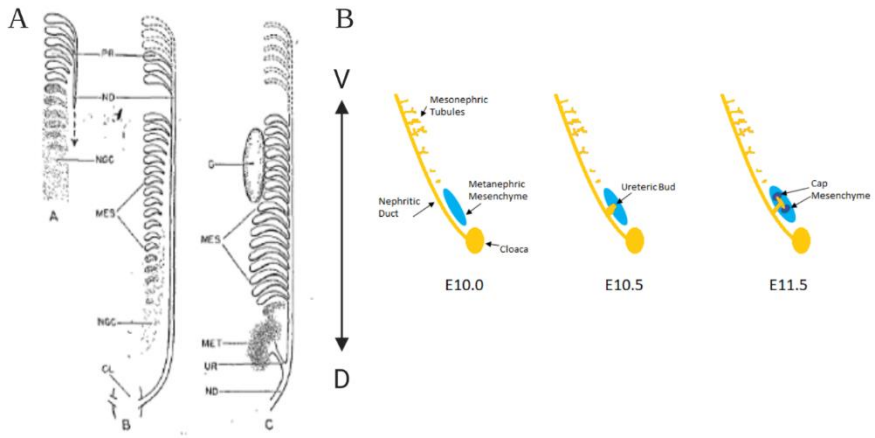

Figure 2: Early Metanephros Kidney Development
A) Figure from Banks 1955 showing the development of the nephric system in vertebrate organogenesis. PR: pronephric duct., ND: nephric duct, NGC: nephrogenic cord, G: gonad, MES: mesonephric units, MET: metanephros, UR: ureter, CL: cloaca. B) The ureteric bud grows from the nephritic duct, both shown in yellow, into the metanephric mesenchyme cells, shown in light blue, at embryonic day 10. The UB cells signal the condensing of metanephric mesenchyme into the cap mesenchymes of nephron progenitor cells, shown in dark blue. At e11.5 two cap mesenchymes will be present at the end of the ureteric branches with two caps at the end of a t-shaped UB. Adapted from Banks 1955, Li 2014, and Dressler 2009.

The metanephros begins to form at e10 in mice, week 5 in human gestation, with the secretion of GDNF and FGF10 from the MM towards the nephric duct activating receptor tyrosine kinases (RTKs). RTK activation in the nephric duct creates a single UB that migrates

and invades the bean shaped MM. The MM at this point already contains the progenitor cell populations that form all epithelial and stroma tissues and some of the vascular components of the developed kidney (Kopan, Chen, & Little 2014). Angioblasts form from the mesoderm germ layer and migrate based on angiogenic signals for proliferation, differentiate into endothelial cells, and develop into blood vessels (Gomez, Norwood, Tufro-McReddie, 1997). Angioblasts are endothelial precursors and guided by angiogenic signals. The angiogenic signals for angioblasts are growth factors and cytokines including VEGF, TNF-α, FGF, TGF-β, FGF-2, and PDGF. Angiogenesis is directed by intrinsic and extrinsic factors of the vascular precursor cells and the tissue progenitor cells the vascularization is occurring in. The tissue specific factors include the extra-cellular matrix and its receptors (Ucuzian, A.A., Gassma, A.A., East, A.T., Greisler, H.P. 2010). The UB will give rise to the collecting ducts of the developed kidneys. MM cells condense to form cap mesenchymes

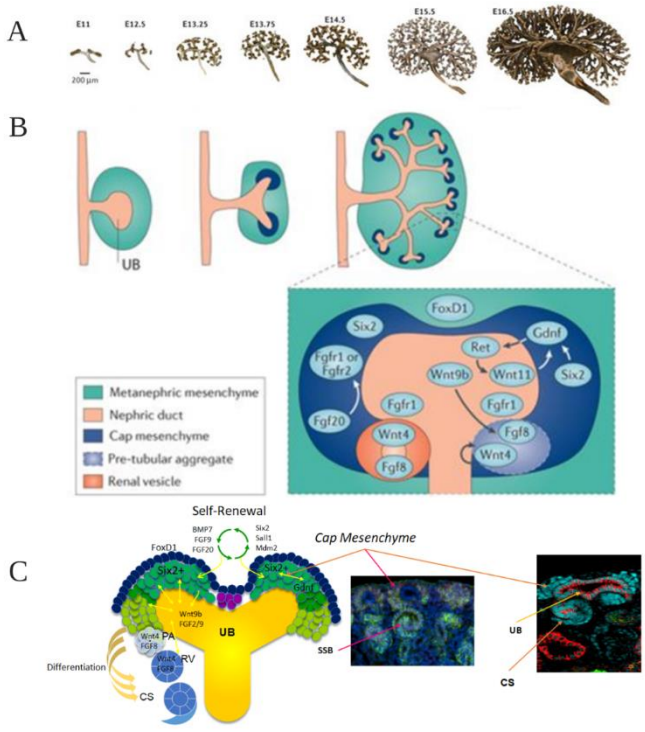

Figure 3: Sequential Ureteric Branching
A) The UB branches sequentially spliting the cap mesenchymes and growing the embryonic kidney. At e11.5 there is a single T shaped UB with two cap mesenchymes. As development progresses the UB branches further forming more cap mesenchymes made up of nephron progenitor cells and expanding the embryonic kidney. B) Crosstalk between the ureteric bud, the cap mesenchyme, and the stroma. The ureteric bud signals for cap maintenance and differentiation. From Short, K. M., & Smyth, I. M. (2016). C) Cross talk and staining of the cap mesenchyme (Sall1), UB (Ecad), CSB (Sall1), SSB (Sall1), differentiating structures. C) Crosstalk maintains the cap mesenchyme, UBTCs, and supports/signals differentiation of the pre-tubular aggregare (PA), the renal vesicly, the comma shaped body (CS), and the S-shaped body (SSB). Marked by NCAM, Sall1 (CM, CS, RV, SSB).

(CMs) of NPCs with the interstitial stroma cells above and beside CMs. The CMs surround the UB whose branches are led by UB tip cells.

The UB outgrowth from the nephric duct at e10.5, invades the adjacent MM (Figure 2B). Reciprocal induction is the two-way signaling between neighboring cell types. The epithelial-mesenchymal interaction during kidney development is a form of reciprocal induction between tissue types. The UB is an epithelial sheet of polarized cells which will interact with the nonpolarized MM that formed from the nephric cord. The loss of the MM will stop UB branching in an embryonic kidney and UB mutants for induction signals will have arrested differentiation of the MM into epithelial and not form functional structures. The two tissues rely on signals from each other to continue development (Berk, Zipursky, et. al. 2000). Reiterative branching of the UB with differentiation of NPCs expands the kidney and forms the major and minor calyces in the UB through e13.5. After this the ureteric branches elongate and form collecting ducts. The elongated ureteric branches produce the medulla at the core of the kidney with the cortex at the periphery filled with the nephrogenic zone made up of UB tips, CM, and the differentiating nascent nephrons, and comma-shaped and s-shaped bodies (CSB and SSB). The normal mouse UB will go through 11 cycles of branching and elongations with branching ending between birth and postnatal day 3 or 4 (Kopan & Costantini 2010, Hartman, Lai, & Patterson 2007) [Figure 3A &B]. Defects in branching can cause fewer cap mesenchymes and smaller kidneys (Carroll & Das 2013, Dressler 2009, Kopan & Costantini 2010).

Lindström et. al. 2018 demonstrated the temporal role in $Six2^{+}$ NPCs as they are recruited into epithelializing in the renal vesicle (RV). Three-dimensional imaging of NPCs in the human CM showed gradients to the expression of NPC markers decreasing along the proximal to distal axis. NPC markers decrease and do not switch off with differentiation. NPCs initiating pre

tubular aggregate formation were directly adjacent to the UB and under the branch tip. NPCs are recruited after a PTA or RV has been established by the first recruits and incorporated into the proximal end of the PTA or RV. Single-cell transcriptome analysis combined with prediction modeling and immunostaining showed that the NPCs that are at the top of the CM are progenitors renewing the NPC pool. A distinct population will be primed to differentiate while remaining mesenchymal. Further along the proximal to distal axis will be the induced cells. The induced cells have been epigenetically reprogrammed and await recruitment into the PTA or RV by those first NPCs. Lindström et. al. adds that the timing of this recruitment determines final cell fate. The final nephron will have 14 distinct cell types and the epithelialized PTA, RV, and SSB already show distinct cell populations with differing cell fates. The first NPC recruits will form the distal precursors and are positive for low Jag1 and low Sox9. These first recruits will connect to the UB and split further into the distal tubule precursors and loop of Henle precursors. The second NPC recruits will be proximal precursors and will not be anchored to the UB instead connecting to the proximal precursors and show no Sox9 expression with high Jag1. The third recruits will be added to the RV and become precursors for the Renal Corpuscle. A proposed source of the expression pattern along the RV and SSB is localized Wnt9b secreted from the UB (Lindström, O., Brandine, G.D., Tran, T., Ransick, A., Suh, G., Guo, J., Kim, A.D., Parvez, R. K., Ruffins, S.W., Rutledge, E. A., Thornton, M. E., Grubbs, B., McMahon, J.A., Smith, A. D., & McMahon, A.P., 2018) (Figure 3B).

The distal part of the polarized RV grows and attaches to the epithelial UB to form CSBs and SSBs (Figure 3B). The proximal, intermediate, and distal sections compose the segmented SSB. SSBs will continue to differentiate and form nephrons, the adult filtering unit of the kidney which contains the glomerulus, the proximal tubule, the loop of Henle, and the distal tubule

which will connect to the collecting duct formed from the UB. The result is the highly specialized structures of the adult kidney.

The glomerulus is dense in capillaries and filters water and solutes out of the blood. The proximal tubule has high surface area to reabsorb and retain necessary substances such as salt, water, glucose, amino acids, potassium, urea, phosphate, and citrate. The proximal tubule also functions in secreting small molecules/drugs and ammonium. The loop of Henle has tightly controlled variation in osmolality, so the descending loop will secrete water and concentrate urea, while the ascending loop of Henle secretes sodium and chloride. This creates concentrated urea and retains water and electrolytes in the body. The distal tubule contains specialized cells to regulate potassium, sodium, calcium and pH in the body and the secreted urea (Carroll & Das 2013, Dressler 2009, Mugford, Spile, McMahon, & McMahon 2008). The function of the adult kidney relies on the proper formation of all these structures in sufficient numbers to allow efficient secretion of waste and the reabsorption of water and solutes as needed.

In both humans and mice nephron formation relies on controlled, induced differentiation of the NPCs to form RVs repeatedly over nephrogenesis while maintaining the NPCs for the entire length of nephrogenesis. The NPC population is maintained by cell survival and proliferation signals. Autonomous cell survival (BMP7, FGF9 and FGF20) and proliferation (Six2, Sall1, Mdm2) along with maintenance signals from the UB (Wnt9b) and survival signals from the UB (FGF2/9) act to maintain the NPC population that makes up the CM (Carroll & Das 2013). Cultured NPCs show decreasing levels of FGF expression over passages with the highest level in freshly isolated NPCs. Introduction of exogenous FGF supported NPC proliferation and stemness (Brown 2011). Wt1 is a regulator of the maintenance signal FGF, the survival signal BMP, and the BMP and MAPK/ERK related signal p-Smad which all regulate NPCs. Motamedi

2014 showed Wt1 as a regulator of FGF, BMP, and p-Smad in kidney development. Chromatin Immunoprecipitation combined with DNA sequencing (ChipSeq) analysis shows the presence of Wt1 binding sites associated with metanephric mesenchyme and kidney development. The Wt1 mutant had no change in Six2, but BMP, FGF, p-Smad, and Wnt/β-catenin were all dysregulated. Supplementing with BMPs and FGFs rescued the Wt1 mutants. Metanephric mesenchyme survival comes partly from a balance of Wt1, BMP/SMAD, and FGF signaling (Motamedi, F. J., Badro, D. A., Clarkson, M., Rita Lecca, M., Bradford, S. T., Buske, F. A., Saar, K., Hübner, N., Brändli, A. W., & Schedl, A., 2014) [Figure 3B & Figure 4].

1.2 Intermediary metabolism and cell fate decisions:

Glucose when metabolized in the cell can be processed by multiple metabolic pathways depending upon conditions and needs of the cell. Glycolysis is the cytosolic conversion of glucose into lactate via phosphorylation and kinase reactions generating metabolites that are participants or substrates of lipid synthesis, amino acid synthesis via serine, and netting 2 pyruvates, 2 NADH, and 2 ATPs. The second stage of glycolysis involving glucose-6-P either continues through glycolysis or into the pentose phosphate pathway and produces instead NADPH, pentose, and 5-Ribose-phosphate. 5-Ribose-phosphate is a precursor for nucleotide synthesis. Or, just before the conversion to lactate the pyruvate from glycolysis can feed into mitochondrial oxidation producing 6 $NADH^+$, 2 $FADH_2$, 4CO_2, and 2 ATP per Acetyl CoAs (Hamanaka & Chandel 2012). Acetyl CoA made from long chain fatty acids produces mitochondrial oxidation producing the same products in addition to triglycerides, phospholipids, hormones, and ketones (Morino, Peterson, & Shulman 2006). These are major energy pathways of the cell. The hexosamine biosynthetic pathway (HBP) accounts for 2-5% of glucose

metabolism. HBP controls posttranslational modifications of proteins by glycosylation. Most of these reactions occur in the golgi apparatus and produce N and O linked glycosylated proteins.

Glycosylation is part of cell packaging to direct activity, stability, and subcellular localization of proteins (Fardini, Dehennaut, Lefebvre, & Issad 2013 & Fantus, Goldberg, Whiteside, &Topic 2006).

The amino sugar α-linked N-acetylgalactosamine, derived from galactose, is a membrane bound substance along the distal tubules of the kidney. Glycosylation is the enzymatic addition of oligosaccharides to proteins forming glycoproteins. A-linked N-acetylgalactosamine is a mucin; a highly glycosylated protein that forms physical barriers in epithelial cells lining tubes or body cavities in animal bodies. Mucins are made of α-linked N-acetylgalactosamine linked to a serine or threonine residue. The sugars galactose, N-acetylgalactosamine, fucose, or sialic acid extend the mucin chain structures. The enzymes that produce α-linked N-acetylgalactosamine are involved in mammalian disease, physiology, and development. The hydrophilic O-glycans are usually negatively charged allowing them to bind water and salts. Polysialylation used to

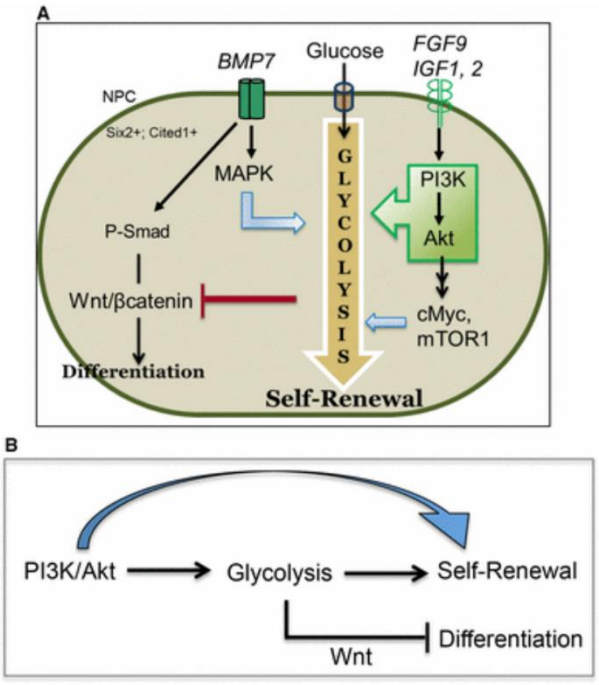

Figure 4: Interaction of Glycolysis with NPC Renewal and differentiation Pathways
A) NPC cell responding to exogenous signals with glycolysis as an intermediary between MAPK, PI3K/AKT, cMyc, and mTOR1, and the Self-Renewal of NPCs and the inhibition of differentiation signaling. It is when glycolysis is low that differentiation signals are strengthened, and self-renewal signals weakened. B) Glycolysis is not essential for self-renewal, but its removal primes NPCs for differentiation rather than self-renewal and maintenance. Liu, J., Edgington-Giordano, F., Dugas, C., Abrams, A., Katakam, P., Satou, R., & Saifudeen, Z. (2017).

extend the DBA recognized α-linked N-acetylgalactosamine is also present in neural cell adhesion molecule (NCAM) when present in the basolateral membrane bound NCAM in the nascent nephron. Lackie, Zuber, and Roth's 1990 development paper showed differences in NCAM when staining mesenchyme and epithelial structures of the rat kidney. E13 immunostaining showed strong PSA staining of the UB and the condensed MM. E14 showed PSA and NCAM present in both the MM and CSB. The PSA staining was stronger and concentrated at the membrane rather than diffuse through the cell as in the MM at e13 and 14. E18 staining for PSA showed intense PSA staining in multiple CSBs and SSBs except for the lower part of SSBs that give rise to podocytes in the developed kidney. NCAM epithelial staining in the embryonic rat kidney co-stained with polysialic acid in the basolateral membrane. It was noted by Roth e. al. that the PSA staining localized where cell to cell adhesion changed during kidney nephrogenesis. PSA, cell-to-cell adhesion, and NCAM are known to work in concert in neural development (Galuska, Lütteke, & Galuska 2017).

During the roughly twelve embryonic days in mice and 29 weeks in humans of kidney development, the embryonic environment is in constant contact with the maternal environment. Maternal food source determines nutrient availability and thus cell metabolism. This does not just mean caloric restriction as shown by famine studies, but also micronutrients epitomized by the developmental importance of folic acid. Cell fuel sources change cell behavior and character in adult tissue and have staggering impacts on developing tissues. Cancer research shines a light on the likely mechanisms. The Warburg effect theorizes cancer cells not just dependent on ATP production, but also the utilization of all metabolic products. High glycolysis means excess carbon for producing nucleotides, lipids, and proteins to increase biosynthesis, and NADPH as a reducing agent in proliferating cells. Both cancer cells and developing organs exist in a

microenvironment. Tumors find themselves in environments with little oxygen and abundant glucose and must efficiently use the resources they have while competing with other cells (Liberti & Locasale 2017). Metabolism usage changes during development. Zhang et. al. 2014 showed human embryonic stem cells (hESCs) have a unique energy phenotype to adult stem cells. hESCs had higher uncoupled oxygen consumption. hESCs were reliant on glutamine to proliferate in culture, but when partly differentiated the cells lost that reliance and had decreased glutamine metabolism. Chen 2009 showed variation in mitochondria number and function as human mesenchymal stem cells (hMSCs) differentiated. Undifferentiated hMSCs were reliant on glycolytic enzymes and lactate production while the differentiated osteogenic cells had increased mitochondria copy number and increased oxygen consumption showing a shift from glycolysis to oxidative phosphorylation with differentiation.

NPCs rely on glycolysis to renew and maintain the progenitor pool, decreased glycolysis primes NPCs to respond to differentiation signals (Liu, J., Edgington-Giordano, F, Dugas, C., Abrams, A., Katakam, P., Satou, R., & Saifudeen Z., 2017). The balance between maintaining the cap mesenchyme and differentiating into nephrons during development has an internal clock as shown by the Kopan NPC transplant studies (Figure 4). In Chen 2015 a mixture of old (P0/P1) and young (e12.5) NPCs transplanted into young e12.5 niches and cultured for 4 days exited the young CM at different rates. The majority of old NPCs injected exited the young niche while less than 30% of the injected young NPCs exited. This shows that there are intrinsic differences between young and old NPCs that direct cells to self-renewal or differentiation despite new environmental signals. But the extrinsic signals of a young niche did change old cells as shown by the persistence of some old NPCs in young niches. P0/P1 cells following only their internal clock would mass differentiate after a few days at their P3. The presence of old NPCs after their

clock would have run out suggests microenvironment plays a role in NPC fate and can overcome intrinsic cell programing. Old NPCs were more likely to remain in the young niche when associated with young NPCs and had differences in cell-to-cell adhesion. FGF20 co-injection increased the old NPCs that engrafted and remained in the young niche. The signals of the young niche are not a fountain of youth as Kopan showed using single cell RNA-seq that the transcription profiles of NPCs change over development and old Cited1+ NPCs are intrinsically closer to differentiate than young NPCs.

The NPCs have a histone landscape unique from differentiated nascent nephron and further unique histone modification in the epithelial tubules. McLaughlin 2014 showed changes to the histone landscape with differentiation from the CM. Proper histone modification is essential for nephrogenesis as deletion of HDAC 1 and 2 in the NPC population arrests nephrogenesis. HDAC 1 and 2 interact with the NPC regulators Six2, Osr1, and Sall1. HDAC1 and 2 regulate proliferation, differentiation, and p53. Direct interaction between chromatin remodeling molecules and regulators of NPC differentiation shows an entwined relationship between epigenetics and kidney organogenesis. As cells differentiate, they have increased deactivation of parts of their genome through chromatin remodeling. The less differentiated a cell the more of its genome that remains open, with differentiation there is a loss of possibilities in cell fate and a loss in genes available for transcription via chromatin remodeling. This is not a byproduct of differentiation though, it is a part of differentiation as agents of chromatin remodeling are essential in kidney progenitor cell fate (McLaughlin, N., Wang, F., Saifudeen, Z., & El-Dahr, S.S. 2014, Liu, H., Chen, S., Yao, X., Li, Y., Chen, C., Liu, J., Saifudeen, Z., & El-Dahr, S.S. 2018).

Studies in cancer and development have shown that cell behavior is tied to cellular metabolism and their histone landscape. Liu 2017 and Yu 2018 show that changes to cellular metabolism changes cell behavior in kidney development and cancer, respectively. Yu 2018 showed metabolic plasticity of cancer cells allows them to respond to the changing microenvironment by histone modifications that regulate expression of genes involved in proliferation and survival.

De novo nephrogenesis only occurs in utero in humans and up to post-natal day 4 in mice. This is at week 34 of human gestation and P3/4 in mice. Mice have a nephron endowment between 11,000 to 20,000 while humans are from 200,000 to over 2 million with most people having 1 million nephrons at birth. Diminished nephron endowment can be caused by inability to maintain NPCs, inability to differentiate NPCs, and failure to deplete the pool of NPCs at the end of nephrogenesis. As nephrons cannot be regenerated, nephron endowment is set at birth and will only decrease over an organism's lifespan (Keller, Zimmer, Mall, Ritz, & Amann, 2003, Yuan, Tipping, Li, Long, & Woolf, 2002).

1.3 Intrauterine Growth Restriction:

The World Health Organization (WHO) historically defined fetal Intrauterine Growth Restriction (IUGR) as full-term newborns in the 10^{th} percentile of birth weight. WHO abandoned the 10^{th} percentile definition for a set weight based on clinical significance as the 10^{th} percentile body weight in newborns varies over time and between countries. The CDC reports the current 10^{th} percentile body weight of full-term newborns in the United States as 6 lbs., 2 oz. for boys and 6 lbs., 1.2 oz for girls with 8.07% rate of IUGR for all full-term newborns (CDC National Center for Health Statistics and WHO Growth Standards). Worldwide WHO reports IUGR at a

rate of 14.6% but that ranges from 2.4% IUGR in Sweden to 27.8% in Bangladesh (UNICEF, Low Birthweight).

The risk factors for IUGR include external environmental conditions (elevation and water quality), placental insufficiency (decreased nutrient absorption by the placenta), maternal health (diabetes, eclampsia, drug addiction), multiple pregnancies (twins etc.), maternal infections (CMV, rubella), and maternal diet including micro and macro-malnutrition (UNICEF, Low Birthweight, CDC, National Center for Health Statistics Statistics). The variety and increasing rate of risk factors for IUGR is a serious public health concern in both the developing and developed world with the same adult health outcomes regardless of gestational cause. Adult health outcomes of IUGR offspring include increased rates of obesity, insulin resistance, hypertension, and chronic kidney disease. IUGR models have been done in sheep, pig, guinea pig, monkey, rat, and mouse using multiple methods including maternal diabetes, glucocorticoid treatments, hypoxia via a chamber or surgery, umbilical artery ligation, uteroplacental embolization, caruncletomy, bilateral uterine ligation, and macro or micro nutrient deficiency related to iron, protein, or caloric intake. An iso-caloric low protein maternal diet is an

Control Diet			6% Protein Diet		
Ingredient	(g/Kg)		Ingredient	(g/Kg)	
Casein	**230**		**Casein**	**69**	
DL-Methionine	3		DL-Methionine	0.9	
Sucrose	**431.7**		**Sucrose**	**571.8**	
Corn Starch	200		Corn Starch	200	
Corn Oil	52.3		Corn Oil	53.9	
Cellulose	**37.86**		**Cellulose**	**57.82**	
Vitamine Mix, Teklad 40060	10		Vitamine Mix, Teklad 40060	10	
Ethoxyquin, antioxidant	0.01		Ethoxyquin, antioxidant	0.01	
Mineral Mix	13.37		Mineral Mix	13.37	
Calcium Phosphate dibasic	**16.66**		**Calcium Phosphate dibasic**	**21.6**	
Calcium Carbonate	**5.1**		**Calcium Carbonate**	**1.6**	
	% by Weight	% kCal From		% by Weight	% kCal From
Protein	**20.3**	**21.6**	**Protein**	**6.1**	**6.5**
Carbohydrate	61.6	65.4	Carbohydrate	75.6	80.4
Fat	5.5	13	Fat	5.5	13.1
Kcal/g	**3.8**		**Kcal/g**	**3.8**	

Figure 5: Diet Comparison for inducing IUGR:
Ingredients for control and 6% protein diet from Envigo diets. Envigo control diet with 20% protein by weight is Envigo 91352 and Envigo with 6% protein by weight is Envigo 90016. Bolded shows the differences between control and experimental diets. Casein is the protein source, sucrose and cellulose are carbohydrate sources used to maintain equal kilocalories per gram of food, calcium phosphate dibasic and calcium carbonate have changed to account for casein changes. The result is a isocaloric diet that has lower protein by weight and kilocalorie, more carbohydrates, and equal fat content.

established model for IUGR in research animals including mice (Sharma, Shastri, Sharma, 2016, Alexandra-Gouabau, Courant, Le Gall, Moyon, Darmaur, Parnet, Coupé, Antignac, 2013).

Previous studies have linked maternal diet and IUGR through amino acid deficiency**.** Bhasin 2009 used protein restriction to 9% and hypercholesterolemia maternal diets to produce IUGR and found altered maternal plasma amino acid levels. Maternal plasma had reduced levels of phenylalanine, leucine, isoleucine, and valine and increased maternal lysine in the reduced protein model. Jansson 1998 found reduced transport of leucine and lysine across the placenta in human cases of IUGR by studying donated placentas. Intervention studies for IUGR include amino acid supplementation (Jansson, T., Scholtbach, V., & Powell, T.L. 1998, Brown, L. D., Green, A.S., Limesant, S.W., & Rozance, P.J., 2011, Bhasin, K.K.S., Nas, A.V., Martin, L.J., Davis, R.C., Devaskar, S.U., & Lusis, A.J. 2009). The studies took place in human trials before properly characterizing the sharing of nutrients with the developing fetus. Amino acids are actively transported across the placenta from circulation in the maternal plasma. Transport of amino acids relied on relative concentration in maternal plasma and fetus and in the presence and operation of transporters that are specialized based on amino acid structure. The fetus then uses amino acid shuttles reliant on serine and glutamine to retrieve and release the amino acids into circulation. The complex pathways and relationships that result in net transfer of amino acids into the fetus make the pure supplementation with protein an ineffective intervention in IUGR. The result from protein supplementation in pregnancies at high risk for IUGR were then high risk with variable results (Brown, L. D., Green, A.S., Limesant, S.W., & Rozance, P.J., 2011). Amino acids are the building block of proteins and regulate several cell functions including cell signaling, RNA and DNA synthesis, metabolism, stress response, growth, and development. Leucine specifically activates the mTOR pathway known to be related to kidney development,

via regulation of metabolism, proliferation, and growth, and adult kidney injury. Cerqueira et. al. (2019) showed in utero exposure to maternal diabetes impairs nephron progenitor differentiation. Maternal diabetes is a known risk factor for IUGR and nephron deficit in humans. The wildtype offspring of diabetic mice from the *Ins*$2^{+/C96Y}$ mice had no decrease in birth weight but did have impaired kidney development, with a 20% decrease in nephron formation and increased expression of NPC markers Six2 and Cited1 at P2. The inefficient formation of structurally normal glomeruli occurred with decreased Notch and decreased phosphorylated-β-catenin. Notch and Wnt/β-catenin signaling pathways are integral to the differentiation of NPCs. The Wnt differentiation signals from the UB changes stroma, MM, and UB as cross talk between these tissues act to maintain and differentiate these cells during development. Wnt and Notch signals prime NPCs for differentiation by decreasing Six2 expression. A loss of Wnt and Notch would leave Six2 unrepressed and maintain NPC Six2 levels and stemness, stopping differentiation and glomeruli formation. This study further supports the importance of studying maternal environment in kidney development.

1.4 Significance:

Dr. David Barker's hypothesis on the developmental origins of health and disease links low-birth weight directly with adult chronic health conditions connecting nutrition during development with adult health including hypertension and chronic kidney disease (Hales, C.N., Barker, D.J., 1992). The CDC reports that 1 in 3 Americans have hypertension and over 1,100 die each day from complications of hypertension such as heart disease and stroke. Impaired filtration from damage or injury over a period of time results in Chronic kidney disease (CKD), affecting approximately 12-14% of the United States. Treatments for CKD include lifestyle changes and pharmaceuticals to prevent further damage, and for severe cases dialysis and kidney

replacement. The projected number of patients receiving dialysis and kidney transplants are expected to double from 2010 to 2030 (American Kidney Fund, 2019, Calkins, Devasker 2011, "The Impact of Kidney Development on the Life Course: A Consensus Document for Action," 2017).

The Dutch famine cohort follows adults that were gestated during WWII where urban daily rations at times fell below 1000 calories. The cohort consists of adults that gestated on low calories at the beginning, middle, end, or for the entirety of pregnancy. This adult population has increased rates of obesity and coronary heart disease when compared to adults born just before or after the famine. The famine cohort had similar life experiences to the control cohort showing a link between caloric intake during gestation and adult health, specifically related to the kidney. Systolic blood pressure was found to increase with the lower birth weight in the famine cohort (Painter, Roseboom, Bleker 2005, Stein, Zybert, Van der Pal-de Bruin, Lumey, 2006).

Moreover, epidemiological studies in humans and ablation of nephron progenitor cells in mice have shown that kidneys of equal size but lower nephron endowment result in hypertensive organisms and chronic kidney disease in adulthood (Cebrian, C., Asai, N., D'Agati, V., & Costantini, F., 2014). Low nephron endowment at the end of kidney development causes hypertension and chronic kidney disease in adults and the maternal and gestational environments drive nephron endowment. The direct link between gestational conditions, nephron endowment, and adult health shows the importance of studying the kidney in IUGR (Cebrian, Asai, D'Agati, Costantini 2014, Wood-Bradley, Barrand, Giot, Armitage 2015). We hypothesized that disruption of metabolic homeostasis in the nephron progenitor cells in the IUGR fetus impairs nephrogenesis and is the direct link between the maternal environment and nephron endowment leading to adult hypertension and Chronic Kidney Disease.

Chapter 2 Materials and Methods

2.1 Mouse Model and Breeding:

Iso-caloric protein restriction to induce intrauterine growth restriction. The protein restricted experimental diet was the Envigo TD 90016 diet that is as percent of weight 6.1% protein, 75.6% carbohydrate, 5.5% fat and 3.8 Kcal/g. The control diet is Envigo TD 91352 that is as percent of weight 20.3% protein, 61.6% carbohydrate, 5.5% fat and 3.8 Kcal/g. The only differences between the two diets are the amount of protein, and the 6% protein diet having more sucrose and cellulose to maintain an iso-caloric formula (Figure 5).

CD1 female mice and SixCreGFP wildtype male mice from a mixed CD1 and C57BL/6J background were used. Male and female mice were put on diet for 3 weeks starting at 6 weeks of age before pairing and diets were continued during all pairing and pregnancy. Timed pregnancies are defined as female mice being paired with male mice overnight where the next day is counted as E0.5. Postnatal day zero (P0) is the day mice are born. Time points after P0 must account for litter size and breastmilk quality. Female mice have 10 nipples for feeding so all growing litters were 10 pups or smaller, in cases of larger litters pups were sacrificed at P0. This controls for postnatal food access. Protein restriction had a noticeable effect on maternal weight gain with the mice remaining slimmer, showing that maternal growth was changed and thus breastmilk quality could be impacted. To account for this, pups from 6% maternal diet grown past P0 were fostered with a CD1 female mouse that had given birth the same day from either the 20% diet population or from normal vivarium diet of 21% protein. Both IUGR and control would have equal access to milk and similar milk quality postnatally.

Six2Cre GFP males are heterozygous for Cre and the Six2+ NPCs have green fluorescent protein. The NPCs have no developmental changes with the presence of GFP. GFP cells can be sorted for using Fluorescence-Activated Cell Sorting (FACS).

The historical definition of IUGR in humans was term infants at the 10th percentile of body weight. Based on this inclusion/exclusion criteria were developed. A 6% maternal diet does not consistently create IUGR mice and IUGR by definition can occur with a normal maternal diet. All mouse pups were weighed at birth and the 10th percentile for control mice was calculated to be 1.42g. This became the threshold for inclusion and exclusion of samples. Control mice below 1.42g were not considered control and to be considered IUGR pups from the 6% maternal protein diet had to be below 1.42g.

2.2 IUGR Characterization:

All mouse pups were weighed at birth for inclusion/exclusion. Kidney weight from harvested P0 kidneys was measured after removal of ureter and capsule for combined kidney weight. Growth curves for P21 samples were done by daily measurement of body weight until sacrificing. Blood sugar from mice was measured using a Freestyle blood sugar meter and Freestyle test strips. P0 blood came from post decapitation pool and P21 blood sugars came from tail snips. At P21 mice were weighed and kidneys harvested with capsule and ureter removed for combined kidney weight at P21. Animals kept for blood pressure measurements were weighed daily from P0 to P30 with weekly measurements after P30.

2.3 Immunohistochemistry:

Paraffin embedded kidneys were sectioned at 5 µM. Paraffin was removed with xylene and sections were rehydrated using alcohol. Antigen Unmasking with acidic sodium citrate followed by quenching in H_2O_2 (10% solution in TBS). Blocking Buffer for 1 hour at Room Temperature with environmental moisture (TNB (0.5% blocking reagent in TBS) + 10% Normal Donkey Serum + 15µl/ml donkey anti Rabbit Fab anti Mouse Fab).

Primary Antibody mixture is made in Antibody Buffer (TNB (0.5% Blocking Reagent in TBS) + 2% Normal Donkey Serum). Incubated on sections for 1 hour at room temperature or overnight at 4C.

Secondary Antibody at 1:400 with Hoechst nuclear stain at 1:800 in antibody buffer. Lectins are added with secondary antibodies. They are incubated at Room Temperature for 90 minutes.

Samples are then washed and mounted. TBS Washes are used between steps and before mounting. Six2(R) 11562-1-AP 1:200. Mesi1/2 (R) 12744S 1:200+TSA 2 minutes. Mesi1/2/3 (m) MBS605057 1:200+TSA 2 minutes. Sox9 (R) 82630 1:200. Aquaporin 1 (R) 243-261 1:200. Pancytokeratin (m) 1:400. Lhx1 (m) 4F2 1:100. Cleaved PARP (R) 1:200 +TSA 3 minutes. BrdU (m) sc-32323 1:200. E-cadherin (R) ab40772. Sall1 (R) MBS9203689 1:200. P-ATF2 (R) 24329S 1:200. LTA FL-1321 1:400. DBA B-1035 1:400. NCAM (m) C9672 1:400. Calbindin (R) ab108404 1:400. WT1 (R) 1:400.

2.4 Count Data for BrdU Proliferation and PARP Apoptosis:

BrdU is suspended in PBS at a concentration of 10 mg/mL and injected at a dose of 100 mg/kg based on pup weight. Each pup was weighed, injected, and incubated for 3 hours before being sacrificed. The kidneys were fixed with 10% formalin, embedded, and then sectioned at 5 µM for immunohistochemistry. The BrdU mouse antibody thermoFischer B35128 was used at 1:100 with markers for tissues of interest. The immunostaining was imaged at 40X with equal exposure times. All tissue sections were sagittal plane and deep within the kidney showing cortex and ureteric branching to control for part of the CMs and UB tips being counted. CMs and UB tips counted contained a ureteric branch that showed NPCs forming CM on both branches. The staining for Six2, Sall1, and Calbindin was done in consecutive sections Counting was done in NIS Elements 4.5.0. Regions of Interest (ROIs) were selected based on the co-staining and then overlaid on the BrdU channel. The BrdU is then counted by MCH thresholding to create and object count and object catalog. The object catalog is images of each BrdU positive stain. The object catalog was used to check that positive stains have not merged with multiple cells being counted as a single object. The final count for BrdU includes objects manually counted from the object catalog.

PARP counts used the same method with NIS elements. The PARP positive cells were a rare event and object catalog did have merged cells decreasing the count by NIS Elements.

2.5 Magnetic Activated Cell Sorting:

Mice are dissected, and kidneys are isolated with capsule and ureter removed then washed in HBSS. Damaged kidneys are not used. Kidneys are incubated in digestion mixture (Accutase or PBS + Collagenase and Pancreatin) rotating in an incubator at 37C. Digestion is stopped using fetal bovine serum and DNase mixture then incubated for 5 minutes rotating at 37C. Cell suspension is removed and washed using isolation buffer of PBS and bovine serum albumin. Cell suspension is filtered through a Miltinenyl Biotec 30 µM filter. Cells are incubated with PE conjugated primary antibodies: CD105 for endothelial cells, CD140 Foxd1+ stroma cells, CD119 for RBCs and erythroblasts, and CD326 for epithelialized/differentiated cells for 13 minutes on ice. After washing the cells with isolation buffer, the cell suspension is incubated for 18 minutes on ice with Anti-PE beads. After further washing the cell suspension is run through a Miltinenyl Biotec LD column that will collect all cell populations bound to the Anti-PE beads leaving the unbound nephron progenitor cells to flow through the column and isolating them via negative selection. The NPCs are Cited1/Six2 dual positive.

2.6 Fluorescence-Activated Cell Sorting:

Cell suspension is isolated and digested as described in MACS. After filtration, the cell suspension is sorted for GFP+ using a Beckton Dickerson FACS Aria Fusion and the FACS DiVa software v8.02. The isolated population will be Six2+ NPCs.

2.7 RNA-Seq:

NPCs of mouse pups from three independent litters of 6% and 20% maternal diet were isolated as described using MACS. The unexpanded isolated NPCs created 3 biological replicates for experimental and control. Total RNA was isolated using Qiagen RNeasy Mini-kit

(74104) with on column DNase digestion. Samples were sent to Genewiz and passed quality control by them. RNA sequencing was non-strand specific and run-on Illumina-HiSeq 2x150bp per lane. The RNA library was prepared with poly-A tail selection.

Before starting alignment and differential expression FASTQ files are checked for quality control using FASTQC. Alignment of the reads was done using STAR to the mm9 and mm10 genomes, not to provide read counts but to provide the best alignment. This produces wiggle files for visualizing tracts. Wig coverage files can be viewed using UCSC web-based viewer, IGV, or IGB. Junction files show isoforms of RNA reads. RSEM provides read counts and normalizes those counts to create a relative molar concentration for the reads from the FASTQ files. While some programs provide only unique reads, RSEM will look at multiple map locations for reads. Reads in RSEM are normalized based on reads and the exon lengths. RSEM results go into the EBSeq R program to produce what are empirical basian genes showing differential expression data. It uses raw counts, not the normalized ones, to compare groups and show statistically significant differences in expression levels between groups. With a $p<0.05$ there were 6,036 differentially expressed genes, of those 1,694 had a fold change of +1.5 or greater, 2,114 had a fold change of -1.5 of greater, and 2,228 had a fold change between +1.5 and -1.5. Those up or down regulated by 1.5 were put into Ingenuity Pathway Analysis (IPA). iPathway analysis uses a $p<0.05$ and a fold change expression absolute value of at least 0.6.

2.8 Kidney Function:

Blood pressure measurements are from tail-cuff using the Visitech BP-2000 Blood Pressure Analysis System. It takes noninvasive measurements of conscious mice using transmission photoplethysmography to measure light transmission through the tail to measure blood pressure and heart rate. The heartbeat of the mouse pushes out through the vascular system

and the dilation of the blood vessels in the tail correspond to systolic while the end of that pressure wave corresponds to diastolic. Mice where acclimated to the machine with at least 3 trial runs before measurements were taken.

Plasma creatinine is a measure of kidney filtration. Creatinine is a waste product filtered by the kidneys and leaves the body in urine. High serum creatinine shows decreased kidney filtration (CDC: NCCDPHP, 2020). The animal was sacrificed, and blood was collected using heart puncture. At least 500 µL of blood was put into plasma collection tubes which were inverted 10 times to prevent coagulation. Plasma was then spun down and stored at -80 until shipped to the UAB-UCSD O'Brien Center for Acute Kidney Injury to measure creatinine, a marker for filtration, or Blood Urea Nitrogen, another marker for kidney filtration. Urine was also collected from the animals to test for kidney damage by testing for urine albumin.

2.9 Glomerular Count:

Hematoxylin and Eosin stained kidney sections show the glomeruli. A large image grab creates a complete image of the kidney section and NIS elements can count and measure the size of selected structures. Based on the fractionator method described in Aresenault et. al. 2014 glomerular are around 15 µM thick. When sections are 15 µM or more apart the glomerular present would be new structures and not a recounting of the same glomerular. Counting 3 or more mid-sagittal sections that are 15 µM or more apart would represent 3 independent samplings from that kidney and averaging those counts would produce an average count per section for that kidney. Animals were counted at 4 months of age except for 1 IUGR male that was excluded from glomerular count due to poor integrity of sections.

2.10 Six2+ Percent by GFP:

P0 and e13.5 are both counted by kidney pair. Kidney is digested as described in MACS then mechanically broken up by pipetting. Cell suspension is spun down at 350 rpm at 4C to

wash twice in PBS. Then the percent fluorescence is measured using Beckman Colter Gallios Flow Cytometer.

2.11 Extracellular Flux Measurements of MACs P0 NPCs:

NPCs isolated by MACs are not expanded and directly plated on Seahorse Extracellular flux plates. The cellular metabolism is measured in live cultured cells on the XF^e24 Extracellular Flux Analyzer (Agilent Seahorse Technologies). Extracellular cell acidification rate (ECAR) measuring glycolysis, and oxygen consumption rate (OCR) measuring oxidative phosphorylation.

2.12 Statistics:

Body weight, kidney weight, and glomerular counts were compared using a student's t-test. Blood sugar was compared using Mann-Whitney U test. Two-way ANOVA analysis with replication was used for testing the interaction of sex and control versus IUGR in adult samples. A p value cut-off of 0.05 was used for all statistics. Excel and Prism 8 were used for statistical analysis and graph building. Error bars on graphs represent standard error measurements.

Chapter 3: Results

3.1a. Physiology and Vital Statistics of newborn pups from dams on a 20% vs 6% protein diet:

We used a 6% protein maternal diet compared to a 20% protein control diet to produce low birth weight offspring. Figure 5 shows a comparison of the components of the two diets. Casein is the protein used in the diet and is, as expected, lower in the experimental 6% protein diet. DL-Methionine is an essential amino acid found in protein sources; its decrease is part of the restriction of protein. Sucrose and cellulose are both increased to compensate for the loss of kilocalories with decreased protein. The calcium phosphate is increased due to the decreased protein. The casein protein contains phosphorous, with decreased casein the phosphorous levels

have decreased, so calcium phosphate is increased in the 6% diet. Calcium carbonate is then decreased to maintain equal amounts of calcium in the isocaloric diets. The result is isocaloric diets that vary in protein and protein related nutrients and increased carbohydrates (Figure 5). There was no variation in blood sugar between the CD1 mothers on control or experimental diet.

3.1b. Morphology and Morphometrics:

Low protein parental diet (LPD, 6% protein) produced full-term mouse pups with decreased body weight at day of birth Postnatal day zero (P0). The average body weight of P0 pups from parents on 20% (control) protein diet was 1.61g, while pups from 6% parental diet weighed at an average 0.869g, a statistically significant decrease of 54% ($p<0.0001$). Pups from 6% parental diet have significantly smaller kidneys than the control, with an average combined kidney weight of 0.0082g versus 0.0129g, a statistically significant decrease of 37% ($p<0.0001$). Interestingly, the kidney weight/body weight has increased with 6% parental diet (Figure 6 A-C). Whereas control kidneys were 0.8% of body weight, 6% LPD (IUGR) pup kidneys were significantly

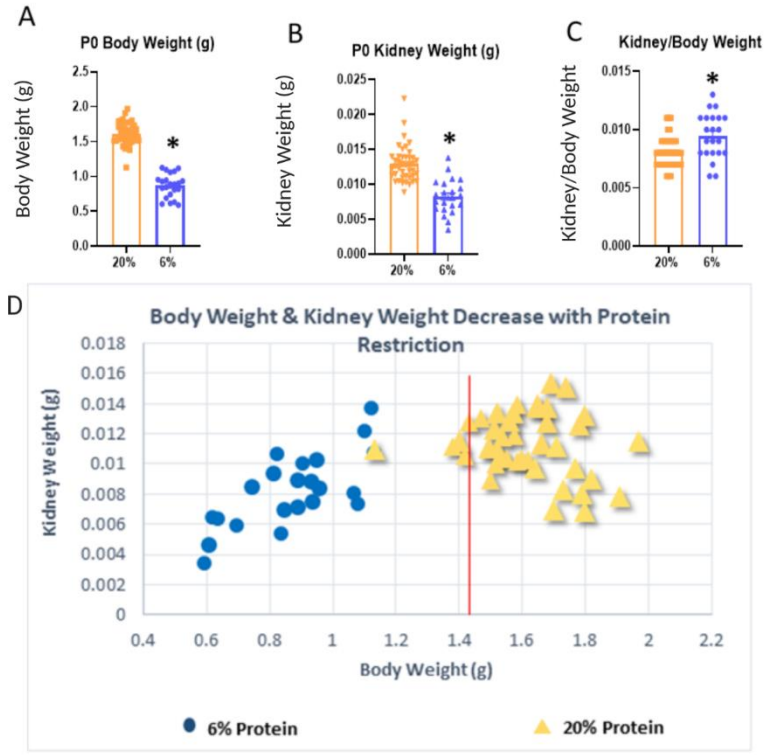

Figure 6: P0 IUGR Mouse Body Weight and Kidney Weight:
A) P0 IUGR have a lower body weight than control p<.0001. B) IUGR mice have decreased kidney weight. p<.0001. C) Kidney weight as percent of body weight is higher in IUGR than control P<.01. D) Kidney and Body weight XY plot. Red line at 1.42 grams is the 10th percentile of control weights at P0. This is the cut off for accepting or rejecting control and IUGR. IUGR n=22, control n=42. These weights were tracked across 5 litters for control and IUGR with control n=26 IUGR n=24.

higher (P<0.01) at 0.95% of body weight. Thus, although IUGR pups have lower body and kidney weight their kidney/body weight ratios are higher than of control pups. These data were collected from 42 pups from 8 control litters and 24 pups from 5 LPD litters.

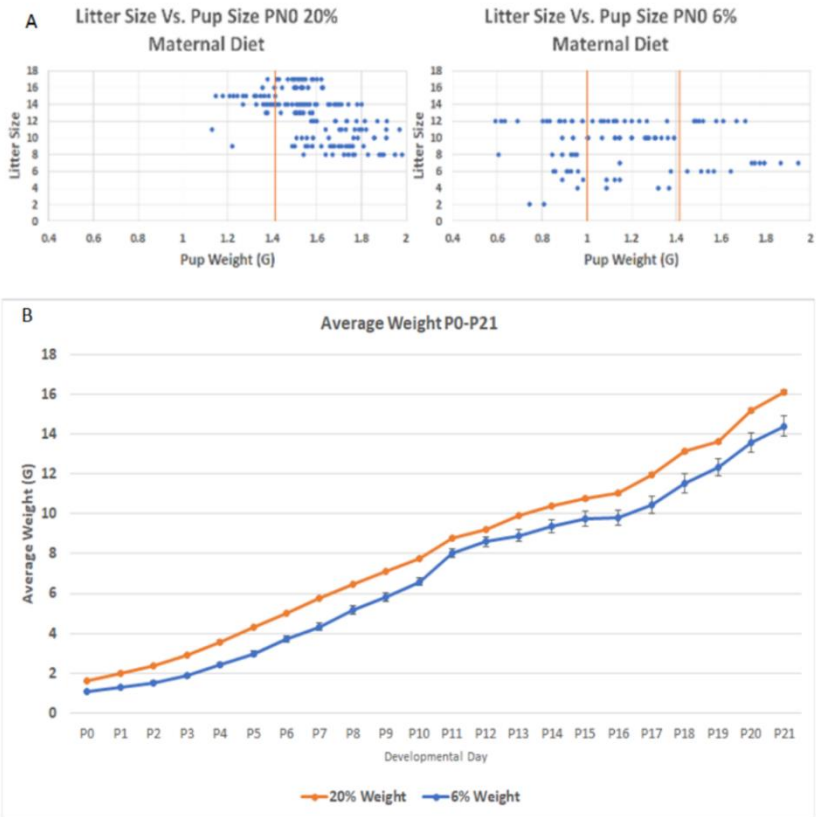

Figure 7: Low Protein Impacts Pup Size, Litter Size, and Growth into adolescence:
A) XY plot of pup weight by litter size of that pup. Graph on the left is only control with the graph on the right only parental protein restricted. Control pup weight at P0 decreases with litter size with larger litters trending towards more pups of lower weight. IUGR weights do not change with litter size. The 1.42 gram cut off for inclusion or exclusion as IUGR and control. Note that there are control mice that have IUGR pups. P0 pups weighing less than 1 gram is only present in 6% protein litters. Control n= 125 from 10 litters. Low Protein n=72 from 7 litters. B) Growth curves for IUGR and control from postnatal day zero and postnatal day 21. IUGR pups are significantly decreased from P0 to P21. All pups tracked were selected using the inclusion/exclusion cut-off of 1.42 grams. These weights were tracked across 5 litters for control and IUGR with control n=26 IUGR n=24.

Due to the variable penetrance of IUGR by LPD and occurrence of IUGR independent of maternal diet criterion for accepting and rejecting P0 samples was established. IUGR in humans was defined as newborns that were full term and-in the bottom-10th percentile by body weight. Extending these to mouse studies, 10th percentile for 42 control pups across eight litters was determined to be 1.42g. Thus, this weight was used as the threshold for defining IUGR versus normal birth weight and denoted by the redline in figure 6 D. P0 control pups weighing less than 1.42g were considered as IUGR and not used. Pups from

LPD with a less than 1.42g are considered as IUGR were used. This criterion was used for P0 immunostaining, cap size measurements at P0, metabolic profile (Seahorse) at P0, and for pups used for P21 and 4-month analysis. The 1.42g criterion was not used for the P0 bulk RNA-seq samples. The embryonic samples from LPD dams showed no change in weight so there was no sample exclusion for this age groups. The significant decrease in P0 body weight and increase in kidney/body weight found in LPD pups represented all samples not just samples accepted or rejected based on the 1.42g cut-off of IUGR.

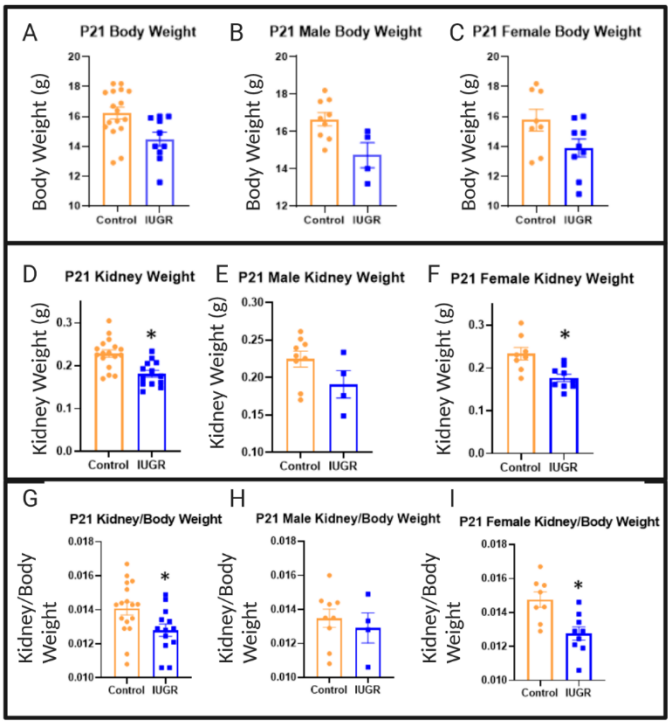

Figure 8: Differences in P21 Body Weight and Kidney Weight
A-C) At postnatal day 21 adolescent IUGR weigh less than control overall, as do male IUGR, female IUGR do not weigh less. D-F) Kidney weight is lower in the IUGR mice overall and in female mice, but not in male mice at the day of weaning postnatal day 21. G-I) Kidney weight as percent of body weight is lower overall and in female IUGR, but not in male IUGR. Showing Male mice are small, with proportionally smaller kidneys at this stage while female mice have caught in body weight with control but have smaller kidneys. At P21 all control n=17, male n=9, female n=8 all IUGR n=10, male n=4, female n=6.

Low protein parental diet impacts the growth of the mouse pups and impacts litter size. Control diet produces a large range of litter size from eight to seventeen pups, while low protein diet produces litters with two to twelve pups. Control diet litters also show a relationship between litter size and pup weight with increasing litter size having lower pup weights. Interestingly, the low protein litters are dissociated from the litter size and pup weight relationship and are small regardless of litter size. This is shown across seven low protein litters and ten control litters,

control n =125 and low protein n=72. This comparison included control pups of low weight and low protein pups of higher weight disregarding inclusion/exclusion criterion at this stage (Figure 7A).

The low birth weight from protein restriction persists to day of weaning (P21), despite controlling for postnatal factors such as milk quality and access. IUGR mice for longitudinal study were fostered by CD1 female mice on normal or control diet that had given birth within a day of IUGR birth. Both IUGR and control litters used for longitudinal study were controlled for size of litter. All longitudinal litters were limited to ten pups to control for access to food as mice possess only ten nipples. This would control for both milk quality and access to milk so that the postnatal environment of IUGR and control pups were similar. Thus, phenotypic differences would be a result of differences in gestational conditions and not postnatal factors. Pups were weighed daily from P0 until postnatal day 21 (P21). The IUGR mice continued to be low weight through P21, at which time they were weaned from their foster mother (Figure 8B). The P0-P21 measurements included IUGR n=24 and control n=26 from five separate litters.

IUGR mice also exhibit differences in postnatal growth and development. At birth IUGR mice were thin with bright red skin and delicate skin. Although the IUGR pups lose the bright red coloring at P2 or P3, they remained more reddish in appearance than the control pups which transitioned from red to pink then a pale white color. The thinness of IUGR pups remained until P9 when some IUGR pups, despite average weight being less than control, looked stouter. Control pups grew a thin but consistent hair cover over their body similar to peach fuzz by P6 with full hair at P9-10. The IUGR pups, however, showed 2-3 days delay in acquiring the peach fuzz at P8-9. Occasionally, the smallest IUGR pups that look like runts until P30 developed the peach fuzz at P10. These pseudo runt mice have shorter bodies and tails with leaner builds. Controls can be

sexed at P8 with prominent nipples on female mice and genital dimorphism being apparent, while IUGR cannot be consistently sexed until P11-12. IUGR mice also showed delayed movement and activity. Whereas at P5 the control mice were active crawlers IUGR pups showed some movement and shift but did not cover great distances until P8 or P9. Therefore, the delayed growth patterns observed in IUGR pups were morphometric and anatomical as well in body weight.

IUGR pups' body weights remained significantly low in males at P21, but not in IUGR females. Averaged combined males plus female body weight at P21 in control pups was 16.23g and 14.49g in IUGR pups. Average weight of control male was 16.66g versus 14.73 in IUGR males. The lowest weight recorded was in one pseudo runt IUGR male that weighed 13.2g. Female offspring did not demonstrate significant weight disparity at P21 (average weight control 15.75g versus IUGR 13.89g) despite the inclusion of two female pseudo runts weighing 10.8g and 11.6g (Figure 8 A-C). Average P21 IUGR kidney weights were lower than control P21 kidney weights particularly in female

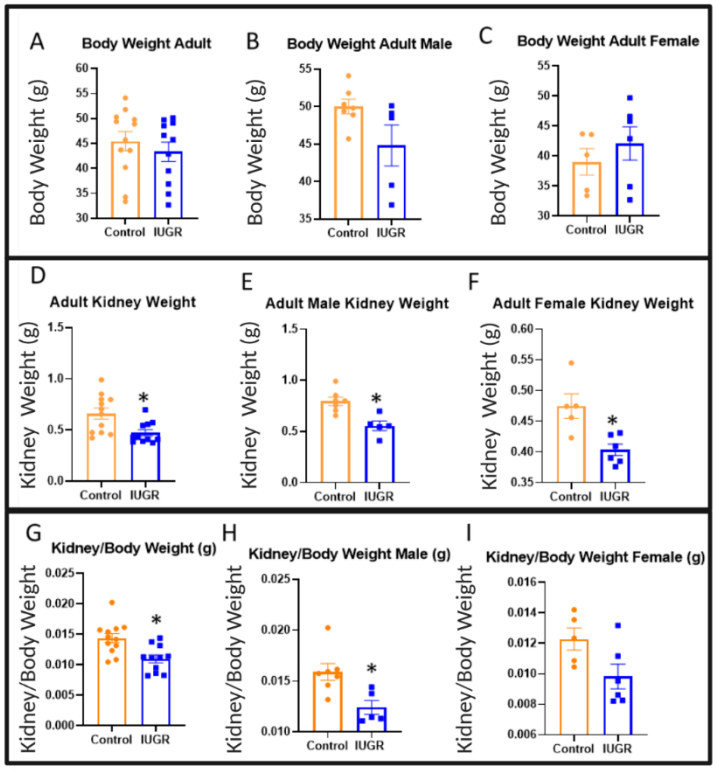

Figure 9: IUGR Adult Body Weight and Kidney Weight Changes

A-C) Adult mice at 3-4 months of age show no difference in body weight overall or for male or female alone. D-F) Shows all IUGR groups have smaller kidneys with sex interaction by ANOVA. G-I) All have a lower kidney weight as percent of body weight. At P21 all control n=17, all IUGR n=10. Control male n=9, IUGR male n=4. Control female n=8, IUGR female n=9. Adult control all n=12 IUGR n=11. Male control n=7 IUGR n=5, female control n=5 IUGR n=6.

offspring. Kidneys from male IUGR offspring did not show significant weight differences from the control. The difference in kidney weight was much smaller than at P0 (Figure 8 D-F). This could come from the mouse kidney continuing through organogenesis postnatally. Mouse kidney development occurs from embryonic day 10 to postnatal day 4 for a total of 16 days with roughly one quarter occurring after birth and removal from the embryonic condition of LPD. But these 4 days of postnatal kidney development were not fully normal despite control and IUGR being under the same conditions postnatally. The lower kidney/body weight ratio persists at P21 in IUGR pups even with female IUGR that have caught up in body weight with control, indicating the lower kidney weight is likely maintained. Furthermore, the kidney/body weight ratio showed differences in kidney development postnatally. The IUGR P0 kidney/body weight ratio was 0.0095 significantly higher than 0.008 in control. At P21 control increased by 75% to 0.0140 while IUGR only increased by 31% to 0.0125. Then at 4 months neither ratio had increased from the P21 ratio (Figure 7C, 8G, 9G). IUGR mice begin with a higher kidney/body weight ratio then by adolescence have a significantly lower kidney/body weight ratio which persists into adulthood. The lower kidney/body weight ratio was present in significantly smaller mice as well (Figure 8 & 9). But the change was from P0 to P21 when control increased their kidney/body ratio while IUGR mice did not. Both had a similar lack of change P21 to 4 months. It was during the 4 days of postnatal kidney development and full 21 days of growth, when control and IUGR were under the same conditions, that IUGR experienced altered kidney development to impact adult kidney/body weight ratio. Thus, despite nearly identical postnatal environment conditions, the IUGR mice maintain morphometric and developmental differences into adolescence. IUGR kidneys retain memory of LPD conditions postnatally and that memory impacts development and growth of the kidney as shown by the changes and sometimes lack of changes from P0 to P21.

At 4 months of age adult IUGR mice (n=11, male n=5 and female n=6), showed no significant difference in body weight from control mice (n=12, male n=7 and female n=5).

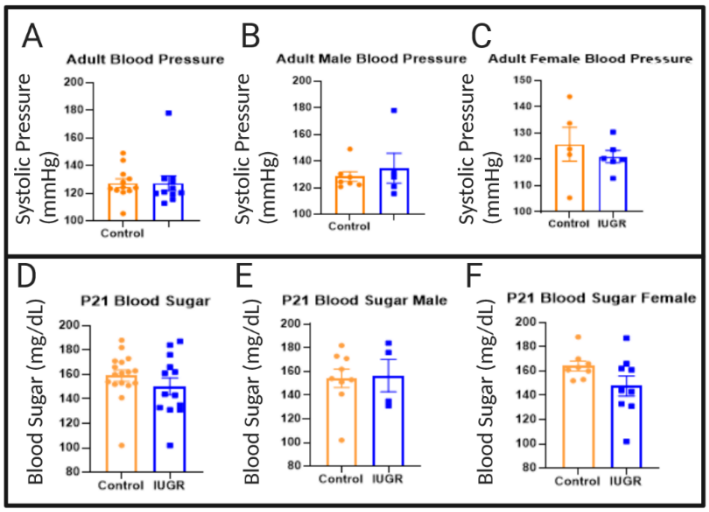

Figure 10: Blood Pressure at 4 months and P21 Blood Sugar Are Unchanged
A-C) No change in blood pressure either over all or in a sex specific analysis. A 6% IUGR male has the highest measured blood pressure of 178.06 mmHg. The average blood pressure for control is 128.4 mmHg and the average for IUGR is 134.7 mmHg. D-F) At postnatal day 21 there is no change in blood sugar overall or in the male or female specific adolescent mice. At P21 all control n=17, all IUGR n=10. Control male n=9, IUGR male n=4. Control female n=8, IUGR female n=9. Adult control all n=12 IUGR n=11. Male control n=7 IUGR n=5, female control n=5 IUGR n=6.

Although male IUGR mice trended lower in body weight than the control, the female IUGR mice showed an opposite trend with higher body weights than the control (Figure 9 A-C). Control males weigh more than control females by about 10g while male and female IUGR adults have no difference in body weight. Female IUGR had caught up at P21 and may be headed towards the higher rate of obesity found in IUGR adult humans. Kidney weights, however, remain lower in the 4-month-old IUGR mice. The IUGR kidneys weigh less when looked at as a group or separated by sex despite male at P21 trending lower in weight with no significance (Figure 9 D-F). Male P21 kidneys not weighing significantly less may be due to small sample size at P21.

Kidney as percent of body weight in 4-month IUGR mice remains lower when comparing both male and female mice, and when comparing male mice alone. The adult IUGR had smaller kidneys in bodies trending towards higher body weight.

3.1b. Blood pressure and kidney function measurements:

Plasma creatinine, urine albumin, and blood urea nitrogen were measured in adult IUGR and control mice as a measure of kidney function. Tail blood was used to measure blood sugar at P21 using a blood sugar meter. These physiological measures are not significantly changed but are of interest. Blood pressure was measured by the tail-cuff method. No significant change in blood pressure was observed in IUGR vs. control mice (Figure 10 A-C). An average blood pressure reading of 128.4 mmHg was recorded in control offspring, with an average reading of 134.7 mmHg in IUGR offspring. The highest blood pressure recorded was 178.06 mmHg from one IUGR male (6.23M1), which contributed to the higher blood pressure trend in IUGR males compared to control males.

Blood sugars were measured at P21 by one-time stick testing on a blood sugar meter. Measurements were done under non-fasting conditions. No changes in levels were observed between control and IUGR mice (Figure 10 D-F).

Plasma creatinine measures kidney function by measuring the waste product of creatine not removed by the kidney. Higher creatinine levels are indicative of decreasing kidney function. Although creatinine levels from adult IUGR mice were not significantly different from control. A strong trend towards increased creatinine was observed, especially when considering values from male mice (figure 11 A-C). The highest plasma creatinine levels were recorded from the adult male 6.23M1 with plasma creatinine of 0.14 mg/dL which is almost 3 times the average creatinine levels of either all controls or control males. The second highest plasma creatinine level was from a female IUGR from the same litter, 6.23F3, with a plasma creatinine level of 0.12 mg/dL (Table 9).

Blood urea nitrogen (BUN) test measures the urea nitrogen in the blood. Urea is produced by the liver when digesting protein. The kidney filters urea as a waste product out of

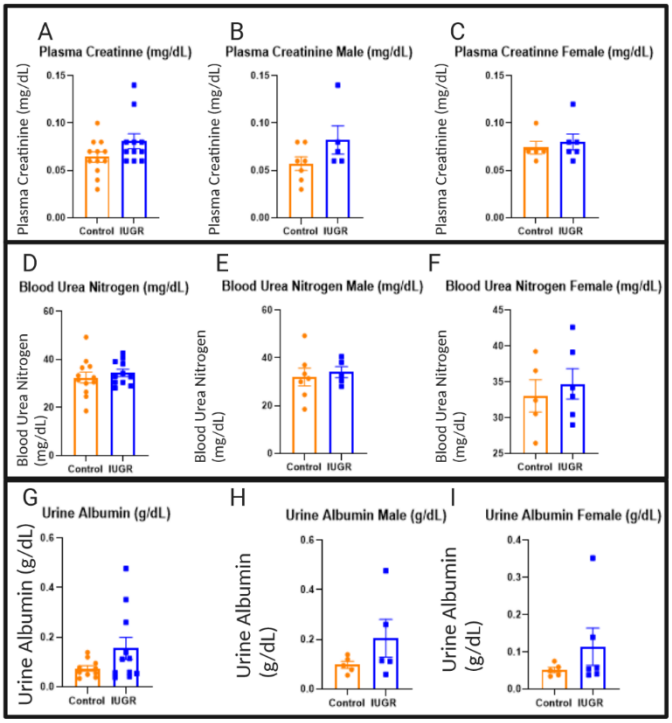

Figure 11: Little Changed in Kidney Function Measures at 4 Months

A-C) Plasma Creatinine is unchanged when comparing all animals and when comparing female, plasma creatinine is higher in male IUGR with the same male with the highest blood pressure having the highest plasma creatinine of 0.14 mg/dL. Control n=12, Control male n=7, female n=5. IUGR n=11, male n=5, female n=6 G-I) Urine albumin is not changed at 4 months, but the male with high blood pressure, and the highest plasma creatinine has the highest urine albumin. An IUGR female with unchanged blood pressure has the second highest urine albumin and the second highest plasma creatinine. This IUGR female and male have high urine albumin of 0.352 g/dL and 0.477 g/dL respectively. Control urine albumin has a mean 0.0744 g/dL. BUN sample sizes are the same, Urine Albumin Control n=10, control male n=5.

the blood. High urea is a sign of poor renal health. High BUN in humans can be caused by a high protein diet, decreased glomerular filtration (GFR), heart failure, hypovolemia, and increased catabolism. Although, there is no significant change in BUN in IUGR adults at 4 months, there is a trend towards increased BUN in IUGR mice. One male control, 20.23M4, had the highest BUN of 49.27 mg/dL. This mouse was otherwise normal. One IUGR female (6.23F3) with second highest BUN of 42.61 mg/dL also has the second highest plasma creatinine. Excluding the control male 20.23M4, the male with the highest BUN is the previously noted 6.23M1 with a BUN of 40.56 mg/dL along with his elevated plasma creatinine levels (Anderson, L., Otto, G., Pritchett-Corning, K., & Whary, M., 2015) (Table 9).

Albumin is a protein found normally in the blood at 36.7 ± 5.2 g/L in males and 46.4 ± 7.0 g/L in females (Anderson, L., Otto, G., Pritchett-Corning, K., & Whary, M. 2015).

Functional kidneys prevent the movement of albumin from blood to urine. Albumin is filtered by the glomerulus of the kidney and reabsorbed by the proximal convoluted tubules, the loop of Henle and distal tubules, and the collecting ducts. Elevated urine albumin is a marker of kidney damage and decreased function. IUGR adult mice do not have significantly increased levels of urine albumin, but there is a definite trend to increased albumin driven mainly by three IUGR animals. The highest urine albumin level was 0.477 g/dL found in 6.23M1 showing one animal with the highest plasma creatinine levels, highest urine albumin and elevated BUN. The second highest urine albumin is 0.352 g/dL from 6.23F3 which had the second highest BUN and second highest plasma creatinine levels. Their IUGR male litter mate 6.23M2 has the third highest urine albumin at 0.26 g/dL. For comparison only four of the 11-control measured had urine albumin over 0.1 g/dL and none of these animals were over 0.14 g/dL. The mean for all control urine albumin was 0.0744 g/dL compared to male IUGR at 0.352 g/dL and 0.477 g/dL for female IUGR (Figure 11 G-I and Table 9).

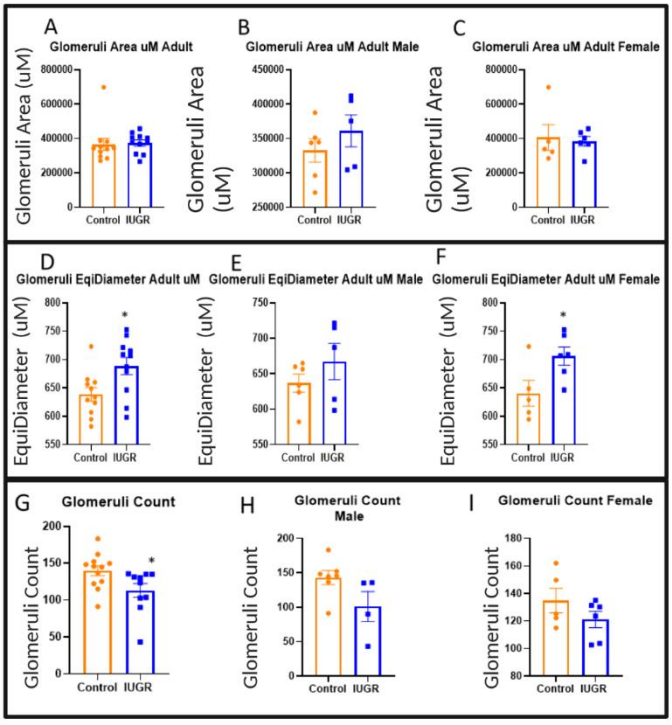

Figure 12: Glomeruli Count and Morphology: A-C) Glomeruli area measured on H&E staining using NIS elements. No change in glomeruli area, but there is a trend of larger glomeruli in male mice. The Eqi diameter is the longest diameter through the glomeruli measured. This is larger overall and in female. G-H) Glomeruli counts from 3 h&e tissue sections 20 uM distance from each other. Glomeruli number is decreased in IUGR. The lowest glomeruli number is from male with cysts visible in histology and the highest blood pressure, plasma creatinine and urine albumin. This data is supported by glomeruli counting from three 10X images per animal and counted independently. Adult control all n=12 IUGR n=10. Male control n=7 IUGR n=4, female control n=5 IUGR n=6.

These physiological measures are not significantly changed but suggest impaired kidney function in offspring from LPD parents. One important consideration here is the genetic background of the mice used – this point is discussed further in the discussion.

There are sex differences in the impact of IUGR. This was first apparent in growth from P0 to P21. ANOVA two-way analysis showed changes to physiology at P21 and adulthood (4 months). There are significant changes in adulthood kidney weight with interaction between sex, IUGR, and kidney weight with IUGR having smaller kidneys than control, IUGR males and females both having smaller kidneys, and IUGR females having the smallest kidneys ($p<0.05$). Control male n=7, total control n=10 with control female n=5. IUGR total n=11, IUGR male n=5, and IUGR female n=6. The adult measurements for body weight, systolic blood pressure, glomeruli count, plasma creatinine, urine albumin, and plasma BUN all showed no interaction. P21

3.1c. Adult Kidney Histology, Glomerular counts, and Immunofluorescence staining of molecular markers:

All control and IUGR adult kidneys were fixed and sectioned for immunostaining. Tissue sections were stained for hematoxylin and eosin. Hematoxylin stains the cell nuclei blue by marking the basic and cationic parts of the tissue. Eosin stains the acidic and anionic parts red

Table 1: Structural Changes in IUGR Relative to Control via Immunostaining

Key NC: No Change +:Up -:Down	Six2	Meis1/2/3	Uhx1	Sall1		DBA	NCAM		Wt1		Sox9		Calbindin	E-Cadherin	LTA/LTL	AQP1			AQP2	Pan Cytokeratin
	Cap Mesenchyme	Stroma	Nascent Nephron	Cap Mesenchyme	Nascent Nephron	Collecting Duct	Cap Mesenchyme	Nascent Nephron, CSB, SSB	Cap Mesenchyme	Podocyte	UB Tip Cells	S-Shaped Body	Ureteric Branching	Distal Tubule, Collecting Duct	Proximal Tubule	Proximal Tubule	Descending Loop of Henle	Descending Vase Recta	Principal Cells Collecting Duct	Collecting Duct
E13.5		NC	-			NC														NC
P0	NC	NC	-	-	NC	-	-	NC	-	-	+	+	NC	NC	-				NC	NC
4 Month						NC							NC	NC	NC	NC	NC	NC	mislocalized	+

showing the extracellular matrix and cytoplasm. The stains also overlap creating different combinations.

IUGR kidneys showed stronger eosin staining and presence of cysts (Figure 13 and 14 A) which were absent in control. Enlarged glomeruli are a sign of kidney disease as the kidney struggles to filter waste. Glomeruli were counted and size estimated on the H&E stained sections. Ten glomeruli were measured per animal from all control and adult IUGR from random fields of stained kidneys. The glomerular area showed no significant difference between control and IUGR kidneys (Figure 12 A-C). Male kidney glomeruli trend towards larger but the difference is not significant (Figure 12 A-C). The EqiDiameter, the longest point across an area, was also measured on the same glomeruli. A significant increase in the EqiDiameter of glomeruli from the female IUGR mice was recorded, with glomeruli from male mice trending towards an increase (Figure 12 D-F). While glomeruli at 4 months were not significantly larger in IUGR kidneys, the shape of glomeruli had changed.

In a young adult glomerular counts reflect glomerular endowment at birth. Glomerular counts showed decreased glomerular number in IUGR kidneys versus control (Figure 12 G). Kidneys from both male and female mice showed a trend towards decreasing glomerular number. The adult glomerular count is the average total count from 3 sections 20 µM apart per animal. This distance provides counts of unique glomeruli based on the established fractionator method (Buzello, 2000, Weibel, E.R., & Gomez, D.M., 1962). Tissue sections were deep showing the cortex, medulla, and ureter. The counts were confirmed by independent counting of glomeruli from three 10X images from the same sections. Both counting methods show IUGR with a significant decrease in glomeruli number (Table 9 and Figure 12). The IUGR male mouse

6.23M1 kidneys had the lowest glomeruli count. This IUGR male also has elevated plasma creatinine, urine albumin, and plasma BUN, and presence of renal cysts by H&E staining.

Consecutive adult kidney sections were stained with antibodies against E-cadherin (Cdh1), lotus tetragonolobus lectin (LTL), aquaporin 1 (Aqp1), pan cytokeratin 8 (CK8), dolichos biflorus agglutinin (DBA), and aquaporin 2 (Aqp2) (Table 9). E-cadherin is a calcium dependent cell adhesion protein that spans the cellular membrane in epithelial cells (Lee, S.-Y., Han, S. M., Kim, J.-E., Chung, K.-Y., & Han, K.-H., 2013). LTL marks the proximal tubules of the kidney by binding to the α-linked L-fucose containing oligosaccharides (Yallowitz, A. R., Hrycaj, S. M., Short, K. M., Smyth, I. M., & Wellik, D. M., 2011). Aquaporin 1 (AQP1) that stains the basolateral and apical plasma membranes of the proximal tubules, the descending loop of Henle, and the descending portion of the vasa recta. AQP1 is a water channel present in cell membranes (Monzani, E., Bazzotti, R., Prego, C., Laporta, C.A.U., 2009) [Brown, D. (2017)].

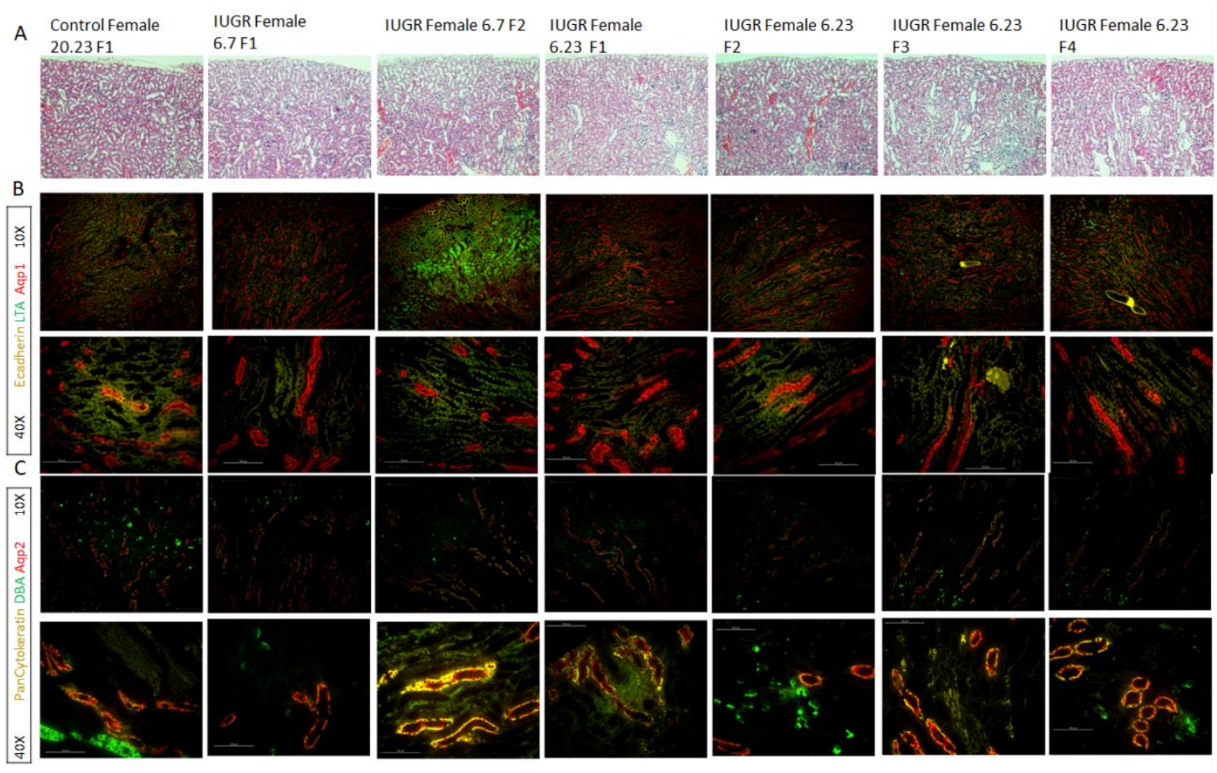

Figure 13 Adult Female Histology:
A) Hematoxylin and eosin staining of tissue sections from a control female and all IUGR females. This shows the presence of cysts including fluid filled cysts in 6.23 F3 and F4. B) Low and high magnification of immunofluorescence. E-cadherin stains the distal tubule and collecting ducts of the kidney. LTA lectin stains the proximal tubules. Aquaporin 1 marks the basolateral and apical plasma membrane in the proximal tubules and the descending loop of Henle. The fluid filled cysts that are pink in H&E are positive for E-cadherin. C) Low and high magnification of pan cytokeratin marking distal tubule, DBA lectin marks the distal tubules, and aquaporin2 marks the apical membrane of the collecting ducts. Staining done on Control females n=5, IUGR females n=6.

Figures 13 and 14 B shows at high and low magnification that IUGR adults have normal distal tubules, collecting ducts, proximal tubules, and loop of Henle. The cells of these structures are present and normally organized. LTL marking of the proximal tubules was decreased in adult IUGR kidneys compared to control.

Separate consecutive sections in all adult control and IUGR were stained with Pan cytokeratin (CK8) marking the collecting ducts. Cytokeratins are proteins found in the cytoskeleton of epithelial cells, specifically the intermediate filaments. There are 29 types of

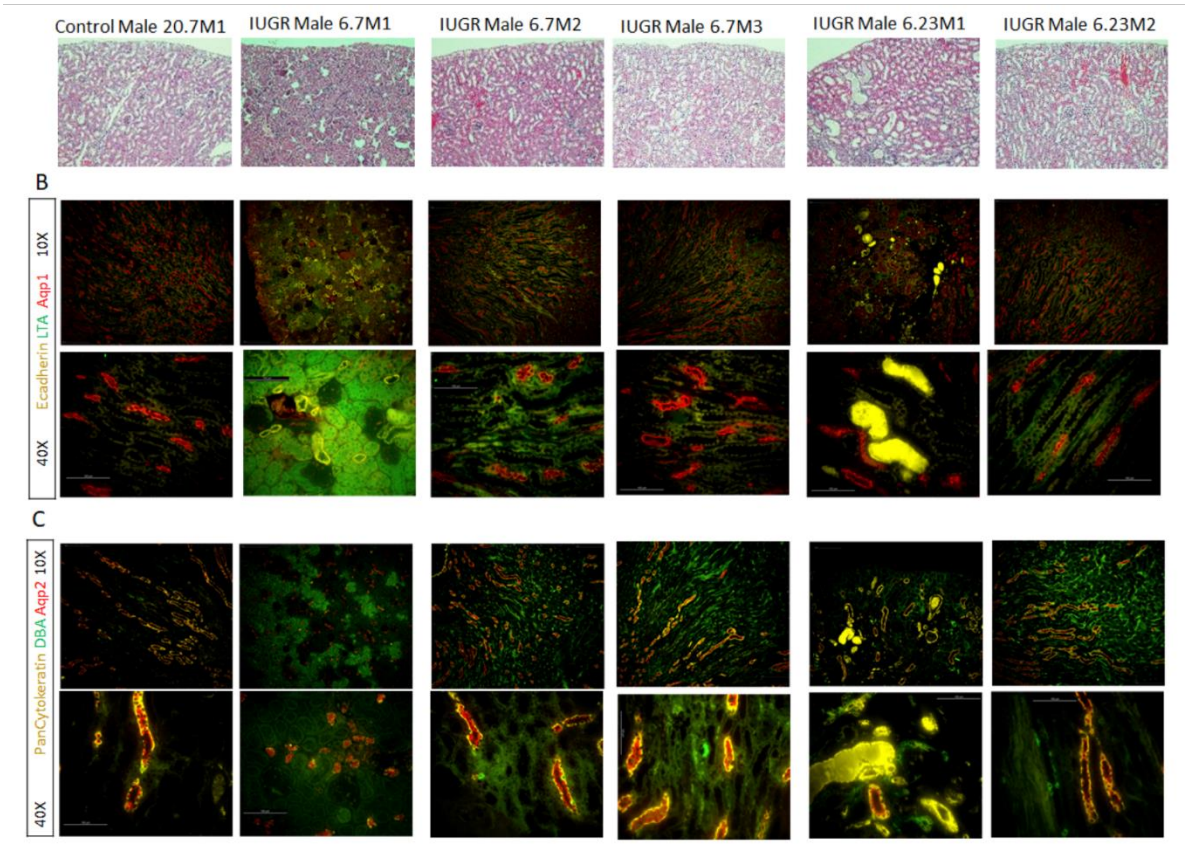

Figure 14 Adult Male Histology:
A) Hematoxylin and eosin staining of tissue sections from a control male and all IUGR males. This shows the presence of cysts including fluid filled cysts in 6.23 F3 and F4. B) Low and high magnification of immunofluorescence. E-cadherin stains the distal tubule and collecting ducts of the kidney. LTA lectin stains the proximal tubules. Aquaporin 1 marks the basolateral and apical plasma membrane in the proximal tubules and the descending loop of Henle. The fluid filled cysts that are pink in H&E are positive for E-cadherin. C) Low and high magnification of pan cytokeratin marking distal tubule, DBA lectin marks the distal tubules, and aquaporin2 marks the apical membrane of the collecting ducts. The fluid filled cysts are visibly stained with E-cadherin and pan cytokeratin. Staining done on Control males n=7, IUGR males n=5.

cytokeratins, the antibody used has nonspecific affinity for cytokeratins (Bates, C., Kharzai, S., Erwin, T., Rossant, J., & Parada, L., 2000). DBA marks the collecting ducts by binding the carbohydrate α-linked N-acetylgalactosamine (Holthöfer, H., Schulte, B. A., & Spicer, S. S., 1987). Aquaporin 2 (AQP2) marks the apical membrane of the collecting ducts. AQP2 is a second water transporter essential for water balance maintained by the kidney (Monzani et. al.

2009) [Brown, D. (2017)]. Figures 13 and 14 C confirms the normal formation of distal tubules and the collecting ducts. There was no loss of DBA in adult IUGR.

The 4-month-old IUGR mice had fluid filled cysts visible with H&E staining (13A and 14A). Epithelial cell staining by E-cadherin of the distal tubule and collecting ducts marked the fluid filled cysts in 6.23M1, 6.23F3, and 6.23F4 (Figure 13B & 14B). The cysts were also positive for the collecting duct marker pan cytokeratin (Figure 13C & 14C). DBA, another collecting duct marker, does not stain the cysts and was not changed between control and IUGR. Aqp2 marks the apical membrane of the principal cells of the collecting ducts. IUGR kidneys had more disperse Aqp2 staining not specific to the apical membrane irrespective of sex and presence of cysts.

IUGR adult kidneys were damaged with 6.23M1 showing the worst histology. 6.23M1 had the most and largest cysts and the brightest staining for E-cadherin and pan cytokeratin in the cysts. This damage coincides with markers of kidney function like blood pressure, plasma creatinine, urine albumin, and blood urea nitrogen (Table 9).

3.2 Embryonic Kidney Development in IUGR vs. Control Mice:

E13.5 and P0 kidneys were collected for molecular marker analysis. P0 pups were weighed and exclusion criteria were applied to ensure pups from LPD mothers reflected IUGR by body weight. Embryonic mice were not weighed so there was no cut-off for inclusion of exclusion of the e13.5 samples. These results are summarized in table 1. by body weight. Embryonic mice were not weighed so there was no cut-off for inclusion of exclusion of the e13.5 samples. These results are summarized in table 1.

3.2a Embryonic IUGR Kidneys have decreased Cap Mesenchyme and Ureteric Branching:

Size of CM was explored by FACS, kidney section staining, and whole organ immunostaining. *Six2CreGFP*$^{+}$ kidneys were fully digested and then counted for percent GFP+ by FACS count to determine the size of the Six2+ CMs. Ureteric branching was determined by kidney section staining, and whole organ immunostaining. Immunostaining of E13.5 organs and sections at the beginning of kidney development shows inconclusive results for cap size. The Six2+ staining in whole organ appears larger at times in the 10 IUGR and 8 control kidneys stained and imaged. Although the IUGR kidneys are smaller with less UB branching from pan cytokeratin staining (Figure 16 A and B). Sectioned e13.5 kidneys appear to have fewer Six2+ cells that are more dispersed, giving the appearance of more diffuse caps around the ureteric tips, and NPCs that are

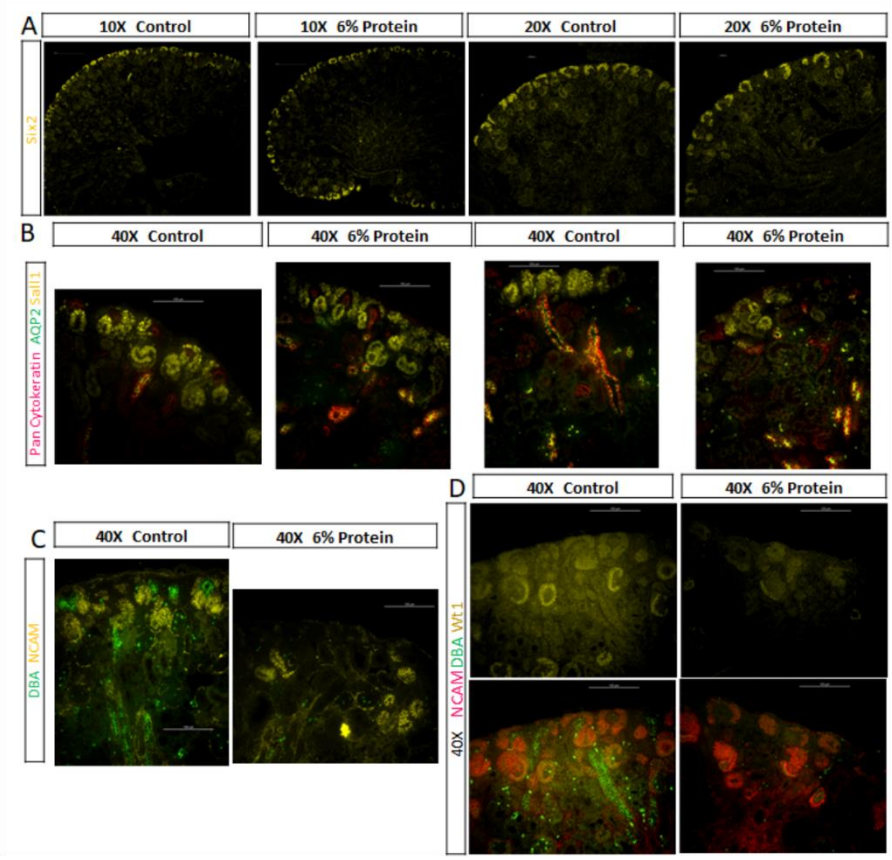

Figure 15: Cap Mesenchyme Markers at P0
A) There is no consistent change in CM size by Six2 staining at P0. The CMs of the smaller IUGR kidneys are diffuse in the cortex with more space between CMs. B) Sall1 staining of the CM is dimmer and smaller in IUGR with no change to Sall1 staining of nascent nephrons. C) NCAM staining of the CM is drastically decreased despite the presence of CM, this loss is often but not always accompanied by a loss of DBA staining in the ureteric branching. D) Wt1 staining in the CM is decreased along with a decrease in NCAM. The loss of Wt1 and NCAM occurs with or without the loss of DBA.

not closely aligned with UB tips (Figure 16 B). The lhx1 staining at e13.5 showed no change to nascent nephrons in size, number, or molecular character in section staining (Figure 16 B) [Cirio et. al. 2011].

Unnormalized percent GFP+ of digested kidneys shows the significant decrease in Six2+ NPC at e13.5 in LPD embryos. To quantify Six2+ NPC in IUGR kidneys, Six2+/GFP+ NPC were counted per kidney pair by flow cytometry at P0 (control n=3;IUGR n=5) and e13.5 (control n=3; IUGR n=4). E13.5 IUGR kidneys have 40% less GFP+ Six2 cells compared to control E13.5 kidneys. Over development, a 37.5% decrease in Six2+/GFP+ NPC was observed. This significant decline in Six2+/GFP+ NPC number from e13.5 to P0 in control is expected as the NPC population differentiates during development. An age-related decline in Six2+ NPC was not observed in IUGR kidneys (Figure 16 C).

Ureteric branching of pan cytokeratin positive structures plays a role in organ size, structure, and the maintenance and differentiation of NPCs (Costantini, F., & Kopan, R., 2010). Whole organ staining of 16 kidneys from 10 control embryos and 10 kidneys from 8 IUGR animals for pan cytokeratin showed changes in the branching at e13.5. DBA co-stained with pan cytokeratin was unchanged at e13.5 (Figure 16 A). Counting the UB tips in the organs shows a significant decrease in branching in IUGR embryonic kidneys. There was nearly a 30% decrease

in average UB tips in IUGR kidneys at e13.5 (Figure 16 E). At e13.5 overall NPC quantity and UB tip number were decreased showing early development of the kidney had changed with LPD.

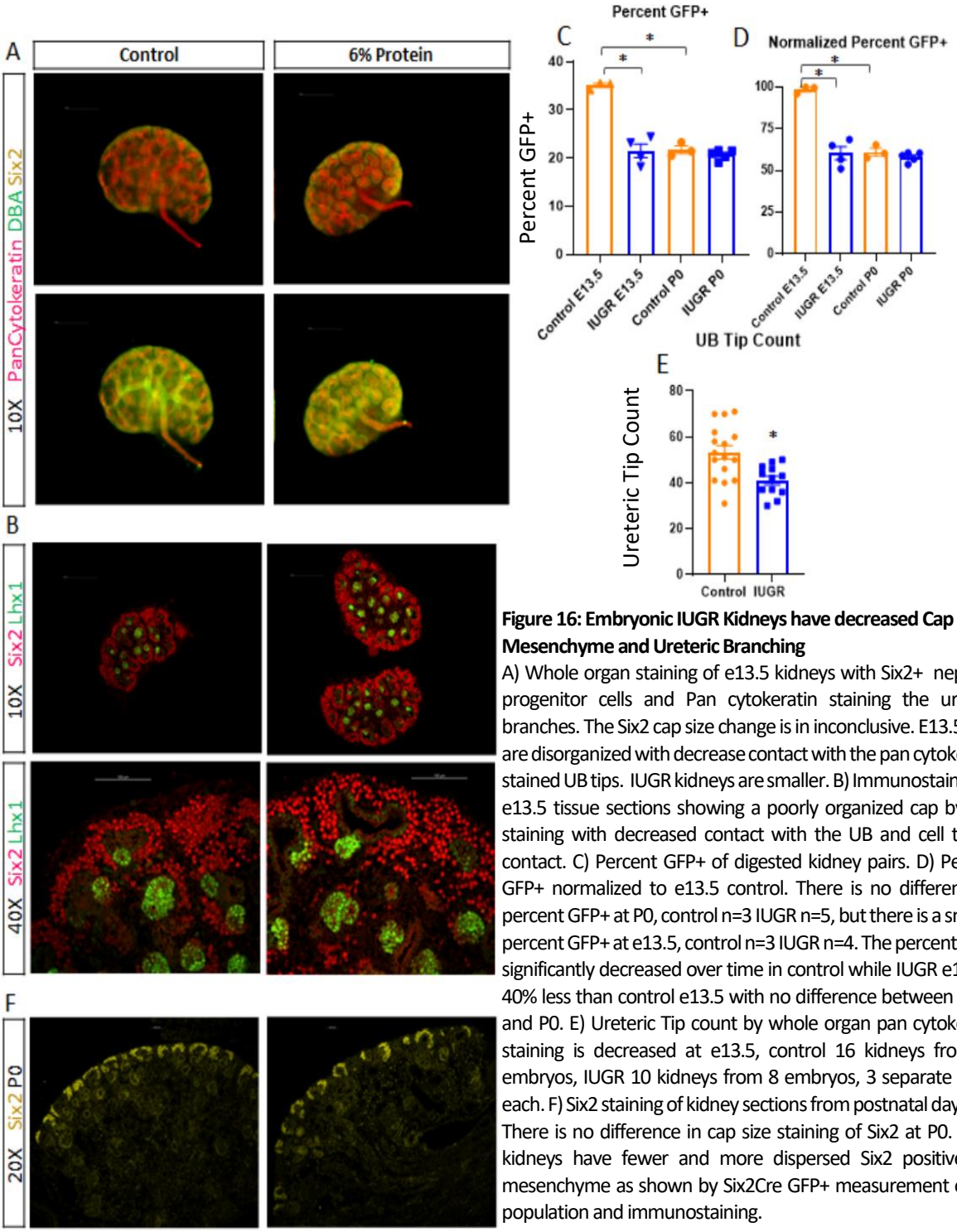

Figure 16: Embryonic IUGR Kidneys have decreased Cap Mesenchyme and Ureteric Branching

A) Whole organ staining of e13.5 kidneys with Six2+ nephron progenitor cells and Pan cytokeratin staining the ureteric branches. The Six2 cap size change is in inconclusive. E13.5 CMs are disorganized with decrease contact with the pan cytokeratin stained UB tips. IUGR kidneys are smaller. B) Immunostaining of e13.5 tissue sections showing a poorly organized cap by Six2 staining with decreased contact with the UB and cell to cell contact. C) Percent GFP+ of digested kidney pairs. D) Percent GFP+ normalized to e13.5 control. There is no difference in percent GFP+ at P0, control n=3 IUGR n=5, but there is a smaller percent GFP+ at e13.5, control n=3 IUGR n=4. The percent GFP+ significantly decreased over time in control while IUGR e13.5 is 40% less than control e13.5 with no difference between e13.5 and P0. E) Ureteric Tip count by whole organ pan cytokeratin staining is decreased at e13.5, control 16 kidneys from 10 embryos, IUGR 10 kidneys from 8 embryos, 3 separate litters each. F) Six2 staining of kidney sections from postnatal day zero. There is no difference in cap size staining of Six2 at P0. E13.5 kidneys have fewer and more dispersed Six2 positive cap mesenchyme as shown by Six2Cre GFP+ measurement of cell population and immunostaining.

3.2b Impact of IUGR on NPC and Nephrogenesis:

Six2 is a transcription factor that regulates the self-renewal and maintenance of the multi-potent NPCs that will differentiate into the nephron. Six2 inhibits the Wnt/β-catenin differentiation signal while activating CM maintenance signals including Osr1, Pax2, and Six2 while signaling the branching of the UB (Katsu et. al. 2012, Barak et. al. 2005, Fleming et. al. 2013). Individual CMs were not changed in IUGR at P0 based on Six2 staining. Six2 did show changes to the overall kidney structure at P0. The smaller IUGR kidneys at low magnification have CMs that are more diffuse along the cortex of the kidney with space between CMs (Figure 15 A). The diffuse caps along the cortex could be evidence of changes to branching in the IUGR kidney.

Sall1 is expressed in the NPC and the differentiated structures of the CM including the pre-tubular aggregate, (RV), CSB, and SSB. Sall1 is activated by Wt1 and is active in the initial UB growth into the metanephric mesenchyme and the successive branching of the UB (Kanda, S., Tanigawa, S., Ohmori, T., Taguchi, A., Kudo, K., Suzuki, Y., Sato, Y., Hino, S., Sander, M., Perantoni, A. O., Sugano, S., Nakao, M., & Nishinakamura, R., 2014). Sall1 expression domain appears smaller, and the staining less intense in IUGR kidney sections (Figure 15 B). The Sall1 transcription factor is required for CM maintenance, UB branching, but not for differentiation Nishinakamura, R., & Takasato, M., 2005).

Neural cell adhesion molecule (NCAM) stains similar cell populations of the kidney as Sall1 marking the CMs and remaining during the mesenchymal to epithelial transition as NPCs differentiate. NCAM is a glycoprotein present on the surface of cells acting as a cell-to-cell adhesion molecule. It is present in development playing a role in cell movement and arrangement during morphogenesis and development (Lackie, Zuber, & Roth, 1990). NCAM staining in the CM was consistently decreased in IUGR kidneys despite the obvious presence of the CM based

on structure and staining of the animals. The loss of NCAM occurred with or without the loss of staining by the lectin DBA which marks the distal tubule by binding the glycosylated protein α-linked N-acetyl galactosamine (Figure 15 C). The tumor suppressor gene and transcription factor Wilm's Tumor 1 (Wt1) is active in the metanephric mesenchyme during the invasion of the UB at the start of kidney development. It activates NPC maintenance signals of Sall1, Pax2, and Bmp7 and the proliferation pathway MAPK/PI3K through FGF16/20. Wt1 is active during differentiation and will regulate differentiation pathways. Wt1 staining at P0 will mark the CM and the differentiated podocyte in mature nephrons (Motamedi et. al. 2014, Nishinakamura, R., & Takasato, M., 2005). The IUGR CM shows decreased Wt1 staining despite the clear presence of defined CMs by the also decreased NCAM co-stain. The low Wt1 is present with IUGR kidneys that show a loss of DBA in the distal tubules (Figure 17 D). The lectin DBA which marks the distal tubule by binding the glycosylated protein α-linked N-acetyl galactosamine (Lackie et. al. 1990).

3.2c Changes in Differentiation Markers Result in Altered Physiology at P0:

Lotus tetragonolobus lectin (ltl) marks the proximal tubules of the kidney by binding α-linked L-fucose containing oligosaccharides. It then marks differentiated and formed structures of the adult kidney (Yallowitz et. al. 2011). IUGR had decreased ltl staining showing fewer

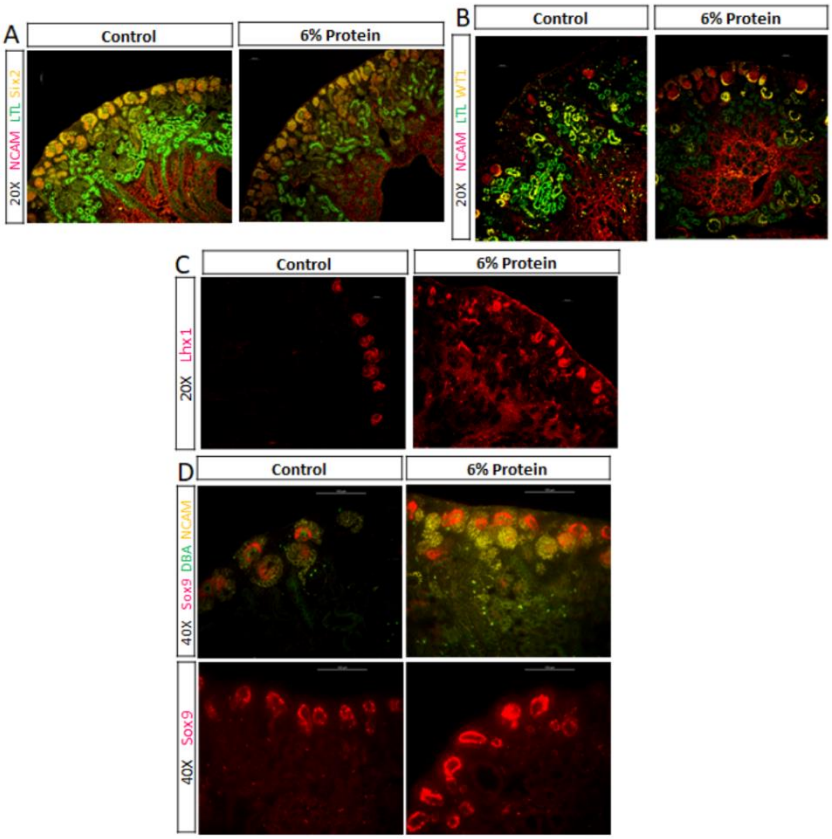

Figure 17: Markers of differentiation and mature glomerular structures at P0:
A) The diffuse cap mesenchymes (CM) are shown by Six2 and NCAM staining with less proximal tubules in IUGR. Control n=10, IUGR n=11. B) The LTL staining for proximal tubules is low in multiple animals along with decreased Wt1 staining for the precursors for the proximal tubules renal vesicle (RV) and comma shaped body (CSB). Control n=8, IUGR n=11. C) Lhx1 marks the nascent nephrons. IUGR has fewer Lhx1+ nascent nephrons that are smaller, and less organized. Control n=6, IUGR n=6. D) Sox9 stains the ureteric tip cells and the interstitial cells of the s-shaped body (SSB). NCAM stains the CM, the RV, and the SSB. DBA stains the ureteric branches (UB). The ureter remains with loss of DBA staining as shown by Sox9 in the tip cells. Sox9 shows more intense staining in the UB tip cells and disorganization of the SSB. Control n=6, IUGR n=6.

proximal tubules (Figure 18 A-B). Proximal tubules form from the epithelialized NPCs. Figure 18B shows low NCAM and Wt1 in the CM with decreased Wt1 positive podocytes and weakly stained and fewer proximal tubules. IUGR nascent nephrons are decreased in number and size by Lhx1 staining (Figure 17 C). IUGR produces disorganized nascent nephrons. The Lhx1 transcription factor is required for the formation of nephrons during development and is under the regulation of Wnt9b from the UB (Cirio e.t al. 2011). IUGR shows changes to the CM and differentiating structures from the CM at P0 that can lead to changes in the adult kidney in the form of structural deficiencies.

Unlike the CM where markers are altered but the CM is unchanged in presence or organization the differentiating structures showed molecular, organizational, and physiological changes. Early markers of differentiation show nascent nephrons, RVs, CSBs, and SSBs are disorganized, smaller, and fewer. This led to a deficit in differentiated structures as shown by decreased in proximal tubules.

3.2d Expression of Ureteric Markers in P0 IUGR Kidneys:

Overall IUGR P0 kidneys have all the structures of ureteric branching with no clear change in the amount and structure of collecting ducts. AQP2 is a water transporter on the surface of principal cells of the collecting duct. Low and high magnification images showed no changes to the presence of AQP2 within the collecting ducts or the amount of collecting duct of the IUGR P0 kidneys (Figure 18 A, C, D). However, AQP2 localizes to the apical membrane and in IUGR it was instead diffuse within the cell (Monzani et. al. 2009) [Brown, D. (2017)]. Diffuse CMs along the cortex shown by Six2 staining is often due to decreased branching of the UB. The diffuse Six2 CMs along the cortex of the kidney with normal AQP2 structures show that while the organization of the CMs at the UB tips has been changed the formation of collecting ducts had not been (Figure 18 A).

E-cadherin is a calcium dependent adhesion molecule present in the distal tubules (Lee et. al. 2013). Figure 18B shows loss of DBA staining with E-cadherin staining present showing a loss of DBA while distal tubule structures are maintained. Figure 18 C confirms normal distal tubule and collecting duct development in IUGR by E-cadherin and AQP2 staining. Pan cytokeratin also marks the collecting ducts of the kidney. Figure 18 D shows no change to the

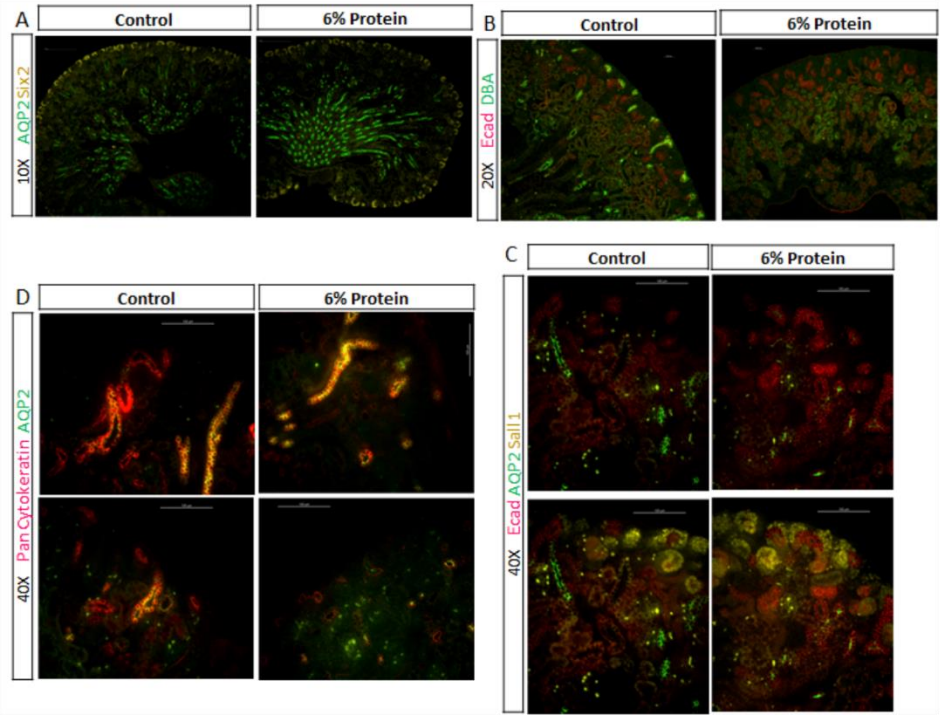

Figure 18: Normal Ureteric Tree Branching:
A) Shows the normal pattern of collecting duct forming in the smaller IUGR kidney by AQP2 staining of the principal cells of the collecting duct. Control n=5, IUGR n=5. B-C) E-cadherin and DBA mark the distal tubules. Even with loss of DBA E-cadherin and distal tubule staining is unchanged in IUGR. Control n=12, IUGR n=16. D) Pan Cytokeratin marks the collecting ducts of the kidney, AQP2 marks the principal cells of the collecting ducts Control n=12, IUGR n=12. Both are unchanged in IUGR. The collecting ducts show normal cell patterns.

collecting ducts in overall structure or in the presence of principal cells of the collecting duct. At P0 the ureteric branching of the kidney is not changed in the smaller IUGR kidneys.

The branching and structures of the collecting duct are not changed in IUGR kidneys at P0, but the UB tip cells are changed. Sox9 is a transcription factor present in the UB tip cells and the intermediate and distal domains of the SSB (Reginensi, A., Clarkson, M., Neirijnck, Y., Lu, B., Ohyama, T., Groves, A. K., Sock, E., Wegner, M., Costantini, F., Chaboissier, M.-C., & Schedl, A., 2011). As shown in Figures 18 A-D Sox9 staining appears qualitatively higher in IUGR P0 kidneys at the UB tips and in the SSB (N control=2; N IUGR=3). IUGR UB tip cells were changed in immunostained e13.5 sections and whole mount, combined with at e13.5. The overall UB tree at e13.5 stained by pan cytokeratin did not show

macroscopic changes to the UB branching, but the UB tip number is significantly decreased (Figure 16 A & E). The IUGR e13.5 kidney also had prominent ampullae formed (Figure 16 B). UB tip development cycles through a t-tip then either into two ampullae or a tri-tip. These have implications for the UB tree formation and for the appearance and organization of the CM. A t-tip has two UB tip ends surrounded by a cloud of continuous NPCs from 1 CM, while the two ampullae have two UB tip ends extending with their own distinct CMs surrounding them. The e13.5 characterized by Short et. al. 2014 showed almost half the number of ampullae as T-tip and Tri-tip with the number and proportion of ampullae increasing over development (Short, K.M., Combes, A. N., Lefevre, J., Ju, A.L., Georgas, K.M., Lamberton, T., Cairncross, O., Rumballe,. B.A., McMahon, A.P., Hamilton, N.A., Smyth, I.M., Little, M.H., 2014). The sectioned IUGR e13.5 staining showed more ampullae than control. The increased ampullae could be impacting the elongation step of UB development and be the reason for the significantly less UB tips counted in whole mount e13.5 IUGR kidneys (Figure 16 E). The IUGR UB having elongation rather than branching changes would explain the normal levels of pan cytokeratin, Aqp2, E-cadherin, and calbindin at e13.5 and P0 with smaller kidneys (Figures 16B, 18A-D, & 19D). Further evidence for the changes in UB tips and elongation are the smaller IUGR kidneys at e13.5 and P0, and the higher staining for UB tip cell marker Sox9 (Figure 17D & 18 A-D).

3.2e Expression of Stromal Markers:

The renal stroma cells are a heterogenous cell population present in the cortex surrounding the CMs and through the medulla. Meis1/2/3 marks the stroma cells that provide structure to the kidney while crosstalk signals with the NPCs of the CM maintain NPC stemness. Stroma cells of the kidney are derived from the same metanephric mesenchyme that gives rise to the NPCs. Stroma cells will give rise to glomerular mesangial cells, pericytes, and vascular smooth muscle cells and vasculature in the adult kidney (Chang-Panesso, M., Kadyrov, F. F., Machado, F. G., Kumar, A., & Humphreys, B. D., 2018). Stroma in the IUGR P0 kidney was unchanged from control with similar thickness of the stroma around the CM (Figure 20).

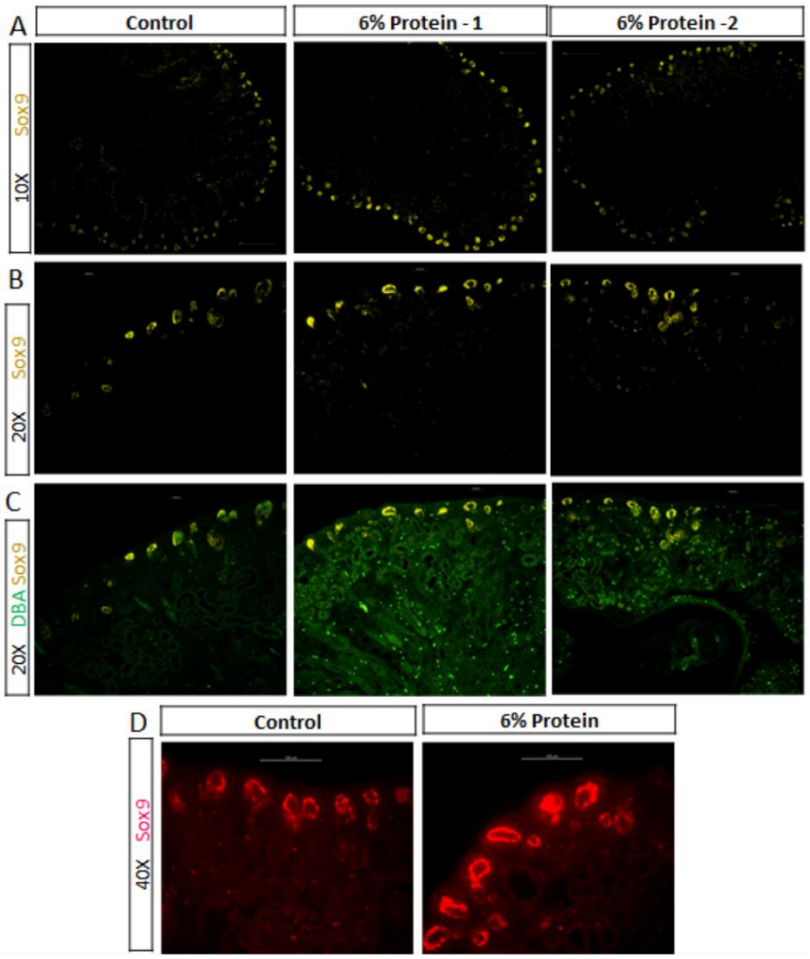

Figure 19: Ureteric Branching Tip Cells:
A-B) Consistent high Sox9 staining in the UB tip cells of IUGR kidneys at P0. Control n=6, IUGR n=6 C) Loss of DBA has no impact on intensity of Sox9 staining.

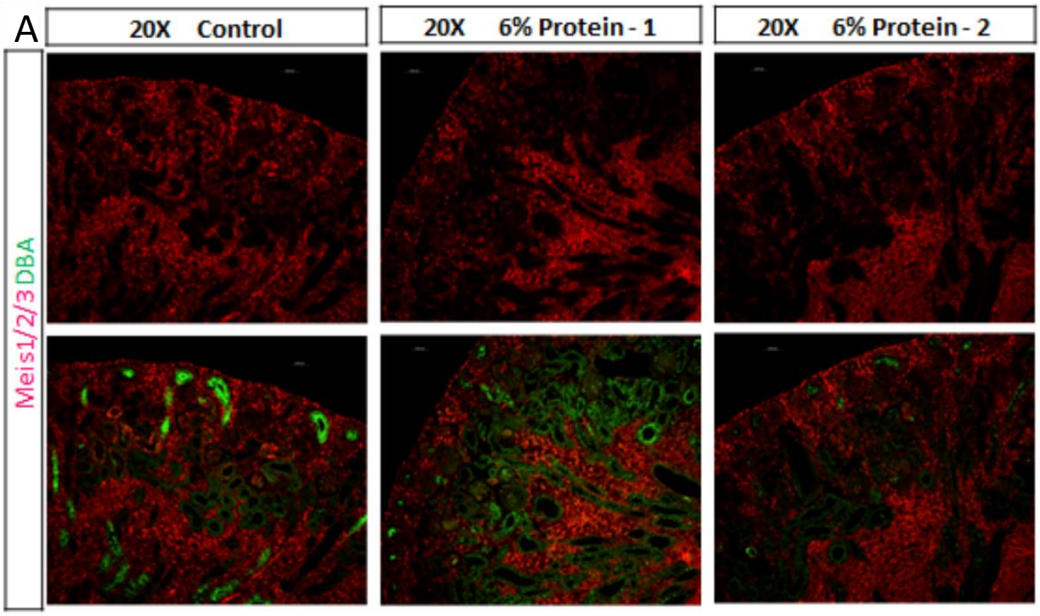

Figure 20: No Change in Cortical Stroma thickness:
Meis1/2/3 staining for the stroma cells of the kidney shows no change in stroma around the cap mesenchyme (CM). There is no thinning or decrease in stroma cells around the CMs.

3.2f Proliferation and Apoptosis in P0 IUGR Kidneys:

Bromodeoxyuridine (BrdU) is an analog for of the nucleotide thymidine. Tissue or cells will take up BrdU and integrate it into the DNA of replicating cells. BrdU can then be immunostained in fixed tissue to identify replicating cells (Muskhelishvili, L., Latendresse, J. R., Kodell, R. L., & Henderson, E. B., 2003).

By co-staining with markers of regions of interest proliferation rates can be found for cell types (Muskhelishvili et. al. 2003). Four control and three IUGR mice were stained and only CMs and nascent nephrons from above a branched UB were counted. The UB tips counted were also always branched. At least 10 unique regions of the sectioned kidneys were counted per animal. Six2, Sall1, and Calbindin was stained in consecutive sections of the kidney. Proliferation in Six2+ stained CM is decreased in IUGR at P0 when looking per CM across animals or per animal. The average number of proliferating cells is decreased by a third in IUGR Six2+ CMs. This is shown when looking per CM measured and when averaged by animal. The

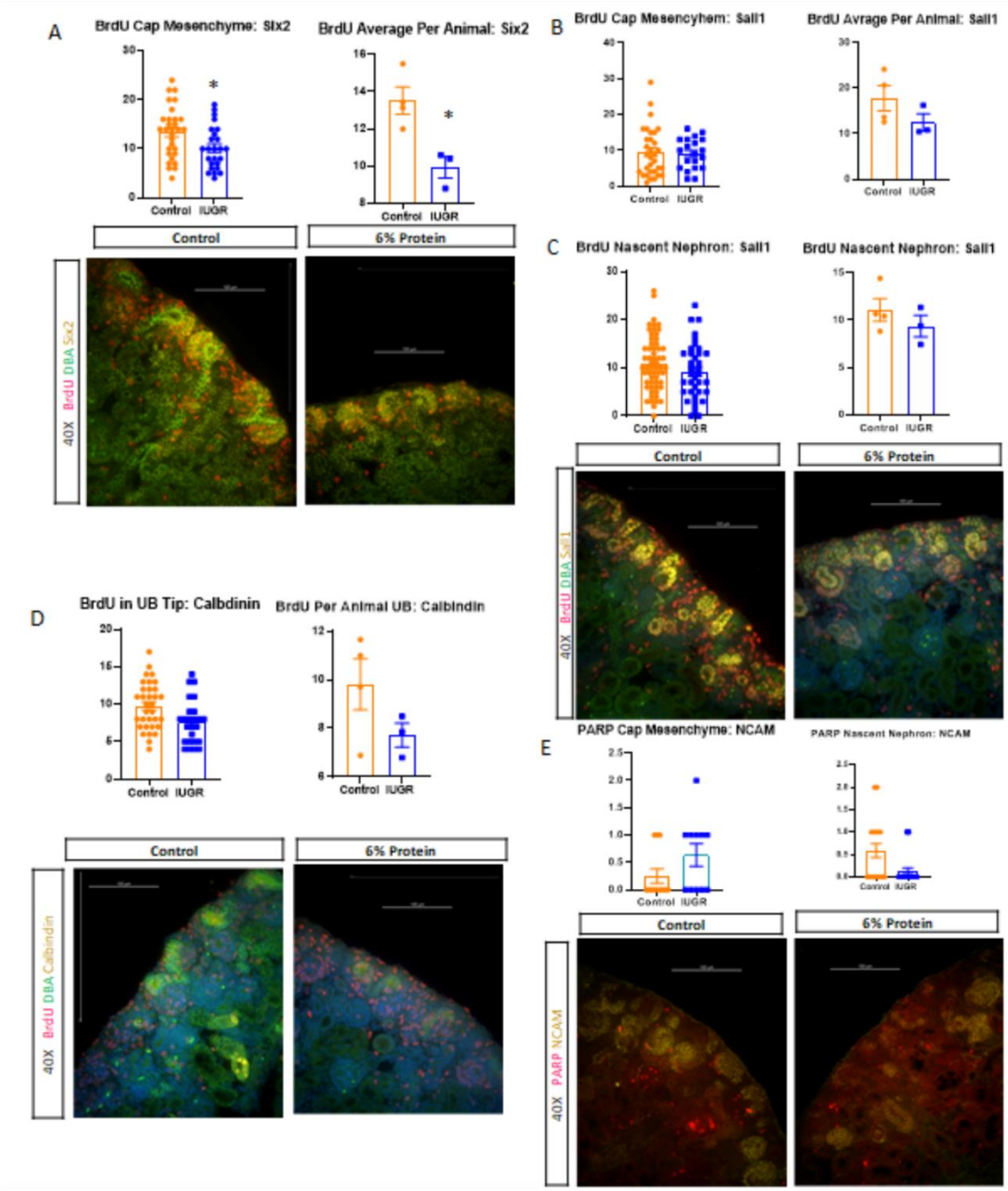

Figure 21: Decreased proliferation in IUGR Six2+ Cap Mesenchyme

A) Decreased replication in the cap mesenchyme by BrdU positive cells in Six2 staining. Co-staining of BrdU for proliferating cells, Six2 for the cap mesenchyme, and DBA for the ureteric branching. B) No change in cap mesenchyme based on Sall1 marked cap mesenchyme. Staining shows BrdU marking proliferating cells, Sall1 marking the cap mesenchyme and the nascent nephrons, and DBA marking the ureteric branching. C) Sall1 marked nascent nephrons has no change in replication. D) Calbindin marked UB tips has no change in replication. Calbindin marks the ureteric branching, DBA marks the ureteric branching, and BrdU marks the proliferating cells. E) PARP marker for apoptosis shows no change in NCAM marked cap mesenchyme or nascent nephrons. BrdU control n=4, IUGR n=3. PARP n=2 for control and IUGR.

IUGR animals used all showed a loss of DBA staining (Figure 21 A). Sall1+ CMs show a trend towards a decrease in proliferation, but it is not significant when looking per CM or per animal. The Sall1 staining for RVs was selected separately and showed no change in proliferation with no trend when looking per nephron. There was a slight trend in decreased proliferation when looking at average per animal per nephron (Figure 21 B-C). The Sall1 RV showed a greater range in proliferation rates compared to the CM. Calbindin marks the ureteric branching of the kidney. The tips of the UB were selected for counting and showed no significant change in proliferation, but there was a trend towards less proliferation in IUGR P0 UB tips (Figure 21 D).

Poly (ADP-ribose) polymerase (PARP) is related to DNA repair, genomic stability, and apoptosis. Here it was used as a marker for apoptosis in the CM and the nascent nephron based on co-staining with NCAM (Muskhelishvili et. al. 2003). IUGR kidneys had no significant change in PARP in the CM or nascent nephron. PARP remains a rare event as shown by the number of control and IUGR kidney fields that had no PARP present in the counted area. There is a trend towards increased apoptosis in the CM and a decrease in the nascent nephrons. The lack of significance might be due to the small sample size of only two control and two IUGR (Figure 21 E).

In summary, NPC, different structures of the nascent nephron, stromal and ureteric components are present in IUGR kidneys. However, decrease in NPC number and fewer nascent nephrons may explain the nephron deficit observed at birth. Maintenance, proliferation, differentiation, and morphogenesis signals have been downregulated.

3.3 RNA-Seq Results:

Three independent P0 control and IUGR RNA samples from MACS isolated NPCs were sequenced on Illumina-HiSeq 2500 platform. Despite low RNA concentrations for 1 control and

1 IUGR sample all were useable for sequencing (Figure 22 A-B). Figure 18C shows samples had between 57 and 67 million with read lengths of 302 base pairs, with the mouse genome being 2.5 x 10^9 bp the samples have a read depth of 8-10X for the 3 control and 3 IUGR RNA samples. Figure 22 D is the Principal Component Analysis (PCA) on the RNA-seq samples. PCA simplifies large data sets into smaller components that retains the components of the full data sets. First the data was standardized so that high value items do not dominate the analysis. For RNA-seq this would be a handful of genes with fold changes in the hundreds being given more weight than hundreds of genes with fold changes below 20. Then the covariance matrix was calculated to determine how variables of the data sets are related to each other, principal components are then calculated to determine the similarity and difference of data sets. The data sets were aligned to mouse genome mm10 and analyzed twice for differential expression.

The first analysis was done by STAR aligner and produced 6,036 differentially expressed genes all with a $p<0.05$. It has 1,694 genes increased by 1.5 or more-fold in IUGR NPCs, 2,114 with a fold change increased or decreased by less than 1.5 but more than 1.005, and 2,228 decreased by more than 1.5-fold in the IUGR NPCs (Figure 22). The genes that are increased or decreased by 1.5-fold or more were then run through Ingenuity Pathway Analysis (IPA) (Supplemental Table 1). IPA by QIAGEN bioinformatics analyzes omics data to arrange it into

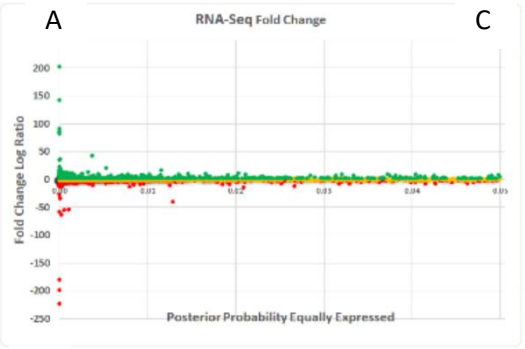

C

All Above Background Signal	Number of Genes
Up-Regulated Greater Than +1.5 Fold Change	1,694
Between -1.5 and 1.5 Fold Change	2,114
Down Regulated Greater Than -1.5 Fold Change	2,228
Total	6,036

B

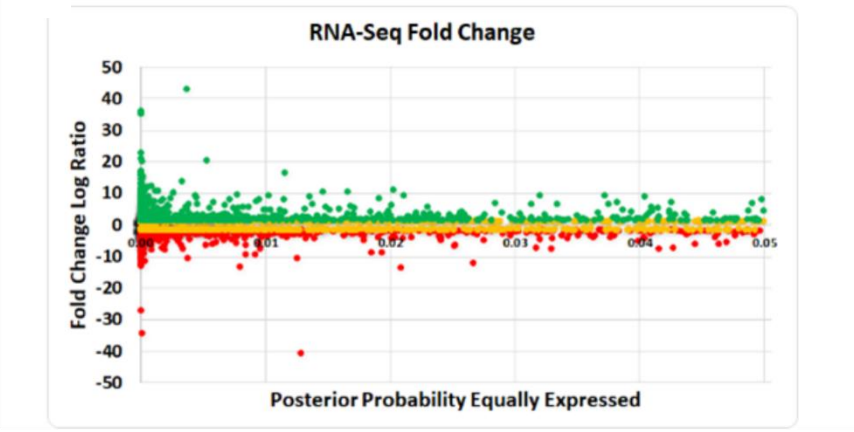

Figure 22 RNA-Seq Differential Expression STAR Aligner:
With a p<.05 there were 6,036 differentially expressed sequences with statistical significance. Of those 1,694 had a fold change of +1.5 or greater show as green dots, 2,114 had a fold change of -1.5 of greater shown as red dots, and 2,228 had a fold change between +1.5 and 1.0001 and -1.5 and -1.0001, shown as yellow dots. All are significant changes. Those up or down regulated by 1.5-fold or more were put into Ingenuity Pathway Analysis (IPA). A) Shows all 6,036 points, B) Y-axis decreased cutting off the 11 points with the largest change. C) Accounting for all points. 28% Upregulated ≥ 1.5, 36.9% are downregulated ≥1.5, 35% are > -1.5 and <1.5, but all 6,036 points are statistically significant.

biological pathways and predict upstream regulators, and downstream outputs including diseases based on published data and biological relationships.

IPA related the 3,992 genes up or down regulated by 1.5-fold as related to diseases and biological functions, regions of the cell, top canonical pathways, predicted causal networks, and predicted upstream regulators based on IPA curated databases and published data. IPA analysis shows development has been altered in the IUGR P0 NPCs. Figure 23 A shows the top diseases and biological functions changed. Diseases and biological functions come from categories of molecular functions from the differentially expressed RNA-seq IPA analysis. Disease and abnormalities at 34% were the most common category with cancer and inflammation the most common subcategories of diseases and

abnormalities. Cell survival was next at 25% of categories including markers of necrosis, cell survival, and apoptosis. Necrosis and apoptosis categories were both up and down regulated in IUGR P0 NPCs. Development and morphology were 19% of categories including proliferation, tissue organization, translation, transcription, and post-translational modification. Cell adhesion and migration represented 14% of categories coming from cell to cell contact and signaling, cell migration, and cell movement of endothelial, epithelial, and mesenchymal cells. Cell adhesion and migration categories decreased in IUGR. Adhesion and migration are related to NPC differentiation as NPCs induced into differentiation migrate out of the CM and condense as they

A

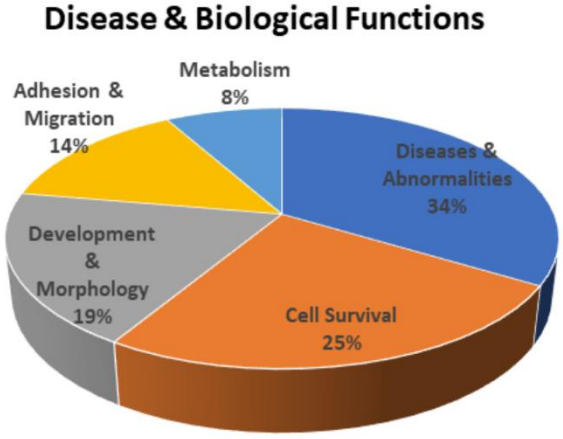

B

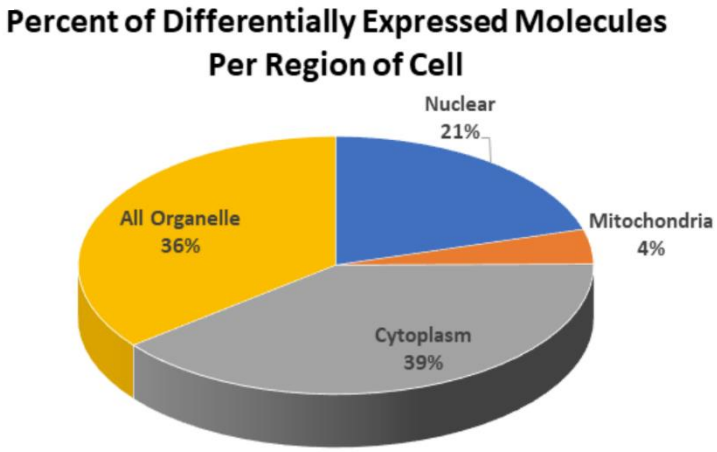

Figure 23 RNA-Seq Differential Expression IPA:
A) The 3,992 genes that are up or downregulated by 1.5-fold or more are associated with cell survival, development and morphology, adhesion and morphology. Adhesion and Migration is of note due to the migration and condensing of epithelizing NPCs when they differentiate. Disease and abnormalities are mostly cancers meaning pathways are developmentally related as well. The dependence of NPCs on glycolysis and shift to oxidative phosphorylation as they age shows that all parts are related to development. B) Parts of the cell with significantly changed RNA expression. The changes are from throughout the cell.

Table 2: Predicted Top Canonical Pathways differentially expressed RNA-seq NPCs by IPA

Top Canonical Pathways	P-Value
EIF2 Signaling	5.95E-19
mTOR Signaling	1.27E-08
Regulation of eIF4 and p70S6K Signaling	4.13E-06
TNFR1 Signaling	8.19E-05
Glycolysis I	9.01E-05

Table 3: Predicted Top Causal Networks from differential expression in NPCs by IPA

Causal Networks	Biological Role	Predicted Activation
MYCN	Proto-oncogene/Development. Transcription dysregulation	Activated
NUPR1	Transcription dysregulation	Activated
SERPINH1	Heat Shock protein 47, Cell Proliferation	Inhibited
Alpha Catenin	Cytoskeleton and Cell polarity	Activated
AMBRA1	Cell senescence and mitophagy	Inhibited

Table 4: Predicted Top Upstream Regulators from RNA-seq differential expression in NPCS by IPA

Top Upstream Regulators	Biological Role	Predicted Activation
MYCN	Proto-oncogene/Development Transcription dysregulation	Activated
POLG	Mitochondrial Polymerase	
NUPR1	Transcription Regulator	Activated
Alpha Catenin	Cytoskeleton and Cell polarity	Activated
RRP1B	Ribosomal RNA processing, Serine/Threonine associated	

epithelize and differentiation. Metabolism contains 8% of categories including carbohydrate metabolism, post-translation related biochemistry, and amino acid metabolism. All categories related to nephron development. Figure 23 B shows changes to molecules located throughout the cell meaning the cytoplasm, nuclease, mitochondria, and organelles.

Top canonical pathways by IPA are predicted to be changed based on the significantly changed RNAs in the RNA-seq differential expression analysis. Table 3 shows the top 5 predicted pathways. Eukaryotic initiation factor 2 or EIF2 signaling regulates the inflammatory

and cytokine response of cells. The 88 molecules changed in the EIF2 signaling pathway includes kinases, transcription and translation regulators, and several ribosomal proteins. mTOR signaling is a central regulator of metabolism, growth, proliferation, and survival. The pathway is targeted in cancer treatment and is associated with diabetes. The 63 molecules changed identified by IPA as associated with mTOR are ribosomal proteins, AKT3, DNA damage response, translation factors, and vascular endothelial growth factors C & D. Regulation of eIF4 & p70S6 kinase is part of the control of translation. It responds to stress, energy balance, hypoxia, hormones, and growth factors. It is regulated by signals from mTORC1, Wnt, and PI3K/AKT. There are 47 molecules identified by IPA as associated with regulation of eIF4 & p70S6 kinase. Among the 47 molecules are several ribosomal proteins, AKT3, a number of translation initiation factors, and insulin receptor substrates. Tumor necrosis factor 1 or TNFR1 signaling

A

Symbol	Entrez Gene Name	Expression Fold Change	Location	Type(s)
ENO1	enolase 1	2.119	Cytoplasm	enzyme
ENO2	enolase 2	3.084	Cytoplasm	enzyme
GAPDH	glyceraldehyde-3-phosphate dehydrogenase	2.577	Cytoplasm	enzyme
GPI	glucose-6-phosphate isomerase	1.844	Extracellular Space	enzyme
PFKL	phosphofructokinase, liver type	2.153	Cytoplasm	kinase
PFKP	phosphofructokinase, platelet	1.706	Cytoplasm	kinase
PGAM1	phosphoglycerate mutase 1	1.672	Cytoplasm	phosphatase
PGK1	phosphoglycerate kinase 1	2.152	Cytoplasm	kinase
PKM	pyruvate kinase, muscle	2.234	Cytoplasm	kinase
TPI1	triosephosphate isomerase 1	2.064	Cytoplasm	enzyme

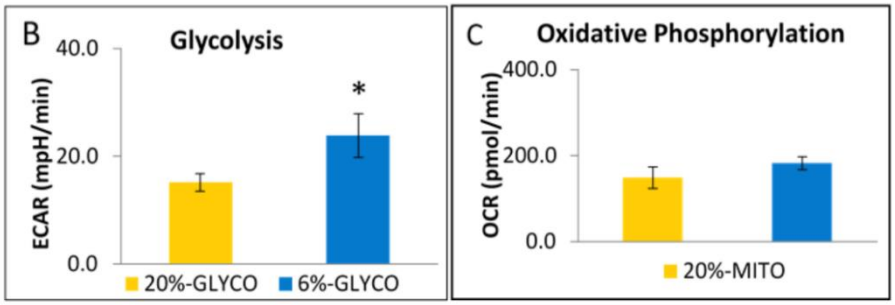

Figure 24 Glycolysis Increased in IUGR P0 Nephron Progenitor Cells: A) Top molecules changed glycolysis by RNA-seq analysis of MACSs isolated P0 nephron progenitor cells (N{PC). Multiple glycolytic enzymes have increased expression in IUGR NPCs leading to glycolysis being a top pathway changed as predicted by IPA and iPathway. B) Seahorse extracellular Flux measurement shows increased glycolysis in MACs isolated NPCs. By ECAR or extracellular acidification rate. C) Seahorse measurement of OCR showing no change in oxidative phosphorylation. N=2 litters for Seahorse.

affects inflammatory response impacting lipid metabolism, coagulation, insulin resistance, and endothelial function. TNFR1 signaling can be for both cell survival and cell death. There were 19 molecules changed in TNFR1 signaling with several apoptosis factors heavily downregulated, and Jun proto-oncogene AP-1 is upregulated. Glycolysis I is a top canonical pathway and has multiple kinases upregulated. The increase in glycolysis is confirmed by measurement of extracellular acidification rate (ECAR) using the Seahorse XF analyzer (Figure 25 A and B). NPCs were isolated using MACs and passage 0 cells were cultured and the Seahorse XF analyzer measured the acidification of seahorse culture media. It showed a significant increase in glycolysis in IUGR NPCs at P0. Oxidative phosphorylation, measured by oxygen consumption rate or OCR, is unchanged in the same IUGR NPCs (Figure 25 C).

IPA predicts the top causal networks from the differentially expressed genes (Table 4). MYCN functions in development and transcription dysregulation and is a proto-oncogene. NUPR1 is a second network activated associated with transcription dysregulation. SERPINH1 is also knows as heat shock protein 47 and is active in cell proliferation and collagen biosynthesis. Alpha catenin is a linker protein that functions in the cytoskeleton and cell polarity. AMBRA1 is inhibited in IUGR NPCs and is active in cell senescence, mitophagy, and autophagy by regulating protein turn over. AMBRA1 relates to cell senescence and mitophagy and is involved in neural development.

Table 4 shows the IPA predicted top upstream regulators based on the pathways IPA predicts to be changed based on the differentially expressed RNAs. MYCN was again present as activated, as was NUPR1 and Alpha Catenin. Polymerase G or POLG is the polymerase active in

A

RNA-Seq Differential Expression Upregulated ≥1.5	RNA-Seq Differential Expression Downregulated ≥1.5
p53 Signaling Pathway	TNFR1 Signaling Pathway
mTOR Signaling Pathway	Mitochondria Apoptotic Signaling
Sonic Hedgehog Pathway	WNt/LrP6 Signaling
Oxidative Stress Induced Gene Expression Via Nrf2	Regulation of Pluripotency of Stem Cells
Glycolysis/Glucogenesis	P53 Signaling Pathway
FOXO Signaling Pathway	

B

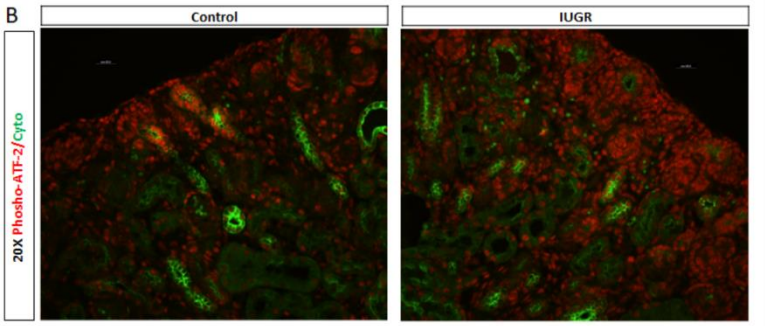

Figure 25 RNA-Seq Differential Expression Up and down regulated ≥1.5:
A) The 1,694 upregulated genes previously used in IPA were uploaded into The **D**atabase for **A**nnotation, **V**isualization and **I**ntegrated **D**iscovery (**DAVID 6.8**) resulting in 1,354 DAVID IDs. The pathways found were P53 Signaling pathway, mTOR signaling pathway, Glycolysis/Glucogenesis, FOXO Signaling Pathway, Sonic Hedgehog Pathway, Oxidative Stress Induced Gene Expression Via Nrf2. B) Phospho-ATF2: stress marker upregulated by immunostaining of P0 tissue at 40X. N=3 for staining.

mitochondria during mitochondrial replication. POLG is known to interact with TP53-inducible glycolysis and apoptosis regulator (TIGAR) and superoxide dismutase 2 (SOD2). TIGAR is a regulator of glycolysis, DNA repair, and cellular degradation of organelles. SOD2 clears reactive oxygen species form mitochondria and is active in oxidative stress and apoptosis. RRP1B is a serine/threonine associated with ribosomal biogenesis. RRP1B is also a transcription factor cofactor for apoptotic signals in response to DNA damage.

There were no molecules that are present in all five top canonical pathways from IPA analysis and none of the predicted upstream regulators are present in all five top canonical pathways. Glycolysis I contained the most unique molecules altered with no shared molecules present in the other 4 top canonical pathways. It does contain the upstream regulators of GPI and

PKM. EIF2 signaling, mTOR pathway, and regulation of eIF4 & p70S6 kinase pathway had the most similarity with over 40 identical molecules changed in all three pathways, most of which are ribosomal proteins. All three also contain the IPA predicted upstream regulators of EIF3E, IRS1, PIK3CG, and PIK3R1. The only duplicated molecule between the TNFR pathway and EIF2 is the upstream regulator XIAP. TNFR also contains the upstream regulators of FADD, JUN, MAP2K4, and MAP3K1. This shows that the top canonical pathways were not driven by the same molecular changes.

The Database for Annotation, Visualization, and Integrated Discovery (DAVID 6.8) is an analysis tool for functional annotation of large biological data sets. It provides functional interpretation based on large data sets. The uploading tool for DAVID allows only for gene lists, not expression level data unlike IPA analysis. DAVID analysis was done by splitting the significant data by up or down regulation (Figure 26 A). The previously identified 1,694 genes upregulated by RNA-seq were analyzed by DAVID (Supplemental Table 1, Figure 25).

There were six pathways identified from upregulated RNA genes shown in Figure 18A. P53 signaling pathway is a tumor suppressor that controls cell cycle progression and apoptosis. It has previously been described as a control mechanism for cell proliferation in first cancer and then development. Normal p53 function is required for normal embryonic development and balancing NPC differentiation and self-renewal with links to cellular metabolism. P53 was found by DAVID analysis of both down and up regulated genes. mTOR signaling is present again. Sonic hedgehog pathway was not in the IPA analysis but present from DAVID. Sonic hedgehog pathway is a developmental pathway that regulates tissue patterning during multicellular organisms, the formation of complex organs including the kidney, and cell polarity. Oxidative Stress Induced Gene Expression Via Nrf2 is a stress response pathway. Nrf2 signaling is related

A Wnt Differentiation Signal Decreased

	6% NPCs			20% NPCs		
Gene Name	TPM	TPM	TPM	TPM	TPM	TPM
Wnt9a	0.48	1.07	0.84	1.63	1.95	1.35
Wnt11	5.49	27.2	9.25	9.4	17.07	7.96
Wnt5a	0.66	0.86	1.82	2.96	4.32	4.05
Wnt16	0.73	0.77	2.33	2.55	2.78	1.98
Wnt5b	7.01	5.3	10.61	19.18	16.46	15.79
Wnt4	89.11	125.36	100.15	131.24	144.18	110.95
Wnt8b	0.18	0.12	0.36	3.39	3.22	3.44

B BMP Proliferation Decreased

	6% NPCs			20% NPCs		
Gene Name	TPM	TPM	TPM	TPM	TPM	TPM
Bmp7	43.55	49.92	56.66	82.63	90.23	64.77
Bmp4	13.11	13.87	23.81	37.6	43.53	43.07
Bmp1	109	142.65	92.17	134.55	162.01	141.28
Bmp2	9.8	9.03	8.73	17.48	18.13	17.93
Bmp3	0.62	0.51	1.6	2.91	4.96	2.62
Bmp2k	11.68	10.09	10.61	7.6	8.04	7.98
Bmp6	4.92	4.89	7.25	7.29	6.77	7.44

C Fgf Signal: NPC Maintenance Downward Trend

	6% NPCs			20% NPCs		
Gene Name	TPM	TPM	TPM	TPM	TPM	TPM
Fgf10	6.22	10.65	9.54	13.2	12.74	10.33
Fgf9	2.57	0.53	4.68	6.87	4.34	5.61
Fgf8	29.42	11.31	39.32	48.49	41.58	50.69
Fgf20	0.69	4.22	2.05	6.96	11.84	5.47
Fgf1	22.99	24.2	35.57	39.87	56.66	30.17
Fgf2	0.42	1.81	1.92	3.37	4.32	2.34
Fgf11	3.43	2.66	5.02	2.95	3.49	3.45

D Histone Modification

	6% NPCs			20% NPCs		
Gene Name	TPM	TPM	TPM	TPM	TPM	TPM
Ezh1	24.66	23.36	42.01	29.46	39.85	35.54
Ezh2	54.06	39.96	94	118.27	112.65	118.65
Hdac5	115.94	128.91	114.97	48.25	54.56	58.74
Hdac2	113.91	114.19	132.85	181.6	171.06	168.6
Hdac7	62.92	69.93	48.83	52.67	55.17	54.39
Hdac3	62.19	66.72	65.96	81.55	79.24	78.33
Hdac4	11.97	12.31	10.86	11.52	11.67	11
Hdac1	111.6	116.27	113.39	123.87	129.57	99.13
Hdac6	27.68	39.02	31.97	37.68	48.54	35.39
Hdac11	16.61	17.33	17.58	17.44	19.94	19.62
Hdac10	9.96	8.44	11.64	11.03	11.83	11.04
Hdac8	5.48	5.88	7.05	6.84	8.63	8.05
Hdac4	12.61	13.57	9.51	11.11	12.21	9.91
Dnmt1	58.36	54.72	81.54	122.26	107.52	107.72
Dnmt3a	34.7	40.71	56.01	73.36	74.86	75.83
Dnmt3b	5.22	4.58	6.56	9.65	10.52	9.87
Sirt2	43.49	46.84	48.74	45.76	48.11	50.77
Sirt1	31.27	32.92	28.73	22.67	25.07	26.5
Sirt7	14.25	16.18	13.86	23.74	28.45	23.56
Sirt3	18.57	19.21	19.83	17.9	18.33	18.83
Sirt4	18.72	22.33	20.21	24.23	30.01	29.29
Sirt6	25.21	36.54	34.52	35.94	45.36	44.83
Sirt5	1.58	1.82	1.98	3.46	4.74	4.57
Trp53	79.24	71.06	133.47	180.9	195.87	193.6
Sin3a	33.88	26.79	47.5	53.59	53.67	65.67
Sin3b	101.65	102.06	109.91	116.4	126.14	110.34
Sap130	15.22	16.01	27.28	37.26	38.11	37.36
Ing1	41.5	53.8	55.43	55.39	56.74	59.8
Ing2	36.28	33.36	32.7	23.47	24.93	28.21
Mta1	151.35	146.62	161.21	157.88	158.3	155
Mta2	108.77	118.29	111.54	117.91	127.11	120.69
Mta3	34.61	40.91	42.59	41.39	38.53	41.53
Mbd1	26.69	31.42	27.97	31.51	34.56	37.2
Mbd2	48.08	50.73	57.32	75.06	75.35	78
Mbd3	173.22	169.04	174.68	238.85	233.94	223.56
Mbd4	4.33	5.69	7.17	10.34	11.56	11.63
Mbd5	22.57	26.95	17.14	17.68	21.06	19.75
Mbd6	100.75	98.62	61.87	66.93	88.72	76.92

Figure 26 RNA-seq TPM Trends:

Transcripts Per Kilobase Million (TPM) is normalized RNA read number. Highlighted yellow are significantly changed in differential expression analysis. Shows average for NPCs from the three control and IUGR litters used for RNA-seq analysis.

A) The Wnt differential signal is decreased. B) BMP proliferation signal is decreased. C) Downward trend in Fgf maintenance signal. D) Histone modification signals are changed. HDACs associated with NPC maturation are decreased and HDACs that are associated with NPC differentiation are decreased. Factors changed are related to acetylation, methylation, glycosylation, and chromatin remodeling. Many are significantly changed while others are trends in TPM levels.

to environmental and metabolic stress. Glycolysis is the enzymatic breakdown of glucose producing energy and pyruvic acid while glucogenesis is the formation of glucose from glycolysis products. FOXO signaling pathway regulates apoptosis, cell cycle, glucose metabolism, and oxidative stress resistance. A major down regulator of FOXO signaling is the activation of Akt/PI3K pathways via insulin or growth factor signaling. FOXO is activated by JNK and AMPK, which respond to energy availability and nutrient stress. The activity of these pathways is related to phosphorylation, acetylation, methylation, and ubiquitylation as post-translational modifications (Figure 25 A).

The 1,354 downregulated genes DAVID analyzed provided five pathways. TNFR1 signaling pathway was also present in the IPA results, confirming changes related to cell death and survival signaling, further confirmed by mitochondria apoptotic signaling. LrP6 is from the Wnt canonical pathway. Wnt canonical pathway feeds into β-catenin, a necessary part of NPC differentiation. Finally, the ability to maintain stemness is changed in the regulation of pluripotency of stem cells. The changes to cell stress are shown by staining of P0 tissue sections. There is an increase in Phospho-ATF2 throughout the kidney, but especially in the cap mesenchyme above the pan cytokeratin staining ureteric branching (Figure 25 B).

The sequencing data before differential expression analysis is shown as Transcripts Per Kilobase Million or TPM. TPM is calculated by read counts divided by the length of each gene in kilobases producing the RPK. The RPK values in a sample are counted up and divided by $1x10^6$ and then divide by a scaling factor to produce a TPM per gene for each sample. This provides a read number that is normalized by gene length. Looking at groups of genes related to development showed significantly changed genes and trends. Figure 26 A shows the differential signal Wnt trends down with three significantly decreased (Wnt5a, Wnt5b, and Wnt8b). The

NPC proliferation signal BMP has multiple molecules significantly down with more trending down without significance (Figure 26B). A second NPC maintenance signal Fgf trends down but with no molecules significantly changed (Figure 26C).

Previous work has shown that NPC differentiation and maintenance is regulated by the histone modification pathways HDAC and their co-factors. HDACs 1-4, 7, and 9 decrease with embryonic maturation. HDAC5, 6, and 8 are constitutively expressed, while HDAC1, 2, and 3 decrease with differentiation in NPCs and HDAC3 is high in podocytes. Histone modifications are known to respond to environmental factors. Figure 26D shows histone associated molecules. Ezh2 is significantly decreased along with Dmnt3a, and Dmnt3b. Ezh2 actively represses differentiation pathways. Hdacs 4, 5, and 7 were all significantly increased in IUGR P0 NPCs. HDACs act with transcription complexes Sin3, Mi-2/NuRD, Co-REST, and SMRT/N-CoR. HDAC/Sin3 complexes regulate cell proliferation, apoptosis, and cell cycle. Mi-2/NuRD is an ATP dependent complex that regulates chromatin remodeling. The Co-REST or RCOR1 complex is downregulated at birth and inhibits neural cell differentiation. SMRT/N-CoR complex is a repressor of cell checkpoint AP-1. The complexes share more components than just HDACs.

Sin3 histone deacetylase complex associated with HDAC 1 and 2, RBBP7 and 4, and SDS3. Sin3a was down regulated 1.27-fold and Sin3b was unchanged. The Sin3 associated growth inhibitor Ing2 is upregulated 1.63-fold. The Mi-2/NuRD complex includes Mta1 and 2 which were both significantly upregulated (1.29 and 1.2). The glycosylation associated Mbd4 was down regulated 1.49-fold with other Mbds trending down. Mbd3 was trending down in IUGR NPCs which inhibits induction of IPSCs. Multiple sirtuins were significantly changed

with IUGR. Sirt1 and 2 were both upregulated (1.62 and 1.27-fold), while Sirt7 is downregulated 1.30-fold while Sirt4-6 have no significant change are all trending down (Figure 26D).

The tumor suppressor gene Trp53 had a fold change of -1.59. Trp53, as previously described, is a link between embryonic development regulating NPC self-renewal and differentiation and metabolism. IUGR P0 NPCs also had significantly decreased Ezh2, Dnmt3a, and Dnmt3b and trending down with no significance were Ezh1 and Dnmt1 (Figure 26D). Ezh2 expression is associated with proliferation in the undifferentiated cells of the embryonic kidney. NPC maintenance and proliferation signals are significantly changed are known intermediaries between environmental signals and transcriptome regulation. This is evidence of changes t histone remodeling, glycosylation, metabolism, and NPC maintenance and differentiation in IUGR P0 NPCs.

The second analysis was by iPathway Guide Analysis. The alignment and differential expression analysis show 3791 differentially expressed genes all with $p<0.05$. There were 282 upregulated over 1.5-fold, 491 downregulated by 1.5-fold, and 3,018 genes statistically significant between -1.5 and +1.5-fold change (Figure 27). All significant genes were analyzed using the Kyoto Encyclopedia of Genes and Genomes (KEGG), Gene Ontology Consortium Database (GO), miRNA analysis from miRibase, and TARGETSCAN databases.

Gene Ontology or GO Analysis with highest FDR selected are in table 5. GO Biological process and molecular function analysis confirmed changes to metabolism and the ribosomal changes found in the IPA RNA-seq analysis. Cellular Macromolecule Metabolic Process are the chemical reactions that process macromolecules. Macromolecules are high molecular mass including proteins, glycoproteins, carbohydrates, polysaccharides, nucleic acids, and lipids. The processing includes metabolic, macromolecule biosynthesis, and methylation. Cellular metabolic

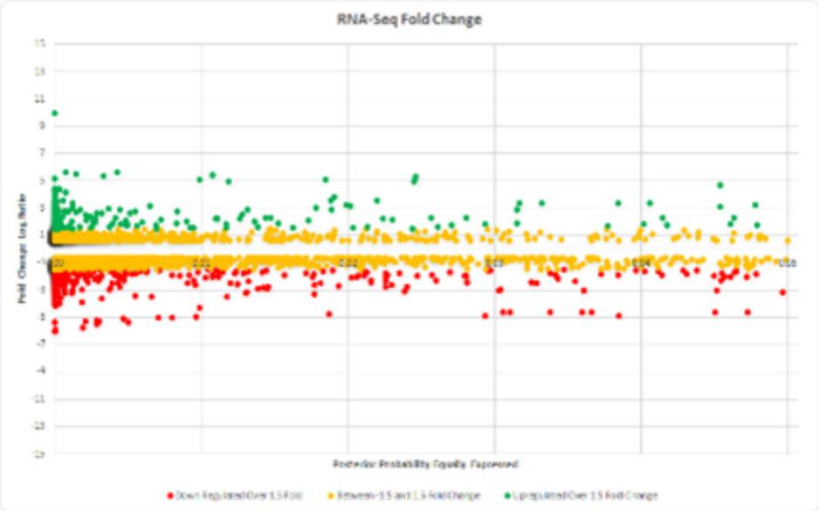

All Statistically Significant	Number of Genes
Up-Regulated Greater Than +1.5 Fold Change	282
Between -1.5 and 1.5 Fold Change	3,018
Down Regulated Greater Than -1.5 Fold Change	491
Total	3,791

Figure 27 RNA-Seq Differential Expression iPathway Guide:
With a p<.05 there were 3791 differentially expressed sequences with statistical significance. Of 23358 genes measured with expression. These genes were analyzed using the Kyoto Encyclopedia of Genes and Genomes (KEGG) database, Gene Ontology Consortium database, miRNAs from the miRbase, and TARGETSCAN databases. A total of 90 pathways were found to be significantly impacted with 2182 Gene Ontology (GO) terms, 41 miRNAs, and 46 diseases found to be significantly enriched. A) Shows the differentially expressed genes found by this analysis with 282 upregulated at or above 1.5-fold, 491 genes downregulated at or above 1.5 fold, and 3,018 between +1.5 and +0.6 and -0.6 and -1.5. All points are statistically significant.

Table 5: Top GO Biological Processes RNA-Seq Differential Expression IUGR NPCs by iPathway Analysis

GO Biological Process Pathways	Differentially Expressed Genes	Total Genes	FDR
Cellular Macromolecule Metabolic Process	1707	7423	1.00E-24
Cellular Metabolic Process	2020	9195	1.00E-24
Primary Metabolic Process	1995	9174	1.00E-24
Nitrogen Compound Metabolic Process	1899	8628	1.00E-24
Metabolic Process	2154	10148	1.00E-24
Macromolecule Metabolic Process	1807	8173	1.00E-24
Organic Substance Metabolic Process	2059	9657	1.00E-24
Cellular Nitrogen Compound Metabolic Process	1336	5691	1.00E-24
Biosynthetic Process	1257	5324	1.00E-24
Organic Substance Biosynthetic Process	1241	5248	1.00E-24

processes are the reactions and pathways that transform molecules into energy for the cell. Primary metabolic process includes lipid metabolism, carbohydrate metabolism, protein metabolism, cellular amino acid derivative metabolic processes, and the metabolism of nucleobase, nucleoside, nucleotide, and nucleic acids. This includes catabolic, maturation, biosynthesis, metabolic, and regulation of these processes. The rest of the Go biological process pathways are subcategories of the previous processes and are nitrogen compound metabolic process, metabolic process, macromolecule metabolic process, organic substance metabolic process, biosynthetic process, and organic substance biosynthetic process.

The top GO molecular function found by iPathway analysis found a series of compound binding pathways (Table 6). The bonds are related to structures of macromolecules (heterocyclic compounds, nucleic acid, organic cyclic, ribosome, protein, and DNA), and cell activity (transcription regulation, transferase). Transferase activity relates to the movement of functional groups between molecules. Functional groups include methyl, alcohol, and others that change the activity and localization of the molecules being modified. The functions found in P0 IUGR relate to transcription activity, protein binding, and protein synthesis changes.

The top altered pathways were ribosome which process messenger and transfer RNA and synthesize polypeptides and proteins (Table 7). The AGE-RAGE signaling pathway in diabetic complications relates to glycation, MAPKs, NF-κB, Il-1, Il-6, TNF-alpha, JAK-STAT, and PI3K-AKT and signals into proliferation and apoptosis. MAPK signaling pathway is a signaling cascade that responds to environmental signals into the cell. MAPK signals relate to cell proliferation, differentiation, and migration.

Glycosphingolipid biosynthesis- globo and ispglobo series is a metabolic and biosynthesis pathway. The globo and isoglobo series specifically process GalNAcα1 into

Table 6: Top GO Molecular Function RNA-Seq Differential Expression IUGR NPCs By iPathway Analysis

GO Molecular Function Analysis	Differentially Expressed Genes	Total Genes	FDR
heterocyclic compound binding	1179	5169	1.00E-24
nucleic acid binding	834	3414	1.00E-24
organic cyclic compound binding	1190	5258	1.00E-24
binding	2491	12604	1.00E-24
structural constituent of ribosome	80	147	1.69E-21
DNA binding transcription factor activity	305	1105	2.73E-15
transcription regulator activity	375	1434	4.26E-15
transferase activity	534	2241	1.43E-13
protein binding	1697	8514	2.07E-12
DNA binding	475	1996	8.45E-12

Table 7: Top Altered Pathways RNA-Seq DE Show Energy Sensing and Stress Response

Pathway Name	Pathway ID	P-Value	P-Value(FDR)	P-Value (Bonferroni)
Ribosome*	3010	1.00E-24	1.00E-24	1.00E-24
AGE-RAGE Signaling pathway in diabetic complications	4933	1.34E-05	0.02	0.004
MAPK Signaling Pathway	4010	2.90E-05	0.003	0.009
Glycosphingolipid biosynthesis- globo and ispglobo series*	603	3.88E-05	0.003	0.012
AMPK Pathway	4152	6.85E-05	0.004	0.021

Table 8: Differential Expression Shows Changes throughout the Cell

Pruning Type: None				Pruning Type: Elim		Pruning Type: Weight	
GO Term	P-value	P-Value (FDR)	P-Value (Bonferroni)	GO Term	P-value	GO Term	P-value
Intracellular	1.00E-24	1.00E-24	1.00E-24	Cytosolic large Ribosomal Subunit	1.00E-24	Organelle	1.00E-24
Intracellular Part	1.00E-24	1.00E-24	1.00E-24	Cytosolic small Ribosomal Subunit	1.40E-18	Cytosolic Ribosome	1.00E-24
Intracellular Organelle	1.00E-24	1.00E-24	1.00E-24	Nucleus	6.10E-12	Intracellular	3.40E-24
Organelle	1.00E-24	1.00E-24	1.00E-24	Cytosol	6.50E-07	Nuclear Lumen	7.40E-10
Membrane-bounded Organelle	1.00E-24	1.00E-24	1.00E-24	Nucleolus	6.90E-07	Focal Adhesion	1.30E-06

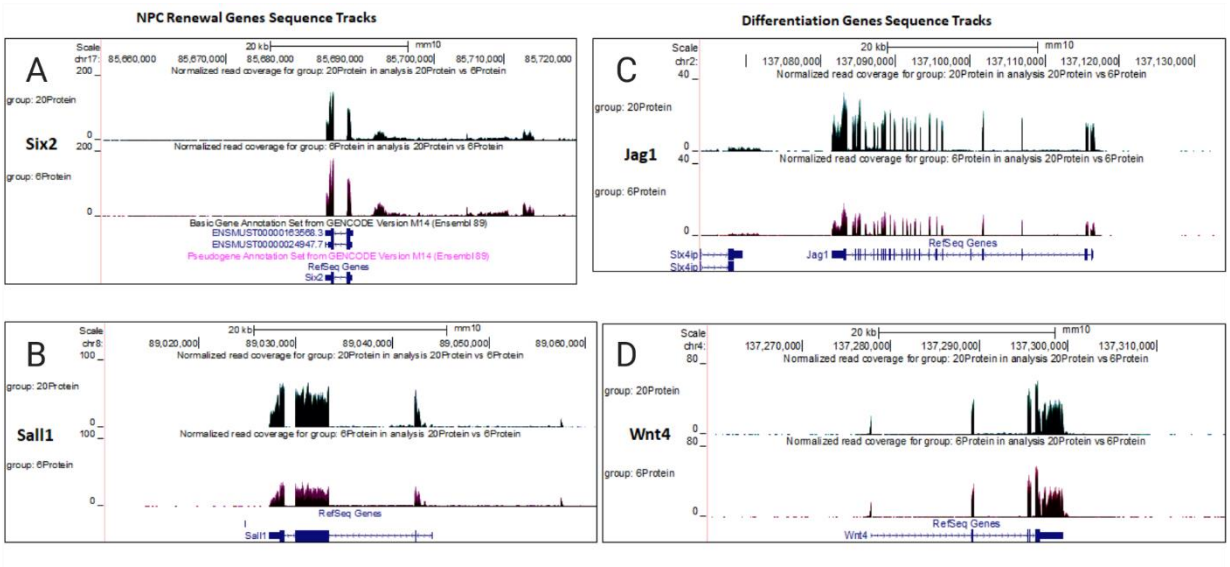

Figure 28 RNA-Seq Differential Expression Gene Track
Gene sequence tracks showing from GENCODE M14. Reference sequence is for mus musculus. The RNA isolated is from Cited1/Sx2 dual positive NPCs. A-B) NPC Renewal markers Six2 and Sall1. IUGR NPCs have no change in Six2 expression. Salll1 is lower in the IUGR NPCs by track and in both analyses. RNA-seq differential expression analysis has -2.246 fold change in IUGR NPCs. C-D) Jagged1 and Wnt4 are differential genes for NPCs. Jagged1 has much smaller peaks and has a fold change of -2.35. The Wnt4 peaks look a bit smaller but differential expression has no significant fold change. Average of 3 litters.

ceramide. AMPK pathway is a sensor of cellular energy status. It activates when the AMP:ATP ratio increases from metabolic stress interfering with ATP production or an increase in ATP use.

Top cellular components show not just changes throughout the cell as shown by IPA analysis but also changes to intracellular components of tissue (Table 8).

NPC renewal genes Six2 and Sall1 tracks show no change to Six2 while Sall1 is decreased a change confirmed by a significant fold change of -2.25 (Figures 28, 15A & 15B). The lack of change in Six2 and decrease in Sall1 is confirmed in staining data previous staining data.

									Plasma Creatinine			Plasma BUN	
Animal	Weight (g)	Kidney Weight (g)	Systolic (mmHg)	Pulse (bpm)	Diastolic (mmHg)	Mean Arterial Pressure (mmHg)	Glomerular Count Average Entire Sections	Glomerular Counts Average 10X Fields	µg/ml	mg/dL (x0.10)	Urine Albumin (g/dL)	Mean urea Conc. (mg/dL)	Mean BUN conc. (mg/dL)
20.7.M.1	48.9	0.99	128.08	711.01	65.8	87.81	183.33	6.67	0.5	0.05		39.66	18.53
20.7.M.2	49.4	0.798	123.43	703.02	67.99	85.89	144.67	6.33	0.8	0.08	0.056	67.15	31.38
20.7.M.3	49.8	0.656	149.07	706.90	83.55	105.12	91.33	6.00	0.8	0.08	0.139	79.30	37.06
20.23.M.1	45.7	0.705	122.33	695.11	72.09	90.75	145.67	6.67	0.4	0.04	0.078	64.24	30.02
20.23.M.2	51.8	0.756	120.83	695.21	68.54	86.17	136.67	5.67	0.3	0.03	0.095	71.18	33.26
20.23.M.3	54.1	0.852	124.46	713.44	67.85	86.66	152.33	7.33	0.6	0.06		52.62	24.59
20.23.M.4	50.3	0.801	130.45	698.29	72.75	92.97	148.33		0.6	0.06	0.12	105.45	49.27
20.7.F.1	43.6	0.456	123.96	561.28	74.01	96.26	115.00	6.67	0.7	0.07	0.034	69.36	32.41
20.7.F.2	43.7	0.475	105.40	546.11	64.79	79.61	125.33	5.33	1.0	0.10	0.059	83.96	39.24
20.7.F.3	40.2	0.545	133.75	658.70	86.54	102.53	122.33	9.00	0.6	0.06	0.05	56.58	26.44
20.23.F.1	34.3	0.4231	121.86	568.15	72.54	92.25	162.00	9.00	0.7	0.07	0.038	78.19	36.54
20.23.F.2	33.4	0.4743	143.88	712.12	85.98	105.33	149.67	6.75	0.7	0.07	0.075	65.31	30.52
6.7.M.1	49.1	0.555	115.65	645.55	59.90	79.45		3.67	0.6	0.06	0.112	70.07	32.74
6.7.M.2	50.1	0.573	127.99	657.41	76.33	94.85	135.00	5.00	0.7	0.07	0.114	60.09	28.08
6.7.M.3	36.9	0.409	131.00	603.15	80.55	98.46	90.00	5.67	0.8	0.08	0.059	81.66	38.16
6.23.M.1	39.5	0.544	178.06	559.92	116.48	137.84	43.33	3.75	1.4	0.14	0.477	86.79	40.56
6.23.M.2	48.5	0.698	120.89	651.66	66.25	86.07	135.67	4.00	0.6	0.06	0.26	65.26	30.49
6.7.F.1	34.9	0.39	119.28	698.58	65.01	84.09	123.67	5.67	0.8	0.08	0.038	73.17	34.19
6.7.F.2	32.7	0.431	130.44	672.87	75.90	95.19	130.33	5.00	0.7	0.07	0.041	65.11	30.43
6.23.F.1	45.8	0.376	130.44	672.87	75.90	95.19	131.33	5.67	0.7	0.07	0.139	83.72	39.12
6.23.F.2	46.6	0.385	119.95	656.74	62.63	79.80	102.67	5.00	0.8	0.08	0.057	70.54	32.96
6.23.F.3	49.7	0.428	112.80	745.05	65.41	83.24	103.67	6.33	1.2	0.12	0.352	91.18	42.61
6.23.F.4	42.9	0.4093	120.37	728.69	71.11	87.21	135.00	5.33	0.6	0.06	0.054	62.04	28.99

Table 9: Adult Summary
Green background are control males, blue are control females, yellow are IUGR males, and orange are IUGR females. Animals come from 4 litters born on 1/7/2019 or 1/23/2019 and are either 20% or 6% parental diet. Systolic pressure has no significance, but IUGR male 6.23.M.1 has the highest systolic and diastolic blood pressure with the highest plasma creatinine and urine albumin levels. The IUGR female 6.23 F.3 has no change to blood pressure but has the second highest Plasma creatinine and urine albumin.

Despite large differences in the number of genes found to be significantly changed by the two analyses the pathways implicated were very similar. Both show changes throughout the cell and related to ribosomes, developmental pathways, metabolism, differentiation, proliferation, and stress responses. The sequencing data itself supports the environmental signals altering pathways that change cell character and activity.

Chapter 4 Discussion:

IUGR mice from LPD are not just small mice at P0, but mice that continue to have developmental differences from control postnatally and into adulthood (table 10). The kidney is physically smaller before changes in size are apparent in with LPD. The severity of changes to kidney size persists even in adult animals that have caught up in weight with adult male 6.7.M.2 and adult females 6.23.f 1 and 2 (table 9). Kidney size is not just decreased in adulthood, but also shows a sex influenced change with IUGR showing female mice with the smallest kidneys in

adulthood. Sex differences are not found at P21 and could not be looked at earlier time points at sex was not recorded for earlier samples. This would be an important future direction when looking at kidneys at P0 and even embryonically as epigenetic regulation, which was greatly altered by the LPD, is known to vary with hormones.

Table 10: Summary and Timeline of Physical Changes

NC: No Change **+**:UP **-**: Down	Body Weight	Body Size	Kidney Weight	Kidney Size	Kidney/ Body Weight
E13.5		**NC**		-	
P0	-	-	-	-	+
P21	-	-	-	-	-
4 Month	**NC**	-	-	-	-

Changes to the skin and hair of IUGR mice postnatally are evidence of changes to cell cycle in stem cells with IUGR. Embryonically the skin begins as a single layer of epidermal stem cells (formed from the ectoderm) which rests on dermis from the paraxial mesoderm (Figure 1). The dermis will form hair follicles, sweat and oil glands, blood capillaries, nerve endings, and lymph vessels. Hair follicles form during embryogenesis from dermal papilla (specialized mesenchymal cells) which experience rapid proliferation postnatally. Hair growth comes from stem cells progressing through cycles of quiescence and activation which lead into proliferation, cell fate choice, differentiation, and apoptosis. This process will continue throughout the life of the organism as hair is lost and regrown. The process is regulated by growth factors, neutrophils, p53, TGFβ, and BMPRIa (a repressor of Wnt). This process relies on a stem cell compartment, cell to cell interaction, and interaction/availability of ECM. It is proposed as a model of stem cell quiescence and activation (Blanpain, C., Horsley, V., & Fuchs, E., 2008, Schmidt-Ulrich, R., & Paus, R., 2005, Alonso, L., & Fuchs, E., 2006). The morphological and morphometric changes in IUGR mice are evidence to changes to mesenchymal derived stem cells. The postnatal delayed skin and hair development supports changes to mesenchymal stem cells in IUGR pups from LPD. The germ layer is the same as the kidney and many signaling pathways for maintenance, proliferation, and

differentiation of the stem cells are the same between the kidney and skin development. The changes in IUGR pups come from changes to stem cell cycling and activation which leads to changes in differentiation and development. Unlike with kidney development, delayed skin and hair development has time to occur on a delayed schedule. Delayed kidney development will run into the wall of mass differentiation of NPCs at P4. Skin and hair development do not have that same end point with skin and hair growth continuing throughout adulthood. Changes in skin and hair development were present in all IUGR mice. Changes that persisted after removal from LPD conditions. As IUGR mice mature they lose the differences from control in appearance, but histology of the skin is a future direction for IUGR research.

IUGR embryonic kidneys have a deficit in Six2+ cells that are in poorly organized CMs as shown by FACS counting and immunostaining of whole organ and tissue section. The IUGR Six2+ population at P0 did not change in quantity from control as shown by count and staining (Figure 16 C, D, F). The deficit in embryonic IUGR kidneys has implications for proliferation and expansion of NPC populations. The lack of change in percent Six2+ population size in IUGR during development has implications for differentiation of NPCs and the intermediate and fully differentiated structures that form from the Six2+ NPCs. These changes are the core of why adult IUGR kidneys show damage and why there is a trend towards diminished kidney function. The changes to CM organization, Six2+ quantity, and Six+ as percent of total embryonic IUGR kidney from LPD are significant statistically and developmentally.

NPC balance between expansion/maintenance and differentiation is regulated by multiple pathways and mechanisms. This balance is essential for successful kidney development. The decreased quantity of Six2+ CM at e13.5 without changes to nascent nephron size or number at e13.5 shows changes to expansion and maintenance of the CMs. Changes to the balance of NPC

maintenance and expansion in the CM versus exiting the CM and differentiating would explain the deficit in differentiated structures in the kidney. This has been seen in previous work altering kidney development. IUGR has the addition of not just tipping the balance away from differentiation, but also decreasing expansion of the NPCs in the CM resulting in the smaller cap early in development and a smaller pool of NPCs for differentiation (Figure 29). The result is not just disordered differentiation, but NPCs that have shifted to survival and maintenance of stemness without expanding the CM they are within. The NPCs are then unable to respond to signals to differentiate at the appropriate time resulting in fewer NPCs to create differentiated structures, NPCs fighting the signal to differentiate through the pathways activated to fight apoptosis and differentiating NPCs that are poorly organized as they continue to signal to

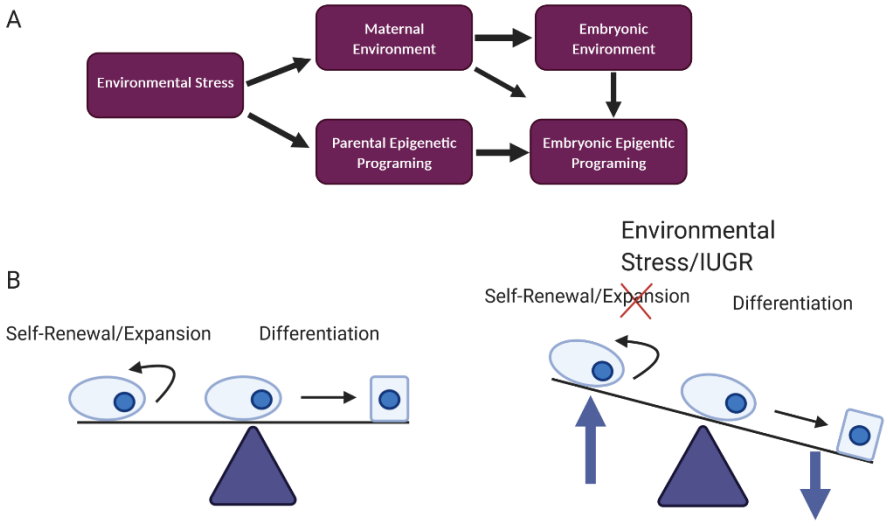

Figure 29: Epigenetic Reprograming Results in Changes to NPC Cell Fate

A) Environmental stress, in this case IUGR from low protein diet changes the epigenetics of parents and alters the maternal environment resulting in changes to the embryonic environment during the pregnancy. The changes to inherited epigenetics from both parents exposed to environmental stresses and changes to the embryonic environment will change the embryonic epigenetic programing from the beginning of embryogenesis.

B) Normal nephrogenesis by nephron progenitor cell (NPC) development requires a balance of Self-Renewal/Expansion in the cap mesenchyme (CM) and differentiation. Environmental stress, low protein diet in this case, changes this balance by decreasing the NPCs differentiating and increasing the Self-Renewal and maintenance of stemness in the CM. But the NPCs are not expanding the NPC population in the CM as shown by the smaller NPC pool at E13.5 and the lack of change in NPC pool over the course of development.

maintain stemness when development tries to progress. This is supported by the RNA-seq analysis and the molecular changes found in the IUGR kidneys.

The changes to the NPCs in the CM are at the start of kidney development. The changes in molecular composition to NPCs at P0 are a result of changes during all of kidney organogenesis (Table 1). Wt1 regulates Sall1, both decreased, and the regulators of NPC maintenance and proliferation BMP, FGF, MAP/ERK, and P-SMAD. All shown changed in RNA-seq at P0. Wt1 can be regulated by hypoxia-inducible factor 1α (Hif1α). Hif1α is regulated in response to environmental signals by phosphorylation of the protein. Hif1α did not change in the RNA-seq, which is expected when regulated on the protein level. Hypoxia-inducible factor 1-alpha inhibitor (Hif1na) is also activated by environmental stress signals to the cells, it is upregulated by 2.72-fold in the RNA-seq. The upregulation of Hif1na and pathways downstream of Hif1α is evidence of its upregulation. Hif1α is an upstream regulator of glucose metabolism, apoptosis, proteolysis, angiogenesis, erythropoiesis, cell proliferation and survival, and pH regulation (Masoud, G. N., & Li, W. 2015). Hif1α regulates p38-MAPK, ARK1/2, VEGF, p53, Myc, and metabolism pathways. This makes Hif1α a strong possibility for the upstream regulator that connects environmental signals of LPD to molecular and physical changes in the developing kidney. This would also explain why so many hypoxia related causes of IUGR exist in epidemiology and in IUGR animal models (glucocorticoid treatments, hypoxia via a chamber or surgery, umbilical artery ligation, uteroplacental embolization). Of further note is the expression of Hif1α in the epithelial cells of the ampullae in the collecting ducts of the kidney which are present in e13.5 IUGR kidneys at an unusually high rate. Hif1α is present in the CSB and SSB during glomerular development, but not in the mature glomerular in rats (Bernhardt, W. M., Schmitt, R., Rosenberger, C., Münchenhagen, P. M., Gröne, H. J., Frei, U., Warnecke, C.,

Bachmann, S., Wiesener, M. S., Willam, C., & Eckardt, K. U., 2006). Making it a candidate for changes in the development of first the UB and then collecting duct of the kidney. Hif2α is also present in the developing kidney and any future work exploring hypoxia inducible signals would need to consider both molecules as candidates for regulators in response to changes in maternal environment.

The pathways changed in the RNA-seq and confirmed in extracellular flux measurements and immunofluorescent staining is likely from epigenetic modifications. Histone modification is a known regulator of NPC maintenance and differentiation. NPCs, nascent nephrons, and epithelial tubules all have unique histone modifications (McLaughlin, et. al. 2014). Old vs. young NPCs show different chromatin landscapes with old NPCs poised for differentiation. The transcription factors Bach2 and AP1 were proposed as a link between renewal signaled by MAPK/AP1 and the Six2/β-catenin regulators of NPC differentiation. In ATAC-seq previous work on the binding motifs of Bach2, AP1, and BATF all showed changes in enrichment of binding sites with NPC age. Bach2 is also an active transcription factor in the distal RV. (Hilliard, S., Song, R.,, Liu, H., Chen, C, Li, Y., Baddoo, M., Flemington, E., Wanek, A., Kolls, J., Saifudeen, Z., & El-Dahr, S.S., 2019). These histone modifications are essential for the formation of mature glomeruli by testing knockouts of HDAC 1 and 2 (Liu, H., Hilliard, S., Chen, S., Yao, C., Li, Y., Chen, C,, Liu, J., Saifudeen, Z., & El-Dahr, S.S., 2018). Multiple HDACs associated with differentiation of the NPCs are decreased while HDACs that decreased with NPC maturation are increased in the IUGR NPCs. The massive dysregulation of epigenetic components like HDAC, Ezh, and Dnmt are a potential source of the large changes found in the RNA-seq. The chromatin regulators associated with differentiation are decreased in IUGR NPCs while maintaining high levels of regulators involved in maintaining stemness. Changes to the

histone landscape of NPCs would come from regulation of these factors and the components used in histone modification. The changes to cellular metabolism found in RNA-seq and cellular flux relate to the histone landscape as products from metabolism are essential for histone modifications. Metabolism products such as nicotinamide adenine dinucleotide (NAD), Acetyl-CoA, SAM, α-keotgluterate, and flavin adenine dinucleotide (FAD) are cofactors for methylation, acetylation, and thus the epigenetic landscape (Berger & Sassone-Corsi 2016). The RNA-seq shows changes to the expression level of many enzymes used in metabolism pathways, and the increased glycolysis measured by extracellular flux confirms changes to pathway activity levels. The difference in kidney growth from P0-P21, outside of LPD conditions and in the same environmental conditions of control pups, is strong evidence that these changes are persistent and alter development and growth of IUGR pups even after progenitor cells have differentiated. The physiological changes are not just to the embryonic or P0 CM.

P0 IUGR pups were smaller than control with smaller kidneys (Table 10). These smaller kidneys had changes to structure and differentiation that began early in development. There are significant changes in branch tip number at e13.5 showing early changes to the developing collecting duct from LPD. At P0 the markers for the collecting duct structures and patterns are unchanged, but the gaps between Six2+ caps along the cortex are evidence of changes in the ureteric tree. Kidney size is driven by ureteric development with decreased branching and elongation leading to smaller kidneys (Short & Smyth, 2016). At the advancing end of ureteric branching in the cortex of the kidney there are the P63+ ureteric bud tip cells (UBTC). The proliferating UBTC are the progenitors of all cells in the collecting duct and will lengthen the ureteric branches, expand the kidney, split the CMs, and through crosstalk signal the maintenance, expansion, and differentiation of the NPCs of the CMs. UBTC maintenance and

proliferation are not perfectly characterized, but Wnt/β-Catenin signaling is known to play a role in the UBTCs that are P63 and Sox9 positive (El-Dahr, et. al. 2017). IUGR at P0 showed increased Sox9 staining at the P63+ UBTCs (Figure 18). P63 is of interest in cancer research where it is known to regulate cell adhesion, movement, and cellular metabolism. P63 maintains proliferative potential of epithelial cells and it activates the transcription of hexokinase 2, the first step in glucose utilization and part of mitochondria function regulating the ADP/ATP ratio. Loss of P63 in transgenic mice causes defects in fatty acid oxidation and obesity (Candi, E., Smirnov, A., Panatta, E., Lena, A. M., Novelli, F., Mancini, M., Viticchiè, G., Piro, M. C., Di Daniele, N., Annicchiarico-Petruzzelli, M., & Melino, G., 2017). P63 in the ureteric branches is temporally and spatially regulated, first being detected in the UBTCs at e15.5 and being lost at P5 (El-Dahr, S. S., Li, Y., Liu, J., Gutierrez, E., Hering-Smith, K. S., Signoretti, S., Pignon, J.-C., Sinha, S., & Saifudeen, Z., 2017). The embryonic branching in IUGR pups and the cells directing that branching were not isolated as the NPCs of the CM were, but they are in a similar microenvironment as the NPCs. The environmental stress signals apparent in the RNA-seq of P0 NPCs will also be interacting with the UBTCs. If P63 regulating metabolism is directing UBTC activity as it does in cancer, then the changes to metabolism found in NPCs is a future direction of study for ureteric branching in normal and IUGR kidneys. Isolating P63+ UBTCs would provide RNA-seq and protein data to show metabolism activity. The branching issues in IUGR could be from increased glycolysis as found in IUGR NPCs as decreasing P63 leads to decreasing glucose metabolism in cancer cells. P63 decreases as UBTCs differentiate to form the ureteric branches behind the UBTCs as the UBs elongate and branch to form first the ureteric tree and then collecting ducts of the kidney. If glycolysis is artificially high the UBTCs would be maintaining a progenitor state and not form the non-progenitor cells that make up the elongating

ureteric branches. Cell adhesion and migration were highly dysregulated in the IUGR P0 NPCs and their products of differentiation. If the stress response pathways are also impacting cell adhesion and migration in the UBTCs, they could be unable to organize and move as needed to elongate the ureteric tree and grow the kidney.

The changes in development across the IUGR mice, the RNA-seq of the P0 NPCs, and the persistence of those changes after exposure to the LPD shows IUGR NPCs and kidneys have changes to the histone landscape. The histone landscape is known to not only change during development of the kidney but to direct and be essential for it. The NPC chromatin landscape changes between young (E13, E16) and old (P0, P2) NPCs via ATAC-seq analysis in Hillard et. al. 2019. The chromatin landscape also varies between high and low GFP NPCs at P0 with GFP varying with level of Six2 as the mice are a Six2CreGFP mouse. The high GFP/Six2 cells are the renewing NPC population while low GFP/Six2 are primed for or beginning the process of differentiation. ATAC-seq analysis of old versus young NPCs showed distinct changes to the chromatin landscape with development. Both NPC populations are Six2+ and yet old NPCs are primed for differentiation and young NPCs are a self-renewing population. There are distinct changes in chromatin accessibility and predicted gene activity with a high presence of stem cell maintenance genes and pathways in young NPCs and high differentiation genes and pathways in old NPCs. Specifically, there is a 2.4-fold increase of Six2 in young versus old NPCs, and a 16-fold change in Old NPCs compared to young for Wnt4. Among the changes from young to old NPCs is the increased accessibility of Bach2/AP1 transcription factors. Overall young NPCs have more cell growth and cell cycle while the old NPCs tend towards differentiation functions like cell-to-cell junction and inactivation of the MAPK pathway (Hilliard, S., Song, R., Liu, H., Chen, C., Li, Y., Baddoo, M., Flemington, E., Wanek, A., Kolls, J., Saifudeen, Z., & El-Dahr,

S.S. 2019). Hillard et. al. 2019 shows that the chromatin landscape changes over development and that the regulation of pathways created NPCs poised for the epithelization which occurs with nephrogenesis. These changes are present in old versus young NPCs and the high versus low GFP/Six2 NPCs sourced from the same P0 kidneys. The changes to the character of the CM niche are intrinsic changes to the cells and not environmental signals from the niche. Hillard et. a. 2019 hypothesizes the chromatin remodeling is mediated by epigenetic machinery like NuRD/HDAC, ATP-dependent chromatin remodelers, and DNA methylation. These are found dysregulated in the IUGR P0 NPC RNA-seq. IUGR does not have the same penetrance and severity as the genetic models of chromatin dysregulation, but the chromatin landscape is clearly changed by LPD and chromatin landscape changes direct NPC renewal and differentiation and has caused fatal mouse phenotypes in knockout models who fail to develop functional renal systems.

H3K27me3 is an epigenetic modification associated with downregulation of nearby genes. The presence of the tri methylated H3K27me3 forms heterochromatic regions that are tightly packed making those regions of the DNA inaccessible to translation machinery. It is enriched in NPCs relative to the rest of the nephrogenic zone. Loss of Ezh1, a component of the complex that mediated methylation of H3K27, does not change the relative prevalence of H3Kme27 in the developing kidney. However, loss of Ezh2 resulted in the loss of H3K27me3 in NPCs and their derivates while its presence in the stroma, UB, and CD is normal. Ezh2 knockout causes a decrease in NPC proliferation, a thinner CM, downregulated Cited1, and fewer nascent nephrons with less Lhx1, Pax8, and Wnt4. There is a 30% decrease in GFP+ NPCs with the Ezh2 knockout. Cell cycle is altered along with an increase in apoptosis. Dual inactivation of Ezh1 and 2 caused early activation of Wnt4, and a decrease in Six2 the net result being early

differentiation of the CM but fewer differentiated structures in the final kidneys along with cysts and poorly developed kidneys. The loss of Ezh1 and 2 in NPCs resulted in premature differentiation as they failed to maintain stemness (Liu, H., Hillard, S., Kelly, E., Chen, C., Saifudeen, Z., & El-Dahr, S.S., 2020). Kidney development requires careful balance that utilizes epigenetic regulation to progress properly. Epigenetic changes are susceptible to environmental signals and result in lifelong changes to organisms.

The IUGR adult mice are not significantly changed in measurements of kidney function. Physiological changes are present in adult IUGR mice. The IUGR adult mice have significantly decreased glomeruli and many of the IUGR adults have damaged kidneys. The lack of disease state from just IUGR is explainable from the multi-hit theory of disease in humans. The multi-hit hypothesis is supported in disease progression of nonalcoholic fatty liver disease (NAFLD) and nonalcoholic steatohepatitis (NASH). NAFLD is the accumulation of triglycerides in the liver without excessive alcohol consumption. NAFLD occurs in approximately 30 to 40 percent of adults in the United States, of those 20 percent have NASH with the rest of NAFLD patients having fatty liver disease. NASH occurs in NAFLD patients where the fat build-up leads to inflammation and scarring, fatty liver patients do not have inflammation (CDC: NCCDPHP, 2020). NAFLD patients with fatty liver disease typically do not have further symptoms, while NASH patients can develop cirrhosis and liver failure requiring a liver transplant. The development of NASH and NAFLD is believed to be caused by a multi-hit system where patient's dietary habits, environment, and genetic predispositions, also causing a high comorbidity with insulin resistance, and obesity, lead to the formation and build up triglycerides in the liver. The build-up of fat in the liver is not itself enough to damage the liver. Triglycerides and inflammation from ER stress and ROS cause inflammation, apoptosis, and fibrosis lead to

the more serious NASH. The ER stress and ROS can be caused by a variety of factors from the environment or genetics with many related to metabolic pathways (Buzzetti, E., Pinzani, M., & Tsochatzis, E. A., 2016). There is also a two-hit hypothesis for Alzheimer's disease with oxidative stress and aberrant mitotic signaling both capable of initiating, but Alzheimer's developing only when both occur (Zhu, X., Lee, H. G., Perry, G., & Smith, M. A., 2007). Alzeheimer's, NAFLD, and NASH are linked to a multi-hit model of disease with both neurological and liver diseases associated with metabolic and inflammatory changes. Metabolic and inflammatory changes are found in the IUGR kidney.

The multi-hit hypothesis is key in the current study and understanding of kidney disease. IgA neuropathy (IgAN) is the most common glomerulonephritis worldwide. It is the inflammation of the filtering glomerulus. The majority of IgAN occurs sporadically while 5-10% occur in families, but both familiar and sporadic IgAN are linked to genetic factors. IgAN is an autoimmune disease with pathology caused by a multi-hit system. Unknown upstream factors lead to the formation of galactose deficient IgA1, which is recognized by an autoantigen, this can then lead to inflammation of the kidney in response to antigen complexes, these immune cells form deposits in the kidney and activate the mesangial cells. Mesangial cell activation causes protein build up and lesions in the glomerulus. It is believed that the multiple steps of this process are regulated by environmental and genetic factors. The galactose deficiency comes from improper O-glycan processing in B cells. IgAN patients show deficiencies in glycosyltransferases and an increase in sialyltransferases. These enzymes are under the regulation of interleukins which respond to cell or organism stress. Mesangial activation by inflammatory signals varies based on receptor activity and sensitivity. The IgAN multi-hit hypothesis of disease comes from layers of environmental and genetic factors coming together

rather than single events of causation (Lai, Tang, Schena, Novak, Tomino, Fogo, Glassock 2016). IUGR kidneys also showed evidence of dysregulation of sialylation and glycosyltransferases. The complete loss of DBA staining in five IUGR mice at P0 is of interest as the DBA lectin binds α-linked N-acetylgalactosamine. As co-staining shows the distal tubules are present it is the specific glycosylated amino sugar that is lost. This is supported by expression changes in glycosylation related genes in the RNA-seq of NPCs. All animals that lack DBA staining have decreased NCAM staining in the CSB and SSB with clear NCAM staining in the mesenchymal CMs. The NCAM loss in differentiating structures is also present in animals that have DBA staining. NCAM is a cell adhesion molecule and as NPCs condense and epithelialize during differentiation NCAM localization changes. It has been shown that NCAM staining is co-localized with staining for polysialic acid along the basolateral membrane of the epithelial structure of the differentiating kidney. This co-localization is not present in the mesenchymal staining by NCAM. NCAM is polysialylated during late embryonic development. Polysialylation is a signal for localization within the cell. NCAM can be at the basolateral membrane in CSB and SSB without polysialylation, but it was suspected that it will not be concentrated there without polysialylation (Lackie, Zuber, & Roth, 1990). The dependence of NCAM localization and binding function is supported by its role in neural development where polysialylation is required for NCAM to NCAM binding during development (Rutishauser, 1988 & Galuska et. al. 2017). IUGR has alterations of molecular modifications that are already known to lead to kidney damage in a multi-hit system.

The separate and combined roles of genetics and environment on nephron endowment and kidney function is supported by research into hypertension. There are genetic components like Pax2 mutations and chromosomal disorders causing oligomeganephronia, or the smaller

kidneys with decreased nephron endowment in p53 mutants and environmental factors, like IUGR and maternal smoking, causing decreased nephron endowment. Extremely low nephron endowment is sufficient to cause hypertension, but this is less common than the wearing down of kidneys born with low endowment. Humans are born with between 250,000 and over 2 million nephrons, with most having 1 million nephrons. Those at the lowest end of the range would have immediate complications when fully one third of the cardiac output is pumped into kidneys with so few structures to process it. But what of those with lower, but more normal nephron endowments? Human nephron endowment is inversely linked to age with an estimated 4500 glomeruli lost per kidney per year through all of adulthood. A person could then expect to lose 450K glomeruli between two kidneys over 5 decades of life. The person starting with 1 million glomeruli and ending with 550K is in much better shape than a person starting with 700K glomeruli and ending with 250K. This level of glomeruli loss comes from the 2010 study Effects of aging on glomerular function and number in living kidney donors by Tan, Busque, Workeneh, Ho, Derby, Blouch, Sommer, Edwars, & Myers. Donors older than 55 compared to those younger than 45 showed the lowest quartile of estimated glomeruli per kidney. Older subjects had nearly a quarter of the median estimated glomeruli per kidney then in the younger group with comparative decrease in kidney function as measured by glomerular filtration rate and increased rates of sclerosis in older subjects.

The multi-hit theory for CDK from IUGR is further supported by a 2011 twin study by Rajan, Barbour, White, and Levin. Where monozygotic twins that are identical in genetics and maternal environment have different kidney disease states as adults with Alport syndrome. The case study traced the more rapid progression of kidney failure to the twin being born with IUGR and decreased nephron endowment at birth. Twin A was 5 lbs. 9.5 ounces at birth and Twin B

was 4 lbs. 9.8 ounces. Twin A just misses the cut off for IUGR in humans, 5 lbs. 8 ounces, while Twin B is clearly IUGR. Both twins have kidney issues as adults, but Twin B has severe problems with kidney function. Both are medicated, but Twin B has had high urine albumin and low estimated glomeruli filtration rate his entire adult life and Twin A has been able to keep urine albumin low and maintained glomeruli filtration into late adulthood. Kidney function is not just genetics or maternal environment as both create a range of outcomes in adulthood. The impact of later challenges to kidney function cannot be ignored in studying kidney disease.

IUGR from LPD alone is not causing hypertension or CDK in adult mice. But given the complexity of disease causation in mice and humans it should not be expected to. IUGR is impacting the developing tissues of the kidney and changing the organ that is formed, but it is not sufficient to cause adult diseases at 4 months. The animals produced would be at high risk if faced with another hit. The next step in IUGR study would be to look at the IUGR model with multiple hits. There are several established genetic models for kidney disease that would serve as a model for populations with genetic predispositions for hypertension combined with an environment of deprivation. This would be of interest for hypertension in African American populations as they have an increased rate of hypertension, CDK, and kidney failure. There are known genetic predispositions in the African American population and the socioeconomic issues faced by the population could easily mimic a genetic predisposition combined with micro or macro malnutrition during development. There are also models for challenging kidney function in adult mice including diet changes, injury, or stress. This would model situations where an adult was gestated during a time of deprivation and faced a challenge to their renal system as an adult by either injury or poor diet. IUGR by parental protein restriction is a sledgehammer to the developing mouse impacting multiple pathways throughout the cell and organism. These

pathways are associated with development and adult renal diseases. For all the changes that occur from IUGR, they are not targeted like genetic models or models of injury in adult mice. The more general harm from these varied changes is of use in further study of ways humans develop hypertension and CDK over a lifetime.

The complexity and severity of the changes in IUGR kidneys means intervention to prevent IUGR can be tested at multiple points and with environmental, drug, and genetic interventions. The first changes with LPD are to the epigenetic programing of the adult mice that will be used for breeding, so changes will be present before fertilization. But a good starting point would be the mesoderm which forms at E6.5 from the primitive streak and further differentiate into many critical organs of the body including the entire urogenital system via the intermediate mesoderm (Figure 1 and 30). The intermediate mesoderm will be marked first by Osr1, then later by Pax2, Pax8, and Lhx1. This offers options for genetic intervention during the development of IUGR mice. Cre-Lox mice can be used to create a knock-in or knock-out genetic model specific to the intermediate mesoderm to rescue partially or completely the pathways impacted by the IUGR signals of stress that re-programmed the developing mouse and its kidneys. Based on the RNA-seq published research into kidney development genetic options include p53, mTOR, one of the changed genes in Glycolysis or a known regulator of Glycolysis. The goal would be to inhibit the stress response of the cells to undo or prevent the epigenetic reprograming caused by IUGR. Intervention at E6 or E6.5 is possible, but difficult and would not model many realities of IUGR. This intervention could work for planned pregnancies for humans with chronic medical conditions, or at high altitude, but would not be useful for humans with other causes of IUGR. Early restriction of calories or micronutrients that was stopped, as in some of the subjects from the Dutch Famine cohort, would the reason for the next potential

intervention point for IUGR. The nephric duct and metanephric mesenchyme have both formed by E10. The development of the metanephros will begin at E10.5 with the growth of the UB out of the nephric duct into the neighboring metanephric mesenchyme and the formation of the cap mesenchyme (Figure 2 and 30). This represents all cells needed to form the adult kidney being in one place for the first time. Embryonic kidneys can be harvested at this time for organ culture providing not just genetic manipulation, but also efficient uptake of drugs as previously used by our lab to change kidney development. Partial glycolysis inhibition, proven to prime NPCs for differentiation under normal conditions, can be done by YN1 and may normalize the IUGR NPCs to create normal differentiation rather than the decreased development found in IUGR. For environmental intervention the maternal diet could be changed to normal at this or other set times, this is unlikely to result in large changes in IUGR as shown by studies like the Dutch Famine cohort and what is known of the long-term changes form epigenetic programing during development. The NPCs at E11.0 are Cited1/Six2 dual positive making genetic models possible either through constitutively active or inducible Cre-Lox systems. These could target known regulators of cellular stress or kidney development. The goal would be to inhibit stress response pathways, and activate cell replication pathways, developmental pathways for the kidney, and to possibly inhibit the stem cell maintenance pathways as maintaining the NPC population is already being done by the IUGR embryos. The smaller pool of NPCs at E13.5 and lack of change in NPC pool over the course of development (Figure 16), shows that stemness is maintained probably to the detriment of the developing kidney and adult structures. Instead Wnt and FGF maintenance signals from the UB and BMP and FGF signals from NPCs should be inhibited so NPCs can be primed for differentiation. Previous work by our lab showed that

partial inhibition of glycolysis will accomplish this priming and it can be done genetically in the Six2 population or by use of many anti-cancer drugs.

Moving into later kidney development an important shift is at E15.5 when NPCs normally change from "young" to "old." At this time their cell metabolism changes from glycolysis dependent to oxidative phosphorylation, epigenetic changes occur showing the NPCs are unique from earlier NPC pools and shifting increasingly into a state primed for differentiation rather than maintenance and expansion of the CM (Liu, 2017). These cells remain Cited1/Six2 dual positive meaning an inducible genetic change is possible at this time. Decreasing glycolysis in the progenitor population, inhibiting p53, or mTOR at this time has the potential to partially rescue the IUGR kidneys as they complete development. A large amount of nephrogenesis occurs at the end of kidney development, with much occurring postnatally in mice. Intervention at this stage is unlikely to fully recue development but would be a realistic model of IUGR in humans when a problem is discovered late in pregnancy. Embryonic organ culture is not an option at this stage, but the isolation of large populations of NPCs either for culturing or analysis is possible. Experiments with NPCs would show a simpler system of the genetic or pharmaceutical changes to developmental pathways and the impact on RNA-seq and the epigenetic landscape from interventions before and at E15.5.

The final time point for intervention is postnatal day zero (P0). There is evidence that subtle intervention at P0 would not improve kidney development as shown by the changes to IUGR in both skin/hair and kidney development despite controlling for breastmilk quality and access in the P21 and adult mouse samples. Despite this it would be easy to access a large number of NPCs for experimentation and easily get drugs or induce genetic mutations at this time point. A large signal to differentiate, either through inhibiting Six2, Sall1, Mdm2,

glycolysis, or the Wnt9b signal from the UB. A combination of these interventions would be possible at P0. This would model late intervention of IUGR in humans which is expected to occur given the lack of access to prenatal care worldwide.

This project focused on the NPCs, CM, and nephrogenesis and did not focus heavily on the UB and the UBTCs. The UBTCs are an important focus in the future of IUGR research not just in relation to the crosstalk with NPCs, but as they are crucial in forming and expanding the kidney. The obviously smaller kidneys with IUGR are strong evidence that UBTCs are changed by IUGR. It is possible to genetically manipulate the UBTCs and any environmental or drug change done in utero would impact the UBTCs. The MACS isolation protocol can be altered to isolate NPCs and UBTCs from the same kidney simultaneously providing an important part of the puzzle. This paper theorized that the changes in the NPCs from environmental stress would be present in the UBTCs as they share a microenvironment and RNA, protein, and epigenetic analysis would easily show not just if the same pathways are changed but provide insight into what those changes have led to in development of the ureteric branching of the IUGR kidney. Any intervention in IUGR must consider the UBTCs neighboring the NPCs explored in this paper.

The interventions also need to consider the appropriate time for determining if the intervention worked. An early indicator are the previously described changes to mouse behavior and delay in growth and development of the skin and hair making the end point around P15. The clearest direction for an end point is having IUGR mice progress to a disease state. Obviously, some IUGR must be grown until they are actually older and not just in the young adult stage of 4 months. IUGR mice grown to 18 – 24 months would provide a model for an elderly IUGR patient and would determine if IUGR alone can cause kidney disease (Hagan, 2017). Models for

the multi-hit theory of disease would likely not need to use mice at that age and would be expected to find disease state much earlier, but still after the 4-month time point used here. The multi-hit model in IUGR could use environmental and genetic as the intervention studies did. High salt and high fat diet have both been used to cause renal injury in mice and could act as a second hit in adult IUGR mice, modeling the poor diet available to many that develop kidney disease. Alternative genetic hits would include the Six2P53 mutants used in the Saifudeen lab, or the combination of diabetic mothers from the *Ins*$2^{+/C96Y}$ mice previously shown in Cerqueira et. al. 2019 to have changes to kidney function in their wild type offspring. The contributing factors for the multi-hit models can be other challenges during development either through genetic changes, or further environmental strain. They could also occur postnatally but during childhood; poor diet post birth using LPD females for poor quality breast milk, low quality diet given to a previously well-fed mouse leading into poor diet then for the IUGR offspring as they wean.

Central to the intervention and multi-hit models for IUGR are the cellular pathways LPD changed to create IUGR. IUGR from LPD adds to kidney research that environmental changes are altering the previously identified metabolic, histone, and cell cycle pathways to change kidney development by early re-programing. Future work with IUGR will be in the exploitation of this, or stopping or re-writing this re-programming.

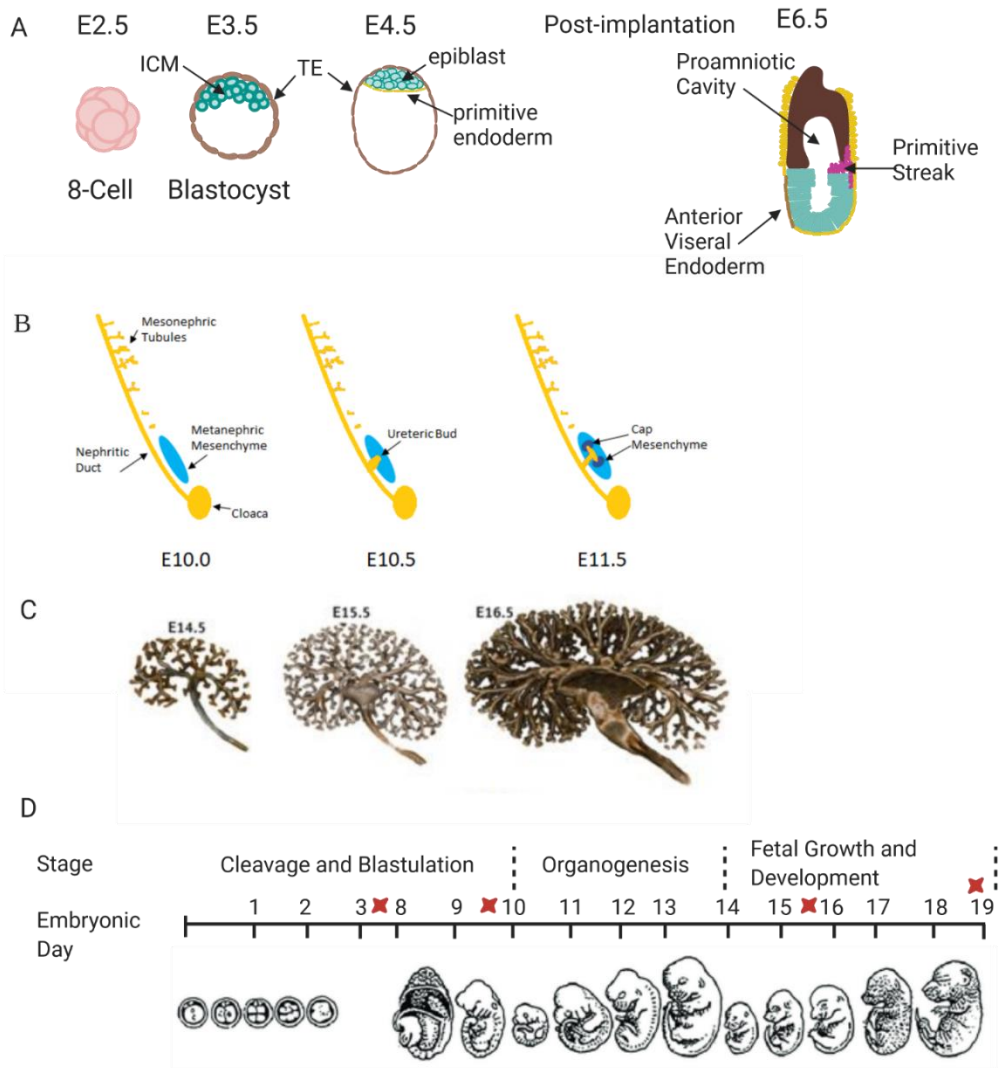

Figure 30: Proposed Points of Intervention for IUGR Development

IUGR from Low protein diet results in changes from the beginning of embryonic development. Multiple points of intervention must then be explored from early in embryo development up to the very end of kidney development. Potential interventions are diet to compensate for thrifty developmental signals, to genetic manipulation of the pathways changed by low protein IUGR. A) Rescue of Mesenchyme: Mouse development runs to approximately embryonic days 18 to 21. At the very beginning cleavage and blastulation starts before the embryo has even implanted. These steps already begin differentiating into germ layers. The mesoderm, the source of mesenchyme which give rise to the urogenital system, forms on e6.0 after implantation. The primitive streak and formation of the mesenchyme are on e6.5. Intervention at this point would change the programing signals of the mesenchyme from low protein parental diet. B) The mesenchyme does not begin formation of the metanephric kidney until E10.5. An intervention at E10.0 or E10.5 could either reprogram the forming cap mesenchymes, or prevent their reprograming by low protein diet if earlier exposure to low protein diet had yet to change their character. C) NPCs, formed from the metanephric mesenchyme and maintained by the signals of UB, shift from "young" to "old" at E15.5. At this time the cell metabolism, epigenetic regulation, and maintenance versus differentiation signals change. IUGR has shown differences to kidney development between e13.5 and P0, this would-be late intervention for the NPCs that have spent 2 weeks receiving the signal from low protein environment. D) The latest point of intervention would be P0. After birth increasing the signal to mass differentiate NPCs as control mice do would be expected to have only a small change in kidney development. But presents a model for human disease intervention. Modified and using graphic from Xu, Y.H., Barnes, S., Sun, Y., & Grabowski, G.A.. 2010.

Supplemental Table 1: RNA-Seq Fold Change in LPD NPCs		
Ensembl_id	**Gene Name**	**Fold Change in LPD RNA**
ENSMUSG00000048938	Nr1h5	202.46
ENSMUSG00000078889	Gm14288	142.55
ENSMUSG00000081516	Gm12470	90.96
ENSMUSG00000090381	Gm6158	85.57
ENSMUSG00000078436	Gm4767	84.42
ENSMUSG00000078284	Cdc73	82.69
ENSMUSG00000091084	BC065403	43.21
ENSMUSG00000070979	Actl7a	36.15
ENSMUSG00000058922	Gm10052	35.24
ENSMUSG00000083650	Gm13357	23.13
ENSMUSG00000037887	Dusp8	21.12
ENSMUSG00000091106	Gm17625	20.61
ENSMUSG00000073741	4732440D04Rik	20.20
ENSMUSG00000048153	Olfr49	17.31
ENSMUSG00000090516	Gm6202	17.03
ENSMUSG00000072451	Gm10359	16.79
ENSMUSG00000083207	Gm14780	16.12
ENSMUSG00000090992	Gm17588	16.02
ENSMUSG00000087579	1500017E21Rik	15.96
ENSMUSG00000082686	Gm12961	15.87
ENSMUSG00000082374	Gm12741	15.33
ENSMUSG00000091997	Gm6611	14.65
ENSMUSG00000090885	Gm3944	14.56
ENSMUSG00000090980	Gm17274	13.98
ENSMUSG00000054136	Adm2	13.35
ENSMUSG00000092509	Gm20394	13.22
ENSMUSG00000089651	Gm16353	13.17
ENSMUSG00000044352	Sowaha	13.13
ENSMUSG00000028553	Angptl3	12.59
ENSMUSG00000079436	Kcnj13	12.38
ENSMUSG00000018865	Sult4a1	12.01
ENSMUSG00000089896	Wnk1	11.80
ENSMUSG00000082265	Gm15547	11.62
ENSMUSG00000067189	Gm7335	11.28
ENSMUSG00000070980	Actl7b	11.09
ENSMUSG00000093717	RP23-345J21.1	11.06
ENSMUSG00000090278	D130062J21Rik	11.01
ENSMUSG00000090604	Gm17378	10.95
ENSMUSG00000058812	0610039K10Rik	10.71
ENSMUSG00000079906	Gm15846	10.69

ENSMUSG00000090070	Gm16577	10.65
ENSMUSG00000041062	Mslnl	10.61
ENSMUSG00000085335	Gm13684	10.56
ENSMUSG00000076433	BC100451	10.46
ENSMUSG00000086625	Gm11831	10.38
ENSMUSG00000085185	BC028777	10.22
ENSMUSG00000078249	Hmga1-rs1	10.09
ENSMUSG00000086062	Gm16853	9.84
ENSMUSG00000039384	Dusp10	9.76
ENSMUSG00000004902	Slc25a18	9.75
ENSMUSG00000081989	Gm13300	9.50
ENSMUSG00000090447	Gm17652	9.47
ENSMUSG00000081801	Dnmt3l-ps1	9.40
ENSMUSG00000079138	Gm8818	9.38
ENSMUSG00000083796	Gm13369	9.35
ENSMUSG00000085364	Gm16641	9.34
ENSMUSG00000082829	Gm15780	9.30
ENSMUSG00000078373	2010109K11Rik	9.29
ENSMUSG00000085289	Gm15337	9.26
ENSMUSG00000082984	Gm10599	9.21
ENSMUSG00000081289	Gm14857	9.14
ENSMUSG00000084792	1700056N10Rik	9.09
ENSMUSG00000091105	Gm5633	9.00
ENSMUSG00000086167	Gm13827	8.94
ENSMUSG00000087373	Gm15892	8.78
ENSMUSG00000093392	RP23-71G16.1	8.78
ENSMUSG00000082806	Rpl13-ps1	8.68
ENSMUSG00000080957	Gm15739	8.67
ENSMUSG00000090888	Gm17429	8.54
ENSMUSG00000026073	Il1r2	8.52
ENSMUSG00000086484	A630071L07Rik	8.48
ENSMUSG00000086192	Gm13609	8.37
ENSMUSG00000024215	Spdef	8.29
ENSMUSG00000069712	4930444G20Rik	8.26
ENSMUSG00000074213	Gm10642	8.25
ENSMUSG00000055691	Gja6	8.21
ENSMUSG00000089281	Scarna6	8.15
ENSMUSG00000037161	4930583H14Rik	8.12
ENSMUSG00000071552	Tigit	8.12
ENSMUSG00000028214	Gem	8.11
ENSMUSG00000026628	Atf3	8.09
ENSMUSG00000086400	Gm16789	8.09
ENSMUSG00000032715	Trib3	8.03

ENSMUSG00000083014	Gm11764	7.78
ENSMUSG00000085471	4933423P22Rik	7.66
ENSMUSG00000084781	D930015M05Rik	7.59
ENSMUSG00000087101	Gm16953	7.58
ENSMUSG00000022863	Btg3	7.57
ENSMUSG00000091831	Gm4707	7.54
ENSMUSG00000092604	Gm20508	7.45
ENSMUSG00000021319	Sfrp4	7.32
ENSMUSG00000090243	Gm16103	7.30
ENSMUSG00000085088	4931413K12Rik	7.21
ENSMUSG00000070330	Cldn27	7.20
ENSMUSG00000026220	Slc16a14	7.19
ENSMUSG00000083339	Gm11693	7.02
ENSMUSG00000086837	Gm16618	7.01
ENSMUSG00000087280	Gm17557	6.99
ENSMUSG00000021070	Bdkrb2	6.97
ENSMUSG00000041872	Il17f	6.89
ENSMUSG00000081156	Gm14425	6.88
ENSMUSG00000090912	4931403G20Rik	6.87
ENSMUSG00000042828	Trim72	6.86
ENSMUSG00000085884	Gm15342	6.80
ENSMUSG00000043186	Dusp8	6.80
ENSMUSG00000085916	Gm16724	6.79
ENSMUSG00000086407	Gm14123	6.79
ENSMUSG00000069804	Gm10277	6.72
ENSMUSG00000038550	Gm129	6.69
ENSMUSG00000058945	Gm10056	6.64
ENSMUSG00000080237	Gm14239	6.63
ENSMUSG00000031297	Slc7a3	6.63
ENSMUSG00000072244	Trim6	6.62
ENSMUSG00000085031	Gm16982	6.61
ENSMUSG00000092028	Gm17500	6.58
ENSMUSG00000020893	Per1	6.53
ENSMUSG00000078125	Gm10916	6.53
ENSMUSG00000086165	Gm15690	6.47
ENSMUSG00000070999	Ccin	6.45
ENSMUSG00000074252	Gm10654	6.44
ENSMUSG00000069196	Gm3511	6.42
ENSMUSG00000086412	Gm16626	6.35
ENSMUSG00000039661	Dusp26	6.32
ENSMUSG00000079160	Gm17608	6.31
ENSMUSG00000089735	Gm8428	6.25
ENSMUSG00000091838	Gm17316	6.18

ENSMUSG00000028341	Nr4a3	6.17
ENSMUSG00000071862	Lrrtm2	6.10
ENSMUSG00000091810	Gm17442	6.10
ENSMUSG00000078240	Gm3550	6.08
ENSMUSG00000027584	Oprl1	6.08
ENSMUSG00000081974	Gm11960	6.04
ENSMUSG00000082345	Gm13622	6.01
ENSMUSG00000040340	1700019B03Rik	5.97
ENSMUSG00000093673	RP23-333M1.4	5.95
ENSMUSG00000050473	Slc35d3	5.95
ENSMUSG00000055430	Nap1l5	5.92
ENSMUSG00000006542	Prkag3	5.88
ENSMUSG00000049649	Gpr3	5.87
ENSMUSG00000061816	Myl1	5.85
ENSMUSG00000071192	Wfikkn1	5.74
ENSMUSG00000056656	Apol8	5.72
ENSMUSG00000087064	Gm11721	5.69
ENSMUSG00000092140	Gm17451	5.65
ENSMUSG00000087620	5330434G04Rik	5.64
ENSMUSG00000070891	Gm12689	5.56
ENSMUSG00000068742	Cry2	5.56
ENSMUSG00000089924	Gm15689	5.56
ENSMUSG00000091318	Gm5415	5.55
ENSMUSG00000034226	Rhov	5.54
ENSMUSG00000046991	Wdr27	5.47
ENSMUSG00000038393	Txnip	5.42
ENSMUSG00000020256	Aldh1l2	5.40
ENSMUSG00000090548	Gm17489	5.30
ENSMUSG00000078965	Gm12033	5.28
ENSMUSG00000030256	Bhlhe41	5.25
ENSMUSG00000051243	Islr2	5.25
ENSMUSG00000084156	Gm14734	5.23
ENSMUSG00000079965	Gm14853	5.20
ENSMUSG00000092011	Gm9793	5.20
ENSMUSG00000089706	B230216N24Rik	5.20
ENSMUSG00000061702	Tmem91	5.19
ENSMUSG00000090836	Gm17475	5.15
ENSMUSG00000018143	Mafk	5.06
ENSMUSG00000071537	Klrg2	5.01
ENSMUSG00000055494	Gm14168	5.00
ENSMUSG00000037613	Tnfrsf23	4.98
ENSMUSG00000031736	4933436C20Rik	4.88
ENSMUSG00000027073	Prg2	4.88

ENSMUSG00000087436	Gm16156	4.85
ENSMUSG00000068417	Pnp2	4.81
ENSMUSG00000062380	Tubb3	4.80
ENSMUSG00000074569	Gcnt7	4.78
ENSMUSG00000067203	H2-K2	4.74
ENSMUSG00000002083	Bbc3	4.73
ENSMUSG00000079489	C030013D06Rik	4.72
ENSMUSG00000081339	Gm16044	4.70
ENSMUSG00000062588	Gm6104	4.68
ENSMUSG00000078933	Ipo11	4.63
ENSMUSG00000085092	Gm16867	4.56
ENSMUSG00000091333	BC051077	4.54
ENSMUSG00000032988	Slc16a8	4.54
ENSMUSG00000085495	Gm16796	4.53
ENSMUSG00000024030	Abcg1	4.52
ENSMUSG00000092098	Gm17529	4.51
ENSMUSG00000085362	C030034L19Rik	4.50
ENSMUSG00000042622	Maff	4.49
ENSMUSG00000090445	Gm17653	4.49
ENSMUSG00000055216	9430025C20Rik	4.48
ENSMUSG00000021680	Crhbp	4.47
ENSMUSG00000034614	Pik3ip1	4.45
ENSMUSG00000071531	Gprin2	4.44
ENSMUSG00000032584	Mst1r	4.42
ENSMUSG00000088170	7SK	4.42
ENSMUSG00000083396	Gm15542	4.41
ENSMUSG00000090489	Gm17415	4.41
ENSMUSG00000085606	Gm15792	4.39
ENSMUSG00000087306	A230004M16Rik	4.39
ENSMUSG00000082484	Gm16177	4.38
ENSMUSG00000001156	Mxd1	4.34
ENSMUSG00000090311	Gm17327	4.24
ENSMUSG00000070880	Gad1	4.24
ENSMUSG00000089798	1700028K03Rik	4.24
ENSMUSG00000087528	9830144P21Rik	4.21
ENSMUSG00000033949	Trim36	4.20
ENSMUSG00000046404	Yod1	4.19
ENSMUSG00000030303	Far2	4.19
ENSMUSG00000048249	A930001N09Rik	4.16
ENSMUSG00000045053	Kcng3	4.16
ENSMUSG00000029607	Ankrd61	4.12
ENSMUSG00000027202	Slc12a1	4.10
ENSMUSG00000034959	5031414D18Rik	4.10

ENSMUSG00000086351	6230400D17Rik	4.10
ENSMUSG00000091513	4731419I09Rik	4.10
ENSMUSG00000066687	Zbtb16	4.09
ENSMUSG00000062461	Gm5453	4.07
ENSMUSG00000002769	Gnmt	4.07
ENSMUSG00000031286	Glt28d2	4.05
ENSMUSG00000091642	Mocs3	4.04
ENSMUSG00000081142	Gm15497	4.03
ENSMUSG00000048758	Rpl29	4.03
ENSMUSG00000091056	Gm17536	4.03
ENSMUSG00000091219	Gm17254	4.01
ENSMUSG00000053164	Gpr21	3.99
ENSMUSG00000087129	Gm16316	3.98
ENSMUSG00000032311	Nrg4	3.97
ENSMUSG00000049969	Plekhf2	3.96
ENSMUSG00000090656	Gm17559	3.95
ENSMUSG00000050957	Insl6	3.94
ENSMUSG00000032936	Camkv	3.94
ENSMUSG00000047604	Frat2	3.94
ENSMUSG00000024524	Gnal	3.93
ENSMUSG00000000276	Dgke	3.93
ENSMUSG00000090630	Gm17403	3.92
ENSMUSG00000073057	Gm10462	3.91
ENSMUSG00000041165	Spem1	3.89
ENSMUSG00000021898	Asb14	3.89
ENSMUSG00000048521	Cxcr6	3.88
ENSMUSG00000042671	Rgs8	3.87
ENSMUSG00000078919	Dpm1	3.86
ENSMUSG00000022176	Rem2	3.85
ENSMUSG00000043807	Ly6g5b	3.83
ENSMUSG00000082596	Gm14227	3.82
ENSMUSG00000047586	Nccrp1	3.80
ENSMUSG00000093677	RP23-102L5.1	3.79
ENSMUSG00000061451	Tmem151a	3.79
ENSMUSG00000091313	Fth-ps2	3.79
ENSMUSG00000093396	RP23-285E19.5	3.78
ENSMUSG00000030730	Atp2a1	3.77
ENSMUSG00000092325	Gm18284	3.76
ENSMUSG00000092595	Gm20427	3.75
ENSMUSG00000087249	Gm16062	3.74
ENSMUSG00000022686	B3gnt5	3.72
ENSMUSG00000039521	Foxp3	3.70
ENSMUSG00000034209	Rasl10a	3.70

ENSMUSG00000023905	Tnfrsf12a	3.69
ENSMUSG00000090157	Gm16534	3.68
ENSMUSG00000044197	Gpr146	3.66
ENSMUSG00000003282	Plag1	3.63
ENSMUSG00000020275	Rel	3.63
ENSMUSG00000056537	Rlim	3.60
ENSMUSG00000085219	Gm16617	3.59
ENSMUSG00000052374	Actn2	3.58
ENSMUSG00000003949	Hlf	3.58
ENSMUSG00000033544	Angptl1	3.57
ENSMUSG00000054556	Gm4876	3.55
ENSMUSG00000038876	Rnf146	3.52
ENSMUSG00000088185	Scarna2	3.51
ENSMUSG00000059229	Gm6802	3.49
ENSMUSG00000032515	Csrnp1	3.48
ENSMUSG00000006218	Fam131c	3.47
ENSMUSG00000038594	Gm9766	3.46
ENSMUSG00000029360	Gm9754	3.46
ENSMUSG00000092837	AC027184.1	3.45
ENSMUSG00000030203	Dusp16	3.45
ENSMUSG00000073102	Ccdc164	3.45
ENSMUSG00000090353	Gm17555	3.44
ENSMUSG00000024186	Rgs11	3.44
ENSMUSG00000085133	B930095G15Rik	3.42
ENSMUSG00000040809	Chi3l3	3.42
ENSMUSG00000091447	Gm17386	3.41
ENSMUSG00000033987	Dnahc17	3.41
ENSMUSG00000085778	Gm16892	3.40
ENSMUSG00000087458	Gm13999	3.39
ENSMUSG00000030268	Bcat1	3.39
ENSMUSG00000091035	Gm17659	3.38
ENSMUSG00000075118	Gpr137b-ps	3.35
ENSMUSG00000079609	Gm17371	3.34
ENSMUSG00000044934	Zfp367	3.33
ENSMUSG00000008686	Zfp955a	3.32
ENSMUSG00000022018	1190002H23Rik	3.31
ENSMUSG00000080885	Gm4167	3.30
ENSMUSG00000072969	Armcx5	3.30
ENSMUSG00000085233	B230208H11Rik	3.30
ENSMUSG00000032262	Elovl4	3.29
ENSMUSG00000079259	Trim71	3.29
ENSMUSG00000054477	Kcnn2	3.26
ENSMUSG00000054999	Naaladl1	3.25

ENSMUSG00000074141	Il4i1	3.25
ENSMUSG00000074277	Phldb3	3.23
ENSMUSG00000039545	4930524L23Rik	3.23
ENSMUSG00000051726	Kcnf1	3.22
ENSMUSG00000020889	Nr1d1	3.22
ENSMUSG00000040840	4930579G18Rik	3.21
ENSMUSG00000086950	Gm16907	3.19
ENSMUSG00000071076	Jund	3.19
ENSMUSG00000040424	Hipk4	3.19
ENSMUSG00000074603	Gm10729	3.19
ENSMUSG00000081305	Gm12879	3.19
ENSMUSG00000070803	Cited4	3.17
ENSMUSG00000051455	Gm1564	3.17
ENSMUSG00000068614	Actc1	3.17
ENSMUSG00000039770	Ypel5	3.17
ENSMUSG00000035329	Fbxo33	3.16
ENSMUSG00000032531	Amotl2	3.16
ENSMUSG00000030161	Gabarapl1	3.14
ENSMUSG00000091877	Gm17699	3.14
ENSMUSG00000038132	Rbm24	3.14
ENSMUSG00000053774	Ubxn7	3.14
ENSMUSG00000083907	Plk-ps1	3.13
ENSMUSG00000020282	Rhbdf1	3.13
ENSMUSG00000087359	Gm17478	3.13
ENSMUSG00000037885	Stk35	3.12
ENSMUSG00000000078	Klf6	3.12
ENSMUSG00000024843	Chka	3.11
ENSMUSG00000036840	Siah1a	3.11
ENSMUSG00000086472	Gm16172	3.10
ENSMUSG00000091943	A730099G02Rik	3.10
ENSMUSG00000037638	Zbtb42	3.09
ENSMUSG00000042246	Tmc7	3.09
ENSMUSG00000068105	Tnfrsf13c	3.09
ENSMUSG00000004267	Eno2	3.08
ENSMUSG00000040010	Slc7a5	3.08
ENSMUSG00000012123	Aim1l	3.08
ENSMUSG00000083849	Gm13477	3.06
ENSMUSG00000085964	Gm16983	3.05
ENSMUSG00000084925	1810062O18Rik	3.04
ENSMUSG00000046085	4931422A03Rik	3.03
ENSMUSG00000028681	Ptch2	3.03
ENSMUSG00000085612	Gm15868	3.02
ENSMUSG00000066538	Gm6254	3.02

ENSMUSG00000086143	Gm16685	3.01
ENSMUSG00000029752	Asns	3.01
ENSMUSG00000022280	Rnf19a	3.01
ENSMUSG00000055657	E030030I06Rik	3.00
ENSMUSG00000041025	Iffo2	3.00
ENSMUSG00000028836	Slc30a2	3.00
ENSMUSG00000090426	Gm17392	3.00
ENSMUSG00000085950	Gm13589	2.99
ENSMUSG00000082985	Gm14042	2.99
ENSMUSG00000071658	Gng3	2.98
ENSMUSG00000090299	Gm17295	2.98
ENSMUSG00000032285	Dnaja4	2.98
ENSMUSG00000086597	F420014N23Rik	2.97
ENSMUSG00000085246	Gm15893	2.97
ENSMUSG00000032525	Nktr	2.97
ENSMUSG00000067199	Frat1	2.96
ENSMUSG00000090377	Gm8281	2.95
ENSMUSG00000029186	Pi4k2b	2.95
ENSMUSG00000091956	C2cd4b	2.94
ENSMUSG00000051246	A930005I04Rik	2.93
ENSMUSG00000072623	Zfp9	2.92
ENSMUSG00000024486	Hbegf	2.91
ENSMUSG00000038239	Hrc	2.91
ENSMUSG00000074102	Rbm15b	2.89
ENSMUSG00000026788	Zbtb43	2.89
ENSMUSG00000049092	Gpr137c	2.89
ENSMUSG00000024014	Pim1	2.89
ENSMUSG00000033478	Fam160b1	2.89
ENSMUSG00000027071	P2rx3	2.88
ENSMUSG00000063254	B230325K18Rik	2.86
ENSMUSG00000087077	Gm12480	2.86
ENSMUSG00000050240	Hic2	2.86
ENSMUSG00000020482	Ccdc117	2.86
ENSMUSG00000024402	Lta	2.84
ENSMUSG00000092023	Gm17496	2.83
ENSMUSG00000049799	Lrrc19	2.82
ENSMUSG00000080768	Gm12219	2.82
ENSMUSG00000056749	Nfil3	2.82
ENSMUSG00000069053	Ube1y1	2.81
ENSMUSG00000018169	Mfng	2.81
ENSMUSG00000069806	Cacng7	2.80
ENSMUSG00000091833	Gm17317	2.80
ENSMUSG00000051949	2010005H15Rik	2.80

ENSMUSG00000052040	Klf13	2.79
ENSMUSG00000087126	1700109K24Rik	2.79
ENSMUSG00000090986	Gm17275	2.78
ENSMUSG00000049692	4933425O20Rik	2.78
ENSMUSG00000020234	4930404N11Rik	2.78
ENSMUSG00000029314	Agpat9	2.77
ENSMUSG00000093650	RP23-454G7.1	2.76
ENSMUSG00000048732	Klhl11	2.76
ENSMUSG00000006675	P4htm	2.74
ENSMUSG00000039967	Zfp292	2.74
ENSMUSG00000039968	Rsbn1l	2.74
ENSMUSG00000061532	Zfp955b	2.73
ENSMUSG00000008855	Hdac5	2.73
ENSMUSG00000090286	Gm17615	2.73
ENSMUSG00000093470	RP23-164N15.3	2.73
ENSMUSG00000036450	Hif1an	2.72
ENSMUSG00000078859	Gm17491	2.72
ENSMUSG00000025408	Ddit3	2.72
ENSMUSG00000080830	Gm12671	2.72
ENSMUSG00000033107	Rnf125	2.71
ENSMUSG00000048807	Slc35e4	2.70
ENSMUSG00000079615	Hspa14	2.70
ENSMUSG00000031559	4930555F03Rik	2.69
ENSMUSG00000045176	2310047M10Rik	2.69
ENSMUSG00000040423	Rc3h1	2.69
ENSMUSG00000087267	4933427J07Rik	2.69
ENSMUSG00000031266	Gla	2.68
ENSMUSG00000024347	Psd2	2.68
ENSMUSG00000040435	Ppp1r15a	2.68
ENSMUSG00000025515	Muc2	2.67
ENSMUSG00000085328	Gm17131	2.67
ENSMUSG00000028680	Plk3	2.67
ENSMUSG00000085963	Gm15249	2.66
ENSMUSG00000078667	1700094D03Rik	2.66
ENSMUSG00000033998	Kcnk1	2.66
ENSMUSG00000022429	Dmc1	2.66
ENSMUSG00000021752	Kctd6	2.66
ENSMUSG00000027196	4921507L20Rik	2.65
ENSMUSG00000020948	Klhl28	2.65
ENSMUSG00000092279	1500011B03Rik	2.64
ENSMUSG00000006494	Pdk1	2.64
ENSMUSG00000036181	Hist1h1c	2.63
ENSMUSG00000078808	Vmn1r58	2.63

ENSMUSG00000034117	Gpr44	2.63
ENSMUSG00000091944	Gm17517	2.63
ENSMUSG00000006930	Hap1	2.62
ENSMUSG00000064032	Gm10143	2.62
ENSMUSG00000053411	Cbx7	2.62
ENSMUSG00000019558	Slc6a8	2.62
ENSMUSG00000030748	Il4ra	2.62
ENSMUSG00000021770	Samd8	2.61
ENSMUSG00000015312	Gadd45b	2.61
ENSMUSG00000090384	Gm17492	2.61
ENSMUSG00000079254	Itprip	2.61
ENSMUSG00000086782	E130102H24Rik	2.59
ENSMUSG00000029385	Ccng2	2.59
ENSMUSG00000067626	Gm17245	2.59
ENSMUSG00000018427	Ypel2	2.59
ENSMUSG00000007812	Zfp655	2.59
ENSMUSG00000090599	AL626783.1	2.59
ENSMUSG00000073060	Zxda	2.58
ENSMUSG00000084835	Gm12352	2.58
ENSMUSG00000030963	Umod	2.58
ENSMUSG00000090435	Gm6410	2.58
ENSMUSG00000047227	Gm527	2.58
ENSMUSG00000035828	Pim3	2.58
ENSMUSG00000057666	Gapdh	2.58
ENSMUSG00000086607	4930511M06Rik	2.58
ENSMUSG00000062519	Zfp398	2.57
ENSMUSG00000060036	Rpl3	2.57
ENSMUSG00000021678	F2rl1	2.57
ENSMUSG00000050459	Gm17646	2.56
ENSMUSG00000047141	Zfp654	2.56
ENSMUSG00000046962	Zfp295	2.56
ENSMUSG00000020108	Ddit4	2.56
ENSMUSG00000087298	Gm9392	2.55
ENSMUSG00000048794	Ccdc37	2.55
ENSMUSG00000071562	Stfa1	2.54
ENSMUSG00000031770	Herpud1	2.54
ENSMUSG00000070644	Etnk2	2.54
ENSMUSG00000078624	Olfr613	2.53
ENSMUSG00000086878	Miat	2.53
ENSMUSG00000007021	Syngr3	2.52
ENSMUSG00000044068	Zrsr1	2.52
ENSMUSG00000021032	Ngb	2.52
ENSMUSG00000030310	Slc6a1	2.52

ENSMUSG00000025450	Gm9752	2.52
ENSMUSG00000035992	Fnip1	2.51
ENSMUSG00000027555	Car13	2.51
ENSMUSG00000085829	Gm4285	2.50
ENSMUSG00000016559	H3f3b	2.50
ENSMUSG00000074925	Ptar1	2.50
ENSMUSG00000030327	Necap1	2.50
ENSMUSG00000056445	5730446D14Rik	2.50
ENSMUSG00000049878	Rlf	2.50
ENSMUSG00000074422	Gm17312	2.50
ENSMUSG00000037214	Thap1	2.49
ENSMUSG00000033933	Vhl	2.49
ENSMUSG00000080850	Gm12439	2.49
ENSMUSG00000022553	Maf1	2.49
ENSMUSG00000044636	Csrnp2	2.48
ENSMUSG00000026977	March7	2.48
ENSMUSG00000028850	Gpatch3	2.48
ENSMUSG00000049800	Sertad2	2.48
ENSMUSG00000025612	Bach1	2.47
ENSMUSG00000085623	Gm16041	2.47
ENSMUSG00000025019	Lcor	2.47
ENSMUSG00000051343	Rab11fip5	2.47
ENSMUSG00000092341	Malat1	2.47
ENSMUSG00000009876	Cox4i2	2.47
ENSMUSG00000038700	Hoxb5	2.46
ENSMUSG00000038894	Irs2	2.46
ENSMUSG00000090673	Gm340	2.46
ENSMUSG00000083594	Gm13722	2.46
ENSMUSG00000048911	Rnf24	2.46
ENSMUSG00000040714	Klc3	2.46
ENSMUSG00000059277	R74862	2.46
ENSMUSG00000085913	Gm15601	2.45
ENSMUSG00000021189	Atxn3	2.45
ENSMUSG00000033883	D3Ertd254e	2.45
ENSMUSG00000086723	Gm16601	2.45
ENSMUSG00000061331	Gm17132	2.45
ENSMUSG00000039452	Snx22	2.45
ENSMUSG00000025025	Mxi1	2.45
ENSMUSG00000078936	2410002O22Rik	2.45
ENSMUSG00000086841	2410006H16Rik	2.44
ENSMUSG00000047115	D330028D13Rik	2.44
ENSMUSG00000047153	Khnyn	2.44
ENSMUSG00000021733	Slc4a7	2.44

ENSMUSG00000084834	4930565N06Rik	2.44
ENSMUSG00000093385	A330044P14Rik	2.44
ENSMUSG00000043415	Otud1	2.44
ENSMUSG00000038646	Fam103a1	2.44
ENSMUSG00000022124	Fbxl3	2.43
ENSMUSG00000032219	Tex9	2.43
ENSMUSG00000090721	Gm17632	2.43
ENSMUSG00000002266	Zim1	2.43
ENSMUSG00000035840	Lysmd3	2.43
ENSMUSG00000052684	Jun	2.43
ENSMUSG00000072566	Pvt1	2.42
ENSMUSG00000020363	Gfpt2	2.42
ENSMUSG00000042501	Cpa6	2.42
ENSMUSG00000044519	Zfp488	2.42
ENSMUSG00000091737	Gm17543	2.42
ENSMUSG00000038002	Cramp1l	2.42
ENSMUSG00000044037	Als2cl	2.41
ENSMUSG00000020894	Vamp2	2.41
ENSMUSG00000054178	Gm9938	2.41
ENSMUSG00000025762	Larp1b	2.40
ENSMUSG00000021028	Mbip	2.39
ENSMUSG00000066278	Vps37b	2.39
ENSMUSG00000028933	Xrcc2	2.39
ENSMUSG00000052763	Zfp212	2.39
ENSMUSG00000084364	Gm15801	2.38
ENSMUSG00000089954	Gm8783	2.38
ENSMUSG00000051639	Gm5812	2.38
ENSMUSG00000037857	Nufip2	2.38
ENSMUSG00000079470	Utp14b	2.38
ENSMUSG00000059146	Ntrk3	2.38
ENSMUSG00000020485	Supt4h1	2.38
ENSMUSG00000055926	Gm14137	2.37
ENSMUSG00000090541	Gm17487	2.36
ENSMUSG00000017418	Arl5b	2.36
ENSMUSG00000034686	Prr7	2.36
ENSMUSG00000074909	Ranbp6	2.36
ENSMUSG00000090674	Gm17082	2.36
ENSMUSG00000040167	Ikzf5	2.36
ENSMUSG00000043614	Vps37d	2.35
ENSMUSG00000001270	Ckb	2.34
ENSMUSG00000047632	Fgfbp3	2.34
ENSMUSG00000053600	Zfp472	2.33
ENSMUSG00000084845	Gm5151	2.33

ENSMUSG00000091384	Gm17574	2.32
ENSMUSG00000027164	Traf6	2.32
ENSMUSG00000022178	Jub	2.32
ENSMUSG00000038352	Arl5c	2.32
ENSMUSG00000062861	Zfp28	2.32
ENSMUSG00000040302	C030048B08Rik	2.31
ENSMUSG00000048271	Rbm33	2.31
ENSMUSG00000029627	Zkscan14	2.31
ENSMUSG00000017639	Rab11fip4	2.31
ENSMUSG00000052979	6530403G13Rik	2.31
ENSMUSG00000044814	Olfr543	2.30
ENSMUSG00000091784	Gm17022	2.30
ENSMUSG00000033863	Klf9	2.29
ENSMUSG00000033770	Clcnka	2.29
ENSMUSG00000042507	C130039O16Rik	2.29
ENSMUSG00000027896	Slc16a4	2.28
ENSMUSG00000047155	Cyp4x1	2.28
ENSMUSG00000073421	H2-Ab1	2.28
ENSMUSG00000029027	Dffb	2.28
ENSMUSG00000089647	Gm2245	2.28
ENSMUSG00000020525	Ppm1d	2.28
ENSMUSG00000014353	Tmem87b	2.28
ENSMUSG00000062175	Tgif2	2.27
ENSMUSG00000090264	Eif4ebp3	2.27
ENSMUSG00000031340	Gabre	2.27
ENSMUSG00000087696	Gm16957	2.27
ENSMUSG00000028865	Cd164l2	2.27
ENSMUSG00000027427	Polr3f	2.27
ENSMUSG00000048109	Rbm15	2.27
ENSMUSG00000004661	Arid3b	2.27
ENSMUSG00000051316	Taf7	2.26
ENSMUSG00000030672	Mylpf	2.26
ENSMUSG00000028348	Murc	2.26
ENSMUSG00000049907	Rasl11b	2.26
ENSMUSG00000085635	Gm14565	2.26
ENSMUSG00000063730	Hsd3b2	2.26
ENSMUSG00000087566	C920006O11Rik	2.26
ENSMUSG00000024459	H2-M5	2.26
ENSMUSG00000074580	4931440P22Rik	2.25
ENSMUSG00000026289	Atg16l1	2.25
ENSMUSG00000062098	Btbd3	2.25
ENSMUSG00000048216	Gpr85	2.25
ENSMUSG00000035694	Caps2	2.25

ENSMUSG00000048701	Ccdc6	2.24
ENSMUSG00000023707	Ogfod2	2.24
ENSMUSG00000075389	2810410L24Rik	2.24
ENSMUSG00000092086	Gm6793	2.24
ENSMUSG00000028967	Errfi1	2.24
ENSMUSG00000037111	Setd7	2.24
ENSMUSG00000032294	Pkm2	2.23
ENSMUSG00000089736	Gm14378	2.23
ENSMUSG00000023067	Cdkn1a	2.22
ENSMUSG00000027803	Wwtr1	2.22
ENSMUSG00000075701	H47	2.22
ENSMUSG00000048696	Mex3d	2.22
ENSMUSG00000078671	Chd2	2.22
ENSMUSG00000044349	Snhg11	2.22
ENSMUSG00000030695	Aldoa	2.22
ENSMUSG00000042595	Fam199x	2.22
ENSMUSG00000028630	Dyrk2	2.22
ENSMUSG00000063229	Ldha	2.22
ENSMUSG00000017412	Cacnb4	2.21
ENSMUSG00000041096	Tspyl2	2.21
ENSMUSG00000031765	Mt1	2.21
ENSMUSG00000033319	Fem1c	2.21
ENSMUSG00000084903	Gm16624	2.21
ENSMUSG00000017740	Slc12a5	2.21
ENSMUSG00000091909	Gm17282	2.21
ENSMUSG00000042724	Map3k9	2.21
ENSMUSG00000085685	Gm15253	2.21
ENSMUSG00000085988	Gm16896	2.21
ENSMUSG00000085492	Trmt61b	2.20
ENSMUSG00000029449	Rhof	2.20
ENSMUSG00000026094	Stk17b	2.20
ENSMUSG00000042650	Alkbh5	2.20
ENSMUSG00000027660	Skil	2.20
ENSMUSG00000032424	Snhg5	2.20
ENSMUSG00000038526	Car14	2.20
ENSMUSG00000031490	Eif4ebp1	2.19
ENSMUSG00000029001	Fbxo44	2.19
ENSMUSG00000028389	Zfp37	2.19
ENSMUSG00000086537	Nespas	2.19
ENSMUSG00000069114	Zbtb10	2.19
ENSMUSG00000027806	Tsc22d2	2.19
ENSMUSG00000032375	Aph1b	2.19
ENSMUSG00000086859	2810008D09Rik	2.19

ENSMUSG00000051495	Irf2bp2	2.19
ENSMUSG00000028035	Dnajb4	2.19
ENSMUSG00000049723	Mmp12	2.19
ENSMUSG00000050310	Rictor	2.18
ENSMUSG00000038806	BC031781	2.18
ENSMUSG00000022051	Bnip3l	2.18
ENSMUSG00000000942	Hoxa4	2.18
ENSMUSG00000085767	Gm13563	2.18
ENSMUSG00000062044	Lmtk3	2.18
ENSMUSG00000041548	Hspb8	2.17
ENSMUSG00000042675	Ypel3	2.17
ENSMUSG00000052415	Tchh	2.17
ENSMUSG00000034300	Fam53c	2.17
ENSMUSG00000037239	Spred3	2.17
ENSMUSG00000032135	Mcam	2.17
ENSMUSG00000045005	Fzd5	2.17
ENSMUSG00000017754	Pltp	2.17
ENSMUSG00000063652	Slc22a21	2.17
ENSMUSG00000081094	Rpl19-ps11	2.16
ENSMUSG00000054364	Rhob	2.16
ENSMUSG00000085360	Gm11647	2.16
ENSMUSG00000039989	Cbx4	2.16
ENSMUSG00000032238	Rora	2.16
ENSMUSG00000037876	Jmjd1c	2.16
ENSMUSG00000034640	Tiparp	2.16
ENSMUSG00000073761	4933427I04Rik	2.16
ENSMUSG00000037474	Dtl	2.15
ENSMUSG00000024924	Vldlr	2.15
ENSMUSG00000024570	Rbfa	2.15
ENSMUSG00000020277	Pfkl	2.15
ENSMUSG00000062070	Pgk1	2.15
ENSMUSG00000032251	Irak1bp1	2.15
ENSMUSG00000092400	Gm20469	2.15
ENSMUSG00000031860	Pbx4	2.15
ENSMUSG00000050097	Ces2b	2.15
ENSMUSG00000081471	Gm14735	2.15
ENSMUSG00000086753	Gm15751	2.14
ENSMUSG00000024530	Slmo1	2.14
ENSMUSG00000089940	Gm4117	2.14
ENSMUSG00000023966	Rsph9	2.14
ENSMUSG00000021265	Slc25a29	2.14
ENSMUSG00000038705	Gmeb2	2.13
ENSMUSG00000001864	Aif1l	2.13

ENSMUSG00000086894	Gm15708	2.13
ENSMUSG00000019916	P4ha1	2.13
ENSMUSG00000040943	Tet2	2.13
ENSMUSG00000006262	Mob1b	2.13
ENSMUSG00000087562	Gm16754	2.13
ENSMUSG00000085444	Gm13936	2.12
ENSMUSG00000085795	Zfp703	2.12
ENSMUSG00000023336	Wfdc1	2.12
ENSMUSG00000048429	1810026J23Rik	2.12
ENSMUSG00000084842	Pabpc1l2b-ps	2.12
ENSMUSG00000063524	Eno1	2.12
ENSMUSG00000027829	Ccnl1	2.12
ENSMUSG00000083405	Gm15725	2.12
ENSMUSG00000070858	Gm1673	2.12
ENSMUSG00000028081	Rps3a	2.12
ENSMUSG00000015837	Sqstm1	2.12
ENSMUSG00000040540	Gm9770	2.12
ENSMUSG00000074264	Amy1	2.11
ENSMUSG00000089828	Gm16300	2.11
ENSMUSG00000020653	Klf11	2.11
ENSMUSG00000093412	RP23-103L13.8	2.11
ENSMUSG00000040594	Ranbp17	2.11
ENSMUSG00000084824	Gm16344	2.11
ENSMUSG00000035399	3230401D17Rik	2.11
ENSMUSG00000031837	Necab2	2.11
ENSMUSG00000078599	Skint8	2.11
ENSMUSG00000058906	Zfp353	2.10
ENSMUSG00000030087	Klf15	2.10
ENSMUSG00000029797	Sspo	2.10
ENSMUSG00000031530	Dusp4	2.10
ENSMUSG00000035929	H2-Q4	2.10
ENSMUSG00000006445	Epha2	2.10
ENSMUSG00000046456	Tmem150b	2.10
ENSMUSG00000028701	1520402A15Rik	2.10
ENSMUSG00000042750	Bex2	2.10
ENSMUSG00000042506	Usp22	2.09
ENSMUSG00000029576	Radil	2.09
ENSMUSG00000037108	Zcwpw1	2.09
ENSMUSG00000041779	Tram2	2.09
ENSMUSG00000053666	Gm9917	2.09
ENSMUSG00000062627	Mysm1	2.09
ENSMUSG00000087299	Gm12953	2.09
ENSMUSG00000021460	Auh	2.09

ENSMUSG00000086615	Gm16862	2.09
ENSMUSG00000028521	Slc35d1	2.09
ENSMUSG00000059013	Sh2d3c	2.08
ENSMUSG00000022507	1810013L24Rik	2.08
ENSMUSG00000073433	Arhgdig	2.08
ENSMUSG00000006585	Cdt1	2.08
ENSMUSG00000040918	Slc19a2	2.08
ENSMUSG00000039137	Whrn	2.08
ENSMUSG00000068394	Cep152	2.08
ENSMUSG00000021215	Net1	2.08
ENSMUSG00000022999	Lmbr1l	2.08
ENSMUSG00000022490	Ppp1r1a	2.07
ENSMUSG00000015342	Xk	2.07
ENSMUSG00000002799	Jag2	2.07
ENSMUSG00000029068	Ccnl2	2.07
ENSMUSG00000047976	Kcna1	2.07
ENSMUSG00000048027	Rgmb	2.06
ENSMUSG00000041679	Lrrc29	2.06
ENSMUSG00000031861	Lpar2	2.06
ENSMUSG00000023456	Tpi1	2.06
ENSMUSG00000040929	Rfx3	2.06
ENSMUSG00000047843	Bri3	2.06
ENSMUSG00000028793	Rnf19b	2.06
ENSMUSG00000015202	Cnksr3	2.06
ENSMUSG00000051379	Flrt3	2.06
ENSMUSG00000041040	Fam117b	2.06
ENSMUSG00000090613	Gm17630	2.06
ENSMUSG00000092232	Gm20521	2.06
ENSMUSG00000040715	Rsc1a1	2.06
ENSMUSG00000032593	Amigo3	2.06
ENSMUSG00000067786	Nnat	2.06
ENSMUSG00000066442	Mthfs	2.06
ENSMUSG00000090739	D930016D06Rik	2.05
ENSMUSG00000092149	Gm17453	2.05
ENSMUSG00000001930	Vwf	2.05
ENSMUSG00000040441	Slc26a10	2.05
ENSMUSG00000044617	Zbtb39	2.05
ENSMUSG00000006014	Prg4	2.05
ENSMUSG00000039376	Synpo2l	2.05
ENSMUSG00000053094	0610007L01Rik	2.05
ENSMUSG00000036934	4921524J17Rik	2.05
ENSMUSG00000038738	Shank1	2.05
ENSMUSG00000037993	Dhx38	2.05

ENSMUSG00000091952	Gm17709	2.04
ENSMUSG00000034059	Ypel4	2.04
ENSMUSG00000027961	Lrrc39	2.04
ENSMUSG00000087502	Gm16091	2.04
ENSMUSG00000082894	Gm6480	2.04
ENSMUSG00000062901	Klhl24	2.04
ENSMUSG00000003031	Cdkn1b	2.04
ENSMUSG00000018554	Ybx2	2.04
ENSMUSG00000032599	Ip6k2	2.03
ENSMUSG00000073374	C030034I22Rik	2.03
ENSMUSG00000019897	Ccdc59	2.03
ENSMUSG00000029110	Rnf4	2.03
ENSMUSG00000093709	RP23-278M16.2	2.03
ENSMUSG00000033054	Npat	2.03
ENSMUSG00000057914	Cacnb2	2.03
ENSMUSG00000000282	Mnt	2.03
ENSMUSG00000047370	Gm7367	2.03
ENSMUSG00000087231	E230016M11Rik	2.03
ENSMUSG00000087590	2410004N09Rik	2.03
ENSMUSG00000016984	Etaa1	2.03
ENSMUSG00000042032	Mat2b	2.03
ENSMUSG00000029389	Ddx55	2.02
ENSMUSG00000063160	Numbl	2.02
ENSMUSG00000070822	Zscan18	2.01
ENSMUSG00000022619	Mapk8ip2	2.01
ENSMUSG00000074220	Zfp382	2.01
ENSMUSG00000074873	AI606181	2.01
ENSMUSG00000042688	Mapk6	2.01
ENSMUSG00000026457	Adipor1	2.01
ENSMUSG00000004347	Pde1c	2.01
ENSMUSG00000074115	Saa1	2.01
ENSMUSG00000025938	Slco5a1	2.01
ENSMUSG00000038174	Fam126b	2.00
ENSMUSG00000037573	Tob1	2.00
ENSMUSG00000027245	2310003F16Rik	2.00
ENSMUSG00000039789	Zfp597	2.00
ENSMUSG00000036898	Zfp157	2.00
ENSMUSG00000044628	Rnf208	2.00
ENSMUSG00000055725	Paqr3	2.00
ENSMUSG00000042390	Gatad2b	2.00
ENSMUSG00000038572	Bpifb5	1.99
ENSMUSG00000027397	Slc20a1	1.99
ENSMUSG00000037808	Fam76b	1.99

ENSMUSG00000022837	Iqcb1	1.99
ENSMUSG00000070424	Art5	1.99
ENSMUSG00000044551	9930012K11Rik	1.99
ENSMUSG00000045466	Zfp956	1.99
ENSMUSG00000024695	Zfp91	1.98
ENSMUSG00000033594	Spata2l	1.98
ENSMUSG00000085936	2610307P16Rik	1.98
ENSMUSG00000049357	4933408B17Rik	1.97
ENSMUSG00000052783	Grk4	1.97
ENSMUSG00000026458	Ppfia4	1.97
ENSMUSG00000074794	Arrdc3	1.97
ENSMUSG00000027324	Rpusd2	1.97
ENSMUSG00000085337	Gm15964	1.97
ENSMUSG00000000531	Grasp	1.97
ENSMUSG00000029290	Zfp326	1.97
ENSMUSG00000046727	0610010O12Rik	1.96
ENSMUSG00000020875	Hoxb9	1.96
ENSMUSG00000028654	Mycl1	1.96
ENSMUSG00000021772	Nkiras1	1.96
ENSMUSG00000086627	Gm16702	1.96
ENSMUSG00000038612	Mcl1	1.96
ENSMUSG00000022415	Syngr1	1.96
ENSMUSG00000027954	Efna1	1.96
ENSMUSG00000050628	Fam100b	1.96
ENSMUSG00000009741	Ubp1	1.96
ENSMUSG00000060260	Pwwp2b	1.95
ENSMUSG00000034429	Zfp707	1.95
ENSMUSG00000087026	A230103J11Rik	1.95
ENSMUSG00000038206	Fbxo8	1.95
ENSMUSG00000079036	Alkbh1	1.95
ENSMUSG00000017009	Sdc4	1.95
ENSMUSG00000085373	B130046B21Rik	1.95
ENSMUSG00000035235	Trim13	1.95
ENSMUSG00000069895	Atxn1l	1.95
ENSMUSG00000041731	Pgm5	1.95
ENSMUSG00000082609	Gm15464	1.95
ENSMUSG00000028463	Car9	1.95
ENSMUSG00000060981	Hist1h4h	1.95
ENSMUSG00000074165	Zfp788	1.95
ENSMUSG00000024298	Zfp871	1.94
ENSMUSG00000041483	Zfp281	1.94
ENSMUSG00000068396	Rpl34-ps1	1.94
ENSMUSG00000086189	Gm15462	1.94

ENSMUSG00000078302	Foxd1	1.94
ENSMUSG00000034908	Sidt2	1.94
ENSMUSG00000052656	Rnf103	1.94
ENSMUSG00000032712	2810474O19Rik	1.94
ENSMUSG00000028195	Cyr61	1.94
ENSMUSG00000050192	Eif5a2	1.94
ENSMUSG00000044792	Isca1	1.94
ENSMUSG00000042308	Setd1a	1.94
ENSMUSG00000047417	Rexo1	1.93
ENSMUSG00000043993	2900052L18Rik	1.93
ENSMUSG00000055128	Cgrrf1	1.93
ENSMUSG00000019756	Prl8a1	1.93
ENSMUSG00000023286	Ube2j2	1.93
ENSMUSG00000046999	1110032F04Rik	1.93
ENSMUSG00000045114	Prrt2	1.93
ENSMUSG00000040722	Scamp5	1.92
ENSMUSG00000032641	Gpr19	1.92
ENSMUSG00000021699	Pde4d	1.92
ENSMUSG00000016526	Dyrk3	1.92
ENSMUSG00000028527	Ak4	1.92
ENSMUSG00000026638	Irf6	1.92
ENSMUSG00000049504	2810046L04Rik	1.92
ENSMUSG00000017386	Traf4	1.92
ENSMUSG00000062591	Tubb4a	1.92
ENSMUSG00000050394	Armcx6	1.92
ENSMUSG00000053581	Zfand2a	1.92
ENSMUSG00000042922	D130020L05Rik	1.92
ENSMUSG00000022358	Fbxo32	1.91
ENSMUSG00000022564	Grina	1.91
ENSMUSG00000047514	Tspyl1	1.91
ENSMUSG00000018648	Dusp14	1.91
ENSMUSG00000085008	Gm13399	1.91
ENSMUSG00000042198	Chchd7	1.91
ENSMUSG00000026643	Nmt2	1.91
ENSMUSG00000018322	Tomm34	1.91
ENSMUSG00000028857	Tmem222	1.90
ENSMUSG00000019977	Hbs1l	1.90
ENSMUSG00000024248	Cox7a2l	1.90
ENSMUSG00000026064	Ptp4a1	1.90
ENSMUSG00000028277	Ube2j1	1.90
ENSMUSG00000028134	Ptbp2	1.90
ENSMUSG00000027285	Haus2	1.90
ENSMUSG00000058558	Rpl5	1.90

ENSMUSG00000027739	Rab33b	1.90
ENSMUSG00000015127	Unkl	1.90
ENSMUSG00000061186	Sfmbt2	1.89
ENSMUSG00000019876	Pkib	1.89
ENSMUSG00000020354	Sgcd	1.89
ENSMUSG00000048997	Atxn7l2	1.89
ENSMUSG00000051166	Eml5	1.89
ENSMUSG00000027171	Prrg4	1.89
ENSMUSG00000071253	Slc25a16	1.89
ENSMUSG00000021830	Txndc16	1.89
ENSMUSG00000033618	Map3k13	1.89
ENSMUSG00000072774	Zfp951	1.89
ENSMUSG00000039879	Heca	1.89
ENSMUSG00000055200	Sertad3	1.89
ENSMUSG00000053198	Prx	1.89
ENSMUSG00000031812	Map1lc3b	1.89
ENSMUSG00000021306	Gpr137b	1.88
ENSMUSG00000021948	Prkcd	1.88
ENSMUSG00000038271	Iffo1	1.88
ENSMUSG00000034460	Six4	1.88
ENSMUSG00000037826	Ppm1k	1.88
ENSMUSG00000014704	Hoxa2	1.88
ENSMUSG00000025959	Klf7	1.88
ENSMUSG00000036411	9530077C05Rik	1.88
ENSMUSG00000037652	Phc3	1.88
ENSMUSG00000040415	Dtx3	1.88
ENSMUSG00000060550	H2-Q7	1.88
ENSMUSG00000058600	Rpl30	1.88
ENSMUSG00000044533	Rps2	1.88
ENSMUSG00000059920	4930453N24Rik	1.87
ENSMUSG00000044864	Ankrd50	1.87
ENSMUSG00000030704	Rab6a	1.87
ENSMUSG00000031450	Grk1	1.87
ENSMUSG00000043843	Tmem145	1.87
ENSMUSG00000090361	Gm17621	1.87
ENSMUSG00000073455	Gm3435	1.87
ENSMUSG00000011179	Odc1	1.87
ENSMUSG00000038909	Myst2	1.87
ENSMUSG00000030815	Phkg2	1.87
ENSMUSG00000013415	Igf2bp1	1.87
ENSMUSG00000039130	Zc3hc1	1.87
ENSMUSG00000089945	Gm20459	1.86
ENSMUSG00000032420	Nt5e	1.86

ENSMUSG00000073557	Ppp1r12b	1.86
ENSMUSG00000020205	Phlda1	1.86
ENSMUSG00000015120	Ube2i	1.86
ENSMUSG00000089989	Flt3l	1.86
ENSMUSG00000087142	Gm12454	1.86
ENSMUSG00000027936	Crtc2	1.86
ENSMUSG00000049804	Armcx4	1.86
ENSMUSG00000050071	Bex1	1.86
ENSMUSG00000021139	Gm20498	1.86
ENSMUSG00000081051	Gm15427	1.85
ENSMUSG00000021477	Ctsl	1.85
ENSMUSG00000024190	Dusp1	1.85
ENSMUSG00000001786	Fbxo7	1.85
ENSMUSG00000057751	Megf6	1.85
ENSMUSG00000052293	Taf9	1.85
ENSMUSG00000042197	Zfp451	1.85
ENSMUSG00000009630	Ppp2cb	1.85
ENSMUSG00000022453	Naga	1.85
ENSMUSG00000036427	Gpi1	1.84
ENSMUSG00000024410	3110002H16Rik	1.84
ENSMUSG00000084315	Vmn1r-ps128	1.84
ENSMUSG00000043085	Tmem82	1.84
ENSMUSG00000087490	A330076H08Rik	1.84
ENSMUSG00000029179	Zcchc4	1.84
ENSMUSG00000020680	Taf15	1.84
ENSMUSG00000051469	Zfp191	1.84
ENSMUSG00000087141	Plcxd2	1.84
ENSMUSG00000038872	Zfhx3	1.84
ENSMUSG00000029279	Brdt	1.84
ENSMUSG00000025723	Nmb	1.83
ENSMUSG00000015377	Fam116b	1.83
ENSMUSG00000021892	Sh3bp5	1.83
ENSMUSG00000025078	Nhlrc2	1.83
ENSMUSG00000036478	Btg1	1.83
ENSMUSG00000006127	Inpp5k	1.83
ENSMUSG00000048154	Mll2	1.83
ENSMUSG00000030276	Ttll3	1.83
ENSMUSG00000036390	Gadd45a	1.83
ENSMUSG00000031955	Bcar1	1.83
ENSMUSG00000020131	Pcsk4	1.82
ENSMUSG00000073474	A330023F24Rik	1.82
ENSMUSG00000031728	Zfp821	1.82
ENSMUSG00000014905	Dnajb9	1.82

ENSMUSG00000032010	Usp2	1.82
ENSMUSG00000021096	Ppm1a	1.82
ENSMUSG00000026121	Sema4c	1.82
ENSMUSG00000030337	Vamp1	1.82
ENSMUSG00000053293	Pom121	1.82
ENSMUSG00000067235	H2-Q10	1.82
ENSMUSG00000004843	Chmp2b	1.82
ENSMUSG00000074505	Fat3	1.82
ENSMUSG00000037321	Tap1	1.82
ENSMUSG00000038692	Hoxb4	1.82
ENSMUSG00000020561	Twistnb	1.82
ENSMUSG00000019808	Adat2	1.82
ENSMUSG00000024949	Sf1	1.82
ENSMUSG00000023505	Cdca3	1.81
ENSMUSG00000018906	P4ha2	1.81
ENSMUSG00000014602	Kif1a	1.81
ENSMUSG00000016940	Kctd2	1.81
ENSMUSG00000047844	Bex4	1.81
ENSMUSG00000055202	Zfp811	1.81
ENSMUSG00000033917	Gde1	1.81
ENSMUSG00000055436	Srsf11	1.81
ENSMUSG00000010067	Rassf1	1.81
ENSMUSG00000073867	AA474408	1.81
ENSMUSG00000046591	5730590G19Rik	1.81
ENSMUSG00000047648	Fbxo30	1.81
ENSMUSG00000074818	Pdzd7	1.81
ENSMUSG00000031970	Dbndd1	1.81
ENSMUSG00000042659	Arrdc4	1.81
ENSMUSG00000055296	D730040F13Rik	1.81
ENSMUSG00000042185	Nfrkb	1.81
ENSMUSG00000022884	Eif4a2	1.80
ENSMUSG00000044167	Foxo1	1.80
ENSMUSG00000034522	Zfp395	1.80
ENSMUSG00000017716	Birc5	1.80
ENSMUSG00000072960	BC065397	1.80
ENSMUSG00000032239	Rp9	1.80
ENSMUSG00000058779	Tomm20	1.80
ENSMUSG00000024462	Gabbr1	1.80
ENSMUSG00000036057	Ptpn23	1.80
ENSMUSG00000040663	Clcf1	1.80
ENSMUSG00000030059	Tmf1	1.80
ENSMUSG00000016528	Mapkapk2	1.80
ENSMUSG00000089993	Gm5822	1.79

ENSMUSG00000024301	Kifc5b	1.79
ENSMUSG00000029922	Mkrn1	1.79
ENSMUSG00000035293	G2e3	1.79
ENSMUSG00000029823	Luc7l2	1.79
ENSMUSG00000034248	Slc25a37	1.79
ENSMUSG00000047547	Cltb	1.79
ENSMUSG00000040321	Zfp770	1.79
ENSMUSG00000033307	Mif	1.79
ENSMUSG00000040006	BC013529	1.79
ENSMUSG00000003762	Adck4	1.79
ENSMUSG00000026822	Lcn2	1.79
ENSMUSG00000000594	Gm2a	1.79
ENSMUSG00000029022	Miip	1.79
ENSMUSG00000000753	Serpinf1	1.79
ENSMUSG00000064043	Trerf1	1.79
ENSMUSG00000027678	Ncoa3	1.79
ENSMUSG00000073647	Gm10557	1.79
ENSMUSG00000022947	Cbr3	1.78
ENSMUSG00000026436	Elk4	1.78
ENSMUSG00000001909	Trmt1	1.78
ENSMUSG00000040511	Pvr	1.78
ENSMUSG00000030967	Zranb1	1.78
ENSMUSG00000036185	Ng23	1.78
ENSMUSG00000035476	Tab3	1.78
ENSMUSG00000074129	Rpl13a	1.78
ENSMUSG00000036278	Macrod1	1.78
ENSMUSG00000021703	Serinc5	1.78
ENSMUSG00000026930	Gpsm1	1.78
ENSMUSG00000046364	Rpl27a	1.78
ENSMUSG00000000346	Dazap2	1.78
ENSMUSG00000007039	Ddah2	1.78
ENSMUSG00000046589	Lrrc8e	1.78
ENSMUSG00000007122	Casq1	1.78
ENSMUSG00000025034	Trim8	1.78
ENSMUSG00000042599	Jhdm1d	1.78
ENSMUSG00000042743	Sgtb	1.78
ENSMUSG00000035545	Leng8	1.77
ENSMUSG00000037415	Ranbp10	1.77
ENSMUSG00000027999	Pla2g12a	1.77
ENSMUSG00000082286	Pisd-ps1	1.77
ENSMUSG00000020105	Lrig3	1.77
ENSMUSG00000024889	Rce1	1.77
ENSMUSG00000041135	Ripk2	1.77

ENSMUSG00000033713	Foxn3	1.77
ENSMUSG00000064345	mt-Nd2	1.77
ENSMUSG00000031327	Chic1	1.77
ENSMUSG00000034317	Trim59	1.77
ENSMUSG00000038486	Sv2a	1.77
ENSMUSG00000074578	1500012F01Rik	1.77
ENSMUSG00000024002	Brd4	1.77
ENSMUSG00000030124	Lag3	1.77
ENSMUSG00000050299	Gm9843	1.76
ENSMUSG00000050368	Hoxd10	1.76
ENSMUSG00000029328	Hnrpdl	1.76
ENSMUSG00000067274	Rplp0	1.76
ENSMUSG00000056153	Socs6	1.76
ENSMUSG00000056501	Cebpb	1.76
ENSMUSG00000024163	Mapk8ip3	1.76
ENSMUSG00000031762	Mt2	1.76
ENSMUSG00000020978	Klhdc2	1.76
ENSMUSG00000014786	Slc9a5	1.76
ENSMUSG00000038227	Hoxa9	1.76
ENSMUSG00000034173	2410018M08Rik	1.76
ENSMUSG00000044258	Ctla2a	1.76
ENSMUSG00000042406	Atf4	1.76
ENSMUSG00000062929	Cfl2	1.76
ENSMUSG00000037174	Elf2	1.76
ENSMUSG00000073702	Rpl31	1.75
ENSMUSG00000042364	Snx18	1.75
ENSMUSG00000045282	Tmem86b	1.75
ENSMUSG00000037243	Zfp692	1.75
ENSMUSG00000020070	Rufy2	1.75
ENSMUSG00000020806	Rhbdf2	1.75
ENSMUSG00000039633	Lonrf1	1.75
ENSMUSG00000020265	Sumo3	1.75
ENSMUSG00000022009	Nufip1	1.75
ENSMUSG00000034953	1700047I17Rik2	1.75
ENSMUSG00000073083	Fam177a	1.75
ENSMUSG00000026426	Arl8a	1.75
ENSMUSG00000082016	Pgam1-ps2	1.74
ENSMUSG00000078429	Ctdsp2	1.74
ENSMUSG00000024608	Rps14	1.74
ENSMUSG00000040794	C1qtnf4	1.74
ENSMUSG00000026655	Fam107b	1.74
ENSMUSG00000020863	Luc7l3	1.74
ENSMUSG00000022974	Gcfc1	1.74

ENSMUSG00000044348	Mcart6	1.74
ENSMUSG00000048769	H1f0	1.74
ENSMUSG00000021661	Ankra2	1.74
ENSMUSG00000005802	Slc30a4	1.74
ENSMUSG00000030744	Rps3	1.74
ENSMUSG00000032595	Cdhr4	1.74
ENSMUSG00000016758	Bik	1.74
ENSMUSG00000048763	Hoxb3	1.74
ENSMUSG00000044912	Syt16	1.74
ENSMUSG00000035173	A630007B06Rik	1.74
ENSMUSG00000020109	Dnajb12	1.73
ENSMUSG00000028057	Rit1	1.73
ENSMUSG00000083705	Gm8624	1.73
ENSMUSG00000023495	Pcbp4	1.73
ENSMUSG00000070002	Ell	1.73
ENSMUSG00000023266	Frs3	1.73
ENSMUSG00000033417	2700078E11Rik	1.73
ENSMUSG00000029634	Rnf6	1.73
ENSMUSG00000029603	Dtx1	1.73
ENSMUSG00000052133	Sema5b	1.73
ENSMUSG00000011257	Pabpc4	1.73
ENSMUSG00000024379	Tslp	1.73
ENSMUSG00000022552	Sharpin	1.73
ENSMUSG00000050373	Snx21	1.73
ENSMUSG00000038520	Tbc1d17	1.72
ENSMUSG00000022389	Tef	1.72
ENSMUSG00000041841	Rpl37	1.72
ENSMUSG00000025872	Thoc3	1.72
ENSMUSG00000037369	Kdm6a	1.72
ENSMUSG00000033658	Ddx19b	1.72
ENSMUSG00000029714	Gigyf1	1.72
ENSMUSG00000029780	Nt5c3	1.72
ENSMUSG00000024112	Cacna1h	1.72
ENSMUSG00000008153	Clstn3	1.72
ENSMUSG00000031532	Tmem66	1.72
ENSMUSG00000050229	Pigm	1.72
ENSMUSG00000083097	Gm14494	1.72
ENSMUSG00000020284	1810043G02Rik	1.72
ENSMUSG00000024791	Cdca5	1.72
ENSMUSG00000034457	Eda2r	1.72
ENSMUSG00000038150	Ormdl3	1.72
ENSMUSG00000080727	C920021L13Rik	1.72
ENSMUSG00000023043	Krt18	1.72

ENSMUSG00000056895	Hist3h2ba	1.71
ENSMUSG00000055531	Cpsf6	1.71
ENSMUSG00000041560	Gltscr2	1.71
ENSMUSG00000041775	Mapk1ip1	1.71
ENSMUSG00000086252	C030044B11Rik	1.71
ENSMUSG00000057933	Gsta2	1.71
ENSMUSG00000039154	Shd	1.71
ENSMUSG00000047675	Rps8	1.71
ENSMUSG00000058838	Rps27a-ps2	1.71
ENSMUSG00000045128	Rpl18a	1.71
ENSMUSG00000039221	Rpl22l1	1.71
ENSMUSG00000084416	Rpl10a-ps1	1.71
ENSMUSG00000025899	Alkbh8	1.71
ENSMUSG00000003273	Car11	1.71
ENSMUSG00000021196	Pfkp	1.71
ENSMUSG00000052291	5330438D12Rik	1.71
ENSMUSG00000029131	Dnajb6	1.70
ENSMUSG00000037742	Eef1a1	1.70
ENSMUSG00000061232	H2-K1	1.70
ENSMUSG00000049517	Rps23	1.70
ENSMUSG00000069682	Gm10275	1.70
ENSMUSG00000025509	Pnpla2	1.70
ENSMUSG00000043168	4930426D05Rik	1.70
ENSMUSG00000067870	Gm8759	1.70
ENSMUSG00000032449	Slc25a36	1.70
ENSMUSG00000035725	Prkx	1.70
ENSMUSG00000032469	Dbr1	1.70
ENSMUSG00000019254	Ppp1r12c	1.70
ENSMUSG00000008348	Ubc	1.70
ENSMUSG00000023018	Smarcd1	1.70
ENSMUSG00000061167	Rpl15-ps3	1.70
ENSMUSG00000000296	Tpd52l1	1.70
ENSMUSG00000052253	Zfp622	1.70
ENSMUSG00000091171	Gm10060	1.70
ENSMUSG00000028788	Ptp4a2	1.70
ENSMUSG00000040857	Erf	1.70
ENSMUSG00000054150	4831426I19Rik	1.70
ENSMUSG00000064326	Siva1	1.70
ENSMUSG00000032518	Rpsa	1.69
ENSMUSG00000029056	Pank4	1.69
ENSMUSG00000038502	Ptov1	1.69
ENSMUSG00000066838	Zfp772	1.69
ENSMUSG00000028191	Bcl10	1.69

ENSMUSG00000025794	Rpl14	1.69
ENSMUSG00000087370	Tmem170b	1.69
ENSMUSG00000022426	Josd1	1.69
ENSMUSG00000082536	Gm13456	1.69
ENSMUSG00000027811	4930579G24Rik	1.69
ENSMUSG00000072568	Fam84b	1.69
ENSMUSG00000027162	Lin7c	1.69
ENSMUSG00000006333	Rps9	1.69
ENSMUSG00000040111	Gramd1b	1.69
ENSMUSG00000032399	Rpl4	1.69
ENSMUSG00000004952	Rasa4	1.69
ENSMUSG00000051790	Nlgn2	1.69
ENSMUSG00000071286	Sowahc	1.69
ENSMUSG00000066892	Fbxl12	1.69
ENSMUSG00000059811	Atl2	1.69
ENSMUSG00000018899	Irf1	1.69
ENSMUSG00000023904	Hcfc1r1	1.69
ENSMUSG00000045546	Rnf113a2	1.68
ENSMUSG00000034168	6430527G18Rik	1.68
ENSMUSG00000029844	Hoxa1	1.68
ENSMUSG00000026511	Srp9	1.68
ENSMUSG00000045248	Med26	1.68
ENSMUSG00000041895	Wipi1	1.68
ENSMUSG00000025407	Gli1	1.68
ENSMUSG00000025508	Rplp2	1.68
ENSMUSG00000008393	Carhsp1	1.68
ENSMUSG00000090137	Uba52	1.68
ENSMUSG00000045319	5430407P10Rik	1.68
ENSMUSG00000049764	Zfp280b	1.68
ENSMUSG00000029528	Pxn	1.68
ENSMUSG00000004951	Hspb1	1.68
ENSMUSG00000015882	Lcorl	1.68
ENSMUSG00000017390	Aldoc	1.68
ENSMUSG00000090000	Ier3ip1	1.67
ENSMUSG00000003131	Pafah1b2	1.67
ENSMUSG00000041642	Kif21b	1.67
ENSMUSG00000042524	Sun2	1.67
ENSMUSG00000011752	Pgam1	1.67
ENSMUSG00000048047	Zbtb33	1.67
ENSMUSG00000030494	Rhpn2	1.67
ENSMUSG00000002728	Naa20	1.67
ENSMUSG00000032041	Tirap	1.67
ENSMUSG00000028653	Trit1	1.67

ENSMUSG00000034994	Eef2	1.67
ENSMUSG00000056952	Tatdn2	1.67
ENSMUSG00000056476	Med12l	1.67
ENSMUSG00000052146	Rps10	1.67
ENSMUSG00000058799	Nap1l1	1.67
ENSMUSG00000005687	Bcas2	1.67
ENSMUSG00000071796	6820431F20Rik	1.67
ENSMUSG00000001248	Gramd1a	1.67
ENSMUSG00000025024	Smndc1	1.67
ENSMUSG00000025035	Arl3	1.67
ENSMUSG00000037563	Rps16	1.67
ENSMUSG00000047215	Rpl9	1.67
ENSMUSG00000031609	Sap30	1.67
ENSMUSG00000031150	Ccdc120	1.67
ENSMUSG00000050708	Ftl1	1.67
ENSMUSG00000028234	Rps20	1.67
ENSMUSG00000060636	Rpl35a	1.67
ENSMUSG00000053552	Ebf4	1.66
ENSMUSG00000027887	Sypl2	1.66
ENSMUSG00000057841	Rpl32	1.66
ENSMUSG00000042814	Mcts2	1.66
ENSMUSG00000006471	Ndor1	1.66
ENSMUSG00000036620	Mgat4b	1.66
ENSMUSG00000044807	Zfp354c	1.66
ENSMUSG00000020460	Rps27a	1.66
ENSMUSG00000030652	Coq7	1.66
ENSMUSG00000028955	Vamp3	1.66
ENSMUSG00000012848	Rps5	1.66
ENSMUSG00000025232	Hexa	1.66
ENSMUSG00000093752	RP23-391M18.7	1.66
ENSMUSG00000029684	Wasl	1.66
ENSMUSG00000029249	Rest	1.66
ENSMUSG00000001750	Tcirg1	1.66
ENSMUSG00000010607	Pigyl	1.66
ENSMUSG00000079252	Tor1aip2	1.66
ENSMUSG00000028809	Srrm1	1.66
ENSMUSG00000034928	Rnf44	1.66
ENSMUSG00000092416	Zfp141	1.66
ENSMUSG00000026223	Itm2c	1.66
ENSMUSG00000028381	Ugcg	1.66
ENSMUSG00000041921	Metap1d	1.66
ENSMUSG00000025816	Sec61a2	1.66
ENSMUSG00000052135	Foxo6	1.66

ENSMUSG00000006373	Pgrmc1	1.65
ENSMUSG00000079429	Heatr7b1	1.65
ENSMUSG00000020472	Zkscan17	1.65
ENSMUSG00000031922	Cep57	1.65
ENSMUSG00000079555	Haus3	1.65
ENSMUSG00000035530	Eif1	1.65
ENSMUSG00000072692	Gm13826	1.65
ENSMUSG00000031700	Gpt2	1.65
ENSMUSG00000027257	Pacsin3	1.65
ENSMUSG00000029769	Ccdc136	1.65
ENSMUSG00000048910	2810453I06Rik	1.65
ENSMUSG00000057036	Gm7536	1.65
ENSMUSG00000086583	Gm15500	1.65
ENSMUSG00000061983	Rps12	1.65
ENSMUSG00000072940	Gm10443	1.65
ENSMUSG00000024059	Clip4	1.65
ENSMUSG00000039001	Rps21	1.65
ENSMUSG00000007892	Rplp1	1.65
ENSMUSG00000037434	Slc30a1	1.65
ENSMUSG00000071711	Mpst	1.65
ENSMUSG00000034156	Bzrap1	1.65
ENSMUSG00000054770	Kctd18	1.65
ENSMUSG00000007097	Atp1a2	1.65
ENSMUSG00000021242	Npc2	1.65
ENSMUSG00000047446	Arl4a	1.65
ENSMUSG00000043439	E130012A19Rik	1.65
ENSMUSG00000064354	mt-Co2	1.65
ENSMUSG00000021901	Bap1	1.64
ENSMUSG00000038180	Spag4	1.64
ENSMUSG00000041126	H2afv	1.64
ENSMUSG00000030034	Ino80b	1.64
ENSMUSG00000062647	Rpl7a	1.64
ENSMUSG00000091845	Gm4604	1.64
ENSMUSG00000063457	Rps15	1.64
ENSMUSG00000087153	Gm6483	1.64
ENSMUSG00000026384	Ptpn4	1.64
ENSMUSG00000079547	H2-DMb1	1.64
ENSMUSG00000020633	Dcdc2c	1.64
ENSMUSG00000045294	Insig1	1.64
ENSMUSG00000024052	Lpin2	1.64
ENSMUSG00000021660	Btf3	1.64
ENSMUSG00000040952	Rps19	1.64
ENSMUSG00000031838	Ifi30	1.64

ENSMUSG00000078813	Leng1	1.64
ENSMUSG00000031939	Taf1d	1.64
ENSMUSG00000015745	Plekho1	1.64
ENSMUSG00000021041	2700073G19Rik	1.64
ENSMUSG00000030741	Spns1	1.64
ENSMUSG00000050608	Minos1	1.64
ENSMUSG00000032425	Zfp949	1.64
ENSMUSG00000002578	Ikzf4	1.64
ENSMUSG00000029238	Clock	1.64
ENSMUSG00000066798	Zbtb6	1.64
ENSMUSG00000008683	Rps15a	1.63
ENSMUSG00000031880	Rrad	1.63
ENSMUSG00000063049	Ing2	1.63
ENSMUSG00000025290	Rps24	1.63
ENSMUSG00000032324	Tspan3	1.63
ENSMUSG00000025484	Bet1l	1.63
ENSMUSG00000055943	2900064A13Rik	1.63
ENSMUSG00000059291	Rpl11	1.63
ENSMUSG00000020409	Slu7	1.63
ENSMUSG00000061477	Rps7	1.63
ENSMUSG00000003154	Foxj2	1.63
ENSMUSG00000022617	Chkb	1.63
ENSMUSG00000027805	Pfn2	1.63
ENSMUSG00000038085	4921517L17Rik	1.63
ENSMUSG00000055633	Zfp580	1.63
ENSMUSG00000019188	H13	1.63
ENSMUSG00000022500	Litaf	1.63
ENSMUSG00000022971	Ifnar2	1.63
ENSMUSG00000049647	Purb	1.63
ENSMUSG00000025351	Cd63	1.63
ENSMUSG00000085396	6720401G13Rik	1.62
ENSMUSG00000022601	Rpl24	1.62
ENSMUSG00000023079	Gtf2ird1	1.62
ENSMUSG00000042073	Abhd14b	1.62
ENSMUSG00000038342	Mlxip	1.62
ENSMUSG00000039756	Dnttip2	1.62
ENSMUSG00000058546	Rpl23a	1.62
ENSMUSG00000030224	Strap	1.62
ENSMUSG00000044600	9130011J15Rik	1.62
ENSMUSG00000029535	Triap1	1.62
ENSMUSG00000058655	Eif4b	1.62
ENSMUSG00000061207	Stk19	1.62
ENSMUSG00000050390	C77080	1.62

ENSMUSG00000029655	N4bp2l2	1.62
ENSMUSG00000045896	Paip2b	1.62
ENSMUSG00000020063	Sirt1	1.62
ENSMUSG00000045106	Ccdc73	1.62
ENSMUSG00000091588	Gm17279	1.62
ENSMUSG00000007783	Cpt1c	1.62
ENSMUSG00000028041	Adam15	1.62
ENSMUSG00000000740	Rpl13	1.62
ENSMUSG00000029208	Guf1	1.62
ENSMUSG00000026158	Ogfrl1	1.61
ENSMUSG00000066440	Zfyve26	1.61
ENSMUSG00000024604	Rbm22	1.61
ENSMUSG00000084883	Ccdc85c	1.61
ENSMUSG00000003778	Brd8	1.61
ENSMUSG00000025417	Pip4k2c	1.61
ENSMUSG00000018537	Pcgf2	1.61
ENSMUSG00000037075	Rnf139	1.61
ENSMUSG00000002550	Uck1	1.61
ENSMUSG00000024206	Rfx2	1.61
ENSMUSG00000069020	Urm1	1.61
ENSMUSG00000036863	Syde2	1.61
ENSMUSG00000002058	Unc119	1.61
ENSMUSG00000030942	Thumpd1	1.61
ENSMUSG00000030432	Rpl28	1.61
ENSMUSG00000003378	Grik5	1.61
ENSMUSG00000032519	Slc25a38	1.61
ENSMUSG00000019856	Fam184a	1.61
ENSMUSG00000060126	Tpt1	1.61
ENSMUSG00000022635	Zcrb1	1.61
ENSMUSG00000028461	Ccdc107	1.61
ENSMUSG00000024191	Bnip1	1.61
ENSMUSG00000050621	Gm9846	1.60
ENSMUSG00000035356	Nfkbiz	1.60
ENSMUSG00000039824	Myl6b	1.60
ENSMUSG00000042331	Specc1	1.60
ENSMUSG00000032384	Csnk1g1	1.60
ENSMUSG00000022034	Esco2	1.60
ENSMUSG00000015087	B230208H17Rik	1.60
ENSMUSG00000074682	Zcchc3	1.60
ENSMUSG00000025967	Eef1b2	1.60
ENSMUSG00000021493	Pdlim7	1.60
ENSMUSG00000057863	Rpl36	1.60
ENSMUSG00000021893	Capn7	1.60

ENSMUSG00000044783	Hjurp	1.60
ENSMUSG00000025366	Esyt1	1.60
ENSMUSG00000019872	Smpdl3a	1.60
ENSMUSG00000085399	9130206I24Rik	1.60
ENSMUSG00000041817	Fam169a	1.60
ENSMUSG00000037295	Ldlrap1	1.60
ENSMUSG00000042712	Wbp5	1.60
ENSMUSG00000091586	Cyp4f17	1.60
ENSMUSG00000018900	Slc22a5	1.60
ENSMUSG00000028936	Rpl22	1.60
ENSMUSG00000029504	Ddx51	1.60
ENSMUSG00000003970	Rpl8	1.60
ENSMUSG00000054717	Hmgb2	1.59
ENSMUSG00000055835	Zfp1	1.59
ENSMUSG00000020385	Clk4	1.59
ENSMUSG00000043342	Hoxd9	1.59
ENSMUSG00000046330	Rpl37a	1.59
ENSMUSG00000039886	Tmem120a	1.59
ENSMUSG00000062116	Zfp954	1.59
ENSMUSG00000020372	Gnb2l1	1.59
ENSMUSG00000044927	H1fx	1.59
ENSMUSG00000039007	Pgcp	1.59
ENSMUSG00000061411	8430427H17Rik	1.59
ENSMUSG00000091524	2610020C07Rik	1.59
ENSMUSG00000059895	Ptp4a3	1.59
ENSMUSG00000011114	Tbrg1	1.59
ENSMUSG00000034892	Rps29	1.59
ENSMUSG00000028249	Sdcbp	1.59
ENSMUSG00000057322	Rpl38	1.59
ENSMUSG00000035637	Grhpr	1.59
ENSMUSG00000009291	Pttg1ip	1.59
ENSMUSG00000029390	Tmed2	1.59
ENSMUSG00000038900	Rpl12	1.59
ENSMUSG00000037788	Vopp1	1.59
ENSMUSG00000008206	Lass4	1.59
ENSMUSG00000040165	Cd209c	1.59
ENSMUSG00000042686	Jph1	1.59
ENSMUSG00000040331	Nsmce4a	1.58
ENSMUSG00000045180	Shroom2	1.58
ENSMUSG00000052557	Gan	1.58
ENSMUSG00000023348	Trip6	1.58
ENSMUSG00000084319	Tpt1-ps3	1.58
ENSMUSG00000017404	Rpl19	1.58

ENSMUSG00000003429	Rps11	1.58
ENSMUSG00000040128	Pnrc1	1.58
ENSMUSG00000035722	Abca7	1.58
ENSMUSG00000059070	Rpl18	1.58
ENSMUSG00000004558	Ndrg2	1.58
ENSMUSG00000071103	1700029J07Rik	1.58
ENSMUSG00000007038	Neu1	1.58
ENSMUSG00000013663	Pten	1.58
ENSMUSG00000040649	Rimklb	1.58
ENSMUSG00000040414	Slc25a28	1.58
ENSMUSG00000015759	Cnih	1.58
ENSMUSG00000008682	Rpl10	1.58
ENSMUSG00000028609	Magoh	1.58
ENSMUSG00000034485	Uaca	1.58
ENSMUSG00000022450	Ndufa6	1.58
ENSMUSG00000059866	Tnip2	1.58
ENSMUSG00000063406	Tmed5	1.58
ENSMUSG00000031428	Zcchc18	1.58
ENSMUSG00000083773	Gm13394	1.58
ENSMUSG00000079641	Rpl39	1.58
ENSMUSG00000022312	Eif3h	1.58
ENSMUSG00000028060	2810403A07Rik	1.58
ENSMUSG00000022434	Fam118a	1.58
ENSMUSG00000022336	Eif3e	1.58
ENSMUSG00000035299	Mid1	1.57
ENSMUSG00000064145	Arih2	1.57
ENSMUSG00000022982	Sod1	1.57
ENSMUSG00000038095	Sbno1	1.57
ENSMUSG00000028150	Rorc	1.57
ENSMUSG00000036916	Zfp280c	1.57
ENSMUSG00000060860	Ube2s	1.57
ENSMUSG00000071722	Spin4	1.57
ENSMUSG00000061787	Rps17	1.57
ENSMUSG00000028572	Hook1	1.57
ENSMUSG00000027630	Tbl1xr1	1.57
ENSMUSG00000002043	Trappc6a	1.57
ENSMUSG00000009927	Rps25	1.57
ENSMUSG00000025140	Pycr1	1.57
ENSMUSG00000069972	Gm10159	1.57
ENSMUSG00000037845	Fdxacb1	1.57
ENSMUSG00000024121	Atp6v0c	1.57
ENSMUSG00000027079	Clp1	1.57
ENSMUSG00000080875	Gm7332	1.57

ENSMUSG00000039842	Mcph1	1.57
ENSMUSG00000009555	Cdk9	1.57
ENSMUSG00000025237	Parp6	1.57
ENSMUSG00000068876	Cgn	1.57
ENSMUSG00000027680	Fxr1	1.57
ENSMUSG00000032172	Olfm2	1.57
ENSMUSG00000068290	Ddrgk1	1.57
ENSMUSG00000021982	Cdadc1	1.57
ENSMUSG00000053128	Rnf26	1.57
ENSMUSG00000079435	Rpl36a	1.57
ENSMUSG00000005800	Mmp8	1.57
ENSMUSG00000068240	Gm11808	1.56
ENSMUSG00000089944	Gm8292	1.56
ENSMUSG00000034042	Gpbp1l1	1.56
ENSMUSG00000025173	Wdr45l	1.56
ENSMUSG00000029614	Rpl6	1.56
ENSMUSG00000040146	Rgl3	1.56
ENSMUSG00000003380	Rabac1	1.56
ENSMUSG00000031628	Casp3	1.56
ENSMUSG00000026411	Tmem9	1.56
ENSMUSG00000002409	Dyrk1b	1.56
ENSMUSG00000057113	Npm1	1.56
ENSMUSG00000029426	Scarb2	1.56
ENSMUSG00000031751	Amfr	1.56
ENSMUSG00000029863	Casp2	1.56
ENSMUSG00000040865	Ino80d	1.56
ENSMUSG00000070420	Zfp498	1.56
ENSMUSG00000002767	Mrpl2	1.56
ENSMUSG00000071415	Rpl23	1.56
ENSMUSG00000040280	Ndufa4l2	1.56
ENSMUSG00000046432	Ngfrap1	1.56
ENSMUSG00000036989	Trim3	1.56
ENSMUSG00000030530	Furin	1.56
ENSMUSG00000021466	Ptch1	1.56
ENSMUSG00000037197	Rbm17	1.56
ENSMUSG00000021054	Sgpp1	1.56
ENSMUSG00000060935	AI597468	1.56
ENSMUSG00000039218	Srrm2	1.55
ENSMUSG00000034551	Hdx	1.55
ENSMUSG00000006378	Gcat	1.55
ENSMUSG00000003382	Etv3	1.55
ENSMUSG00000029560	Snx8	1.55
ENSMUSG00000006599	Gtf2h1	1.55

ENSMUSG00000069892	9930111J21Rik2	1.55
ENSMUSG00000048142	Nat8l	1.55
ENSMUSG00000021591	Glrx	1.55
ENSMUSG00000017723	Wfdc2	1.55
ENSMUSG00000051278	4930422G04Rik	1.55
ENSMUSG00000081453	Gm6767	1.55
ENSMUSG00000066705	Fxyd6	1.55
ENSMUSG00000028618	Tmem59	1.55
ENSMUSG00000055067	Smyd3	1.55
ENSMUSG00000033701	Acbd6	1.55
ENSMUSG00000028291	Akirin2	1.55
ENSMUSG00000027716	Trpc3	1.55
ENSMUSG00000043716	Rpl7	1.55
ENSMUSG00000039382	Wdr45	1.55
ENSMUSG00000067148	Polr1c	1.55
ENSMUSG00000030083	Abtb1	1.55
ENSMUSG00000046807	AI646023	1.55
ENSMUSG00000021986	Fam123a	1.55
ENSMUSG00000041120	Nbl1	1.55
ENSMUSG00000043510	Hscb	1.55
ENSMUSG00000023092	Fhl1	1.55
ENSMUSG00000032388	Spg21	1.54
ENSMUSG00000030806	Stx1b	1.54
ENSMUSG00000085622	3110056K07Rik	1.54
ENSMUSG00000023972	Ptk7	1.54
ENSMUSG00000022199	Slc22a17	1.54
ENSMUSG00000081406	Gm13654	1.54
ENSMUSG00000039323	Igfbp2	1.54
ENSMUSG00000035236	Scai	1.54
ENSMUSG00000070436	Serpinh1	1.54
ENSMUSG00000025855	Prkar1b	1.54
ENSMUSG00000028834	Trim63	1.54
ENSMUSG00000033684	Qsox1	1.54
ENSMUSG00000028495	Rps6	1.54
ENSMUSG00000002055	Spag5	1.54
ENSMUSG00000025982	Sf3b1	1.54
ENSMUSG00000036707	Cab39	1.54
ENSMUSG00000020190	Mknk2	1.54
ENSMUSG00000034071	Zfp551	1.54
ENSMUSG00000050954	Zfp169	1.54
ENSMUSG00000054648	Zfp869	1.54
ENSMUSG00000023944	Hsp90ab1	1.54
ENSMUSG00000062997	Rpl35	1.54

ENSMUSG00000001419	Mef2d	1.54
ENSMUSG00000026790	Odf2	1.53
ENSMUSG00000045365	Rbm15b	1.53
ENSMUSG00000031029	Eif3f	1.53
ENSMUSG00000007891	Ctsd	1.53
ENSMUSG00000036208	BC027231	1.53
ENSMUSG00000031059	Ndufb11	1.53
ENSMUSG00000013367	Iglon5	1.53
ENSMUSG00000002265	Peg3	1.53
ENSMUSG00000064125	BC068157	1.53
ENSMUSG00000030067	Foxp1	1.53
ENSMUSG00000002732	Fkbp7	1.53
ENSMUSG00000041180	Hectd2	1.53
ENSMUSG00000058317	Ube2e2	1.53
ENSMUSG00000026374	Tsn	1.53
ENSMUSG00000035596	Mboat7	1.53
ENSMUSG00000048495	1110034B05Rik	1.53
ENSMUSG00000020311	Erlec1	1.53
ENSMUSG00000019189	Rnf145	1.53
ENSMUSG00000027408	Cpxm1	1.53
ENSMUSG00000058756	Thra	1.53
ENSMUSG00000024792	Zfpl1	1.53
ENSMUSG00000034685	Fam171a2	1.53
ENSMUSG00000026455	Klhl12	1.53
ENSMUSG00000000787	Ddx3x	1.53
ENSMUSG00000069171	Nr2f1	1.53
ENSMUSG00000027381	Bcl2l11	1.53
ENSMUSG00000022194	Pabpn1	1.53
ENSMUSG00000024217	Snrpc	1.53
ENSMUSG00000034158	Lrrc58	1.53
ENSMUSG00000058569	Tmed9	1.53
ENSMUSG00000022558	Heatr7a	1.53
ENSMUSG00000021486	Prelid1	1.52
ENSMUSG00000049516	Spty2d1	1.52
ENSMUSG00000041995	Zbed3	1.52
ENSMUSG00000059486	Kbtbd2	1.52
ENSMUSG00000035458	Tnni3	1.52
ENSMUSG00000042210	Abhd14a	1.52
ENSMUSG00000064368	mt-Nd6	1.52
ENSMUSG00000028278	Rragd	1.52
ENSMUSG00000025207	Sema4g	1.52
ENSMUSG00000025060	Slk	1.52
ENSMUSG00000034083	C130022K22Rik	1.52

ENSMUSG00000071267	Zfp942	1.52
ENSMUSG00000028464	Tpm2	1.52
ENSMUSG00000031103	Elf4	1.52
ENSMUSG00000067288	Rps28	1.52
ENSMUSG00000002413	Braf	1.52
ENSMUSG00000040749	Siah1b	1.52
ENSMUSG00000029151	Slc30a3	1.52
ENSMUSG00000026489	Adck3	1.52
ENSMUSG00000061315	Naca	1.52
ENSMUSG00000010095	Slc3a2	1.52
ENSMUSG00000071454	Dtnb	1.52
ENSMUSG00000024188	Luc7l	1.52
ENSMUSG00000021731	Mrps30	1.52
ENSMUSG00000021709	Erbb2ip	1.52
ENSMUSG00000083364	Gm14535	1.52
ENSMUSG00000021495	Fam193b	1.52
ENSMUSG00000039841	Zfp800	1.52
ENSMUSG00000033096	2310001A20Rik	1.52
ENSMUSG00000006575	Rundc3a	1.52
ENSMUSG00000073987	Ggh	1.52
ENSMUSG00000020994	Pnn	1.52
ENSMUSG00000056770	Setd3	1.51
ENSMUSG00000030788	Rnf141	1.51
ENSMUSG00000039328	Rnf122	1.51
ENSMUSG00000029348	Asphd2	1.51
ENSMUSG00000035011	Zbtb7a	1.51
ENSMUSG00000035297	Cops4	1.51
ENSMUSG00000039747	Orai2	1.51
ENSMUSG00000020577	Tspan13	1.51
ENSMUSG00000004637	Wwox	1.51
ENSMUSG00000020029	Nudt4	1.51
ENSMUSG00000060671	Atp8b2	1.51
ENSMUSG00000040054	Baz2a	1.51
ENSMUSG00000025200	Cwf19l1	1.51
ENSMUSG00000026958	Dpp7	1.51
ENSMUSG00000060419	Rps16-ps2	1.51
ENSMUSG00000031066	Usp11	1.51
ENSMUSG00000025159	Mms19	1.51
ENSMUSG00000032253	Phip	1.51
ENSMUSG00000015126	0610007P22Rik	1.51
ENSMUSG00000071723	Gspt2	1.51
ENSMUSG00000024943	Smc5	1.51
ENSMUSG00000030539	Sema4b	1.51

ENSMUSG00000008200	Fnbp4	1.51
ENSMUSG00000029404	Arl6ip4	1.51
ENSMUSG00000033106	Slc7a6os	1.51
ENSMUSG00000091207	Purb	1.51
ENSMUSG00000036779	Papd5	1.51
ENSMUSG00000034731	Dgkh	1.51
ENSMUSG00000031320	Rps4x	1.51
ENSMUSG00000036026	Tmem63b	1.50
ENSMUSG00000019854	Reps1	1.50
ENSMUSG00000047407	Tgif1	1.50
ENSMUSG00000023940	Sgol1	1.50
ENSMUSG00000038702	Dsel	1.50
ENSMUSG00000053398	Phgdh	1.50
ENSMUSG00000010110	Stx5a	1.50
ENSMUSG00000028445	Enho	1.50
ENSMUSG00000042903	Foxo4	1.50
ENSMUSG00000054737	Zfp182	1.50
ENSMUSG00000025521	Tmem192	1.50
ENSMUSG00000031447	Lamp1	1.50
ENSMUSG00000073640	Rpl27-ps3	1.50
ENSMUSG00000030609	Aen	-1.50
ENSMUSG00000020808	Fam64a	-1.50
ENSMUSG00000037752	Xkr8	-1.50
ENSMUSG00000036845	Lin37	-1.50
ENSMUSG00000043671	Dpy19l3	-1.50
ENSMUSG00000022064	Pibf1	-1.50
ENSMUSG00000034573	Ptpn13	-1.50
ENSMUSG00000026754	Golga1	-1.50
ENSMUSG00000039031	Arhgap18	-1.50
ENSMUSG00000042066	Tmcc2	-1.50
ENSMUSG00000039145	Camk1d	-1.51
ENSMUSG00000071317	Bves	-1.51
ENSMUSG00000067851	Arfgef1	-1.51
ENSMUSG00000026239	Pde6d	-1.51
ENSMUSG00000048899	Rimkla	-1.51
ENSMUSG00000020439	Smtn	-1.51
ENSMUSG00000049553	Polr1a	-1.51
ENSMUSG00000038217	Tlcd2	-1.51
ENSMUSG00000025133	Ints4	-1.51
ENSMUSG00000051341	Zfp52	-1.51
ENSMUSG00000025575	Cant1	-1.51
ENSMUSG00000025384	2310003H01Rik	-1.51
ENSMUSG00000034487	Kdelc2	-1.51

ENSMUSG00000021981	Cab39l	-1.51
ENSMUSG00000021670	Hmgcr	-1.51
ENSMUSG00000032014	Oaf	-1.51
ENSMUSG00000031657	Heatr3	-1.51
ENSMUSG00000031984	2810004N23Rik	-1.51
ENSMUSG00000031548	Sfrp1	-1.51
ENSMUSG00000005871	Apc	-1.51
ENSMUSG00000033722	BC034090	-1.51
ENSMUSG00000020974	Pole2	-1.51
ENSMUSG00000063808	Gpatch1	-1.51
ENSMUSG00000026623	Lpgat1	-1.51
ENSMUSG00000037010	Apln	-1.51
ENSMUSG00000038280	Ostm1	-1.51
ENSMUSG00000028020	Glrb	-1.51
ENSMUSG00000029782	Tmem209	-1.51
ENSMUSG00000031826	Usp10	-1.51
ENSMUSG00000000958	Slc7a7	-1.51
ENSMUSG00000010554	Mettl16	-1.52
ENSMUSG00000055435	Maf	-1.52
ENSMUSG00000055963	Gm11818	-1.52
ENSMUSG00000074782	4833422C13Rik	-1.52
ENSMUSG00000070425	Trpc2	-1.52
ENSMUSG00000033458	Fan1	-1.52
ENSMUSG00000034152	Exoc3	-1.52
ENSMUSG00000020952	Scfd1	-1.52
ENSMUSG00000029633	Gm5578	-1.52
ENSMUSG00000049493	Pls1	-1.52
ENSMUSG00000031631	4933411K20Rik	-1.52
ENSMUSG00000022773	Ypel1	-1.52
ENSMUSG00000024451	Arap3	-1.52
ENSMUSG00000005672	Kit	-1.52
ENSMUSG00000041741	Pde3a	-1.52
ENSMUSG00000038371	Sbf2	-1.52
ENSMUSG00000024666	Tmem138	-1.52
ENSMUSG00000020288	Ahsa2	-1.52
ENSMUSG00000042851	Zc3h6	-1.52
ENSMUSG00000041245	Wnk3-ps	-1.52
ENSMUSG00000052137	C430048L16Rik	-1.52
ENSMUSG00000027582	Zgpat	-1.52
ENSMUSG00000061650	Med9	-1.52
ENSMUSG00000034320	Slc26a2	-1.52
ENSMUSG00000020843	Timm22	-1.52
ENSMUSG00000040034	Nup43	-1.52

ENSMUSG00000047003	Zfp41	-1.52
ENSMUSG00000027176	Cstf3	-1.52
ENSMUSG00000049680	Urgcp	-1.52
ENSMUSG00000027167	Elp4	-1.52
ENSMUSG00000028703	Lrrc41	-1.52
ENSMUSG00000025860	Xiap	-1.53
ENSMUSG00000020152	Actr2	-1.53
ENSMUSG00000022774	Ncbp2	-1.53
ENSMUSG00000037892	Pcdh18	-1.53
ENSMUSG00000055041	Commd5	-1.53
ENSMUSG00000062646	Ganc	-1.53
ENSMUSG00000055235	Wdr86	-1.53
ENSMUSG00000021756	Il6st	-1.53
ENSMUSG00000014813	Stc1	-1.53
ENSMUSG00000047409	Ctdspl	-1.53
ENSMUSG00000053985	Zfp14	-1.53
ENSMUSG00000023800	Tiam2	-1.53
ENSMUSG00000004266	Ptpn6	-1.53
ENSMUSG00000037216	Lipt1	-1.53
ENSMUSG00000038102	D030016E14Rik	-1.53
ENSMUSG00000038766	Gabpb2	-1.53
ENSMUSG00000039759	Thap3	-1.53
ENSMUSG00000072494	Ppp1r3e	-1.53
ENSMUSG00000035382	Pcsk7	-1.53
ENSMUSG00000031605	Klhl2	-1.53
ENSMUSG00000038732	Mboat1	-1.53
ENSMUSG00000020484	Xbp1	-1.53
ENSMUSG00000039062	Anpep	-1.53
ENSMUSG00000041949	Tmco7	-1.53
ENSMUSG00000036613	Tssc1	-1.54
ENSMUSG00000032977	1810008A18Rik	-1.54
ENSMUSG00000025332	Kdm5c	-1.54
ENSMUSG00000041215	Yeats2	-1.54
ENSMUSG00000030079	Ruvbl1	-1.54
ENSMUSG00000029063	Nadk	-1.54
ENSMUSG00000031171	Ftsj1	-1.54
ENSMUSG00000025171	Ubtd1	-1.54
ENSMUSG00000051674	Dcun1d4	-1.54
ENSMUSG00000042428	Mgat3	-1.54
ENSMUSG00000031634	Ufsp2	-1.54
ENSMUSG00000043015	Tmem194b	-1.54
ENSMUSG00000031367	Ap1s2	-1.54
ENSMUSG00000021540	Smad5	-1.54

ENSMUSG00000070544	Top1	-1.54
ENSMUSG00000033880	Lgals3bp	-1.54
ENSMUSG00000022960	Donson	-1.54
ENSMUSG00000037617	Spag1	-1.54
ENSMUSG00000021065	Fut8	-1.54
ENSMUSG00000026841	Fibcd1	-1.54
ENSMUSG00000032459	Mrps22	-1.54
ENSMUSG00000055652	Klhl25	-1.54
ENSMUSG00000019899	Lama2	-1.54
ENSMUSG00000031099	Smarca1	-1.54
ENSMUSG00000028700	Pomgnt1	-1.54
ENSMUSG00000042389	Tsen2	-1.54
ENSMUSG00000038762	Abcf1	-1.54
ENSMUSG00000021978	Extl3	-1.55
ENSMUSG00000000561	Wdr77	-1.55
ENSMUSG00000074876	Spata5l1	-1.55
ENSMUSG00000033732	Sf3b3	-1.55
ENSMUSG00000029916	Agk	-1.55
ENSMUSG00000034601	2700049A03Rik	-1.55
ENSMUSG00000021257	Angel1	-1.55
ENSMUSG00000025933	Tmem14a	-1.55
ENSMUSG00000026098	Pms1	-1.55
ENSMUSG00000072501	Phf20l1	-1.55
ENSMUSG00000000776	Polr3d	-1.55
ENSMUSG00000022793	B4galt4	-1.55
ENSMUSG00000020876	Snx11	-1.55
ENSMUSG00000031901	Dus2l	-1.55
ENSMUSG00000035829	Ppp1r26	-1.55
ENSMUSG00000026872	Zeb2	-1.55
ENSMUSG00000020590	Snx13	-1.55
ENSMUSG00000032244	Fem1b	-1.55
ENSMUSG00000037315	Phf16	-1.55
ENSMUSG00000054509	Parp4	-1.55
ENSMUSG00000059552	Trp53	-1.55
ENSMUSG00000026810	Dpm2	-1.55
ENSMUSG00000037669	1110057K04Rik	-1.55
ENSMUSG00000015697	Setdb1	-1.55
ENSMUSG00000025224	Gbf1	-1.55
ENSMUSG00000053801	Grwd1	-1.55
ENSMUSG00000046691	Chtf8	-1.55
ENSMUSG00000078143	Gm17344	-1.55
ENSMUSG00000024537	Psmg2	-1.55
ENSMUSG00000042225	Ammecr1	-1.55

ENSMUSG00000003559	As3mt	-1.55
ENSMUSG00000027957	Slc35a3	-1.55
ENSMUSG00000019849	Prep	-1.55
ENSMUSG00000026014	Raph1	-1.55
ENSMUSG00000013736	Trnt1	-1.55
ENSMUSG00000022514	Il1rap	-1.55
ENSMUSG00000001228	Uhrf1	-1.56
ENSMUSG00000015335	Zdhhc12	-1.56
ENSMUSG00000021266	Wars	-1.56
ENSMUSG00000029345	Tfip11	-1.56
ENSMUSG00000035051	Dhx57	-1.56
ENSMUSG00000024947	Men1	-1.56
ENSMUSG00000040549	Ckap5	-1.56
ENSMUSG00000025789	St8sia2	-1.56
ENSMUSG00000026111	Unc50	-1.56
ENSMUSG00000082585	Gm15387	-1.56
ENSMUSG00000026185	Igfbp5	-1.56
ENSMUSG00000021468	Sptlc1	-1.56
ENSMUSG00000034282	Evpl	-1.56
ENSMUSG00000001751	Naglu	-1.56
ENSMUSG00000039826	Trub2	-1.56
ENSMUSG00000005057	Sh2b2	-1.56
ENSMUSG00000019979	Apaf1	-1.56
ENSMUSG00000015971	Actr8	-1.56
ENSMUSG00000020476	Dbnl	-1.56
ENSMUSG00000022760	Thap7	-1.56
ENSMUSG00000016257	Slmo2	-1.56
ENSMUSG00000026027	Stradb	-1.56
ENSMUSG00000018923	Med11	-1.56
ENSMUSG00000072704	2700089E24Rik	-1.56
ENSMUSG00000031349	Nsdhl	-1.56
ENSMUSG00000002455	Prpf6	-1.56
ENSMUSG00000024982	Zdhhc6	-1.56
ENSMUSG00000037896	Rcor1	-1.56
ENSMUSG00000019789	Hey2	-1.56
ENSMUSG00000026784	Pdss1	-1.56
ENSMUSG00000023019	Gpd1	-1.56
ENSMUSG00000062210	Tnfaip8	-1.57
ENSMUSG00000032123	Dpagt1	-1.57
ENSMUSG00000024581	Napg	-1.57
ENSMUSG00000031891	Hsd11b2	-1.57
ENSMUSG00000024816	Frmd8	-1.57
ENSMUSG00000061559	Wdr61	-1.57

ENSMUSG00000026042	Col5a2	-1.57
ENSMUSG00000079605	Zbtb9	-1.57
ENSMUSG00000050931	Sgms2	-1.57
ENSMUSG00000040896	Kcnd3	-1.57
ENSMUSG00000030447	Cyfip1	-1.57
ENSMUSG00000079662	Ntn3	-1.57
ENSMUSG00000032418	Me1	-1.57
ENSMUSG00000026675	Hsd17b7	-1.57
ENSMUSG00000022528	Hes1	-1.57
ENSMUSG00000002820	Atg4d	-1.57
ENSMUSG00000060548	Tnfrsf19	-1.57
ENSMUSG00000049672	Zfp161	-1.57
ENSMUSG00000022951	Rcan1	-1.57
ENSMUSG00000026249	Serpine2	-1.57
ENSMUSG00000025782	Taf3	-1.57
ENSMUSG00000036377	C530008M17Rik	-1.57
ENSMUSG00000067034	Zfp960	-1.57
ENSMUSG00000006705	Pknox1	-1.57
ENSMUSG00000031681	Smad1	-1.57
ENSMUSG00000046947	Adck2	-1.57
ENSMUSG00000010651	Acaa1b	-1.57
ENSMUSG00000040621	Gemin8	-1.57
ENSMUSG00000014606	Slc25a11	-1.57
ENSMUSG00000026439	Rbbp5	-1.57
ENSMUSG00000074166	AW146154	-1.58
ENSMUSG00000031974	Abcb10	-1.58
ENSMUSG00000026443	Lrrn2	-1.58
ENSMUSG00000023066	Rttn	-1.58
ENSMUSG00000035161	Ints6	-1.58
ENSMUSG00000040195	Tmem194	-1.58
ENSMUSG00000063281	Zfp35	-1.58
ENSMUSG00000021597	Ankrd32	-1.58
ENSMUSG00000008763	Man1a2	-1.58
ENSMUSG00000040687	Madd	-1.58
ENSMUSG00000020075	Ddx21	-1.58
ENSMUSG00000020392	Cdkn2aipnl	-1.58
ENSMUSG00000044095	2410075B13Rik	-1.58
ENSMUSG00000031823	Zdhhc7	-1.58
ENSMUSG00000026657	Frmd4a	-1.58
ENSMUSG00000020640	Itsn2	-1.58
ENSMUSG00000031617	Tmem184c	-1.58
ENSMUSG00000022090	Pdlim2	-1.58
ENSMUSG00000028497	Ptplad2	-1.58

ENSMUSG00000035495	Tstd2	-1.58
ENSMUSG00000033906	Zdhhc15	-1.58
ENSMUSG00000040928	S100pbp	-1.58
ENSMUSG00000035845	Alg12	-1.58
ENSMUSG00000020457	Drg1	-1.58
ENSMUSG00000041671	Pyroxd1	-1.58
ENSMUSG00000038024	Dennd4c	-1.58
ENSMUSG00000040774	Cept1	-1.58
ENSMUSG00000071350	Setdb2	-1.59
ENSMUSG00000032952	Ap4b1	-1.59
ENSMUSG00000040383	Aqr	-1.59
ENSMUSG00000035933	Cog5	-1.59
ENSMUSG00000027001	Dusp19	-1.59
ENSMUSG00000028188	Spata1	-1.59
ENSMUSG00000052214	Opa3	-1.59
ENSMUSG00000075227	Znhit2-ps	-1.59
ENSMUSG00000056941	Commd7	-1.59
ENSMUSG00000031072	Oraov1	-1.59
ENSMUSG00000029376	Mthfd2l	-1.59
ENSMUSG00000057098	Ebf1	-1.59
ENSMUSG00000031309	Rps6ka3	-1.59
ENSMUSG00000039242	B3galnt2	-1.59
ENSMUSG00000027286	Lrrc57	-1.59
ENSMUSG00000035109	Shc4	-1.59
ENSMUSG00000066357	Wdr6	-1.59
ENSMUSG00000029474	Rnf34	-1.59
ENSMUSG00000028127	Abcd3	-1.59
ENSMUSG00000042292	Mkl1	-1.59
ENSMUSG00000079444	Prickle4	-1.59
ENSMUSG00000021583	Erap1	-1.59
ENSMUSG00000003062	Stard3nl	-1.59
ENSMUSG00000086040	Wipf3	-1.59
ENSMUSG00000039697	Ncoa7	-1.59
ENSMUSG00000010529	Gm266	-1.59
ENSMUSG00000029141	Slc4a1ap	-1.59
ENSMUSG00000023032	Slc4a8	-1.59
ENSMUSG00000035310	Lin54	-1.59
ENSMUSG00000030084	Plxna1	-1.59
ENSMUSG00000025006	Sorbs1	-1.59
ENSMUSG00000042821	Snai1	-1.59
ENSMUSG00000027822	Slc33a1	-1.59
ENSMUSG00000047821	Trim16	-1.60
ENSMUSG00000031534	AI316807	-1.60

ENSMUSG00000022300	Dcaf13	-1.60
ENSMUSG00000031583	Wrn	-1.60
ENSMUSG00000035239	Neu3	-1.60
ENSMUSG00000033009	Ogfod1	-1.60
ENSMUSG00000033216	Eefsec	-1.60
ENSMUSG00000023961	Enpp4	-1.60
ENSMUSG00000038482	Tfdp1	-1.60
ENSMUSG00000028243	Ubxn2b	-1.60
ENSMUSG00000039115	Itga9	-1.60
ENSMUSG00000030850	Ate1	-1.60
ENSMUSG00000006463	Zdhhc24	-1.60
ENSMUSG00000042569	Dhrs7b	-1.60
ENSMUSG00000036430	Tbcc	-1.60
ENSMUSG00000001823	Hoxd12	-1.60
ENSMUSG00000086780	Gm16707	-1.60
ENSMUSG00000021816	Ppp3cb	-1.60
ENSMUSG00000034379	Wdr5b	-1.60
ENSMUSG00000029502	Golga3	-1.60
ENSMUSG00000026767	Fam188a	-1.60
ENSMUSG00000038668	Lpar1	-1.60
ENSMUSG00000021611	Tert	-1.60
ENSMUSG00000032911	Cspg4	-1.60
ENSMUSG00000054519	Zfp867	-1.60
ENSMUSG00000035133	Arhgap5	-1.61
ENSMUSG00000003623	Crot	-1.61
ENSMUSG00000032571	Pik3r4	-1.61
ENSMUSG00000028436	Dcaf12	-1.61
ENSMUSG00000041605	5730559C18Rik	-1.61
ENSMUSG00000029575	Mmab	-1.61
ENSMUSG00000025184	D19Ertd386e	-1.61
ENSMUSG00000019577	Pdk4	-1.61
ENSMUSG00000027695	Pld1	-1.61
ENSMUSG00000028414	Fktn	-1.61
ENSMUSG00000024135	Srbd1	-1.61
ENSMUSG00000074030	Exoc8	-1.61
ENSMUSG00000029725	Ppp1r35	-1.61
ENSMUSG00000027259	Adal	-1.61
ENSMUSG00000060862	Zbtb40	-1.61
ENSMUSG00000041112	Elmo1	-1.61
ENSMUSG00000078908	Mon1b	-1.61
ENSMUSG00000026589	Sec16b	-1.61
ENSMUSG00000024170	Telo2	-1.61
ENSMUSG00000032026	Rexo2	-1.61

ENSMUSG00000078786	BC024978	-1.61
ENSMUSG00000021532	Fastkd3	-1.61
ENSMUSG00000056131	Pgm3	-1.61
ENSMUSG00000030780	BC017158	-1.61
ENSMUSG00000023330	Dtwd1	-1.62
ENSMUSG00000033799	BC016423	-1.62
ENSMUSG00000039157	Fam102a	-1.62
ENSMUSG00000032058	Ppp2r1b	-1.62
ENSMUSG00000091512	Lamtor3	-1.62
ENSMUSG00000028295	1810030N24Rik	-1.62
ENSMUSG00000029669	Tspan12	-1.62
ENSMUSG00000028212	Ccne2	-1.62
ENSMUSG00000031684	Slc10a7	-1.62
ENSMUSG00000001661	Hoxc6	-1.62
ENSMUSG00000035367	Rmi1	-1.62
ENSMUSG00000036955	2510003E04Rik	-1.62
ENSMUSG00000038495	Otud7b	-1.62
ENSMUSG00000021068	Nin	-1.62
ENSMUSG00000002617	Zfp40	-1.62
ENSMUSG00000035441	Myo1d	-1.62
ENSMUSG00000079450	3110007F17Rik	-1.62
ENSMUSG00000075419	Dolk	-1.62
ENSMUSG00000022106	Rcbtb2	-1.62
ENSMUSG00000034684	Sema3f	-1.62
ENSMUSG00000032849	Abcc4	-1.62
ENSMUSG00000027993	Trim2	-1.62
ENSMUSG00000043065	Spice1	-1.63
ENSMUSG00000024472	Dcp2	-1.63
ENSMUSG00000016181	Diexf	-1.63
ENSMUSG00000020817	Rabep1	-1.63
ENSMUSG00000024483	Ankhd1	-1.63
ENSMUSG00000023277	Twf2	-1.63
ENSMUSG00000027944	Hax1	-1.63
ENSMUSG00000031060	Rbm10	-1.63
ENSMUSG00000041278	Ttc1	-1.63
ENSMUSG00000013646	Sh3bp5l	-1.63
ENSMUSG00000034274	Thoc5	-1.63
ENSMUSG00000027312	Atrn	-1.63
ENSMUSG00000070814	6330408A02Rik	-1.63
ENSMUSG00000090290	Gm17296	-1.63
ENSMUSG00000075703	Ept1	-1.63
ENSMUSG00000001065	Zfp276	-1.63
ENSMUSG00000035311	Gnptab	-1.63

ENSMUSG00000002718	Cse1l	-1.63
ENSMUSG00000020305	Asb3	-1.63
ENSMUSG00000033557	Fam20b	-1.63
ENSMUSG00000021408	Ripk1	-1.63
ENSMUSG00000031924	Cyb5b	-1.63
ENSMUSG00000039103	Nexn	-1.64
ENSMUSG00000021327	Zkscan3	-1.64
ENSMUSG00000041684	Bivm	-1.64
ENSMUSG00000034021	Pds5b	-1.64
ENSMUSG00000026933	Camsap1	-1.64
ENSMUSG00000039047	Pigk	-1.64
ENSMUSG00000030042	Pole4	-1.64
ENSMUSG00000028690	Mmachc	-1.64
ENSMUSG00000026918	Brd3	-1.64
ENSMUSG00000034800	Zfp661	-1.64
ENSMUSG00000078496	Gm13152	-1.64
ENSMUSG00000052299	Ltn1	-1.64
ENSMUSG00000015112	Slc25a13	-1.64
ENSMUSG00000035234	Fam175a	-1.64
ENSMUSG00000025995	Wdr75	-1.64
ENSMUSG00000039050	Osbpl2	-1.64
ENSMUSG00000026799	Med27	-1.64
ENSMUSG00000040836	Gpr161	-1.64
ENSMUSG00000021036	Sptlc2	-1.64
ENSMUSG00000025821	Zfp282	-1.64
ENSMUSG00000032786	Alas1	-1.64
ENSMUSG00000026275	Ppp1r7	-1.64
ENSMUSG00000039275	Foxk2	-1.64
ENSMUSG00000042063	Zfp386	-1.64
ENSMUSG00000041426	Hibch	-1.64
ENSMUSG00000039936	Pik3cd	-1.64
ENSMUSG00000034105	4632415K11Rik	-1.64
ENSMUSG00000028779	Pef1	-1.64
ENSMUSG00000038023	Atp6v0a2	-1.64
ENSMUSG00000046550	Spin2	-1.64
ENSMUSG00000037029	Zfp146	-1.64
ENSMUSG00000024976	Shoc2	-1.64
ENSMUSG00000001785	Pwp1	-1.64
ENSMUSG00000022401	Xpnpep3	-1.65
ENSMUSG00000026627	Tmem206	-1.65
ENSMUSG00000044991	1110034G24Rik	-1.65
ENSMUSG00000055172	C1ra	-1.65
ENSMUSG00000047230	Cldn2	-1.65

ENSMUSG00000020032	Nuak1	-1.65
ENSMUSG00000031616	Ednra	-1.65
ENSMUSG00000004018	Fancl	-1.65
ENSMUSG00000040236	Trappc5	-1.65
ENSMUSG00000029438	Bcl7a	-1.65
ENSMUSG00000027353	Mcm8	-1.65
ENSMUSG00000022197	Pdzd2	-1.65
ENSMUSG00000044442	N6amt1	-1.65
ENSMUSG00000021760	Gpx8	-1.65
ENSMUSG00000023022	Lima1	-1.65
ENSMUSG00000051615	Rap2a	-1.65
ENSMUSG00000029270	Fam69a	-1.65
ENSMUSG00000040521	Tsfm	-1.65
ENSMUSG00000022797	Tfrc	-1.65
ENSMUSG00000078878	Gm14305	-1.65
ENSMUSG00000061536	Sec22c	-1.65
ENSMUSG00000045281	Gpr20	-1.65
ENSMUSG00000004631	Sgce	-1.65
ENSMUSG00000019303	Psmc3ip	-1.65
ENSMUSG00000026663	Atf6	-1.66
ENSMUSG00000070643	Sox13	-1.66
ENSMUSG00000039065	Fam173b	-1.66
ENSMUSG00000059981	Taok2	-1.66
ENSMUSG00000091244	Gm17690	-1.66
ENSMUSG00000057103	Cml1	-1.66
ENSMUSG00000025962	Fastkd2	-1.66
ENSMUSG00000018547	Pip4k2b	-1.66
ENSMUSG00000038046	Rnmtl1	-1.66
ENSMUSG00000032512	Wdr48	-1.66
ENSMUSG00000067430	Zfp763	-1.66
ENSMUSG00000026174	Rqcd1	-1.66
ENSMUSG00000078584	AU022252	-1.66
ENSMUSG00000033624	Pdpr	-1.66
ENSMUSG00000028890	Mtf1	-1.66
ENSMUSG00000025722	Wdr73	-1.66
ENSMUSG00000002227	Mov10	-1.66
ENSMUSG00000042042	Csgalnact2	-1.66
ENSMUSG00000045268	Zfp691	-1.66
ENSMUSG00000031916	Cog8	-1.66
ENSMUSG00000029580	Actb	-1.67
ENSMUSG00000020387	Phf15	-1.67
ENSMUSG00000032177	Pde4a	-1.67
ENSMUSG00000070780	Rbm47	-1.67

ENSMUSG00000025209	Peo1	-1.67
ENSMUSG00000022682	Rrn3	-1.67
ENSMUSG00000026339	Ccdc93	-1.67
ENSMUSG00000086084	2610528B01Rik	-1.67
ENSMUSG00000036291	Mudeng	-1.67
ENSMUSG00000019796	Lrp11	-1.67
ENSMUSG00000028016	Ints12	-1.67
ENSMUSG00000043008	Klhl6	-1.67
ENSMUSG00000034040	Wbscr17	-1.67
ENSMUSG00000000884	Gnb1l	-1.67
ENSMUSG00000068134	Zfp120	-1.67
ENSMUSG00000025050	Pcgf6	-1.67
ENSMUSG00000024969	Mark2	-1.67
ENSMUSG00000038072	Galnt11	-1.67
ENSMUSG00000044513	9930014A18Rik	-1.67
ENSMUSG00000078902	Gm14443	-1.67
ENSMUSG00000028197	Col24a1	-1.67
ENSMUSG00000036850	Mrpl41	-1.67
ENSMUSG00000001119	Col6a1	-1.67
ENSMUSG00000031925	Maml2	-1.67
ENSMUSG00000046079	Lrrc8d	-1.68
ENSMUSG00000036959	Bcorl1	-1.68
ENSMUSG00000022472	Pppde2	-1.68
ENSMUSG00000000127	Fer	-1.68
ENSMUSG00000063683	Glyat	-1.68
ENSMUSG00000034854	Mfsd12	-1.68
ENSMUSG00000031216	Stard8	-1.68
ENSMUSG00000019699	Akt3	-1.68
ENSMUSG00000044707	Ccnjl	-1.68
ENSMUSG00000041199	Rpusd1	-1.68
ENSMUSG00000035045	Zc3h12b	-1.68
ENSMUSG00000029338	Antxr2	-1.68
ENSMUSG00000025076	Casp7	-1.68
ENSMUSG00000039100	March6	-1.68
ENSMUSG00000003184	Irf3	-1.68
ENSMUSG00000032468	Armc8	-1.68
ENSMUSG00000034321	Exosc1	-1.68
ENSMUSG00000027469	Tpx2	-1.68
ENSMUSG00000022299	Slc25a32	-1.68
ENSMUSG00000004609	Cd33	-1.68
ENSMUSG00000021263	Degs2	-1.68
ENSMUSG00000037426	Depdc5	-1.68
ENSMUSG00000005958	Ephb3	-1.68

ENSMUSG00000040389	Wdr47	-1.69
ENSMUSG00000052533	Nup188	-1.69
ENSMUSG00000002147	Stat6	-1.69
ENSMUSG00000003234	Abcf3	-1.69
ENSMUSG00000075254	Heg1	-1.69
ENSMUSG00000030051	Aplf	-1.69
ENSMUSG00000073393	B230354K17Rik	-1.69
ENSMUSG00000051786	Tubgcp6	-1.69
ENSMUSG00000021418	Rpp40	-1.69
ENSMUSG00000029594	Rbm19	-1.69
ENSMUSG00000005225	Plekha8	-1.69
ENSMUSG00000032409	Atr	-1.69
ENSMUSG00000050930	4933403G14Rik	-1.69
ENSMUSG00000022515	Anks3	-1.69
ENSMUSG00000078862	Gm14326	-1.69
ENSMUSG00000027699	Ect2	-1.69
ENSMUSG00000035401	2210018M11Rik	-1.69
ENSMUSG00000029283	Cdc7	-1.69
ENSMUSG00000046096	BC030336	-1.69
ENSMUSG00000072640	1810012P15Rik	-1.69
ENSMUSG00000031093	Dock11	-1.69
ENSMUSG00000018733	Pex12	-1.69
ENSMUSG00000070348	Ccnd1	-1.69
ENSMUSG00000033222	Ttf2	-1.69
ENSMUSG00000041231	Ublcp1	-1.70
ENSMUSG00000071855	Ccdc112	-1.70
ENSMUSG00000029471	Camkk2	-1.70
ENSMUSG00000045312	Lhfpl2	-1.70
ENSMUSG00000036931	Nfkbid	-1.70
ENSMUSG00000035498	Cdcp1	-1.70
ENSMUSG00000074582	Arfgef2	-1.70
ENSMUSG00000068551	Zfp467	-1.70
ENSMUSG00000035504	Reep6	-1.70
ENSMUSG00000045103	Dmd	-1.70
ENSMUSG00000024246	Thumpd2	-1.70
ENSMUSG00000026740	Dnajc1	-1.70
ENSMUSG00000028771	Ptpn12	-1.70
ENSMUSG00000038893	Fam117a	-1.70
ENSMUSG00000006390	Elovl1	-1.70
ENSMUSG00000028683	Eif2b3	-1.70
ENSMUSG00000040616	Tmem51	-1.70
ENSMUSG00000022711	Pmm2	-1.70
ENSMUSG00000026575	Nme7	-1.70

ENSMUSG00000036892	Prodh2	-1.70
ENSMUSG00000074634	Gm7120	-1.70
ENSMUSG00000026806	Ddx31	-1.70
ENSMUSG00000022228	Zfp187	-1.70
ENSMUSG00000025940	Tmem70	-1.70
ENSMUSG00000018599	Smcr7	-1.70
ENSMUSG00000031196	F8	-1.70
ENSMUSG00000031935	Med17	-1.70
ENSMUSG00000045980	Tmem104	-1.70
ENSMUSG00000024236	Svil	-1.71
ENSMUSG00000000194	Gpr107	-1.71
ENSMUSG00000033728	Lrrc14	-1.71
ENSMUSG00000042793	Lgr6	-1.71
ENSMUSG00000026078	Pdcl3	-1.71
ENSMUSG00000046516	Cox17	-1.71
ENSMUSG00000028675	Pnrc2	-1.71
ENSMUSG00000031375	Bgn	-1.71
ENSMUSG00000029657	Hsph1	-1.71
ENSMUSG00000046808	Atp10d	-1.71
ENSMUSG00000036339	6720456H20Rik	-1.71
ENSMUSG00000050619	Zscan29	-1.71
ENSMUSG00000038563	Eftud1	-1.71
ENSMUSG00000056234	Ncoa4	-1.71
ENSMUSG00000018334	Ksr1	-1.71
ENSMUSG00000074807	Gm10762	-1.71
ENSMUSG00000024065	Ehd3	-1.71
ENSMUSG00000042155	Klhl23	-1.71
ENSMUSG00000050132	Sarm1	-1.71
ENSMUSG00000035376	Ptplb	-1.71
ENSMUSG00000068114	Ccdc134	-1.72
ENSMUSG00000025644	Gm7628	-1.72
ENSMUSG00000028088	Fmo5	-1.72
ENSMUSG00000070426	Rnf121	-1.72
ENSMUSG00000022911	Arl13b	-1.72
ENSMUSG00000005501	Usp40	-1.72
ENSMUSG00000027080	Med19	-1.72
ENSMUSG00000030282	Cmas	-1.72
ENSMUSG00000028621	Cyb5rl	-1.72
ENSMUSG00000023959	Clic5	-1.72
ENSMUSG00000008575	Nfib	-1.72
ENSMUSG00000017376	Nlk	-1.72
ENSMUSG00000084867	Enox	-1.72
ENSMUSG00000041406	BC055324	-1.72

ENSMUSG00000025277	Abhd6	-1.73
ENSMUSG00000055228	Zfp935	-1.73
ENSMUSG00000026709	Dars2	-1.73
ENSMUSG00000031864	Ints10	-1.73
ENSMUSG00000029687	Ezh2	-1.73
ENSMUSG00000065979	Cpped1	-1.73
ENSMUSG00000086635	4932415G12Rik	-1.73
ENSMUSG00000030170	Wnt5b	-1.73
ENSMUSG00000033578	Tmem35	-1.73
ENSMUSG00000020605	Hs1bp3	-1.73
ENSMUSG00000042745	Id1	-1.73
ENSMUSG00000041954	Tnfrsf18	-1.73
ENSMUSG00000037458	Azin1	-1.73
ENSMUSG00000027650	Tti1	-1.73
ENSMUSG00000038368	BC057079	-1.73
ENSMUSG00000047867	Gimap6	-1.73
ENSMUSG00000015747	Vps45	-1.73
ENSMUSG00000040105	Ppapdc2	-1.73
ENSMUSG00000024007	Ppil1	-1.73
ENSMUSG00000054640	Slc8a1	-1.73
ENSMUSG00000074384	AI429214	-1.74
ENSMUSG00000041390	Mdfic	-1.74
ENSMUSG00000021185	9030617O03Rik	-1.74
ENSMUSG00000040102	Klhdc5	-1.74
ENSMUSG00000032560	Dnajc13	-1.74
ENSMUSG00000037098	Rab11fip3	-1.74
ENSMUSG00000020744	Slc25a19	-1.74
ENSMUSG00000035181	Heatr5a	-1.74
ENSMUSG00000038305	Spats2l	-1.74
ENSMUSG00000040209	Zfp704	-1.74
ENSMUSG00000041729	Coro2b	-1.74
ENSMUSG00000053950	Adnp2	-1.74
ENSMUSG00000042918	Mamstr	-1.74
ENSMUSG00000026585	Kifap3	-1.74
ENSMUSG00000046768	Rhoj	-1.74
ENSMUSG00000078970	Wdr92	-1.74
ENSMUSG00000029851	Fam115c	-1.74
ENSMUSG00000038119	Cdon	-1.74
ENSMUSG00000048481	Mypop	-1.74
ENSMUSG00000020003	Pex7	-1.74
ENSMUSG00000037972	Snn	-1.74
ENSMUSG00000047654	Tssk6	-1.75
ENSMUSG00000026820	Ptges2	-1.75

ENSMUSG00000031951	Tmem231	-1.75
ENSMUSG00000031539	Ap3m2	-1.75
ENSMUSG00000045725	Prr15	-1.75
ENSMUSG00000056602	Fry	-1.75
ENSMUSG00000090523	Gypc	-1.75
ENSMUSG00000030213	Atf7ip	-1.75
ENSMUSG00000056753	C330011M18Rik	-1.75
ENSMUSG00000033857	Engase	-1.75
ENSMUSG00000027088	Phospho2	-1.75
ENSMUSG00000021850	1700011H14Rik	-1.75
ENSMUSG00000026942	Traf2	-1.75
ENSMUSG00000022684	Bfar	-1.75
ENSMUSG00000018750	Zbtb4	-1.75
ENSMUSG00000007646	Rad51c	-1.75
ENSMUSG00000026004	1110028C15Rik	-1.75
ENSMUSG00000031380	Figf	-1.75
ENSMUSG00000005897	Nr2c1	-1.75
ENSMUSG00000042680	Fam59a	-1.75
ENSMUSG00000041594	Tmtc4	-1.75
ENSMUSG00000033985	Tesk2	-1.76
ENSMUSG00000066880	Zfp617	-1.76
ENSMUSG00000018661	Cog1	-1.76
ENSMUSG00000022144	Gdnf	-1.76
ENSMUSG00000081126	Gm15784	-1.76
ENSMUSG00000029407	Uso1	-1.76
ENSMUSG00000074916	Chst14	-1.76
ENSMUSG00000005514	Por	-1.76
ENSMUSG00000033610	Pank1	-1.76
ENSMUSG00000012076	Brms1l	-1.76
ENSMUSG00000036667	Fam115a	-1.76
ENSMUSG00000026976	Pax8	-1.76
ENSMUSG00000037946	Fgd3	-1.76
ENSMUSG00000075028	Prdm11	-1.76
ENSMUSG00000067928	Zfp760	-1.76
ENSMUSG00000041498	Kif14	-1.76
ENSMUSG00000054252	Fgfr3	-1.76
ENSMUSG00000022195	6030458C11Rik	-1.76
ENSMUSG00000090015	Gm15446	-1.76
ENSMUSG00000046167	Gldn	-1.76
ENSMUSG00000034066	Farp2	-1.77
ENSMUSG00000027357	Crls1	-1.77
ENSMUSG00000010721	Lmbr1	-1.77
ENSMUSG00000063895	Nupl1	-1.77

ENSMUSG00000022575	Gsdmd	-1.77
ENSMUSG00000019832	Rab32	-1.77
ENSMUSG00000024082	2410091C18Rik	-1.77
ENSMUSG00000029263	Pigg	-1.77
ENSMUSG00000032092	Mpzl2	-1.77
ENSMUSG00000033739	Fkbpl	-1.77
ENSMUSG00000042473	Tbc1d8b	-1.77
ENSMUSG00000048000	Gigyf2	-1.77
ENSMUSG00000039063	Echdc3	-1.77
ENSMUSG00000032579	Hemk1	-1.77
ENSMUSG00000004044	Ptrf	-1.77
ENSMUSG00000071653	1810009A15Rik	-1.77
ENSMUSG00000022849	Hspbap1	-1.77
ENSMUSG00000074519	Etohi1	-1.77
ENSMUSG00000062040	Zfp27	-1.77
ENSMUSG00000043162	Pigy	-1.77
ENSMUSG00000046027	Stard5	-1.78
ENSMUSG00000019948	Actr6	-1.78
ENSMUSG00000074024	4632427E13Rik	-1.78
ENSMUSG00000085214	0610005C13Rik	-1.78
ENSMUSG00000038009	Dnajc22	-1.78
ENSMUSG00000045519	Zfp560	-1.78
ENSMUSG00000032757	Bet1	-1.78
ENSMUSG00000078877	Gm14295	-1.78
ENSMUSG00000061353	Cxcl12	-1.78
ENSMUSG00000017446	C1qtnf1	-1.78
ENSMUSG00000049904	Tmem17	-1.78
ENSMUSG00000043419	A030009H04Rik	-1.78
ENSMUSG00000072770	Acrbp	-1.78
ENSMUSG00000001440	Kpnb1	-1.78
ENSMUSG00000016520	Lnx2	-1.78
ENSMUSG00000043964	Orai3	-1.78
ENSMUSG00000027865	Gdap2	-1.78
ENSMUSG00000020962	Gtf2a1	-1.78
ENSMUSG00000029722	Agfg2	-1.78
ENSMUSG00000003680	Taf6l	-1.78
ENSMUSG00000050666	E130203B14Rik	-1.78
ENSMUSG00000031767	Nudt7	-1.79
ENSMUSG00000020441	2310033P09Rik	-1.79
ENSMUSG00000085814	1810014B01Rik	-1.79
ENSMUSG00000056481	Cd248	-1.79
ENSMUSG00000000530	Acvrl1	-1.79
ENSMUSG00000056919	4922501C03Rik	-1.79

ENSMUSG00000034981	Parm1	-1.79
ENSMUSG00000022962	Gart	-1.79
ENSMUSG00000049307	Fut4	-1.79
ENSMUSG00000036412	Arsi	-1.79
ENSMUSG00000042961	Egflam	-1.79
ENSMUSG00000022887	Masp1	-1.79
ENSMUSG00000032537	Ephb1	-1.79
ENSMUSG00000024421	Lama3	-1.79
ENSMUSG00000055334	Snupn	-1.79
ENSMUSG00000018995	Nars2	-1.79
ENSMUSG00000032502	Stac	-1.80
ENSMUSG00000060397	Zfp128	-1.80
ENSMUSG00000040170	Fmo2	-1.80
ENSMUSG00000054517	Trim65	-1.80
ENSMUSG00000020993	Trappc6b	-1.80
ENSMUSG00000030220	Arhgdib	-1.80
ENSMUSG00000075411	Bin2	-1.80
ENSMUSG00000070282	3000002C10Rik	-1.80
ENSMUSG00000059000	Zfp799	-1.80
ENSMUSG00000003228	Grk5	-1.80
ENSMUSG00000032834	Pwp2	-1.80
ENSMUSG00000050945	Zfp438	-1.80
ENSMUSG00000017801	Mlx	-1.80
ENSMUSG00000056216	Cebpg	-1.80
ENSMUSG00000041762	Gpr155	-1.80
ENSMUSG00000025602	Zfp202	-1.80
ENSMUSG00000032000	Birc3	-1.80
ENSMUSG00000033499	Larp4b	-1.80
ENSMUSG00000032580	Rbm5	-1.80
ENSMUSG00000029638	Glcci1	-1.80
ENSMUSG00000057842	Zfp595	-1.80
ENSMUSG00000034853	Acot11	-1.80
ENSMUSG00000000093	Tbx2	-1.80
ENSMUSG00000070509	Rgma	-1.80
ENSMUSG00000026245	Farsb	-1.80
ENSMUSG00000052446	Zfp961	-1.80
ENSMUSG00000039286	Fndc3b	-1.80
ENSMUSG00000039519	Cyp7b1	-1.80
ENSMUSG00000020520	Galnt10	-1.80
ENSMUSG00000022742	Cpox	-1.80
ENSMUSG00000029047	Pex10	-1.81
ENSMUSG00000022335	Zfat	-1.81
ENSMUSG00000024899	Papss2	-1.81

ENSMUSG00000020638	Cmpk2	-1.81
ENSMUSG00000000142	Axin2	-1.81
ENSMUSG00000036580	Spg20	-1.81
ENSMUSG00000049858	Suox	-1.81
ENSMUSG00000078931	Pdf	-1.81
ENSMUSG00000041632	Mrps27	-1.81
ENSMUSG00000047342	Zfp286	-1.81
ENSMUSG00000042228	Lyn	-1.81
ENSMUSG00000004798	Ulk2	-1.81
ENSMUSG00000018740	Slc25a35	-1.81
ENSMUSG00000041559	Fmod	-1.81
ENSMUSG00000019814	Ltv1	-1.82
ENSMUSG00000039206	Daglb	-1.82
ENSMUSG00000078872	Gm14401	-1.82
ENSMUSG00000005774	Rfx5	-1.82
ENSMUSG00000020272	Stk10	-1.82
ENSMUSG00000022131	Gpr180	-1.82
ENSMUSG00000068566	Myadm	-1.82
ENSMUSG00000030613	Ccdc90b	-1.82
ENSMUSG00000056204	Pgpep1	-1.82
ENSMUSG00000027882	Stxbp3a	-1.82
ENSMUSG00000051671	1810063B05Rik	-1.82
ENSMUSG00000078853	Igtp	-1.82
ENSMUSG00000051351	Zfp46	-1.82
ENSMUSG00000026088	Mitd1	-1.82
ENSMUSG00000025937	Lactb2	-1.82
ENSMUSG00000084128	Esrp2	-1.82
ENSMUSG00000034764	1700006J14Rik	-1.82
ENSMUSG00000030218	Mgp	-1.82
ENSMUSG00000031723	Txnl4b	-1.82
ENSMUSG00000031934	Panx1	-1.82
ENSMUSG00000022560	Slc52a2	-1.82
ENSMUSG00000069713	4933406P04Rik	-1.82
ENSMUSG00000056310	Tyw1	-1.83
ENSMUSG00000037813	D630003M21Rik	-1.83
ENSMUSG00000079469	Pigb	-1.83
ENSMUSG00000022790	Igsf11	-1.83
ENSMUSG00000030752	Jmjd5	-1.83
ENSMUSG00000032470	Mras	-1.83
ENSMUSG00000035704	Alg8	-1.83
ENSMUSG00000000532	Acvr1b	-1.83
ENSMUSG00000036334	Igsf10	-1.83
ENSMUSG00000038080	Kdm1b	-1.83

ENSMUSG00000026180	Cxcr2	-1.83
ENSMUSG00000030264	Thumpd3	-1.83
ENSMUSG00000020706	Ftsj3	-1.83
ENSMUSG00000060090	Rp2h	-1.83
ENSMUSG00000020644	Id2	-1.83
ENSMUSG00000002458	Rgs19	-1.83
ENSMUSG00000021697	Depdc1b	-1.83
ENSMUSG00000061544	Zfp229	-1.84
ENSMUSG00000057982	Zfp809	-1.84
ENSMUSG00000027933	Ints3	-1.84
ENSMUSG00000020652	Cenpo	-1.84
ENSMUSG00000024378	Stard4	-1.84
ENSMUSG00000028678	Kif2c	-1.84
ENSMUSG00000024083	Pja2	-1.84
ENSMUSG00000022952	Runx1	-1.84
ENSMUSG00000079144	A130010J15Rik	-1.84
ENSMUSG00000034453	Polr3b	-1.84
ENSMUSG00000020241	Col6a2	-1.84
ENSMUSG00000068270	Shroom4	-1.84
ENSMUSG00000039116	Gpr126	-1.84
ENSMUSG00000019124	Scrn1	-1.85
ENSMUSG00000026694	Mettl13	-1.85
ENSMUSG00000032342	Mto1	-1.85
ENSMUSG00000035305	Ror1	-1.85
ENSMUSG00000029209	Gnpda2	-1.85
ENSMUSG00000059401	Mamld1	-1.85
ENSMUSG00000079334	Nat6	-1.85
ENSMUSG00000074867	Zfp808	-1.85
ENSMUSG00000045237	1110012L19Rik	-1.85
ENSMUSG00000032478	Nme6	-1.85
ENSMUSG00000040690	Col16a1	-1.85
ENSMUSG00000090125	Pou3f1	-1.85
ENSMUSG00000035351	Nup37	-1.85
ENSMUSG00000025421	Hdhd2	-1.86
ENSMUSG00000074865	Zfp934	-1.86
ENSMUSG00000020864	Ankrd40	-1.86
ENSMUSG00000048960	Prex2	-1.86
ENSMUSG00000022718	Dgcr8	-1.86
ENSMUSG00000030451	Herc2	-1.86
ENSMUSG00000060314	Zfp941	-1.86
ENSMUSG00000073858	Itpripl2	-1.86
ENSMUSG00000032806	Slc10a3	-1.86
ENSMUSG00000050244	Heatr1	-1.86

ENSMUSG00000028688	Toe1	-1.86
ENSMUSG00000027387	Zc3h8	-1.86
ENSMUSG00000020697	Lig3	-1.86
ENSMUSG00000066735	Vkorc1l1	-1.87
ENSMUSG00000037275	Gemin5	-1.87
ENSMUSG00000003198	Zfp959	-1.87
ENSMUSG00000039055	Eme1	-1.87
ENSMUSG00000033111	3830406C13Rik	-1.87
ENSMUSG00000023886	Smoc2	-1.87
ENSMUSG00000051238	2310047B19Rik	-1.87
ENSMUSG00000052085	Dock8	-1.87
ENSMUSG00000037206	Islr	-1.87
ENSMUSG00000032590	Apeh	-1.87
ENSMUSG00000003037	Rab8a	-1.87
ENSMUSG00000074671	Tspyl3	-1.87
ENSMUSG00000008429	Herpud2	-1.87
ENSMUSG00000031652	N4bp1	-1.87
ENSMUSG00000019779	Frk	-1.88
ENSMUSG00000020648	Dus4l	-1.88
ENSMUSG00000042505	Acn9	-1.88
ENSMUSG00000044501	Zfp758	-1.88
ENSMUSG00000005103	Wdr1	-1.88
ENSMUSG00000028007	Snx7	-1.88
ENSMUSG00000022351	Sqle	-1.88
ENSMUSG00000037151	Lrrc20	-1.88
ENSMUSG00000016128	Stard13	-1.88
ENSMUSG00000032883	Acsl3	-1.88
ENSMUSG00000040651	D14Abb1e	-1.88
ENSMUSG00000025326	Ube3a	-1.88
ENSMUSG00000000876	Pxmp4	-1.88
ENSMUSG00000041417	Pik3r1	-1.88
ENSMUSG00000007827	Ankrd26	-1.88
ENSMUSG00000055733	Nap1l3	-1.88
ENSMUSG00000054400	Cklf	-1.88
ENSMUSG00000090935	Synj2bp	-1.88
ENSMUSG00000005470	Asf1b	-1.88
ENSMUSG00000059475	Zfp426	-1.88
ENSMUSG00000040447	Spns2	-1.88
ENSMUSG00000031832	Taf1c	-1.89
ENSMUSG00000028419	Chmp5	-1.89
ENSMUSG00000031781	Ciapin1	-1.89
ENSMUSG00000015405	Ace2	-1.89
ENSMUSG00000037395	Rcor3	-1.89

ENSMUSG00000086158	Gm5918	-1.89
ENSMUSG00000021276	Cinp	-1.89
ENSMUSG00000026856	Dolpp1	-1.89
ENSMUSG00000031561	Odz3	-1.89
ENSMUSG00000051497	Kcnj16	-1.89
ENSMUSG00000021696	Elovl7	-1.90
ENSMUSG00000024906	Mus81	-1.90
ENSMUSG00000048787	Dcun1d3	-1.90
ENSMUSG00000046157	Tmem229b	-1.90
ENSMUSG00000048163	Selplg	-1.90
ENSMUSG00000048222	Mfap1b	-1.90
ENSMUSG00000004665	Cnn2	-1.90
ENSMUSG00000091683	Gm17357	-1.90
ENSMUSG00000028292	Rars2	-1.90
ENSMUSG00000021273	Fdft1	-1.90
ENSMUSG00000042992	Loh12cr1	-1.90
ENSMUSG00000022248	Rad1	-1.90
ENSMUSG00000091747	D17H6S56E-5	-1.90
ENSMUSG00000031774	Fam192a	-1.91
ENSMUSG00000034587	8430429K09Rik	-1.91
ENSMUSG00000044734	Serpinb1a	-1.91
ENSMUSG00000049687	Fam109b	-1.91
ENSMUSG00000031963	Bmper	-1.91
ENSMUSG00000003721	Insig2	-1.91
ENSMUSG00000028995	Fam126a	-1.91
ENSMUSG00000030335	Mrpl51	-1.91
ENSMUSG00000061013	Mkx	-1.91
ENSMUSG00000046567	4930430F08Rik	-1.91
ENSMUSG00000038279	Nop2	-1.91
ENSMUSG00000020887	A230052G05Rik	-1.91
ENSMUSG00000057604	Lmcd1	-1.91
ENSMUSG00000049957	Ccdc137	-1.91
ENSMUSG00000068479	Mfap1a	-1.91
ENSMUSG00000034532	Fbxo16	-1.92
ENSMUSG00000024370	Cdc23	-1.92
ENSMUSG00000024349	Tmem173	-1.92
ENSMUSG00000021047	Nova1	-1.92
ENSMUSG00000021835	Bmp4	-1.92
ENSMUSG00000022973	Synj1	-1.92
ENSMUSG00000022814	Umps	-1.92
ENSMUSG00000045854	Lyrm2	-1.92
ENSMUSG00000039901	9130011E15Rik	-1.92
ENSMUSG00000024096	Ralbp1	-1.92

ENSMUSG00000023832	Acat2	-1.92
ENSMUSG00000043257	Pigv	-1.92
ENSMUSG00000040818	Fam116a	-1.93
ENSMUSG00000056174	Col8a2	-1.93
ENSMUSG00000044676	Zfp612	-1.93
ENSMUSG00000069727	Gm5595	-1.93
ENSMUSG00000033016	Nfatc1	-1.93
ENSMUSG00000058258	Idi1	-1.93
ENSMUSG00000020492	Fam33a	-1.93
ENSMUSG00000021607	Mrpl36	-1.93
ENSMUSG00000092558	Med20	-1.93
ENSMUSG00000053935	Atf7ip	-1.93
ENSMUSG00000021958	Pinx1	-1.93
ENSMUSG00000021706	Zfyve16	-1.93
ENSMUSG00000040412	5330417C22Rik	-1.93
ENSMUSG00000032006	Pdgfd	-1.93
ENSMUSG00000030782	Tgfb1i1	-1.93
ENSMUSG00000052301	Doc2a	-1.93
ENSMUSG00000021613	Hapln1	-1.93
ENSMUSG00000054967	Zfp647	-1.93
ENSMUSG00000053965	Pde5a	-1.93
ENSMUSG00000071285	Zfp87	-1.93
ENSMUSG00000053907	Mat2a	-1.94
ENSMUSG00000025583	Rptor	-1.94
ENSMUSG00000048755	Mcat	-1.94
ENSMUSG00000037349	Nudt22	-1.94
ENSMUSG00000009647	Ccdc109a	-1.94
ENSMUSG00000037820	Tgm2	-1.94
ENSMUSG00000040187	Arntl2	-1.94
ENSMUSG00000022781	Pak2	-1.94
ENSMUSG00000050721	Plekho2	-1.94
ENSMUSG00000020456	Ogdh	-1.94
ENSMUSG00000024645	1700034H14Rik	-1.94
ENSMUSG00000078789	Dph1	-1.94
ENSMUSG00000028289	Epha7	-1.94
ENSMUSG00000087060	2810442I21Rik	-1.94
ENSMUSG00000042590	Ipo11	-1.95
ENSMUSG00000030208	Emp1	-1.95
ENSMUSG00000015189	Casd1	-1.95
ENSMUSG00000067150	Xpo5	-1.95
ENSMUSG00000026828	Galnt5	-1.95
ENSMUSG00000090093	Gm14399	-1.95
ENSMUSG00000020258	Glyctk	-1.95

ENSMUSG00000002020	Ltbp2	-1.95
ENSMUSG00000021824	Ap3m1	-1.95
ENSMUSG00000037921	Ddx60	-1.95
ENSMUSG00000055884	Fancm	-1.95
ENSMUSG00000033276	Stk36	-1.95
ENSMUSG00000010914	Pdhx	-1.95
ENSMUSG00000020829	Slc46a1	-1.95
ENSMUSG00000084972	9030407P20Rik	-1.95
ENSMUSG00000025083	Afap1l2	-1.95
ENSMUSG00000041301	Cftr	-1.95
ENSMUSG00000091764	Zfp964	-1.95
ENSMUSG00000036636	Clcn7	-1.96
ENSMUSG00000028899	Taf12	-1.96
ENSMUSG00000029804	Herc3	-1.96
ENSMUSG00000059493	Nhs	-1.96
ENSMUSG00000017697	Ada	-1.96
ENSMUSG00000083718	Ccnb2-ps	-1.96
ENSMUSG00000031840	Rab3a	-1.96
ENSMUSG00000028696	Ipp	-1.96
ENSMUSG00000048833	Slc39a9	-1.96
ENSMUSG00000007216	Zfp775	-1.96
ENSMUSG00000048497	Mmgt2	-1.96
ENSMUSG00000021271	Zfp839	-1.97
ENSMUSG00000024069	Slc30a6	-1.97
ENSMUSG00000005836	Gata6	-1.97
ENSMUSG00000049562	Gm962	-1.97
ENSMUSG00000038729	Akap2	-1.97
ENSMUSG00000026826	Nr4a2	-1.97
ENSMUSG00000027963	Extl2	-1.97
ENSMUSG00000034473	Sec22a	-1.97
ENSMUSG00000015133	Lrrk1	-1.97
ENSMUSG00000055184	Fam72a	-1.97
ENSMUSG00000030168	Adipor2	-1.97
ENSMUSG00000049580	Tsku	-1.97
ENSMUSG00000003849	Nqo1	-1.97
ENSMUSG00000040260	Daam2	-1.98
ENSMUSG00000020696	Rffl	-1.98
ENSMUSG00000046447	Camk2n1	-1.98
ENSMUSG00000033965	Slc16a2	-1.98
ENSMUSG00000092286	Gm20448	-1.98
ENSMUSG00000070304	Scn2b	-1.98
ENSMUSG00000047963	Stbd1	-1.98
ENSMUSG00000039662	Icmt	-1.98

ENSMUSG00000035799	Twist1	-1.98
ENSMUSG00000028273	Pdlim5	-1.98
ENSMUSG00000021710	Nln	-1.98
ENSMUSG00000027102	Hoxd8	-1.98
ENSMUSG00000001288	Rarg	-1.98
ENSMUSG00000001123	Lgals9	-1.98
ENSMUSG00000055313	Pgbd1	-1.99
ENSMUSG00000035069	Oma1	-1.99
ENSMUSG00000016477	E2f3	-1.99
ENSMUSG00000037007	Zfp113	-1.99
ENSMUSG00000027076	Timm10	-1.99
ENSMUSG00000049287	A230051G13Rik	-1.99
ENSMUSG00000042340	Ctf1	-1.99
ENSMUSG00000042694	Obfc1	-1.99
ENSMUSG00000031378	Abcd1	-1.99
ENSMUSG00000028108	Ecm1	-1.99
ENSMUSG00000024180	Tmem8	-1.99
ENSMUSG00000074890	Lcmt2	-1.99
ENSMUSG00000028894	Inpp5b	-2.00
ENSMUSG00000027652	Ralgapb	-2.00
ENSMUSG00000024142	Mlst8	-2.00
ENSMUSG00000027254	Mtap1a	-2.00
ENSMUSG00000004356	Utp20	-2.00
ENSMUSG00000028318	Polr1e	-2.00
ENSMUSG00000031753	Cog4	-2.00
ENSMUSG00000042426	Dhx29	-2.00
ENSMUSG00000052934	Fbxo31	-2.00
ENSMUSG00000022765	Snap29	-2.00
ENSMUSG00000022554	Fam203a	-2.00
ENSMUSG00000044341	Gm5601	-2.00
ENSMUSG00000022969	Il10rb	-2.00
ENSMUSG00000092262	Gm20434	-2.01
ENSMUSG00000037419	Endod1	-2.01
ENSMUSG00000018428	Akap1	-2.01
ENSMUSG00000022120	Rnf219	-2.01
ENSMUSG00000001767	Crnkl1	-2.01
ENSMUSG00000027428	Rbbp9	-2.01
ENSMUSG00000021998	Lcp1	-2.01
ENSMUSG00000032487	Ptgs2	-2.01
ENSMUSG00000074178	Gm10638	-2.01
ENSMUSG00000022519	Srl	-2.02
ENSMUSG00000090373	Gm17435	-2.02
ENSMUSG00000035378	Shq1	-2.02

ENSMUSG00000029610	Aimp2	-2.02
ENSMUSG00000034919	Ttc22	-2.02
ENSMUSG00000015468	Notch4	-2.02
ENSMUSG00000022833	Ccdc14	-2.02
ENSMUSG00000030341	Tnfrsf1a	-2.02
ENSMUSG00000031520	Vegfc	-2.02
ENSMUSG00000022123	Scel	-2.02
ENSMUSG00000071660	Ttc9c	-2.02
ENSMUSG00000029661	Col1a2	-2.02
ENSMUSG00000030610	Det1	-2.02
ENSMUSG00000031568	Rwdd4a	-2.02
ENSMUSG00000079002	C030006K11Rik	-2.03
ENSMUSG00000057778	Cyb5d2	-2.03
ENSMUSG00000036273	Lrrk2	-2.03
ENSMUSG00000056069	Fam105a	-2.03
ENSMUSG00000072763	5430403G16Rik	-2.03
ENSMUSG00000032332	Col12a1	-2.03
ENSMUSG00000029790	Tsga14	-2.03
ENSMUSG00000071042	Rasgrp3	-2.03
ENSMUSG00000002343	Armc6	-2.03
ENSMUSG00000021275	Tecpr2	-2.03
ENSMUSG00000093726	RP23-358B23.3	-2.03
ENSMUSG00000037536	Fbxo34	-2.03
ENSMUSG00000028702	Rad54l	-2.03
ENSMUSG00000024222	Fkbp5	-2.04
ENSMUSG00000026395	Ptprc	-2.04
ENSMUSG00000052539	Magi3	-2.04
ENSMUSG00000060568	Fam78b	-2.04
ENSMUSG00000030319	Cand2	-2.04
ENSMUSG00000045629	Sh3tc2	-2.04
ENSMUSG00000021111	Papola	-2.04
ENSMUSG00000031993	Snx19	-2.04
ENSMUSG00000079164	Tlr5	-2.05
ENSMUSG00000026203	Dnajb2	-2.05
ENSMUSG00000060176	Kif27	-2.05
ENSMUSG00000025373	Rnf41	-2.05
ENSMUSG00000020122	Egfr	-2.05
ENSMUSG00000067017	Gm3608	-2.05
ENSMUSG00000038214	Bend3	-2.05
ENSMUSG00000059058	Gm15431	-2.05
ENSMUSG00000068122	Agtr2	-2.05
ENSMUSG00000009733	Tfcp2	-2.05
ENSMUSG00000078863	Gm14325	-2.05

ENSMUSG00000020639	Pfn4	-2.05
ENSMUSG00000066637	Ttc32	-2.05
ENSMUSG00000037085	Trmt12	-2.05
ENSMUSG00000092260	Zfp963	-2.05
ENSMUSG00000036932	Aifm1	-2.05
ENSMUSG00000039153	Runx2	-2.05
ENSMUSG00000000739	Sult5a1	-2.05
ENSMUSG00000005078	Jkamp	-2.05
ENSMUSG00000023885	Thbs2	-2.05
ENSMUSG00000031641	Cbr4	-2.06
ENSMUSG00000027742	Cog6	-2.06
ENSMUSG00000031730	Dhodh	-2.06
ENSMUSG00000028976	Slc2a5	-2.06
ENSMUSG00000024172	St6gal2	-2.06
ENSMUSG00000041482	Fam38b	-2.06
ENSMUSG00000038540	Tmc3	-2.06
ENSMUSG00000024600	Slc27a6	-2.06
ENSMUSG00000028786	Tmem54	-2.06
ENSMUSG00000054920	Klhl5	-2.06
ENSMUSG00000020628	Ttc15	-2.06
ENSMUSG00000073452	Zfp97	-2.06
ENSMUSG00000028772	Zcchc17	-2.06
ENSMUSG00000057594	Arl16	-2.06
ENSMUSG00000058192	Zfp846	-2.07
ENSMUSG00000025759	Mfsd8	-2.07
ENSMUSG00000053091	Lins	-2.07
ENSMUSG00000046679	C87436	-2.07
ENSMUSG00000026029	Casp8	-2.07
ENSMUSG00000028082	Sh3d19	-2.07
ENSMUSG00000031953	Tmem170	-2.07
ENSMUSG00000003534	Ddr1	-2.07
ENSMUSG00000058447	Zfp82	-2.07
ENSMUSG00000039058	Ak5	-2.07
ENSMUSG00000024878	Cbwd1	-2.07
ENSMUSG00000050550	Gm11868	-2.07
ENSMUSG00000038888	Ctu1	-2.07
ENSMUSG00000067942	Zfp160	-2.08
ENSMUSG00000046794	Ppp1r3b	-2.08
ENSMUSG00000063531	Sema3e	-2.08
ENSMUSG00000028069	Gpatch4	-2.08
ENSMUSG00000037169	Mycn	-2.08
ENSMUSG00000074408	Gm10687	-2.08
ENSMUSG00000031931	Ankrd49	-2.08

ENSMUSG00000018362	Kpna2	-2.08
ENSMUSG00000052496	Pkdrej	-2.08
ENSMUSG00000074282	Zfp94	-2.08
ENSMUSG00000078954	Arhgap8	-2.08
ENSMUSG00000022676	Snai2	-2.08
ENSMUSG00000037514	Pank2	-2.08
ENSMUSG00000033352	Map2k4	-2.08
ENSMUSG00000037621	Atoh8	-2.08
ENSMUSG00000041360	D19Bwg1357e	-2.08
ENSMUSG00000024501	Dpysl3	-2.08
ENSMUSG00000047037	Nipa1	-2.09
ENSMUSG00000020774	Aspa	-2.09
ENSMUSG00000045817	Zfp36l2	-2.09
ENSMUSG00000009013	Dynll1	-2.09
ENSMUSG00000024999	Noc3l	-2.09
ENSMUSG00000044794	9330133O14Rik	-2.09
ENSMUSG00000074211	Sdhaf1	-2.09
ENSMUSG00000006638	Abhd1	-2.09
ENSMUSG00000028980	H6pd	-2.09
ENSMUSG00000034617	Mtrr	-2.09
ENSMUSG00000074136	4930513N10Rik	-2.10
ENSMUSG00000074364	Ehd2	-2.10
ENSMUSG00000079057	Cyp4v3	-2.10
ENSMUSG00000059316	Slc27a4	-2.10
ENSMUSG00000078899	Gm4631	-2.10
ENSMUSG00000087189	D130017N08Rik	-2.10
ENSMUSG00000028636	Ppcs	-2.10
ENSMUSG00000021891	Mettl6	-2.10
ENSMUSG00000074207	Adh1	-2.10
ENSMUSG00000032812	Arap1	-2.11
ENSMUSG00000086502	B130055M24Rik	-2.11
ENSMUSG00000051721	BC068281	-2.11
ENSMUSG00000035104	Fam176a	-2.11
ENSMUSG00000021676	Iqgap2	-2.11
ENSMUSG00000037278	Tmem97	-2.11
ENSMUSG00000035049	Rrp12	-2.11
ENSMUSG00000039804	Ncoa5	-2.11
ENSMUSG00000042350	1110018G07Rik	-2.11
ENSMUSG00000050010	Shisa3	-2.11
ENSMUSG00000027531	Impa1	-2.11
ENSMUSG00000061371	Zfp873	-2.12
ENSMUSG00000029920	Smarcad1	-2.12
ENSMUSG00000037762	Slc16a9	-2.12

ENSMUSG00000066007	Zfp600	-2.12
ENSMUSG00000052384	Lrrc33	-2.12
ENSMUSG00000032640	Chsy1	-2.12
ENSMUSG00000050866	Clrn3	-2.12
ENSMUSG00000071252	2210408I21Rik	-2.12
ENSMUSG00000042380	BC003266	-2.13
ENSMUSG00000028159	Dapp1	-2.13
ENSMUSG00000023156	Rpp14	-2.13
ENSMUSG00000039725	2810408M09Rik	-2.13
ENSMUSG00000025915	Sgk3	-2.13
ENSMUSG00000026389	Steap3	-2.13
ENSMUSG00000028565	Nfia	-2.13
ENSMUSG00000074579	Lekr1	-2.13
ENSMUSG00000038145	Snrk	-2.13
ENSMUSG00000002603	Tgfb1	-2.13
ENSMUSG00000066720	Cldn9	-2.14
ENSMUSG00000005686	Ampd3	-2.14
ENSMUSG00000031453	Rasa3	-2.14
ENSMUSG00000020785	Camkk1	-2.14
ENSMUSG00000044674	Fzd1	-2.14
ENSMUSG00000026142	Rhbdd1	-2.14
ENSMUSG00000045975	C2cd2	-2.14
ENSMUSG00000022220	Adcy4	-2.14
ENSMUSG00000037531	Mrpl47	-2.14
ENSMUSG00000074064	Mlycd	-2.14
ENSMUSG00000033554	Dph5	-2.14
ENSMUSG00000046245	Pilra	-2.14
ENSMUSG00000030922	Lyrm1	-2.14
ENSMUSG00000066113	Adamtsl1	-2.14
ENSMUSG00000020132	Rab21	-2.14
ENSMUSG00000028550	Atg4c	-2.14
ENSMUSG00000058446	Znrf2	-2.14
ENSMUSG00000031627	Irf2	-2.14
ENSMUSG00000051498	Tlr6	-2.15
ENSMUSG00000085208	4632419I22Rik	-2.15
ENSMUSG00000030871	Ears2	-2.15
ENSMUSG00000021457	Syk	-2.15
ENSMUSG00000028439	2310028H24Rik	-2.15
ENSMUSG00000047996	Prrg1	-2.15
ENSMUSG00000070802	Pnmal2	-2.15
ENSMUSG00000027339	Rassf2	-2.15
ENSMUSG00000023873	1700010I14Rik	-2.15
ENSMUSG00000021991	Cacna2d3	-2.15

ENSMUSG00000024511	Rab27b	-2.15
ENSMUSG00000037104	Socs5	-2.16
ENSMUSG00000039069	Gtpbp5	-2.16
ENSMUSG00000019312	Grb7	-2.16
ENSMUSG00000043279	Trim56	-2.16
ENSMUSG00000022179	4931414P19Rik	-2.16
ENSMUSG00000027323	Rad51	-2.16
ENSMUSG00000022792	Yars2	-2.16
ENSMUSG00000038379	Ttk	-2.16
ENSMUSG00000000148	Baat1	-2.16
ENSMUSG00000087598	Zfp111	-2.16
ENSMUSG00000078580	E430018J23Rik	-2.17
ENSMUSG00000004994	Ccdc130	-2.17
ENSMUSG00000028780	Sema3c	-2.17
ENSMUSG00000042371	Slc5a10	-2.17
ENSMUSG00000038510	Rpf2	-2.17
ENSMUSG00000026946	Nmi	-2.17
ENSMUSG00000024247	Pkdcc	-2.17
ENSMUSG00000028274	Rngtt	-2.17
ENSMUSG00000020679	Hnf1b	-2.18
ENSMUSG00000036983	Tfb1m	-2.18
ENSMUSG00000041644	Slc5a12	-2.18
ENSMUSG00000066026	Dhrs3	-2.18
ENSMUSG00000057060	Slc35f3	-2.18
ENSMUSG00000007908	Hmgcll1	-2.18
ENSMUSG00000026617	Bpnt1	-2.18
ENSMUSG00000055480	Zfp458	-2.18
ENSMUSG00000015943	Bola1	-2.18
ENSMUSG00000001707	Eef1e1	-2.18
ENSMUSG00000021707	Dhfr	-2.18
ENSMUSG00000038058	Nod1	-2.18
ENSMUSG00000048126	Col6a3	-2.18
ENSMUSG00000028907	Utp11l	-2.18
ENSMUSG00000048351	2010305A19Rik	-2.18
ENSMUSG00000024274	Zscan30	-2.18
ENSMUSG00000063888	Rpl7l1	-2.19
ENSMUSG00000034329	Brip1	-2.19
ENSMUSG00000013539	D16H22S680E	-2.19
ENSMUSG00000034037	Fgd5	-2.19
ENSMUSG00000027800	Tm4sf1	-2.19
ENSMUSG00000035184	Fam124a	-2.19
ENSMUSG00000036902	Neto2	-2.20
ENSMUSG00000055660	Mettl4	-2.20

ENSMUSG00000039929	Urb1	-2.20
ENSMUSG00000032718	Mansc1	-2.20
ENSMUSG00000029012	Orc5	-2.20
ENSMUSG00000055493	Epm2a	-2.20
ENSMUSG00000022371	Col14a1	-2.20
ENSMUSG00000054619	Mettl7a1	-2.20
ENSMUSG00000026814	Eng	-2.20
ENSMUSG00000092119	Gm17523	-2.20
ENSMUSG00000045932	Ifit2	-2.21
ENSMUSG00000021904	Sema3g	-2.21
ENSMUSG00000030306	Tmtc1	-2.21
ENSMUSG00000053799	Exoc6	-2.21
ENSMUSG00000028629	Dem1	-2.21
ENSMUSG00000017776	Crk	-2.21
ENSMUSG00000004568	Arhgef18	-2.21
ENSMUSG00000002944	Cd36	-2.21
ENSMUSG00000026035	Ppil3	-2.22
ENSMUSG00000050079	Rspry1	-2.22
ENSMUSG00000079376	Gm3383	-2.22
ENSMUSG00000026803	Ttf1	-2.22
ENSMUSG00000026235	Epha4	-2.22
ENSMUSG00000004748	Mtfp1	-2.22
ENSMUSG00000039000	Ube3c	-2.23
ENSMUSG00000039768	Dnajc11	-2.23
ENSMUSG00000010054	Tusc2	-2.23
ENSMUSG00000007877	Tcap	-2.23
ENSMUSG00000025810	Nrp1	-2.23
ENSMUSG00000006386	Tek	-2.23
ENSMUSG00000043535	Setx	-2.23
ENSMUSG00000089824	Rbm12	-2.23
ENSMUSG00000031887	Tradd	-2.23
ENSMUSG00000039414	Heatr5b	-2.23
ENSMUSG00000032583	Mon1a	-2.24
ENSMUSG00000073016	Uprt	-2.24
ENSMUSG00000040795	Iqcc	-2.24
ENSMUSG00000029480	Dhx37	-2.24
ENSMUSG00000042672	Dcst1	-2.24
ENSMUSG00000000159	Igsf5	-2.24
ENSMUSG00000084910	C630043F03Rik	-2.24
ENSMUSG00000039763	Dnajc28	-2.24
ENSMUSG00000026072	Il1r1	-2.24
ENSMUSG00000021392	Nol8	-2.25
ENSMUSG00000022799	Arhgap31	-2.25

ENSMUSG00000048728	Zfp454	-2.25
ENSMUSG00000047040	Prr15l	-2.25
ENSMUSG00000031665	Sall1	-2.25
ENSMUSG00000042229	Rabif	-2.25
ENSMUSG00000080981	Gm12161	-2.25
ENSMUSG00000030725	Lipt2	-2.25
ENSMUSG00000021951	N6amt2	-2.25
ENSMUSG00000031608	Galnt7	-2.25
ENSMUSG00000034810	Scn7a	-2.25
ENSMUSG00000033809	Alg3	-2.25
ENSMUSG00000029999	Tgfa	-2.26
ENSMUSG00000021285	Ppp1r13b	-2.26
ENSMUSG00000045316	Fahd1	-2.26
ENSMUSG00000091002	Tcerg1l	-2.26
ENSMUSG00000078886	Gm2026	-2.27
ENSMUSG00000024620	Pdgfrb	-2.27
ENSMUSG00000023259	Slc26a6	-2.27
ENSMUSG00000005089	Slc1a2	-2.27
ENSMUSG00000047583	Tyw3	-2.28
ENSMUSG00000051373	Ppapdc3	-2.28
ENSMUSG00000040548	Tex2	-2.28
ENSMUSG00000030469	Zfp719	-2.28
ENSMUSG00000031673	Cdh11	-2.28
ENSMUSG00000020810	Cygb	-2.28
ENSMUSG00000056091	St3gal5	-2.28
ENSMUSG00000007777	0610009B22Rik	-2.28
ENSMUSG00000045464	2810002D19Rik	-2.28
ENSMUSG00000034744	Nagk	-2.28
ENSMUSG00000018927	Ccl6	-2.28
ENSMUSG00000037405	Icam1	-2.28
ENSMUSG00000024668	Sdhaf2	-2.29
ENSMUSG00000022324	Matn2	-2.29
ENSMUSG00000019988	Nedd1	-2.29
ENSMUSG00000075502	Gm5465	-2.29
ENSMUSG00000026222	Sp100	-2.29
ENSMUSG00000043487	Acot6	-2.29
ENSMUSG00000056220	Pla2g4a	-2.29
ENSMUSG00000041609	Ccdc64	-2.29
ENSMUSG00000034518	Hmgxb4	-2.29
ENSMUSG00000034187	Nsf	-2.29
ENSMUSG00000019975	Ikbip	-2.30
ENSMUSG00000069227	Gprin1	-2.30
ENSMUSG00000022130	Tgds	-2.30

ENSMUSG00000032513	Gorasp1	-2.30
ENSMUSG00000025766	D3Ertd751e	-2.30
ENSMUSG00000049235	Gm7324	-2.31
ENSMUSG00000032344	E330016A19Rik	-2.31
ENSMUSG00000040703	Cyp2s1	-2.31
ENSMUSG00000072582	Ptrh2	-2.31
ENSMUSG00000073427	Gm4924	-2.31
ENSMUSG00000027463	Slc52a3	-2.31
ENSMUSG00000090817	Gm4450	-2.31
ENSMUSG00000035575	Utp6	-2.31
ENSMUSG00000014177	Fam18b	-2.31
ENSMUSG00000021759	Ppap2a	-2.31
ENSMUSG00000046667	Rbm12b	-2.32
ENSMUSG00000023921	Mut	-2.32
ENSMUSG00000028992	Nmnat1	-2.32
ENSMUSG00000028031	Dkk2	-2.32
ENSMUSG00000044702	Palb2	-2.32
ENSMUSG00000053846	Lipg	-2.32
ENSMUSG00000025958	Creb1	-2.32
ENSMUSG00000030614	Tmem126b	-2.32
ENSMUSG00000056492	Gpr116	-2.32
ENSMUSG00000039934	Pion	-2.32
ENSMUSG00000020527	Myo19	-2.32
ENSMUSG00000032235	Narg2	-2.33
ENSMUSG00000039883	Lrrc17	-2.33
ENSMUSG00000058099	Nfam1	-2.33
ENSMUSG00000070583	Fv1	-2.33
ENSMUSG00000052117	D630039A03Rik	-2.33
ENSMUSG00000048970	C1galt1c1	-2.33
ENSMUSG00000045827	Serpinb9	-2.33
ENSMUSG00000064128	Cenpj	-2.33
ENSMUSG00000050188	Lsm10	-2.33
ENSMUSG00000001911	Nfix	-2.34
ENSMUSG00000028655	Mfsd2a	-2.34
ENSMUSG00000078202	Nrarp	-2.34
ENSMUSG00000040429	Mterf	-2.34
ENSMUSG00000044647	Csrnp3	-2.35
ENSMUSG00000049755	Zfp672	-2.35
ENSMUSG00000027276	Jag1	-2.35
ENSMUSG00000038736	Nudcd1	-2.35
ENSMUSG00000053297	AI854703	-2.35
ENSMUSG00000074732	Zfp950	-2.36
ENSMUSG00000020100	Slc29a3	-2.36

ENSMUSG00000034738	Nostrin	-2.36
ENSMUSG00000037991	A630055G03Rik	-2.36
ENSMUSG00000023988	Bysl	-2.36
ENSMUSG00000075585	6330403L08Rik	-2.36
ENSMUSG00000022526	Zfp251	-2.36
ENSMUSG00000049939	Lrrc4	-2.36
ENSMUSG00000093445	Lrch4	-2.36
ENSMUSG00000054939	Zfp174	-2.37
ENSMUSG00000024268	Celf4	-2.37
ENSMUSG00000043190	Rfesd	-2.37
ENSMUSG00000075012	Fjx1	-2.37
ENSMUSG00000022674	Ube2v2	-2.38
ENSMUSG00000047735	Samd9l	-2.38
ENSMUSG00000049112	Oxtr	-2.38
ENSMUSG00000039316	Rftn1	-2.38
ENSMUSG00000036067	Slc2a6	-2.38
ENSMUSG00000017929	B4galt5	-2.38
ENSMUSG00000043518	Rai2	-2.38
ENSMUSG00000034639	Setmar	-2.38
ENSMUSG00000090394	4930523C07Rik	-2.39
ENSMUSG00000040061	Plcb2	-2.39
ENSMUSG00000046909	1110002N22Rik	-2.39
ENSMUSG00000022894	Adamts5	-2.39
ENSMUSG00000054676	1600014C10Rik	-2.39
ENSMUSG00000006362	Cbfa2t3	-2.39
ENSMUSG00000033777	Tlr13	-2.39
ENSMUSG00000052821	Cysltr1	-2.40
ENSMUSG00000015950	Ncf1	-2.40
ENSMUSG00000046603	D9Ertd402e	-2.40
ENSMUSG00000029832	Nfe2l3	-2.40
ENSMUSG00000073771	Btbd19	-2.40
ENSMUSG00000067480	Gm14403	-2.40
ENSMUSG00000050751	Pgbd5	-2.40
ENSMUSG00000032202	Rab27a	-2.40
ENSMUSG00000035407	Kank4	-2.40
ENSMUSG00000022724	Mina	-2.41
ENSMUSG00000042097	Zfp239	-2.41
ENSMUSG00000022325	Pop1	-2.41
ENSMUSG00000089857	Zfp882	-2.41
ENSMUSG00000026354	Lct	-2.41
ENSMUSG00000052917	Senp7	-2.41
ENSMUSG00000021071	Trim9	-2.41
ENSMUSG00000044811	AF251705	-2.41

ENSMUSG00000022639	5330426P16Rik	-2.41
ENSMUSG00000043991	Pura	-2.42
ENSMUSG00000038074	Fkbp14	-2.42
ENSMUSG00000020553	Pctp	-2.42
ENSMUSG00000050668	Ccdc75	-2.42
ENSMUSG00000030800	Prss8	-2.42
ENSMUSG00000001774	Chordc1	-2.42
ENSMUSG00000033900	Mtap9	-2.43
ENSMUSG00000024558	Mapk4	-2.43
ENSMUSG00000026365	Cfh	-2.43
ENSMUSG00000054383	Pnma1	-2.43
ENSMUSG00000024087	Cyp1b1	-2.43
ENSMUSG00000021871	Pnp	-2.43
ENSMUSG00000018604	Tbx3	-2.43
ENSMUSG00000056383	AI987944	-2.44
ENSMUSG00000025993	Slc40a1	-2.44
ENSMUSG00000046610	5330437I02Rik	-2.44
ENSMUSG00000036834	Plch1	-2.44
ENSMUSG00000068407	Rnase12	-2.44
ENSMUSG00000075304	Sp5	-2.44
ENSMUSG00000062545	Tlr12	-2.44
ENSMUSG00000033961	Zfp446	-2.44
ENSMUSG00000024276	Zfp397	-2.45
ENSMUSG00000035878	Agphd1	-2.45
ENSMUSG00000000392	Fap	-2.45
ENSMUSG00000048486	Fitm2	-2.45
ENSMUSG00000022898	Dscr3	-2.45
ENSMUSG00000020621	Rdh14	-2.45
ENSMUSG00000029084	Cd38	-2.46
ENSMUSG00000036461	Elf1	-2.46
ENSMUSG00000034110	Kctd7	-2.46
ENSMUSG00000027859	Ngf	-2.46
ENSMUSG00000034203	Chchd4	-2.46
ENSMUSG00000092534	Gm20418	-2.46
ENSMUSG00000022367	Has2	-2.46
ENSMUSG00000058897	Col25a1	-2.46
ENSMUSG00000029482	Aacs	-2.46
ENSMUSG00000074643	Cpne1	-2.47
ENSMUSG00000022664	Slc35a5	-2.47
ENSMUSG00000024694	Keg1	-2.47
ENSMUSG00000045757	Zfp764	-2.47
ENSMUSG00000034848	Ttc21b	-2.47
ENSMUSG00000022146	Osmr	-2.47

ENSMUSG00000031870	Pgr	-2.47
ENSMUSG00000029163	Emilin1	-2.48
ENSMUSG00000026994	Galnt3	-2.48
ENSMUSG00000050973	D330012F22Rik	-2.48
ENSMUSG00000026241	Nppc	-2.49
ENSMUSG00000037015	Tmem185b	-2.49
ENSMUSG00000048458	6530418L21Rik	-2.49
ENSMUSG00000043140	Tmem186	-2.49
ENSMUSG00000048581	E130311K13Rik	-2.49
ENSMUSG00000074417	Gm14548	-2.49
ENSMUSG00000002885	Cd97	-2.49
ENSMUSG00000030711	Sult1a1	-2.49
ENSMUSG00000028544	Slc5a9	-2.50
ENSMUSG00000027684	Mecom	-2.50
ENSMUSG00000018999	Slc35b4	-2.50
ENSMUSG00000026043	Col3a1	-2.50
ENSMUSG00000091828	5033417F24Rik	-2.50
ENSMUSG00000038527	C1rl	-2.50
ENSMUSG00000068299	1700019G17Rik	-2.50
ENSMUSG00000036327	Qsox2	-2.50
ENSMUSG00000038630	Zkscan16	-2.50
ENSMUSG00000051359	Ncald	-2.51
ENSMUSG00000027962	Vcam1	-2.51
ENSMUSG00000071281	Zfp71-rs1	-2.51
ENSMUSG00000025892	Gria4	-2.51
ENSMUSG00000029919	Hpgds	-2.51
ENSMUSG00000004462	Tbccd1	-2.52
ENSMUSG00000090919	Pabpc4l	-2.52
ENSMUSG00000086877	A230072C01Rik	-2.52
ENSMUSG00000031101	Sash3	-2.52
ENSMUSG00000030616	Sytl2	-2.52
ENSMUSG00000048814	Lonrf2	-2.52
ENSMUSG00000030283	St8sia1	-2.52
ENSMUSG00000019861	Gopc	-2.52
ENSMUSG00000045691	Thtpa	-2.52
ENSMUSG00000022512	Cldn1	-2.52
ENSMUSG00000028546	Elavl4	-2.53
ENSMUSG00000019864	Rtn4ip1	-2.53
ENSMUSG00000044164	Rnf182	-2.53
ENSMUSG00000048100	Taf13	-2.53
ENSMUSG00000024579	Pcyox1l	-2.53
ENSMUSG00000024897	Apba1	-2.53
ENSMUSG00000021716	Srek1ip1	-2.53

ENSMUSG00000028599	Tnfrsf1b	-2.53
ENSMUSG00000038028	9630033F20Rik	-2.54
ENSMUSG00000043602	Zfp3	-2.54
ENSMUSG00000085028	Slc2a4rg-ps	-2.54
ENSMUSG00000032572	Col6a4	-2.54
ENSMUSG00000053025	Sv2b	-2.54
ENSMUSG00000038268	Ovca2	-2.54
ENSMUSG00000075033	Fam55c	-2.55
ENSMUSG00000053062	Jam2	-2.55
ENSMUSG00000038560	Sp6	-2.55
ENSMUSG00000060466	Thap6	-2.56
ENSMUSG00000090622	A930033H14Rik	-2.56
ENSMUSG00000075273	Ttc30b	-2.56
ENSMUSG00000068457	Uty	-2.56
ENSMUSG00000048022	Tmem229a	-2.56
ENSMUSG00000021390	Ogn	-2.56
ENSMUSG00000020053	Igf1	-2.57
ENSMUSG00000015653	Steap2	-2.57
ENSMUSG00000020380	Rad50	-2.57
ENSMUSG00000032035	Ets1	-2.57
ENSMUSG00000044881	Chchd8	-2.57
ENSMUSG00000020752	Recql5	-2.58
ENSMUSG00000034968	Lbx2	-2.58
ENSMUSG00000001506	Col1a1	-2.58
ENSMUSG00000053012	Krcc1	-2.58
ENSMUSG00000034157	2310044G17Rik	-2.58
ENSMUSG00000055373	Fut9	-2.58
ENSMUSG00000046351	Zfp322a	-2.58
ENSMUSG00000033126	Ybey	-2.59
ENSMUSG00000023953	Polh	-2.60
ENSMUSG00000031073	Fgf15	-2.60
ENSMUSG00000060380	C030014I23Rik	-2.60
ENSMUSG00000028479	Gne	-2.60
ENSMUSG00000051506	Wdfy4	-2.61
ENSMUSG00000039680	Mrps6	-2.61
ENSMUSG00000079224	Gm6565	-2.61
ENSMUSG00000091183	Gm3604	-2.61
ENSMUSG00000030016	Zfml	-2.61
ENSMUSG00000051735	Rinl	-2.61
ENSMUSG00000063894	Zfp192	-2.62
ENSMUSG00000055150	Zfp78	-2.63
ENSMUSG00000042579	4632404H12Rik	-2.63
ENSMUSG00000029193	Cckar	-2.63

ENSMUSG00000055319	Sec23ip	-2.63
ENSMUSG00000068196	Col8a1	-2.64
ENSMUSG00000090576	Gm17055	-2.64
ENSMUSG00000037490	Slc2a12	-2.64
ENSMUSG00000057497	Fam136a	-2.64
ENSMUSG00000028864	Hgf	-2.65
ENSMUSG00000029178	Klf3	-2.65
ENSMUSG00000030347	D6Wsu163e	-2.65
ENSMUSG00000028619	2210012G02Rik	-2.65
ENSMUSG00000071256	Zfp213	-2.65
ENSMUSG00000082361	Btc	-2.65
ENSMUSG00000056888	Glipr1	-2.65
ENSMUSG00000075054	1600012F09Rik	-2.66
ENSMUSG00000074283	Zfp109	-2.66
ENSMUSG00000048965	Mrgpre	-2.66
ENSMUSG00000019913	Sim1	-2.66
ENSMUSG00000032802	Srxn1	-2.66
ENSMUSG00000056529	Ptafr	-2.66
ENSMUSG00000026858	Fam73b	-2.67
ENSMUSG00000000378	Ccm2	-2.67
ENSMUSG00000032744	Heyl	-2.67
ENSMUSG00000036298	Slc2a13	-2.67
ENSMUSG00000062382	Gm10116	-2.67
ENSMUSG00000018698	Lhx1	-2.68
ENSMUSG00000085282	Gm15663	-2.68
ENSMUSG00000019838	Slc16a10	-2.68
ENSMUSG00000049922	Slc35c1	-2.69
ENSMUSG00000023994	Nfya	-2.69
ENSMUSG00000092035	Peg10	-2.69
ENSMUSG00000042842	Serpinb6b	-2.70
ENSMUSG00000021711	2410002O22Rik	-2.70
ENSMUSG00000047205	Dusp18	-2.70
ENSMUSG00000012429	2810021B07Rik	-2.70
ENSMUSG00000022510	Trp63	-2.70
ENSMUSG00000043019	Edem3	-2.70
ENSMUSG00000063535	Zfp773	-2.71
ENSMUSG00000022306	Zfpm2	-2.71
ENSMUSG00000031910	Has3	-2.71
ENSMUSG00000027173	Depdc7	-2.71
ENSMUSG00000061742	Slc22a12	-2.71
ENSMUSG00000039958	4833442J19Rik	-2.72
ENSMUSG00000047649	Cd3eap	-2.72
ENSMUSG00000069089	Cdk7	-2.72

ENSMUSG00000047180	Neurl3	-2.73
ENSMUSG00000003418	St8sia6	-2.73
ENSMUSG00000051235	Gen1	-2.73
ENSMUSG00000085615	A330035P11Rik	-2.73
ENSMUSG00000025804	Ccr1	-2.73
ENSMUSG00000001494	Sost	-2.73
ENSMUSG00000021754	Map3k1	-2.73
ENSMUSG00000035681	Kcnc2	-2.73
ENSMUSG00000059173	Pde1a	-2.73
ENSMUSG00000025931	Paqr8	-2.73
ENSMUSG00000029676	Pot1a	-2.74
ENSMUSG00000037262	Kin	-2.74
ENSMUSG00000033233	Trim45	-2.74
ENSMUSG00000018405	Mrm1	-2.74
ENSMUSG00000021906	Oxnad1	-2.74
ENSMUSG00000036295	Lrrn3	-2.75
ENSMUSG00000026674	Ddr2	-2.75
ENSMUSG00000047773	Ankfn1	-2.75
ENSMUSG00000020427	Igfbp3	-2.76
ENSMUSG00000046441	Ftsjd1	-2.76
ENSMUSG00000032252	Glce	-2.76
ENSMUSG00000034308	Sdr42e1	-2.76
ENSMUSG00000036975	Tmem177	-2.77
ENSMUSG00000040133	Gpr176	-2.77
ENSMUSG00000078190	Dnm3os	-2.77
ENSMUSG00000003283	Hck	-2.77
ENSMUSG00000026435	Slc45a3	-2.77
ENSMUSG00000031604	Sc4mol	-2.77
ENSMUSG00000032652	Crebl2	-2.77
ENSMUSG00000073791	Efcab7	-2.77
ENSMUSG00000063239	Grm4	-2.78
ENSMUSG00000089876	Tmem102	-2.78
ENSMUSG00000051256	Jagn1	-2.78
ENSMUSG00000030443	Zfp583	-2.78
ENSMUSG00000022687	Boc	-2.78
ENSMUSG00000036599	Chst12	-2.79
ENSMUSG00000086843	E030013I19Rik	-2.80
ENSMUSG00000024697	Gna14	-2.80
ENSMUSG00000087107	AI662270	-2.81
ENSMUSG00000048582	Gja3	-2.81
ENSMUSG00000048865	Arhgap30	-2.81
ENSMUSG00000045573	Penk	-2.81
ENSMUSG00000038400	Pmepa1	-2.81

ENSMUSG00000044149	Nkrf	-2.81
ENSMUSG00000026786	Apbb1ip	-2.81
ENSMUSG00000053886	Sh2d4a	-2.82
ENSMUSG00000031952	Chst5	-2.82
ENSMUSG00000041757	Plekha6	-2.82
ENSMUSG00000051727	Kctd14	-2.83
ENSMUSG00000091994	E130317F20Rik	-2.83
ENSMUSG00000035455	Fignl1	-2.83
ENSMUSG00000050714	Zbtb26	-2.83
ENSMUSG00000078779	Zfp59	-2.83
ENSMUSG00000050471	Fam118b	-2.83
ENSMUSG00000025185	Loxl4	-2.83
ENSMUSG00000048280	Zfp738	-2.83
ENSMUSG00000057123	Gja5	-2.83
ENSMUSG00000000359	Rem1	-2.84
ENSMUSG00000055148	Klf2	-2.84
ENSMUSG00000026317	Cln8	-2.85
ENSMUSG00000021359	Tfap2a	-2.85
ENSMUSG00000028698	Pik3r3	-2.85
ENSMUSG00000053286	1190005F20Rik	-2.85
ENSMUSG00000026698	Pigc	-2.85
ENSMUSG00000074500	Zfp558	-2.86
ENSMUSG00000089942	Pira2	-2.86
ENSMUSG00000081683	Fzd10	-2.87
ENSMUSG00000068962	Zfp114	-2.87
ENSMUSG00000053684	BC048403	-2.87
ENSMUSG00000034116	Vav1	-2.88
ENSMUSG00000047786	Lix1	-2.88
ENSMUSG00000072962	Gm16401	-2.88
ENSMUSG00000028247	Coq3	-2.88
ENSMUSG00000044921	Rassf9	-2.88
ENSMUSG00000050541	Adra1b	-2.88
ENSMUSG00000063087	Gm10125	-2.89
ENSMUSG00000083246	Gm11839	-2.89
ENSMUSG00000020309	Chac2	-2.89
ENSMUSG00000027750	Postn	-2.89
ENSMUSG00000014763	Fam120b	-2.90
ENSMUSG00000038506	Dcun1d2	-2.90
ENSMUSG00000022244	Amacr	-2.90
ENSMUSG00000045680	Tcf21	-2.90
ENSMUSG00000020614	Fam20a	-2.91
ENSMUSG00000005611	Mrvi1	-2.92
ENSMUSG00000057143	Trim12c	-2.92

ENSMUSG00000006403	Adamts4	-2.92
ENSMUSG00000021903	Galntl2	-2.92
ENSMUSG00000051124	Gimap9	-2.92
ENSMUSG00000026104	Stat1	-2.92
ENSMUSG00000041079	Rwdd2b	-2.92
ENSMUSG00000091596	3110083C13Rik	-2.93
ENSMUSG00000027015	Cybrd1	-2.93
ENSMUSG00000091302	2310043M15Rik	-2.93
ENSMUSG00000018008	Cyth4	-2.93
ENSMUSG00000030247	Kcnj8	-2.93
ENSMUSG00000033579	Fa2h	-2.93
ENSMUSG00000024592	C330018D20Rik	-2.94
ENSMUSG00000043592	Unc5cl	-2.94
ENSMUSG00000025475	Gpr123	-2.94
ENSMUSG00000015652	Steap1	-2.95
ENSMUSG00000079364	Gm3558	-2.95
ENSMUSG00000038582	Pptc7	-2.95
ENSMUSG00000029335	Bmp3	-2.95
ENSMUSG00000056735	A930024E05Rik	-2.96
ENSMUSG00000056025	Clca1	-2.96
ENSMUSG00000004500	Zfp324	-2.97
ENSMUSG00000040003	Magi2	-2.98
ENSMUSG00000060950	Trmt61a	-2.98
ENSMUSG00000025352	Gdf11	-2.98
ENSMUSG00000085379	2310058D17Rik	-2.99
ENSMUSG00000044362	Ccdc89	-2.99
ENSMUSG00000030559	Rab38	-2.99
ENSMUSG00000057137	Tmem140	-2.99
ENSMUSG00000028028	Alpk1	-2.99
ENSMUSG00000024900	Cpt1a	-2.99
ENSMUSG00000026656	Fcgr2b	-2.99
ENSMUSG00000044288	Cnr1	-3.00
ENSMUSG00000055760	Gemin6	-3.00
ENSMUSG00000074676	Foxs1	-3.00
ENSMUSG00000041378	Cldn5	-3.00
ENSMUSG00000050697	Prkaa1	-3.01
ENSMUSG00000047635	2810006K23Rik	-3.01
ENSMUSG00000071456	1110002L01Rik	-3.01
ENSMUSG00000033313	Fbxl8	-3.01
ENSMUSG00000042529	Kcnj12	-3.02
ENSMUSG00000030047	Arhgap25	-3.03
ENSMUSG00000078349	AW011738	-3.04
ENSMUSG00000049536	Tceal1	-3.05

ENSMUSG00000044231	Nhlrc1	-3.06
ENSMUSG00000010047	Hyal2	-3.07
ENSMUSG00000025429	Pstpip2	-3.07
ENSMUSG00000048550	Thnsl1	-3.07
ENSMUSG00000020513	Tubd1	-3.07
ENSMUSG00000058883	Zfp708	-3.07
ENSMUSG00000040253	Gbp7	-3.07
ENSMUSG00000085566	A730017L22Rik	-3.07
ENSMUSG00000021895	Arhgef3	-3.07
ENSMUSG00000048920	Fkrp	-3.08
ENSMUSG00000038094	Atp13a4	-3.08
ENSMUSG00000022061	Nkx3-1	-3.09
ENSMUSG00000047759	Hs3st3a1	-3.09
ENSMUSG00000062743	Zfp677	-3.10
ENSMUSG00000041773	Enc1	-3.10
ENSMUSG00000027368	Dusp2	-3.10
ENSMUSG00000031077	Fadd	-3.10
ENSMUSG00000026602	Nphs2	-3.10
ENSMUSG00000091138	E530011L22Rik	-3.11
ENSMUSG00000042460	C1galt1	-3.11
ENSMUSG00000042938	Gm14117	-3.11
ENSMUSG00000052504	Epha3	-3.11
ENSMUSG00000021786	Oxsm	-3.11
ENSMUSG00000027955	Fam198b	-3.11
ENSMUSG00000032446	Eomes	-3.12
ENSMUSG00000037188	Grhl3	-3.12
ENSMUSG00000040229	Gpr34	-3.13
ENSMUSG00000043311	D17H6S53E	-3.13
ENSMUSG00000036078	Sigmar1	-3.14
ENSMUSG00000021245	Mlh3	-3.14
ENSMUSG00000050953	Gja1	-3.14
ENSMUSG00000023017	Accn2	-3.15
ENSMUSG00000043969	Emx2	-3.15
ENSMUSG00000074892	B3galt5	-3.15
ENSMUSG00000028005	Gucy1b3	-3.16
ENSMUSG00000090369	4933411K16Rik	-3.16
ENSMUSG00000054057	A930004D18Rik	-3.18
ENSMUSG00000047728	BC025446	-3.18
ENSMUSG00000042857	Gm9776	-3.18
ENSMUSG00000041781	Cpsf2	-3.19
ENSMUSG00000054435	Gimap4	-3.19
ENSMUSG00000020902	Ntn1	-3.19
ENSMUSG00000033730	Egr3	-3.19

ENSMUSG00000036948	BC037034	-3.20
ENSMUSG00000039005	Tlr4	-3.20
ENSMUSG00000058914	C1qtnf3	-3.21
ENSMUSG00000045569	Mc2r	-3.21
ENSMUSG00000021994	Wnt5a	-3.21
ENSMUSG00000090433	9430037G07Rik	-3.22
ENSMUSG00000048251	Bcl11b	-3.23
ENSMUSG00000005043	Sgsh	-3.24
ENSMUSG00000039253	Fn3krp	-3.24
ENSMUSG00000056418	BC043934	-3.25
ENSMUSG00000063047	Zfp780b	-3.25
ENSMUSG00000021565	Slc6a19	-3.28
ENSMUSG00000085013	4930556M19Rik	-3.28
ENSMUSG00000072915	Gm12258	-3.28
ENSMUSG00000023903	Mmp25	-3.28
ENSMUSG00000054931	Zkscan4	-3.29
ENSMUSG00000039164	Naif1	-3.29
ENSMUSG00000039706	Ldb2	-3.29
ENSMUSG00000040599	Mis12	-3.30
ENSMUSG00000024228	Nudt12	-3.30
ENSMUSG00000039628	Hs3st6	-3.30
ENSMUSG00000023947	Nfkbie	-3.31
ENSMUSG00000070942	Il1rl2	-3.31
ENSMUSG00000027270	6330527O06Rik	-3.31
ENSMUSG00000004069	Dnaja3	-3.32
ENSMUSG00000029915	Clec5a	-3.32
ENSMUSG00000056019	Zfp709	-3.32
ENSMUSG00000056258	Kcnq3	-3.32
ENSMUSG00000026051	1500015O10Rik	-3.32
ENSMUSG00000040969	D630013G24Rik	-3.33
ENSMUSG00000030543	Mesp2	-3.33
ENSMUSG00000045551	Fpr1	-3.34
ENSMUSG00000057156	Homez	-3.35
ENSMUSG00000026979	Psd4	-3.35
ENSMUSG00000085261	Gm13814	-3.35
ENSMUSG00000013150	Gfod2	-3.36
ENSMUSG00000041468	Gpr12	-3.37
ENSMUSG00000041797	Abca9	-3.37
ENSMUSG00000029312	Klhl8	-3.37
ENSMUSG00000041623	D11Wsu47e	-3.37
ENSMUSG00000022292	Rrm2b	-3.37
ENSMUSG00000074860	Gm10778	-3.38
ENSMUSG00000023243	Kcnk5	-3.38

ENSMUSG00000061535	C1qtnf7	-3.38
ENSMUSG00000085154	C130046K22Rik	-3.38
ENSMUSG00000017679	Ttpal	-3.39
ENSMUSG00000049285	Mblac1	-3.39
ENSMUSG00000020901	Pik3r5	-3.39
ENSMUSG00000044367	Slc16a13	-3.40
ENSMUSG00000064294	Aox3	-3.41
ENSMUSG00000054988	Agtr1b	-3.43
ENSMUSG00000063488	Zfp167	-3.44
ENSMUSG00000045515	Pou3f3	-3.45
ENSMUSG00000028540	Dph2	-3.45
ENSMUSG00000046731	Kctd11	-3.45
ENSMUSG00000022828	Gtf2e1	-3.45
ENSMUSG00000028331	5830415F09Rik	-3.46
ENSMUSG00000033356	Pus7l	-3.47
ENSMUSG00000046805	Mpeg1	-3.47
ENSMUSG00000055305	Zfp93	-3.47
ENSMUSG00000043572	Pars2	-3.48
ENSMUSG00000049950	Rpp38	-3.48
ENSMUSG00000057457	Phex	-3.48
ENSMUSG00000033634	Cml2	-3.48
ENSMUSG00000020573	Pik3cg	-3.49
ENSMUSG00000085957	Syna	-3.50
ENSMUSG00000034584	Exph5	-3.51
ENSMUSG00000039563	2210406O10Rik	-3.51
ENSMUSG00000038608	Dock10	-3.51
ENSMUSG00000039057	Myo16	-3.52
ENSMUSG00000055782	Abcd2	-3.53
ENSMUSG00000084779	4921504A21Rik	-3.53
ENSMUSG00000000317	Bcl6b	-3.54
ENSMUSG00000027274	Mkks	-3.54
ENSMUSG00000034041	Lyl1	-3.54
ENSMUSG00000028607	Cpt2	-3.55
ENSMUSG00000049717	Lig4	-3.55
ENSMUSG00000040310	Alx4	-3.55
ENSMUSG00000047746	Fbxo40	-3.56
ENSMUSG00000079293	Clec7a	-3.57
ENSMUSG00000037640	Zfp60	-3.57
ENSMUSG00000091018	Rplp2-ps1	-3.57
ENSMUSG00000019295	Tmem129	-3.60
ENSMUSG00000032105	Pdzd3	-3.60
ENSMUSG00000032841	Prr5l	-3.61
ENSMUSG00000078234	Klhdc7a	-3.63

ENSMUSG00000062944	9130023H24Rik	-3.63
ENSMUSG00000074598	Ufm1	-3.63
ENSMUSG00000086568	9130020K20Rik	-3.64
ENSMUSG00000021120	Pigh	-3.65
ENSMUSG00000058794	Nfe2	-3.65
ENSMUSG00000067586	S1pr3	-3.65
ENSMUSG00000078700	D030028A08Rik	-3.66
ENSMUSG00000074766	Ism1	-3.66
ENSMUSG00000049130	C5ar1	-3.66
ENSMUSG00000086515	Gm16292	-3.66
ENSMUSG00000045140	Pigw	-3.67
ENSMUSG00000051444	Bbs12	-3.68
ENSMUSG00000048776	Pthlh	-3.68
ENSMUSG00000026069	Il1rl1	-3.68
ENSMUSG00000078922	Tgtp1	-3.68
ENSMUSG00000038843	Gcnt1	-3.69
ENSMUSG00000054675	Tmem119	-3.69
ENSMUSG00000079554	Aox3l1	-3.69
ENSMUSG00000089862	Gm16039	-3.70
ENSMUSG00000030237	Slco1a4	-3.72
ENSMUSG00000006642	Tcf23	-3.73
ENSMUSG00000032758	Kap	-3.73
ENSMUSG00000085184	4933439K11Rik	-3.74
ENSMUSG00000037523	Mavs	-3.75
ENSMUSG00000084020	Gm12282	-3.76
ENSMUSG00000078994	Zfp429	-3.76
ENSMUSG00000013846	St3gal1	-3.78
ENSMUSG00000090418	Gm17585	-3.78
ENSMUSG00000069874	Irgm2	-3.79
ENSMUSG00000024440	Pcdh12	-3.80
ENSMUSG00000030493	C230052I12Rik	-3.81
ENSMUSG00000028883	Sema3a	-3.82
ENSMUSG00000039238	Zfp750	-3.84
ENSMUSG00000044770	Scml4	-3.85
ENSMUSG00000073779	B230314M03Rik	-3.85
ENSMUSG00000006777	Krt23	-3.86
ENSMUSG00000039182	AW209491	-3.88
ENSMUSG00000025645	Ccdc51	-3.88
ENSMUSG00000092118	Fancf	-3.88
ENSMUSG00000002699	Lcp2	-3.88
ENSMUSG00000054626	Xlr	-3.89
ENSMUSG00000084931	1110019D14Rik	-3.89
ENSMUSG00000042190	Cmklr1	-3.90

ENSMUSG00000027300	Ubox5	-3.90
ENSMUSG00000090834	Gm17476	-3.91
ENSMUSG00000069793	Slfn9	-3.92
ENSMUSG00000062961	Gm1568	-3.92
ENSMUSG00000049001	A930038C07Rik	-3.93
ENSMUSG00000039911	Spsb1	-3.94
ENSMUSG00000001983	Taco1	-3.95
ENSMUSG00000049107	Ntf3	-3.96
ENSMUSG00000091641	Gm17593	-3.97
ENSMUSG00000070423	Olfr558	-3.97
ENSMUSG00000089929	Bcl2a1b	-3.97
ENSMUSG00000074971	Fibin	-3.99
ENSMUSG00000036214	Znrd1as	-3.99
ENSMUSG00000043621	Ubxn10	-3.99
ENSMUSG00000025887	Casp12	-4.01
ENSMUSG00000031497	Tnfsf13b	-4.01
ENSMUSG00000022015	Tnfsf11	-4.01
ENSMUSG00000028182	Lrriq3	-4.02
ENSMUSG00000031506	Ptpn7	-4.02
ENSMUSG00000031264	Btk	-4.02
ENSMUSG00000090659	Zfp493	-4.03
ENSMUSG00000030789	Itgax	-4.03
ENSMUSG00000045658	Pid1	-4.03
ENSMUSG00000049608	Gpr55	-4.04
ENSMUSG00000060441	Trim5	-4.06
ENSMUSG00000069184	Zfp72	-4.07
ENSMUSG00000067578	Cbln4	-4.08
ENSMUSG00000011427	Zfp790	-4.08
ENSMUSG00000020707	Rnf135	-4.08
ENSMUSG00000051037	Zfp455	-4.09
ENSMUSG00000021234	Fam161b	-4.10
ENSMUSG00000040710	St8sia4	-4.10
ENSMUSG00000037251	4930444A02Rik	-4.10
ENSMUSG00000050796	B3galt6	-4.10
ENSMUSG00000087676	9230114K14Rik	-4.13
ENSMUSG00000020607	Fam84a	-4.13
ENSMUSG00000014773	Dll1	-4.14
ENSMUSG00000053337	Gm9903	-4.18
ENSMUSG00000058661	Gm7452	-4.19
ENSMUSG00000037185	Krt80	-4.19
ENSMUSG00000034333	Zbed4	-4.20
ENSMUSG00000021186	Fbln5	-4.23
ENSMUSG00000029073	Gltpd1	-4.25

ENSMUSG00000085582	3110099E03Rik	-4.25
ENSMUSG00000056592	Zfp658	-4.27
ENSMUSG00000026107	Obfc2a	-4.27
ENSMUSG00000055900	Tmem69	-4.28
ENSMUSG00000050428	Fbxo46	-4.29
ENSMUSG00000054200	O3far1	-4.29
ENSMUSG00000041362	4930506M07Rik	-4.32
ENSMUSG00000005124	Wisp1	-4.34
ENSMUSG00000041481	Serpina3g	-4.35
ENSMUSG00000052435	Cebpe	-4.35
ENSMUSG00000024810	Il33	-4.35
ENSMUSG00000085119	Gm13644	-4.37
ENSMUSG00000043496	Tril	-4.37
ENSMUSG00000085596	Gm11476	-4.38
ENSMUSG00000031639	Tlr3	-4.41
ENSMUSG00000043099	Hic1	-4.42
ENSMUSG00000047414	Flrt2	-4.45
ENSMUSG00000033910	Gucy1a3	-4.46
ENSMUSG00000022829	Stxbp5l	-4.48
ENSMUSG00000086496	Gm14204	-4.49
ENSMUSG00000079043	Fastkd5	-4.50
ENSMUSG00000037411	Serpine1	-4.50
ENSMUSG00000041849	Card6	-4.53
ENSMUSG00000020434	4921536K21Rik	-4.53
ENSMUSG00000032564	Cpne4	-4.58
ENSMUSG00000051457	Spn	-4.59
ENSMUSG00000060240	Cend1	-4.59
ENSMUSG00000031847	1700030J22Rik	-4.60
ENSMUSG00000020137	Thap2	-4.63
ENSMUSG00000017713	Tha1	-4.70
ENSMUSG00000034538	Zfp418	-4.70
ENSMUSG00000031253	Srpx2	-4.73
ENSMUSG00000012428	Steap4	-4.73
ENSMUSG00000027424	8430406I07Rik	-4.74
ENSMUSG00000028874	Fgr	-4.74
ENSMUSG00000030737	Slco2b1	-4.74
ENSMUSG00000079227	Ccr5	-4.76
ENSMUSG00000078137	Gm1337	-4.77
ENSMUSG00000004709	Cd244	-4.80
ENSMUSG00000085016	Gm11335	-4.83
ENSMUSG00000029231	Pdgfra	-4.83
ENSMUSG00000071661	Zbtb3	-4.83
ENSMUSG00000050234	Gja4	-4.87

ENSMUSG00000031070	Mrgprf	-4.87
ENSMUSG00000050677	Ccdc96	-4.94
ENSMUSG00000045107	1810063B07Rik	-4.95
ENSMUSG00000066170	E230001N04Rik	-4.98
ENSMUSG00000063193	Cd300lb	-4.99
ENSMUSG00000089803	Gm10171	-5.01
ENSMUSG00000045930	Clec14a	-5.04
ENSMUSG00000025597	Klhl4	-5.06
ENSMUSG00000052382	Rnase9	-5.13
ENSMUSG00000046491	C1qtnf2	-5.15
ENSMUSG00000007805	Twist2	-5.18
ENSMUSG00000031461	Myom2	-5.20
ENSMUSG00000066072	Cyp4a10	-5.24
ENSMUSG00000046380	Jrk	-5.26
ENSMUSG00000030157	Clec2d	-5.33
ENSMUSG00000049625	Tifab	-5.36
ENSMUSG00000086942	Gm15489	-5.44
ENSMUSG00000093606	B130034C11Rik	-5.46
ENSMUSG00000079355	Ccrl1	-5.51
ENSMUSG00000026271	Gpr35	-5.56
ENSMUSG00000055489	Ano5	-5.58
ENSMUSG00000054945	Gm9958	-5.60
ENSMUSG00000042549	Gm16516	-5.61
ENSMUSG00000090641	Zfp712	-5.64
ENSMUSG00000039220	Ppp1r10	-5.65
ENSMUSG00000030909	Anks4b	-5.70
ENSMUSG00000054404	Slfn5	-5.70
ENSMUSG00000059555	A830007P12Rik	-5.70
ENSMUSG00000017692	Rhbdl3	-5.72
ENSMUSG00000035759	Bbs10	-5.76
ENSMUSG00000024168	Tmem204	-5.80
ENSMUSG00000022659	Gcet2	-5.85
ENSMUSG00000045871	Slitrk6	-5.90
ENSMUSG00000043795	Gm14492	-5.91
ENSMUSG00000030031	Kbtbd8	-5.98
ENSMUSG00000044055	Otos	-5.98
ENSMUSG00000051682	Treml4	-5.99
ENSMUSG00000054715	Zscan22	-6.05
ENSMUSG00000024691	Fam111a	-6.07
ENSMUSG00000047878	A4galt	-6.07
ENSMUSG00000063234	Gpr84	-6.08
ENSMUSG00000026163	Sphkap	-6.13
ENSMUSG00000056824	Zfp663	-6.17

ENSMUSG00000075271	Ttc30a1	-6.24
ENSMUSG00000002289	Angptl4	-6.25
ENSMUSG00000071470	Ccnb1ip1	-6.28
ENSMUSG00000048988	Elfn1	-6.29
ENSMUSG00000041577	Prelp	-6.31
ENSMUSG00000084127	Gm13169	-6.32
ENSMUSG00000035431	Sstr1	-6.40
ENSMUSG00000038422	Hdhd3	-6.50
ENSMUSG00000063130	Calml3	-6.51
ENSMUSG00000066235	C85492	-6.57
ENSMUSG00000064293	Cntn4	-6.61
ENSMUSG00000016087	Fli1	-6.68
ENSMUSG00000026829	Gbgt1	-6.74
ENSMUSG00000047842	Diras2	-6.91
ENSMUSG00000049396	Gemin4	-6.91
ENSMUSG00000048779	P2ry6	-6.92
ENSMUSG00000068696	Gpr88	-6.94
ENSMUSG00000009670	Tex11	-7.02
ENSMUSG00000066141	Gm11232	-7.03
ENSMUSG00000046561	Arsj	-7.05
ENSMUSG00000021624	Cd180	-7.08
ENSMUSG00000078920	Ifi47	-7.09
ENSMUSG00000057396	Zfp759	-7.09
ENSMUSG00000060735	Rxfp3	-7.27
ENSMUSG00000048001	Hes5	-7.32
ENSMUSG00000045690	Wdr89	-7.32
ENSMUSG00000043461	1110032A04Rik	-7.35
ENSMUSG00000033082	Clec1a	-7.48
ENSMUSG00000021590	Spata9	-7.50
ENSMUSG00000064165	Krt39	-7.59
ENSMUSG00000036362	P2ry13	-7.73
ENSMUSG00000078945	Naip2	-7.88
ENSMUSG00000063727	Tnfrsf11b	-8.03
ENSMUSG00000049241	Gpr81	-8.37
ENSMUSG00000045382	Cxcr4	-8.40
ENSMUSG00000020524	Gria1	-8.49
ENSMUSG00000013523	Bcas1	-8.60
ENSMUSG00000054293	A630033H20Rik	-8.70
ENSMUSG00000040552	C3ar1	-8.97
ENSMUSG00000078650	G6pc	-9.07
ENSMUSG00000022860	Chodl	-9.11
ENSMUSG00000050232	Cxcr3	-9.37
ENSMUSG00000024868	Dkk1	-9.81

ENSMUSG00000051705	Senp8	-10.02
ENSMUSG00000049103	Ccr2	-10.29
ENSMUSG00000050395	Tnfsf15	-10.32
ENSMUSG00000044952	Kctd21	-10.46
ENSMUSG00000070390	Nlrp1b	-10.52
ENSMUSG00000039783	Kmo	-11.27
ENSMUSG00000036961	Wnt8b	-11.44
ENSMUSG00000089702	Gm16568	-12.00
ENSMUSG00000052336	Cx3cr1	-12.22
ENSMUSG00000043017	Ptgir	-12.94
ENSMUSG00000079645	Gm17193	-13.28
ENSMUSG00000080935	Got2-ps1	-13.54
ENSMUSG00000024261	Syt4	-27.05
ENSMUSG00000090723	Gm9625	-34.07
ENSMUSG00000078139	AK157302	-40.59
ENSMUSG00000087412	Gm15501	-53.88
ENSMUSG00000046721	Rpl14-ps1	-55.15
ENSMUSG00000085791	Rpl30-ps9	-58.19
ENSMUSG00000083879	Gm14038	-62.68
ENSMUSG00000069011	Gm10254	-108.04
ENSMUSG00000022591	Gm9747	-180.18
ENSMUSG00000021908	Gm6768	-198.63
ENSMUSG00000047676	Rpsa-ps10	-223.21
ENSMUSG00000059751	Gm9000	-375.87
ENSMUSG00000092329	Gm20388	-498.64
ENSMUSG00000062611	Gm10119	-715.53
ENSMUSG00000083061	Gm12191	-1058.90

Bibliography

Adli, M., Parlak, M., Li, Y., & El-Dahr, S. S. (2015). Epigenetic States of Nephron Progenitors and Epithelial Differentiation. *Journal of Cellular Biochemistry, 116*(6), 893-902. Retrieved from https://onlinelibrary.wiley.com/doi/abs/10.1002/jcb.25048. doi:10.1002/jcb.25048

al-Awqati, Q., & Goldberg, M. R. (1998). Architectural patterns in branching morphogenesis in the kidney. *Kidney Int, 54*(6), 1832-1842. doi:10.1046/j.1523-1755.1998.00196.x

Alexandre-Gouabau, M.-C., Courant, F., Le Gall, G., Moyon, T., Darmaun, D., Parnet, P., Coupé, B., & Antignac, J.-P. (2011). Offspring Metabolomic Response to Maternal Protein Restriction in a Rat Model of Intrauterine Growth Restriction (IUGR). *Journal of Proteome Research, 10*(7), 3292-3302. Retrieved from https://doi.org/10.1021/pr2003193. doi:10.1021/pr2003193

Alexandre-Gouabau, M.-C., Courant, F., Le Gall, G., Moyon, T., Darmaun, D., Parnet, P., Coupé, B., & Antignac, J.-P. (2011). Offspring Metabolomic Response to Maternal Protein Restriction in a Rat Model of Intrauterine Growth Restriction (IUGR). *Journal of Proteome Research, 10*(7), 3292-3302. Retrieved from https://doi.org/10.1021/pr2003193. doi:10.1021/pr2003193

Alonso, L., & Fuchs, E. (2006). The hair cycle. *Journal of Cell Science, 119*(3), 391-393. Retrieved from https://jcs.biologists.org/content/joces/119/3/391.full.pdf. doi:10.1242/jcs.02793

American Kidney Fund. (2019). Chronic Kidney Disease. Retrieved from https://www.kidneyfund.org/kidney-disease/chronic-kidney-disease-ckd/#how_is_ckd_treated

Amu, S., Hahn-Zoric, M., Malik, A., Ashraf, R., Zaman, S., Kjellmer, I., Hagberg, H., Padyukov, L., & Hanson, L. Å. (2006). Cytokines in the Placenta of Pakistani Newborns with and Without Intrauterine Growth Retardation. *Pediatric Research, 59*(2), 254-258. Retrieved from https://doi.org/10.1203/01.pdr.0000196332.37565.7d. doi:10.1203/01.pdr.0000196332.37565.7d

Arsenault, M. G., Miao, Y., Jones, K., Sims, D., Spears, J., Wright, G. M., & Hartwig, S. (2014). Estimation of total glomerular number using an integrated disector method in embryonic and postnatal kidneys. *Canadian journal of kidney health and disease, 1*, 12-12. Retrieved from https://pubmed.ncbi.nlm.nih.gov/25780607 doi:10.1186/2054-3581-1-12

Barak, H., Rosenfelder, L., Schultheiss, T. M., & Reshef, R. (2005). Cell fate specification along the anterior–posterior axis of the intermediate mesoderm. *Developmental Dynamics, 232*(4), 901-914. Retrieved from https://anatomypubs.onlinelibrary.wiley.com/doi/abs/10.1002/dvdy.20263. doi:10.1002/dvdy.20263

Bard, J. B. L., Gordon, A., Sharp, L., & Sellers, W. I. (2001). Early nephron formation in the developing mouse kidney. *Journal of Anatomy, 199*(4), 385-392. Retrieved from https://onlinelibrary.wiley.com/doi/abs/10.1046/j.1469-7580.2001.19940385.x. doi:10.1046/j.1469-7580.2001.19940385.x

Bartha, J. L., Romero-Carmona, R., & Comino-Delgado, R. (2003). Inflammatory cytokines in intrauterine growth retardation. *Acta Obstet Gynecol Scand, 82*(12), 1099-1102. doi:10.1046/j.1600-0412.2003.00259.x

Basgen, J. M., Nicholas, S. B., Mauer, M., Rozen, S., & Nyengaard, J. R. (2006). Comparison of Methods for Counting Cells in the Mouse Glomerulus. *Nephron Experimental Nephrology, 103*(4), e139-e148. Retrieved from https://www.karger.com/DOI/10.1159/000092905. doi:10.1159/000092905

Basta, J. M., Robbins, L., Kiefer, S. M., Dorsett, D., & Rauchman, M. (2014). Sall1 balances self-renewal and differentiation of renal progenitor cells. *Development, 141*(5), 1047-1058. Retrieved from https://pubmed.ncbi.nlm.nih.gov/24550112 doi:10.1242/dev.095851

Bates, C., Kharzai, S., Erwin, T., Rossant, J., & Parada, L. (2000). Role of N-myc in the Developing Mouse Kidney. *Developmental Biology, 222*, 317-325. doi:10.1006/dbio.2000.9716

Beeman, S. C., Cullen-McEwen, L. A., Puelles, V. G., Zhang, M., Wu, T., Baldelomar, E. J., Dowling, J., Charlton, J. R., Forbes, M. S., Ng, A., Wu, Q.-z., Armitage, J. A., Egan, G. F., Bertram, J. F., & Bennett, K. M. (2014). MRI-based glomerular morphology and pathology in whole human kidneys. *Am J Physiol Renal Physiol, 306*(11), F1381-F1390. Retrieved from https://pubmed.ncbi.nlm.nih.gov/24647716 doi:10.1152/ajprenal.00092.2014

Bernhardt, W. M., Schmitt, R., Rosenberger, C., Münchenhagen, P. M., Gröne, H. J., Frei, U., Warnecke, C., Bachmann, S., Wiesener, M. S., Willam, C., & Eckardt, K. U. (2006). Expression of hypoxia-inducible transcription factors in developing human and rat kidneys. *Kidney Int, 69*(1), 114-122. Retrieved from http://www.sciencedirect.com/science/article/pii/S0085253815513288. doi:https://doi.org/10.1038/sj.ki.5000062

Bhasin, K. K. S., van Nas, A., Martin, L. J., Davis, R. C., Devaskar, S. U., & Lusis, A. J. (2009). Maternal Low-Protein Diet or Hypercholesterolemia Reduces Circulating Essential Amino Acids and Leads to Intrauterine Growth Restriction. *Diabetes, 58*(3), 559-566. Retrieved from https://diabetes.diabetesjournals.org/content/diabetes/58/3/559.full.pdf. doi:10.2337/db07-1530

Blank, U., Brown, A., Adams, D. C., Karolak, M. J., & Oxburgh, L. (2009). BMP7 promotes proliferation of nephron progenitor cells via a JNK-dependent mechanism. *Development, 136*(21), 3557-3566. doi:10.1242/dev.036335

Blanpain, C., Horsley, V., & Fuchs, E. (2007). Epithelial stem cells: turning over new leaves. *Cell, 128*(3), 445-458. Retrieved from https://pubmed.ncbi.nlm.nih.gov/17289566 doi:10.1016/j.cell.2007.01.014

Boergermann, J. H., Kopf, J., Yu, P. B., & Knaus, P. (2010). Dorsomorphin and LDN-193189 inhibit BMP-mediated Smad, p38 and Akt signalling in C2C12 cells. *Int J Biochem Cell Biol, 42*(11), 1802-1807. Retrieved from https://pubmed.ncbi.nlm.nih.gov/20691279 doi:10.1016/j.biocel.2010.07.018

Breitwieser, W., Lyons, S., Flenniken, A. M., Ashton, G., Bruder, G., Willington, M., Lacaud, G., Kouskoff, V., & Jones, N. (2007). Feedback regulation of p38 activity via ATF2 is essential for survival of embryonic liver cells. *Genes Dev, 21*(16), 2069-2082. doi:10.1101/gad.430207

Brown, A. C., Adams, D., de Caestecker, M., Yang, X., Friesel, R., & Oxburgh, L. (2011). FGF/EGF signaling regulates the renewal of early nephron progenitors during embryonic development. *Development, 138*(23), 5099-5112. Retrieved from https://dev.biologists.org/content/develop/138/23/5099.full.pdf. doi:10.1242/dev.065995

Brown, A. C., Muthukrishnan, S. D., Guay, J. A., Adams, D. C., Schafer, D. A., Fetting, J. L., & Oxburgh, L. (2013). Role for compartmentalization in nephron progenitor differentiation. *Proc Natl Acad Sci U S A, 110*(12), 4640-4645. doi:10.1073/pnas.1213971110

Brown, A. C., Muthukrishnan, S. D., & Oxburgh, L. (2015). A synthetic niche for nephron progenitor cells. *Dev Cell, 34*(2), 229-241. doi:10.1016/j.devcel.2015.06.021

Brown, D. (2017). The Discovery of Water Channels (Aquaporins). *Annals of Nutrition and Metabolism, 70(suppl 1)*(Suppl. 1), 37-42. Retrieved from https://www.karger.com/DOI/10.1159/000463061. doi:10.1159/000463061

Brown, L. D., Green, A. S., Limesand, S. W., & Rozance, P. J. (2011). Maternal amino acid supplementation for intrauterine growth restriction. *Frontiers in bioscience (Scholar edition), 3*, 428-444. Retrieved from https://pubmed.ncbi.nlm.nih.gov/21196387 doi:10.2741/s162

Burns, R. (1955). Urogenital System. In B. H. Willier, P. A. Weiss, & V. Hamburger (Eds.), *Analysis of Development* (pp. 462-491). Philadelphia: Saunders.

Buzzetti, E., Pinzani, M., & Tsochatzis, E. A. (2016). The multiple-hit pathogenesis of non-alcoholic fatty liver disease (NAFLD). *Metabolism, 65*(8), 1038-1048. Retrieved from http://www.sciencedirect.com/science/article/pii/S0026049515003832. doi:https://doi.org/10.1016/j.metabol.2015.12.012

Cain, J. E., Di Giovanni, V., Smeeton, J., & Rosenblum, N. D. (2010). Genetics of Renal Hypoplasia: Insights Into the Mechanisms Controlling Nephron Endowment. *Pediatric Research, 68*(2), 91-98. Retrieved from https://doi.org/10.1203/PDR.0b013e3181e35a88. doi:10.1203/PDR.0b013e3181e35a88

Cain, J. E., Islam, E., Haxho, F., Chen, L., Bridgewater, D., Nieuwenhuis, E., Hui, C.-C., & Rosenblum, N. D. (2009). GLI3 Repressor Controls Nephron Number via Regulation of Wnt11 and Ret in Ureteric Tip Cells. *PLOS ONE, 4*(10), e7313. Retrieved from https://doi.org/10.1371/journal.pone.0007313. doi:10.1371/journal.pone.0007313

Calkins, K., & Devaskar, S. U. (2011). Fetal origins of adult disease. *Current problems in pediatric and adolescent health care, 41*(6), 158-176. Retrieved from https://pubmed.ncbi.nlm.nih.gov/21684471 doi:10.1016/j.cppeds.2011.01.001

Candi, E., Smirnov, A., Panatta, E., Lena, A. M., Novelli, F., Mancini, M., Viticchiè, G., Piro, M. C., Di Daniele, N., Annicchiarico-Petruzzelli, M., & Melino, G. (2017). Metabolic pathways regulated by p63. *Biochemical and Biophysical Research Communications, 482*(3), 440-444. Retrieved from http://www.sciencedirect.com/science/article/pii/S0006291X16317818. doi:https://doi.org/10.1016/j.bbrc.2016.10.094

Carroll, T. J., & Das, A. (2013). Defining the Signals that Constitute the Nephron Progenitor Niche. *Journal of the American Society of Nephrology, 24*(6), 873-876. Retrieved from https://jasn.asnjournals.org/content/jnephrol/24/6/873.full.pdf. doi:10.1681/asn.2012090931

Cebrian, C., Asai, N., D'Agati, V., & Costantini, F. (2014). The Number of Fetal Nephron Progenitor Cells Limits Ureteric Branching and Adult Nephron Endowment. *Cell Reports, 7*(1), 127-137. Retrieved from https://doi.org/10.1016/j.celrep.2014.02.033. doi:10.1016/j.celrep.2014.02.033

Cebrian, C., Asai, N., D'Agati, V., & Costantini, F. (2014). The Number of Fetal Nephron Progenitor Cells Limits Ureteric Branching and Adult Nephron Endowment. *Cell*

Reports, *7*(1), 127-137. Retrieved from https://doi.org/10.1016/j.celrep.2014.02.033. doi:10.1016/j.celrep.2014.02.033

Cerqueira, D. M., Hemker, S. L., Bodnar, A. J., Ortiz, D. M., Oladipupo, F. O., Mukherjee, E., Gong, Z., Appolonia, C., Muzumdar, R., Sims-Lucas, S., & Ho, J. (2019). In utero exposure to maternal diabetes impairs nephron progenitor differentiation. *American Journal of Physiology-Renal Physiology*, *317*(5), F1318-F1330. Retrieved from https://journals.physiology.org/doi/abs/10.1152/ajprenal.00204.2019. doi:10.1152/ajprenal.00204.2019

Chang-Panesso, M., Kadyrov, F. F., Machado, F. G., Kumar, A., & Humphreys, B. D. (2018). Meis1 is specifically upregulated in kidney myofibroblasts during aging and injury but is not required for kidney homeostasis or fibrotic response. *Am J Physiol Renal Physiol, 315*(2), F275-F290. Retrieved from https://pubmed.ncbi.nlm.nih.gov/29592525 doi:10.1152/ajprenal.00030.2018

Charlton, J. R., & Chevalier, R. L. (2018). Developmental Origins of CKD: Big Problems From Small Packages. *American Journal of Kidney Diseases*, *71*(1), 3-5. Retrieved from https://doi.org/10.1053/j.ajkd.2017.08.022. doi:10.1053/j.ajkd.2017.08.022

Chen, S., Brunskill, E. W., Potter, S. S., Dexheimer, P. J., Salomonis, N., Aronow, B. J., Hong, C. I., Zhang, T., & Kopan, R. (2015). Intrinsic Age-Dependent Changes and Cell-Cell Contacts Regulate Nephron Progenitor Lifespan. *Dev Cell*, *35*(1), 49-62. Retrieved from https://pubmed.ncbi.nlm.nih.gov/26460946 doi:10.1016/j.devcel.2015.09.009

Chen, S., & El-Dahr, S. S. (2013). Histone deacetylases in kidney development: implications for disease and therapy. *Pediatric Nephrology*, *28*(5), 689-698. Retrieved from https://doi.org/10.1007/s00467-012-2223-8. doi:10.1007/s00467-012-2223-8

Chen, Y., Lasaitiene, D., & Friberg, P. (2004). The renin–angiotensin system in kidney development. *Acta Physiologica Scandinavica*, *181*(4), 529-535. Retrieved from https://onlinelibrary.wiley.com/doi/abs/10.1111/j.1365-201X.2004.01327.x. doi:10.1111/j.1365-201X.2004.01327.x

Chen, Y., & Williams, B. R. (2000). The role of NF-kappaB in the regulation of the expression of wilms tumor suppressor gene WT1. *Gene Expr*, *9*(3), 103-114. doi:10.3727/000000001783992614

Chen, Y. W., Chenier, I., Chang, S. Y., Tran, S., Ingelfinger, J. R., & Zhang, S. L. (2011). High glucose promotes nascent nephron apoptosis via NF-kappaB and p53 pathways. *Am J Physiol Renal Physiol*, *300*(1), F147-156. doi:10.1152/ajprenal.00361.2010

Cheng, H.-T., & Kopan, R. (2005). The role of Notch signaling in specification of podocyte and proximal tubules within the developing mouse kidney. *Kidney Int*, *68*(5), 1951-1952. Retrieved from http://www.sciencedirect.com/science/article/pii/S0085253815510703. doi:https://doi.org/10.1111/j.1523-1755.2005.00627.x

Choudhry, Z., Rikani, A. A., Choudhry, A. M., Tariq, S., Zakaria, F., Asghar, M. W., Sarfraz, M. K., Haider, K., Shafiq, A. A., & Mobassarah, N. J. (2014). Sonic hedgehog signalling pathway: a complex network. *Annals of neurosciences*, *21*(1), 28-31. Retrieved from https://pubmed.ncbi.nlm.nih.gov/25206052 doi:10.5214/ans.0972.7531.210109

ur). Lhx1 Is Required for Specification of the Renal Progenitor Cell Field. *PLOS ONE*, *6*(4), e18858. Retrieved from https://doi.org/10.1371/journal.pone.0018858. doi:10.1371/journal.pone.0018858

Clemens, M. J. (2001). Initiation factor eIF2 alpha phosphorylation in stress responses and apoptosis. *Prog Mol Subcell Biol*, *27*, 57-89. doi:10.1007/978-3-662-09889-9_3

Cline, J. M., & Clarkson, T. B. (2015). Chapter 35 - Research in Laboratory Animal and Comparative Medicine. In J. G. Fox, L. C. Anderson, G. M. Otto, K. R. Pritchett-Corning, & M. T. Whary (Eds.), *Laboratory Animal Medicine (Third Edition)* (pp. 1535-1541). Boston: Academic Press.

Combes, A. N., Lefevre, J. G., Wilson, S., Hamilton, N. A., & Little, M. H. (2016). Cap mesenchyme cell swarming during kidney development is influenced by attraction, repulsion, and adhesion to the ureteric tip. *Developmental Biology, 418*(2), 297-306. Retrieved from http://www.sciencedirect.com/science/article/pii/S0012160616303025. doi:https://doi.org/10.1016/j.ydbio.2016.06.028

Costantini, F., & Kopan, R. (2010). Patterning a Complex Organ: Branching Morphogenesis and Nephron Segmentation in Kidney Development. *Dev Cell, 18*(5), 698-712. Retrieved from http://www.sciencedirect.com/science/article/pii/S1534580710002078. doi:https://doi.org/10.1016/j.devcel.2010.04.008

Cunningham, B. A., Hoffman, S., Rutishauser, U., Hemperly, J. J., & Edelman, G. M. (1983). Molecular topography of the neural cell adhesion molecule N-CAM: surface orientation and location of sialic acid-rich and binding regions. *Proceedings of the National Academy of Sciences, 80*(10), 3116-3120. Retrieved from https://www.pnas.org/content/pnas/80/10/3116.full.pdf. doi:10.1073/pnas.80.10.3116

Davidson, A. J. (2010). *Mouse kidney development*. Retrieved from https://www.ncbi.nlm.nih.gov/books/NBK27080/

Davies, J. (1994). Control of calbindin-D28K expression in developing mouse kidney. *Dev Dyn, 199*(1), 45-51. doi:10.1002/aja.1001990105

Deng, S., Yang, B., Ren, Z. J., & Dong, Q. (2018). [Growth Regulation of Factor Inhibiting Hypoxia-Inducible Factor in Renal Carcinoma Cells]. *Sichuan Da Xue Xue Bao Yi Xue Ban, 49*(1), 29-33.

Drabovich, A. P., Pavlou, M. P., Dimitromanolakis, A., & Diamandis, E. P. (2012). Quantitative Analysis of Energy Metabolic Pathways in MCF-7 Breast Cancer Cells by Selected Reaction Monitoring Assay. *Molecular & Cellular Proteomics, 11*(8), 422-434. Retrieved from https://www.mcponline.org/content/mcprot/11/8/422.full.pdf. doi:10.1074/mcp.M111.015214

Dressler, G. R. (2006). The Cellular Basis of Kidney Development. *Annual Review of Cell and Developmental Biology, 22*(1), 509-529. Retrieved from https://www.annualreviews.org/doi/abs/10.1146/annurev.cellbio.22.010305.104340. doi:10.1146/annurev.cellbio.22.010305.104340

Dressler, G. R. (2009). Advances in early kidney specification, development and patterning. *Development, 136*(23), 3863-3874. doi:10.1242/dev.034876

Dressler, G. R. (2009). Advances in early kidney specification, development and patterning. *Development, 136*(23), 3863-3874. Retrieved from https://dev.biologists.org/content/develop/136/23/3863.full.pdf. doi:10.1242/dev.034876

Drummond-Barbosa, D., & Spradling, A. C. (2001). Stem Cells and Their Progeny Respond to Nutritional Changes during Drosophila Oogenesis. *Developmental Biology, 231*(1), 265-278. Retrieved from http://www.sciencedirect.com/science/article/pii/S0012160600901350. doi:https://doi.org/10.1006/dbio.2000.0135

Duan, W. R., Garner, D. S., Williams, S. D., Funckes-Shippy, C. L., Spath, I. S., & Blomme, E. A. (2003). Comparison of immunohistochemistry for activated caspase-3 and cleaved

cytokeratin 18 with the TUNEL method for quantification of apoptosis in histological sections of PC-3 subcutaneous xenografts. *The Journal of Pathology, 199*(2), 221-228. Retrieved from https://onlinelibrary.wiley.com/doi/abs/10.1002/path.1289. doi:10.1002/path.1289

Edgar, R., Mazor, Y., Rinon, A., Blumenthal, J., Golan, Y., Buzhor, E., Livnat, I., Ben-Ari, S., Lieder, I., Shitrit, A., Gilboa, Y., Ben-Yehudah, A., Edri, O., Shraga, N., Bogoch, Y., Leshansky, L., Aharoni, S., West, M. D., Warshawsky, D., & Shtrichman, R. (2013). LifeMap Discovery™: the embryonic development, stem cells, and regenerative medicine research portal. *PLOS ONE, 8*(7), e66629. doi:10.1371/journal.pone.0066629

El-Dahr, S. S. (2019). DNA methylation links intrauterine stress with abnormal nephrogenesis. *Nature Reviews Nephrology, 15*(4), 196-197. Retrieved from https://doi.org/10.1038/s41581-019-0114-y. doi:10.1038/s41581-019-0114-y

El-Dahr, S. S., Li, Y., Liu, J., Gutierrez, E., Hering-Smith, K. S., Signoretti, S., Pignon, J.-C., Sinha, S., & Saifudeen, Z. (2017). p63+ ureteric bud tip cells are progenitors of intercalated cells. *JCI insight, 2*(9), e89996. Retrieved from https://pubmed.ncbi.nlm.nih.gov/28469077 doi:10.1172/jci.insight.89996

Elias, B. C., Das, A., Parekh, D. V., Mernaugh, G., Adams, R., Yang, Z., Brakebusch, C., Pozzi, A., Marciano, D. K., Carroll, T. J., & Zent, R. (2015). Cdc42 regulates epithelial cell polarity and cytoskeletal function during kidney tubule development. *Journal of Cell Science, 128*(23), 4293-4305. Retrieved from https://jcs.biologists.org/content/joces/128/23/4293.full.pdf. doi:10.1242/jcs.164509

Elumalai, G. (2017). "RENAL ECTOPIA" EMBRYOLOGICAL BASIS AND ITS CLINICAL IMPORTANCE. *Elixir Embryology, 103*, 45680-46685.

Etchegaray, J.-P., & Mostoslavsky, R. (2016). Interplay between Metabolism and Epigenetics: A Nuclear Adaptation to Environmental Changes. *Molecular Cell, 62*(5), 695-711. Retrieved from http://www.sciencedirect.com/science/article/pii/S1097276516301927. doi:https://doi.org/10.1016/j.molcel.2016.05.029

Fanni, D., Fanos, V., Monga, G., Gerosa, C., Locci, A., Nemolato, S., Van Eyken, P., & Faa, G. (2011). Expression of WT1 during normal human kidney development. *The Journal of Maternal-Fetal & Neonatal Medicine, 24*(sup2), 44-47. Retrieved from https://doi.org/10.3109/14767058.2011.606619. doi:10.3109/14767058.2011.606619

Fantus, D., Rogers, N. M., Grahammer, F., Huber, T. B., & Thomson, A. W. (2016). Roles of mTOR complexes in the kidney: implications for renal disease and transplantation. *Nature reviews. Nephrology, 12*(10), 587-609. Retrieved from https://pubmed.ncbi.nlm.nih.gov/27477490 doi:10.1038/nrneph.2016.108

Fantus, I. G., Goldberg, H. J., Whiteside, C. I., & Topic, D. (2006). The Hexokinase Pathway. In P. Cortes & C. E. Mogensen (Eds.), *Contemporary Diabtes: The Diabetic Kidney*. Totowa, NJ: Humana Press Inc

Fleming, B. M., Yelin, R., James, R. G., & Schultheiss, T. M. (2013). A role for Vg1/Nodal signaling in specification of the intermediate mesoderm. *Development, 140*(8), 1819-1829. Retrieved from https://dev.biologists.org/content/develop/140/8/1819.full.pdf. doi:10.1242/dev.093740

Forbes, M. S., Thornhill, B. A., & Chevalier, R. L. (2011). Proximal tubular injury and rapid formation of a tubular glomeruli in mice with unilateral ureteral obstruction: a new look at an old model. *Am J Physiol Renal Physiol, 301*(1), F110-F117. Retrieved from https://pubmed.ncbi.nlm.nih.gov/21429968 doi:10.1152/ajprenal.00022.2011

Fujita, K., & Srinivasula, S. M. (2009). Ubiquitination and TNFR1 signaling. *Results Probl Cell Differ, 49*, 87-114. doi:10.1007/400_2009_18

Galuska, C. E., Lütteke, T., & Galuska, S. P. (2017). Is Polysialylated NCAM Not Only a Regulator during Brain Development But also during the Formation of Other Organs? *Biology (Basel), 6*(2). doi:10.3390/biology6020027

Galuska, C. E., Lütteke, T., & Galuska, S. P. (2017). Is Polysialylated NCAM Not Only a Regulator during Brain Development But also during the Formation of Other Organs? *Biology (Basel), 6*(2), 27. Retrieved from https://pubmed.ncbi.nlm.nih.gov/28448440 doi:10.3390/biology6020027

Gao, X., Chen, X., Taglienti, M., Rumballe, B., Little, M. H., & Kreidberg, J. A. (2005). Angioblast-mesenchyme induction of early kidney development is mediated by Wt1 and Vegfa. *Development, 132*(24), 5437-5449. Retrieved from https://dev.biologists.org/content/develop/132/24/5437.full.pdf. doi:10.1242/dev.02095

Godley, L. A., Kopp, J. B., Eckhaus, M., Paglino, J. J., Owens, J., & Varmus, H. E. (1996). Wild-type p53 transgenic mice exhibit altered differentiation of the ureteric bud and possess small kidneys. *Genes Dev, 10*(7), 836-850. doi:10.1101/gad.10.7.836

Goldenberg, R. L., & Cliver, S. P. (1997). Small for gestational age and intrauterine growth restriction: definitions and standards. *Clin Obstet Gynecol, 40*(4), 704-714. doi:10.1097/00003081-199712000-00004

Gomez, R. A., Norwood, V. F., & Tufro-McReddie, A. (1997). Development of the kidney vasculature. *Microscopy Research and Technique, 39*(3), 254-260. Retrieved from https://onlinelibrary.wiley.com/doi/abs/10.1002/%28SICI%291097-0029%2819971101%2939%3A3%3C254%3A%3AAID-JEMT5%3E3.0.CO%3B2-K. doi:10.1002/(sici)1097-0029(19971101)39:3<254::Aid-jemt5>3.0.Co;2-k

Griffin, K. A., Kramer, H., & Bidani, A. K. (2008). Adverse renal consequences of obesity. *American Journal of Physiology-Renal Physiology, 294*(4), F685-F696. Retrieved from https://journals.physiology.org/doi/abs/10.1152/ajprenal.00324.2007. doi:10.1152/ajprenal.00324.2007

Hagan, C., (2017). When Are Mice Considered Old?. *JAX Blog*. https://www.jax.org/news-and-insights/jax-blog/2017/november/when-are-mice-considered-old#:~:text=Mice%20should%20be%20at%20least%2010%20months%20old,ranging%20from%2056%20-%2069%20years%20of%20age.

Hales, C. N., & Barker, D. J. (1992). Type 2 (non-insulin-dependent) diabetes mellitus: the thrifty phenotype hypothesis. *Diabetologia, 35*(7), 595-601. doi:10.1007/bf00400248

Hamanaka, R. B., & Chandel, N. S. (2012). Targeting glucose metabolism for cancer therapy. *Journal of Experimental Medicine, 209*(2), 211-215. Retrieved from https://doi.org/10.1084/jem.20120162. doi:10.1084/jem.20120162

Hasegawa, T., McLeod, D. S., Prow, T., Merges, C., Grebe, R., & Lutty, G. A. (2008). Vascular Precursors in Developing Human Retina. *Investigative Ophthalmology & Visual Science, 49*(5), 2178-2192. Retrieved from https://doi.org/10.1167/iovs.07-0632. doi:10.1167/iovs.07-0632

Hastie, N. D. (2017). Wilms' tumour 1 (WT1) in development, homeostasis and disease. *Development, 144*(16), 2862-2872. Retrieved from https://dev.biologists.org/content/develop/144/16/2862.full.pdf. doi:10.1242/dev.153163

Hayakawa, M., Takemoto, K., Nakayama, A., Saito, A., Sato, Y., Hasegawa, M., Ieda, K., & Mimura, S. (2006). An animal model of intrauterine growth retardation induced by

synthetic thromboxane a(2). *J Soc Gynecol Investig, 13*(8), 566-572. doi:10.1016/j.jsgi.2006.09.007

Hilliard, S., Song, R., Liu, H., Chen, C.-h., Li, Y., Baddoo, M., Flemington, E., Wanek, A., Kolls, J., Saifudeen, Z., & El-Dahr, S. S. (2019). Defining the dynamic chromatin landscape of nephron progenitors. *bioRxiv*, 515429. Retrieved from https://www.biorxiv.org/content/biorxiv/early/2019/01/08/515429.full.pdf. doi:10.1101/515429

Holthöfer, H., Schulte, B. A., & Spicer, S. S. (1987). Expression of binding sites for Dolichos biflorus agglutinin at the apical aspect of collecting duct cells in rat kidney. *Cell and Tissue Research, 249*(3), 481-485. Retrieved from https://doi.org/10.1007/BF00217319. doi:10.1007/BF00217319

Hoy, W. E., Hughson, M. D., Bertram, J. F., Douglas-Denton, R., & Amann, K. (2005). Nephron Number, Hypertension, Renal Disease, and Renal Failure. *Journal of the American Society of Nephrology, 16*(9), 2557-2564. Retrieved from https://jasn.asnjournals.org/content/jnephrol/16/9/2557.full.pdf. doi:10.1681/asn.2005020172

Hsu, P., & Nanan, R. K. H. (2014). Innate and adaptive immune interactions at the fetal-maternal interface in healthy human pregnancy and pre-eclampsia. *Frontiers in immunology, 5*, 125-125. Retrieved from https://pubmed.ncbi.nlm.nih.gov/24734032 doi:10.3389/fimmu.2014.00125

Huang da, W., Sherman, B. T., & Lempicki, R. A. (2009). Bioinformatics enrichment tools: paths toward the comprehensive functional analysis of large gene lists. *Nucleic Acids Res, 37*(1), 1-13. doi:10.1093/nar/gkn923

Huang da, W., Sherman, B. T., & Lempicki, R. A. (2009). Systematic and integrative analysis of large gene lists using DAVID bioinformatics resources. *Nat Protoc, 4*(1), 44-57. doi:10.1038/nprot.2008.211

Ihermann-Hella, A., Hirashima, T., Kupari, J., Kurtzeborn, K., Li, H., Kwon, H. N., Cebrian, C., Soofi, A., Dapkunas, A., Miinalainen, I., Dressler, G. R., Matsuda, M., & Kuure, S. (2018). Dynamic MAPK/ERK Activity Sustains Nephron Progenitors through Niche Regulation and Primes Precursors for Differentiation. *Stem Cell Reports, 11*(4), 912-928. Retrieved from https://pubmed.ncbi.nlm.nih.gov/30220628 doi:10.1016/j.stemcr.2018.08.012

Jacob, S., & Bhargava, P. (1962). New method for the preparation of liver cell suspensions. *Experimental cell research, 27*, 453-467. doi:10.1016/0014-4827(62)90011-3

Jansson, T., Scholtbach, V., & Powell, T. L. (1998). Placental Transport of Leucine and Lysine Is Reduced in Intrauterine Growth Restriction. *Pediatric Research, 44*(4), 532-537. Retrieved from https://doi.org/10.1203/00006450-199810000-00011. doi:10.1203/00006450-199810000-00011

Jones, A. K., Brown, L. D., Rozance, P. J., Serkova, N. J., Hay, W. W., Jr., Friedman, J. E., & Wesolowski, S. R. (2019). Differential effects of intrauterine growth restriction and a hypersinsulinemic-isoglycemic clamp on metabolic pathways and insulin action in the fetal liver. *Am J Physiol Regul Integr Comp Physiol, 316*(5), R427-r440. doi:10.1152/ajpregu.00359.2018

Jordan, J. M., Hibshman, J. D., Webster, A. K., Kaplan, R. E. W., Leinroth, A., Guzman, R., Maxwell, C. S., Chitrakar, R., Bowman, E. A., Fry, A. L., Hubbard, E. J. A., & Baugh, L. R. (2019). Insulin/IGF Signaling and Vitellogenin Provisioning Mediate Intergenerational

Adaptation to Nutrient Stress. *Current Biology, 29*(14), 2380-2388.e2385. Retrieved from https://doi.org/10.1016/j.cub.2019.05.062. doi:10.1016/j.cub.2019.05.062

Kanda, S., Tanigawa, S., Ohmori, T., Taguchi, A., Kudo, K., Suzuki, Y., Sato, Y., Hino, S., Sander, M., Perantoni, A. O., Sugano, S., Nakao, M., & Nishinakamura, R. (2014). Sall1 maintains nephron progenitors and nascent nephrons by acting as both an activator and a repressor. *J Am Soc Nephrol, 25*(11), 2584-2595. doi:10.1681/asn.2013080896

Karantzali, E., Lekakis, V., Ioannou, M., Hadjimichael, C., Papamatheakis, J., & Kretsovali, A. (2011). Sall1 regulates embryonic stem cell differentiation in association with nanog. *J Biol Chem, 286*(2), 1037-1045. doi:10.1074/jbc.M110.170050

Katsu, K., Tokumori, D., Tatsumi, N., Suzuki, A., & Yokouchi, Y. (2012). BMP inhibition by DAN in Hensen's node is a critical step for the establishment of left–right asymmetry in the chick embryo. *Developmental Biology, 363*(1), 15-26. Retrieved from http://www.sciencedirect.com/science/article/pii/S0012160611014357. doi:https://doi.org/10.1016/j.ydbio.2011.12.015

Keith, B., Johnson, R. S., & Simon, M. C. (2011). HIF1α and HIF2α: sibling rivalry in hypoxic tumour growth and progression. *Nature reviews. Cancer, 12*(1), 9-22. Retrieved from https://pubmed.ncbi.nlm.nih.gov/22169972 doi:10.1038/nrc3183

Keller, G., Zimmer, G., Mall, G., Ritz, E., & Amann, K. (2003). Nephron number in patients with primary hypertension. *N Engl J Med, 348*(2), 101-108. doi:10.1056/NEJMoa020549

Kimball, S. R. (1999). Eukaryotic initiation factor eIF2. *Int J Biochem Cell Biol, 31*(1), 25-29. doi:10.1016/s1357-2725(98)00128-9

Kobayashi, A., Valerius, M. T., Mugford, J. W., Carroll, T. J., Self, M., Oliver, G., & McMahon, A. P. (2008). Six2 defines and regulates a multipotent self-renewing nephron progenitor population throughout mammalian kidney development. *Cell stem cell, 3*(2), 169-181. doi:10.1016/j.stem.2008.05.020

Kontou, M., Weidemann, W., Bork, K., & Horstkorte, R. (2009). Beyond glycosylation: sialic acid precursors act as signaling molecules and are involved in cellular control of differentiation of PC12 cells. *Biol Chem, 390*(7), 575-579. doi:10.1515/bc.2009.058

Kopan, R., Chen, S., & Little, M. (2014). Chapter Eleven - Nephron Progenitor Cells: Shifting the Balance of Self-Renewal and Differentiation. In M. Rendl (Ed.), *Curr Top Dev Biol* (Vol. 107, pp. 293-331): Academic Press.

Kopan, R., Chen, S., & Little, M. (2014). Nephron progenitor cells: shifting the balance of self-renewal and differentiation. *Curr Top Dev Biol, 107*, 293-331. doi:10.1016/b978-0-12-416022-4.00011-1

Kurien, B. T., & Scofield, R. H. (1999). Mouse urine collection using clear plastic wrap. *Lab Anim, 33*(1), 83-86. doi:10.1258/002367799780578525

Lackie, P. M., Zuber, C., & Roth, J. (1990). Polysialic acid and N-CAM localisation in embryonic rat kidney: mesenchymal and epithelial elements show different patterns of expression. *Development, 110*(3), 933-947.

Lackie, P. M., Zuber, C., & Roth, J. (1990). Polysialic acid and N-CAM localisation in embryonic rat kidney: mesenchymal and epithelial elements show different patterns of expression. *Development, 110*(3), 933-947.

Lang, K. J., Kappel, A., & Goodall, G. J. (2002). Hypoxia-inducible factor-1alpha mRNA contains an internal ribosome entry site that allows efficient translation during normoxia and hypoxia. *Mol Biol Cell, 13*(5), 1792-1801. doi:10.1091/mbc.02-02-0017

Laplante, M., & Sabatini, D. M. (2009). mTOR signaling at a glance. *Journal of Cell Science, 122*(20), 3589-3594. Retrieved from https://jcs.biologists.org/content/joces/122/20/3589.full.pdf. doi:10.1242/jcs.051011

Laugesen, A., & Helin, K. (2014). Chromatin repressive complexes in stem cells, development, and cancer. *Cell stem cell, 14*(6), 735-751. doi:10.1016/j.stem.2014.05.006

Lee, S.-Y., Han, S. M., Kim, J.-E., Chung, K.-Y., & Han, K.-H. (2013). Expression of E-cadherin in pig kidney. *Journal of veterinary science, 14*(4), 381-386. Retrieved from https://pubmed.ncbi.nlm.nih.gov/23820247 doi:10.4142/jvs.2013.14.4.381

Leng, N., Dawson, J. A., Thomson, J. A., Ruotti, V., Rissman, A. I., Smits, B. M., Haag, J. D., Gould, M. N., Stewart, R. M., & Kendziorski, C. (2013). EBSeq: an empirical Bayes hierarchical model for inference in RNA-seq experiments. *Bioinformatics, 29*(8), 1035-1043. doi:10.1093/bioinformatics/btt087

Li, B., & Dewey, C. N. (2011). RSEM: accurate transcript quantification from RNA-Seq data with or without a reference genome. *BMC Bioinformatics, 12*(1), 323. Retrieved from https://doi.org/10.1186/1471-2105-12-323. doi:10.1186/1471-2105-12-323

Li, Y. (2014). *Novel roles of p53 in regulation of nephron progenitor cell renewal and differentiation during kidney development*. New Orleans, La.: New Orleans, La. : Tulane University.

Li, Y., Liu, J., Li, W., Brown, A., Baddoo, M., Li, M., Carroll, T., Oxburgh, L., Feng, Y., & Saifudeen, Z. (2015). p53 Enables metabolic fitness and self-renewal of nephron progenitor cells. *Development, 142*(7), 1228-1241. doi:10.1242/dev.111617

Li, Y., Liu, J., Li, W., Brown, A., Baddoo, M., Li, M., Carroll, T., Oxburgh, L., Feng, Y., & Saifudeen, Z. (2015). p53 enables metabolic fitness and self-renewal of nephron progenitor cells. *Development, 142*(7), 1228-1241. Retrieved from https://dev.biologists.org/content/develop/142/7/1228.full.pdf. doi:10.1242/dev.111617

Lin, G., Wang, X., Wu, G., Feng, C., Zhou, H., Li, D., & Wang, J. (2014). Improving amino acid nutrition to prevent intrauterine growth restriction in mammals. *Amino Acids, 46*(7), 1605-1623. Retrieved from https://doi.org/10.1007/s00726-014-1725-z. doi:10.1007/s00726-014-1725-z

Lindström, Nils O., Carragher, Neil O., & Hohenstein, P. (2015). The PI3K Pathway Balances Self-Renewal and Differentiation of Nephron Progenitor Cells through β-Catenin Signaling. *Stem Cell Reports, 4*(4), 551-560. Retrieved from https://doi.org/10.1016/j.stemcr.2015.01.021. doi:10.1016/j.stemcr.2015.01.021

Lindström, N. O., De Sena Brandine, G., Tran, T., Ransick, A., Suh, G., Guo, J., Kim, A. D., Parvez, R. K., Ruffins, S. W., Rutledge, E. A., Thornton, M. E., Grubbs, B., McMahon, J. A., Smith, A. D., & McMahon, A. P. (2018). Progressive Recruitment of Mesenchymal Progenitors Reveals a Time-Dependent Process of Cell Fate Acquisition in Mouse and Human Nephrogenesis. *Dev Cell, 45*(5), 651-660.e654. Retrieved from http://www.sciencedirect.com/science/article/pii/S1534580718303678. doi:https://doi.org/10.1016/j.devcel.2018.05.010

Liu, H., Chen, S., Yao, X., Li, Y., Chen, C.-H., Liu, J., Saifudeen, Z., & El-Dahr, S. S. (2018). Histone deacetylases 1 and 2 regulate the transcriptional programs of nephron progenitors and renal vesicles. *Development, 145*(10), dev153619. Retrieved from https://dev.biologists.org/content/develop/145/10/dev153619.full.pdf. doi:10.1242/dev.153619

Liu, H., Hilliard, S., Kelly, E., Chen, C. H., Saifudeen, Z., & El-Dahr, S. S. (2020). The polycomb proteins EZH1 and EZH2 co-regulate chromatin accessibility and nephron progenitor cell lifespan in mice. *J Biol Chem*. doi:10.1074/jbc.RA120.013348

Liu, J., Edgington-Giordano, F., Dugas, C., Abrams, A., Katakam, P., Satou, R., & Saifudeen, Z. (2017). Regulation of Nephron Progenitor Cell Self-Renewal by Intermediary Metabolism. *Journal of the American Society of Nephrology, 28*(11), 3323-3335. Retrieved from https://jasn.asnjournals.org/content/jnephrol/28/11/3323.full.pdf. doi:10.1681/asn.2016111246

Ma, Q. (2013). Role of nrf2 in oxidative stress and toxicity. *Annual review of pharmacology and toxicology, 53*, 401-426. Retrieved from https://pubmed.ncbi.nlm.nih.gov/23294312 https://www.ncbi.nlm.nih.gov/pmc/articles/PMC4680839/. doi:10.1146/annurev-pharmtox-011112-140320

Maeshima, A., Sakurai, H., & Nigam, S. K. (2006). Adult kidney tubular cell population showing phenotypic plasticity, tubulogenic capacity, and integration capability into developing kidney. *J Am Soc Nephrol, 17*(1), 188-198. doi:10.1681/asn.2005040370

Martin, L. J., Meng, Q., Blencowe, M., Lagarrigue, S., Xiao, S., Pan, C., Wier, J., Temple, W. C., Devaskar, S. U., Lusis, A. J., & Yang, X. (2018). Maternal High-Protein and Low-Protein Diets Perturb Hypothalamus and Liver Transcriptome and Metabolic Homeostasis in Adult Mouse Offspring. *Frontiers in Genetics, 9*(642). Retrieved from https://www.frontiersin.org/article/10.3389/fgene.2018.00642. doi:10.3389/fgene.2018.00642

Masoud, G. N., & Li, W. (2015). HIF-1α pathway: role, regulation and intervention for cancer therapy. *Acta Pharmaceutica Sinica B, 5*(5), 378-389. Retrieved from http://www.sciencedirect.com/science/article/pii/S2211383515000817. doi:https://doi.org/10.1016/j.apsb.2015.05.007

Maurer, K. J., & Quimby, F. W. (2015). Chapter 34 - Animal Models in Biomedical Research. In J. G. Fox, L. C. Anderson, G. M. Otto, K. R. Pritchett-Corning, & M. T. Whary (Eds.), *Laboratory Animal Medicine (Third Edition)* (pp. 1497-1534). Boston: Academic Press.

McLaughlin, N., Wang, F., Saifudeen, Z., & El-Dahr, S. S. (2014). In situ histone landscape of nephrogenesis. *Epigenetics, 9*(2), 222-235. Retrieved from https://pubmed.ncbi.nlm.nih.gov/24169366 doi:10.4161/epi.26793

McNeill, H., & Reginensi, A. (2017). Lats1/2 Regulate Yap/Taz to Control Nephron Progenitor Epithelialization and Inhibit Myofibroblast Formation. *Journal of the American Society of Nephrology, 28*(3), 852-861. Retrieved from https://jasn.asnjournals.org/content/jnephrol/28/3/852.full.pdf. doi:10.1681/asn.2016060611

Menon, R., Otto, E. A., Kokoruda, A., Zhou, J., Zhang, Z., Yoon, E., Chen, Y.-C., Troyanskaya, O., Spence, J. R., Kretzler, M., & Cebrián, C. (2018). Single-cell analysis of progenitor cell dynamics and lineage specification in the human fetal kidney. *Development, 145*(16), dev164038. Retrieved from https://dev.biologists.org/content/develop/145/16/dev164038.full.pdf. doi:10.1242/dev.164038

Menshykau, D., Michos, O., Lang, C., Conrad, L., McMahon, A. P., & Iber, D. (2019). Image-based modeling of kidney branching morphogenesis reveals GDNF-RET based Turing-type mechanism and pattern-modulating WNT11 feedback. *Nature Communications*,

10(1), 239. Retrieved from https://doi.org/10.1038/s41467-018-08212-8. doi:10.1038/s41467-018-08212-8

Merrill, A. H., & Sandhoff, K. (2002). Chapter 14 Sphingolipids: metabolism and cell signaling. In *New Comprehensive Biochemistry* (Vol. 36, pp. 373-407): Elsevier.

Militello, M., Pappalardo, E. M., Ermito, S., Dinatale, A., Cavaliere, A., & Carrara, S. (2009). Obstetric management of IUGR. *Journal of prenatal medicine, 3*(1), 6-9. Retrieved from https://pubmed.ncbi.nlm.nih.gov/22439031

Monzani, E., Bazzotti, R., Perego, C., & La Porta, C. A. (2009). AQP1 is not only a water channel: it contributes to cell migration through Lin7/beta-catenin. *PLOS ONE, 4*(7), e6167. doi:10.1371/journal.pone.0006167

Motamedi, F. J., Badro, D. A., Clarkson, M., Rita Lecca, M., Bradford, S. T., Buske, F. A., Saar, K., Hübner, N., Brändli, A. W., & Schedl, A. (2014). WT1 controls antagonistic FGF and BMP-pSMAD pathways in early renal progenitors. *Nature Communications, 5*(1), 4444. Retrieved from https://doi.org/10.1038/ncomms5444. doi:10.1038/ncomms5444

Mugford, J. W., Sipilä, P., McMahon, J. A., & McMahon, A. P. (2008). Osr1 expression demarcates a multi-potent population of intermediate mesoderm that undergoes progressive restriction to an Osr1-dependent nephron progenitor compartment within the mammalian kidney. *Developmental Biology, 324*(1), 88-98. Retrieved from http://www.sciencedirect.com/science/article/pii/S0012160608011950. doi:https://doi.org/10.1016/j.ydbio.2008.09.010

Mukherjee, E., Maringer, K., Papke, E., Bushnell, D., Schaefer, C., Kramann, R., Ho, J., Humphreys, B. D., Bates, C., & Sims-Lucas, S. (2017). Endothelial marker-expressing stromal cells are critical for kidney formation. *American Journal of Physiology-Renal Physiology, 313*(3), F611-F620. Retrieved from https://journals.physiology.org/doi/abs/10.1152/ajprenal.00136.2017. doi:10.1152/ajprenal.00136.2017

Munro, D. A. D., Hohenstein, P., Coate, T. M., & Davies, J. A. (2017). Refuting the hypothesis that semaphorin-3f/neuropilin-2 exclude blood vessels from the cap mesenchyme in the developing kidney. *Dev Dyn, 246*(12), 1047-1056. doi:10.1002/dvdy.24592

Murray, H. C., Swanson, M. E. V., Dieriks, B. V., Turner, C., Faull, R. L. M., & Curtis, M. A. (2018). Neurochemical Characterization of PSA-NCAM(+) Cells in the Human Brain and Phenotypic Quantification in Alzheimer's Disease Entorhinal Cortex. *Neuroscience, 372*, 289-303. doi:10.1016/j.neuroscience.2017.12.019

Musante, L., Tataruch, D. E., & Holthofer, H. (2014). Use and Isolation of Urinary Exosomes as Biomarkers for Diabetic Nephropathy. *Frontiers in Endocrinology, 5*(149). Retrieved from https://www.frontiersin.org/article/10.3389/fendo.2014.00149. doi:10.3389/fendo.2014.00149

Muskhelishvili, L., Latendresse, J. R., Kodell, R. L., & Henderson, E. B. (2003). Evaluation of Cell Proliferation in Rat Tissues with BrdU, PCNA, Ki-67(MIB-5) Immunohistochemistry and In Situ Hybridization for Histone mRNA. *Journal of Histochemistry & Cytochemistry, 51*(12), 1681-1688. Retrieved from https://journals.sagepub.com/doi/abs/10.1177/002215540305101212. doi:10.1177/002215540305101212

Muthukrishnan, S. D. (2016). *Combinatorial growth factor signaling controls nephron progenitor renewal and differentiation.* Retrieved from

http://libproxy.tulane.edu:2048/login?url=https://search.proquest.com/docview/1844966745?accountid=14437

Muthukrishnan, S. D., Yang, X., Friesel, R., & Oxburgh, L. (2015). Concurrent BMP7 and FGF9 signalling governs AP-1 function to promote self-renewal of nephron progenitor cells. *Nature Communications, 6*(1), 10027. Retrieved from https://doi.org/10.1038/ncomms10027. doi:10.1038/ncomms10027

Nadell, C. D., Bucci, V., Drescher, K., Levin, S. A., Bassler, B. L., & Xavier, J. B. (2013). Cutting through the complexity of cell collectives. *Proc Biol Sci, 280*(1755), 20122770. doi:10.1098/rspb.2012.2770

Nagy, I. I., Xu, Q., Naillat, F., Ali, N., Miinalainen, I., Samoylenko, A., & Vainio, S. J. (2016). Impairment of Wnt11 function leads to kidney tubular abnormalities and secondary glomerular cystogenesis. *BMC developmental biology, 16*(1), 30-30. Retrieved from https://pubmed.ncbi.nlm.nih.gov/27582005doi:10.1186/s12861-016-0131-z

CDC (2020). National Center for Health Statistics. Retrieved from https://www.cdc.gov/nchs/index.htm

CDC: NCCDPHP (2020). Chronic Kidney Disease. https://www.cdc.gov/chronicdisease/index.htm

NIH. (2019). Kidney Disease Statistics for the United States. https://www.niddk.nih.gov/health-information/health-statistics/kidney-disease

Nishinakamura, R., & Takasato, M. (2005). Essential roles of Sall1 in kidney development. *Kidney Int, 68*(5), 1948-1950. Retrieved from http://www.sciencedirect.com/science/article/pii/S0085253815510697. doi:https://doi.org/10.1111/j.1523-1755.2005.00626.x

Nyengaard, J. R. (1999). Stereologic methods and their application in kidney research. *J Am Soc Nephrol, 10*(5), 1100-1123.

Nyengaard, J. R., & Bendtsen, T. F. (1992). Glomerular number and size in relation to age, kidney weight, and body surface in normal man. *Anat Rec, 232*(2), 194-201. doi:10.1002/ar.1092320205

Obara-Ishihara, T., Kuhlman, J., Niswander, L., & Herzlinger, D. (1999). The surface ectoderm is essential for nephric duct formation in intermediate mesoderm. *Development, 126*(6), 1103-1108.

O'Brien, L. L., Combes, A. N., Short, K. M., Lindström, N. O., Whitney, P. H., Cullen-McEwen, L. A., Ju, A., Abdelhalim, A., Michos, O., Bertram, J. F., Smyth, I. M., Little, M. H., & McMahon, A. P. (2018). Wnt11 directs nephron progenitor polarity and motile behavior ultimately determining nephron endowment. *eLife, 7*, e40392. Retrieved from https://pubmed.ncbi.nlm.nih.gov/30516471 doi:10.7554/eLife.40392

Oxburgh, L. (2018). Kidney Nephron Determination. *Annual Review of Cell and Developmental Biology, 34*(1), 427-450. Retrieved from https://www.annualreviews.org/doi/abs/10.1146/annurev-cellbio-100616-060647. doi:10.1146/annurev-cellbio-100616-060647

Oxburgh, L., Brown, A. C., Fetting, J., & Hill, B. (2011). BMP signaling in the nephron progenitor niche. *Pediatric Nephrology, 26*(9), 1491-1497. Retrieved from https://doi.org/10.1007/s00467-011-1819-8. doi:10.1007/s00467-011-1819-8

Pai, S. G., Carneiro, B. A., Mota, J. M., Costa, R., Leite, C. A., Barroso-Sousa, R., Kaplan, J. B., Chae, Y. K., & Giles, F. J. (2017). Wnt/beta-catenin pathway: modulating anticancer

immune response. *Journal of Hematology & Oncology*, *10*(1), 101. Retrieved from https://doi.org/10.1186/s13045-017-0471-6. doi:10.1186/s13045-017-0471-6

Painter, R. C., Roseboom, T. J., & Bleker, O. P. (2005). Prenatal exposure to the Dutch famine and disease in later life: an overview. *Reprod Toxicol*, *20*(3), 345-352. doi:10.1016/j.reprotox.2005.04.005

Patterson, L. T., & Potter, S. S. (2003). Hox genes and kidney patterning. *Curr Opin Nephrol Hypertens*, *12*(1), 19-23. doi:10.1097/00041552-200301000-00004

Patterson, L. T., & Potter, S. S. (2004). Atlas of Hox gene expression in the developing kidney. *Dev Dyn*, *229*(4), 771-779. doi:10.1002/dvdy.10474

Pereira, L., Petitt, M., Fong, A., Tsuge, M., Tabata, T., Fang-Hoover, J., Maidji, E., Zydek, M., Zhou, Y., Inoue, N., Loghavi, S., Pepkowitz, S., Kauvar, L. M., & Ogunyemi, D. (2014). Intrauterine growth restriction caused by underlying congenital cytomegalovirus infection. *J Infect Dis*, *209*(10), 1573-1584. doi:10.1093/infdis/jiu019

Polyzos, S. A., Kountouras, J., & Zavos, C. (2009). The multi-hit process and the antagonistic roles of tumor necrosis factor-alpha and adiponectin in non alcoholic fatty liver disease. *Hippokratia*, *13*(2), 127-128. Retrieved from https://pubmed.ncbi.nlm.nih.gov/19561788

Rajan, T., Barbour, S. J., White, C. T., & Levin, A. (2011). Low birth weight and nephron mass and their role in the progression of chronic kidney disease: a case report on identical twins with Alport disease. *Nephrology Dialysis Transplantation*, *26*(12), 4136-4139. Retrieved from https://doi.org/10.1093/ndt/gfr252. doi:10.1093/ndt/gfr252

Reginensi, A., Clarkson, M., Neirijnck, Y., Lu, B., Ohyama, T., Groves, A. K., Sock, E., Wegner, M., Costantini, F., Chaboissier, M.-C., & Schedl, A. (2011). SOX9 controls epithelial branching by activating RET effector genes during kidney development. *Human molecular genetics*, *20*(6), 1143-1153. Retrieved from https://pubmed.ncbi.nlm.nih.gov/21212101 doi:10.1093/hmg/ddq558

Regnault, T. R. H., Friedman, J. E., Wilkening, R. B., Anthony, R. V., & Hay, W. W. (2005). Fetoplacental transport and utilization of amino acids in IUGR — a review. *Placenta*, *26*, S52-S62. Retrieved from http://www.sciencedirect.com/science/article/pii/S0143400405000330. doi:https://doi.org/10.1016/j.placenta.2005.01.003

Richardson, L., Venkataraman, S., Stevenson, P., Yang, Y., Moss, J., Graham, L., Burton, N., Hill, B., Rao, J., Baldock, R. A., & Armit, C. (2013). EMAGE mouse embryo spatial gene expression database: 2014 update. *Nucleic Acids Res*, *42*(D1), D835-D844. Retrieved from https://doi.org/10.1093/nar/gkt1155. doi:10.1093/nar/gkt1155

Ross, J. C., Fennessey, P. V., Wilkening, R. B., Battaglia, F. C., & Meschia, G. (1996). Placental transport and fetal utilization of leucine in a model of fetal growth retardation. *Am J Physiol*, *270*(3 Pt 1), E491-503. doi:10.1152/ajpendo.1996.270.3.E491

Ross, M. G., & Beall, M. H. (2008). Adult sequelae of intrauterine growth restriction. *Seminars in perinatology*, *32*(3), 213-218. Retrieved from https://pubmed.ncbi.nlm.nih.gov/18482624 doi:10.1053/j.semperi.2007.11.005

Rotar, O., Moguchaia, E., Boyarinova, M., Kolesova, E., Khromova, N., Freylikhman, O., Smolina, N., Solntsev, V., Kostareva, A., Konradi, A., & Shlyakhto, E. (2015). Seventy years after the siege of Leningrad: does early life famine still affect cardiovascular risk and aging? *J Hypertens*, *33*(9), 1772-1779; discussion 1779. doi:10.1097/hjh.0000000000000640

Rowan, C. J., Sheybani-Deloui, S., & Rosenblum, N. D. (2017). Origin and Function of the Renal Stroma in Health and Disease. In R. K. Miller (Ed.), *Kidney Development and Disease* (pp. 205-229). Cham: Springer International Publishing.

Safford, S. D., Freemerman, A. J., Langdon, S., Bentley, R., Goyeau, D., Grundy, P. E., & Skinner, M. A. (2005). Decreased E-cadherin expression correlates with higher stage of Wilms' tumors. *Journal of Pediatric Surgery, 40*(2), 341-348. Retrieved from http://www.sciencedirect.com/science/article/pii/S0022346804007092. doi:https://doi.org/10.1016/j.jpedsurg.2004.10.030

Saifudeen, Z. (2017). Tissue-Specific Functions of p53 During Kidney Development. *Results Probl Cell Differ, 60*, 111-136. doi:10.1007/978-3-319-51436-9_5

Sassone-Corsi, P. (2013). When Metabolism and Epigenetics Converge. *Science, 339*(6116), 148-150. Retrieved from https://science.sciencemag.org/content/sci/339/6116/148.full.pdf. doi:10.1126/science.1233423

Saxén, L., & Sariola, H. (1987). Early organogenesis of the kidney. *Pediatric Nephrology, 1*(3), 385-392. Retrieved from https://doi.org/10.1007/BF00849241. doi:10.1007/BF00849241

Schmidt-Ullrich, R., & Paus, R. (2005). Molecular principles of hair follicle induction and morphogenesis. *Bioessays, 27*(3), 247-261. doi:10.1002/bies.20184

Schmidt-Ullrich, R., & Paus, R. (2005). Molecular principles of hair follicle induction and morphogenesis. *Bioessays, 27*(3), 247-261. Retrieved from https://onlinelibrary.wiley.com/doi/abs/10.1002/bies.20184. doi:10.1002/bies.20184

Schmidt-Ullrich, R., & Paus, R. (2005). Molecular principles of hair follicle induction and morphogenesis. *Bioessays, 27*(3), 247-261. doi:10.1002/bies.20184

Schwarzkopf, M., Knobeloch, K.-P., Rohde, E., Hinderlich, S., Wiechens, N., Lucka, L., Horak, I., Reutter, W., & Horstkorte, R. (2002). Sialylation is essential for early development in mice. *Proceedings of the National Academy of Sciences, 99*(8), 5267-5270. Retrieved from https://www.pnas.org/content/pnas/99/8/5267.full.pdf. doi:10.1073/pnas.072066199

Sequeira Lopez, M. L. S., & Gomez, R. A. (2011). Development of the renal arterioles. *J Am Soc Nephrol, 22*(12), 2156-2165. Retrieved from https://pubmed.ncbi.nlm.nih.gov/22052047 doi:10.1681/ASN.2011080818

Sequeira-Lopez, M. L. S., & Torban, E. (2016). New insights into precursors of renal endothelium. *Kidney Int, 90*(2), 244-246. Retrieved from https://pubmed.ncbi.nlm.nih.gov/27418087 doi:10.1016/j.kint.2016.03.043

Sharma, D., Shastri, S., & Sharma, P. (2016). Intrauterine Growth Restriction: Antenatal and Postnatal Aspects. *Clinical medicine insights. Pediatrics, 10*, 67-83. Retrieved from https://pubmed.ncbi.nlm.nih.gov/27441006 doi:10.4137/CMPed.S40070

Short, K. M., & Smyth, I. M. (2016). The contribution of branching morphogenesis to kidney development and disease. *Nature reviews. Nephrology, 12*(12), 754-767. doi:10.1038/nrneph.2016.157

Short, K. M., Combes, Alexander N., Lefevre, J., Ju, Adler L., Georgas, Kylie M., Lamberton, T., Cairncross, O., Rumballe, Bree A., McMahon, Andrew P., Hamilton, Nicholas A., Smyth, Ian M., & Little, Melissa H. (2014). Global Quantification of Tissue Dynamics in the Developing Mouse Kidney. *Dev Cell, 29*(2), 188-202. Retrieved from https://doi.org/10.1016/j.devcel.2014.02.017. doi:10.1016/j.devcel.2014.02.017

Shrestha, N., Bahnan, W., Wiley, D. J., Barber, G., Fields, K. A., & Schesser, K. (2012). Eukaryotic initiation factor 2 (eIF2) signaling regulates proinflammatory cytokine expression and bacterial invasion. *J Biol Chem, 287*(34), 28738-28744. doi:10.1074/jbc.M112.375915

Shyh-Chang, N., Daley, G. Q., & Cantley, L. C. (2013). Stem cell metabolism in tissue development and aging. *Development, 140*(12), 2535-2547. Retrieved from https://dev.biologists.org/content/develop/140/12/2535.full.pdf. doi:10.1242/dev.091777

Sirin, Y., & Pavenstädt, H. (2010). FIH1 (factor inhibiting HIF-1) in the kidney: more than an oxygen sensor? *Kidney Int, 78*(9), 836-837. doi:10.1038/ki.2010.282

Song, X.-F., Ren, H., Andreasen, A., Thomsen, J. S., & Zhai, X.-Y. (2012). Expression of Bcl-2 and Bax in mouse renal tubules during kidney development. *PLOS ONE, 7*(2), e32771-e32771. Retrieved from https://pubmed.ncbi.nlm.nih.gov/22389723 doi:10.1371/journal.pone.0032771

Stein, A. D., Zybert, P. A., van der Pal-de Bruin, K., & Lumey, L. H. (2006). Exposure to famine during gestation, size at birth, and blood pressure at age 59 y: evidence from the Dutch Famine. *Eur J Epidemiol, 21*(10), 759-765. doi:10.1007/s10654-006-9065-2

Takasato, M., & Little, M. H. (2015). The origin of the mammalian kidney: implications for recreating the kidney in vitro. *Development, 142*(11), 1937-1947. Retrieved from https://dev.biologists.org/content/develop/142/11/1937.full.pdf. doi:10.1242/dev.104802

Takasato, M., & Little, M. H. (2015). The origin of the mammalian kidney: implications for recreating the kidney in vitro. *Development, 142*(11), 1937-1947. doi:10.1242/dev.104802

Tan, J. C., Busque, S., Workeneh, B., Ho, B., Derby, G., Blouch, K. L., Sommer, F. G., Edwards, B., & Myers, B. D. (2010). Effects of aging on glomerular function and number in living kidney donors. *Kidney Int, 78*(7), 686-692. Retrieved from https://pubmed.ncbi.nlm.nih.gov/20463656 doi:10.1038/ki.2010.128

Tanner, M. E. (2005). The enzymes of sialic acid biosynthesis. *Bioorg Chem, 33*(3), 216-228. doi:10.1016/j.bioorg.2005.01.005

Tojo, A., & Kinugasa, S. (2012). Mechanisms of Glomerular Albumin Filtration and Tubular Reabsorption. *International Journal of Nephrology, 2012*, 481520. Retrieved from https://doi.org/10.1155/2012/481520. doi:10.1155/2012/481520

The Impact of Kidney Development on the Life Course: A Consensus Document for Action. (2017). *Nephron, 136*(1), 3-49. doi:10.1159/000457967

UNICEF. (2019). Low Birthweight: A Good Start in Life Begins in the Womb. Retrieved from https://data.unicef.org/topic/nutrition/low-birthweight/

Vainio, S., Lehtonen, E., Jalkanen, M., Bernfield, M., & Saxén, L. (1989). Epithelial-mesenchymal interactions regulate the stage-specific expression of a cell surface proteoglycan, syndecan, in the developing kidney. *Dev Biol, 134*(2), 382-391. doi:10.1016/0012-1606(89)90110-3

Vainio, S., & Lin, Y. (2002). Coordinating early kidney development: lessons from gene targeting. *Nat Rev Genet, 3*(7), 533-543. doi:10.1038/nrg842

Vandenbosche, R. C., & Kirchner, J. T. (1998). Intrauterine growth retardation. *Am Fam Physician, 58*(6), 1384-1390, 1393-1384.

Vanslambrouck, J. M., Wilson, S. B., Tan, K. S., Soo, J. Y., Scurr, M., Spijker, H. S., Starks, L. T., Neilson, A., Cui, X., Jain, S., Little, M. H., & Howden, S. E. (2019). A Toolbox to Characterize Human Induced Pluripotent Stem Cell-Derived Kidney Cell Types and Organoids. *J Am Soc Nephrol, 30*(10), 1811-1823. doi:10.1681/asn.2019030303

Velagapudi, C., Nilsson, R.-P., Lee, M. J., Burns, H. S., Ricono, J. M., Arar, M., Barnes, V. L., Abboud, H. E., & Barnes, J. L. (2012). Reciprocal induction of simple organogenesis by mouse kidney progenitor cells in three-dimensional co-culture. *The American journal of pathology, 180*(2), 819-830. Retrieved from https://pubmed.ncbi.nlm.nih.gov/22138298 doi:10.1016/j.ajpath.2011.11.002

Vize, P. D., Seufert, D. W., Carroll, T. J., & Wallingford, J. B. (1997). Model systems for the study of kidney development: use of the pronephros in the analysis of organ induction and patterning. *Dev Biol, 188*(2), 189-204. doi:10.1006/dbio.1997.8629

Vuguin, P. M. (2007). Animal models for small for gestational age and fetal programming of adult disease. *Horm Res, 68*(3), 113-123. Retrieved from https://pubmed.ncbi.nlm.nih.gov/17351325 doi:10.1159/000100545

Wagner, K.-D., Wagner, N., Wellmann, S., Schley, G., Bondke, A., Theres, H., & Scholz, H. (2003). Oxygen-regulated expression of the Wilms' tumor suppressor Wt1 involves hypoxia-inducible factor-1 (HIF-1). *The FASEB Journal, 17*(10), 1364-1366. Retrieved from https://faseb.onlinelibrary.wiley.com/doi/abs/10.1096/fj.02-1065fje. doi:10.1096/fj.02-1065fje

Wajant, H., & Siegmund, D. (2019). TNFR1 and TNFR2 in the Control of the Life and Death Balance of Macrophages. *Frontiers in Cell and Developmental Biology, 7*(91). Retrieved from https://www.frontiersin.org/article/10.3389/fcell.2019.00091. doi:10.3389/fcell.2019.00091

Wang, N., Wang, X., Han, B., Li, Q., Chen, Y., Zhu, C., Chen, Y., Xia, F., Cang, Z., Zhu, C., Lu, M., Meng, Y., Chen, C., Lin, D., Wang, B., Jensen, M. D., & Lu, Y. (2015). Is Exposure to Famine in Childhood and Economic Development in Adulthood Associated With Diabetes? *J Clin Endocrinol Metab, 100*(12), 4514-4523. doi:10.1210/jc.2015-2750

Wang, P., Chen, Y., Yong, J., Cui, Y., Wang, R., Wen, L., Qiao, J., & Tang, F. (2018). Dissecting the Global Dynamic Molecular Profiles of Human Fetal Kidney Development by Single-Cell RNA Sequencing. *Cell Reports, 24*(13), 3554-3567.e3553. Retrieved from http://www.sciencedirect.com/science/article/pii/S2211124718313433. doi:https://doi.org/10.1016/j.celrep.2018.08.056

Wanner, N., Vornweg, J., Combes, A., Wilson, S., Plappert, J., Rafflenbeul, G., Puelles, V. G., Rahman, R.-U., Liwinski, T., Lindner, S., Grahammer, F., Kretz, O., Wlodek, M. E., Romano, T., Moritz, K. M., Boerries, M., Busch, H., Bonn, S., Little, M. H., Bechtel-Walz, W., & Huber, T. B. (2019). DNA Methyltransferase 1 Controls Nephron Progenitor Cell Renewal and Differentiation. *Journal of the American Society of Nephrology, 30*(1), 63-78. Retrieved from https://jasn.asnjournals.org/content/jnephrol/30/1/63.full.pdf. doi:10.1681/asn.2018070736

Watanabe, N., Hiramatsu, K., Miyamoto, R., Yasuda, K., Suzuki, N., Oshima, N., Kiyonari, H., Shiba, D., Nishio, S., Mochizuki, T., Yokoyama, T., Maruyama, S., Matsuo, S., Wakamatsu, Y., & Hashimoto, H. (2009). A murine model of neonatal diabetes mellitus in Glis3-deficient mice. *FEBS Letters, 583*(12), 2108-2113. Retrieved from

http://www.sciencedirect.com/science/article/pii/S0014579309004141. doi:https://doi.org/10.1016/j.febslet.2009.05.039

Weibel, E. R., & Gomez, D. M. (1962). A principle for counting tissue structures on random sections. *J Appl Physiol, 17*, 343-348. doi:10.1152/jappl.1962.17.2.343

Whary, M. T., Baumgarth, N., Fox, J. G., & Barthold, S. W. (2015). Chapter 3 - Biology and Diseases of Mice. In J. G. Fox, L. C. Anderson, G. M. Otto, K. R. Pritchett-Corning, & M. T. Whary (Eds.), *Laboratory Animal Medicine (Third Edition)* (pp. 43-149). Boston: Academic Press.

Wollmann, H. A. (1998). Intrauterine growth restriction: definition and etiology. *Horm Res, 49 Suppl 2*, 1-6. doi:10.1159/000053079

Woolf, A., & Winyard, P. (2015). Oxford Textbook of Clinical Nephrology. In *Human kidney development*: Oxford University Press.

Wu, G. (2010). Functional amino acids in growth, reproduction, and health. *Advances in nutrition (Bethesda, Md.), 1*(1), 31-37. Retrieved from https://pubmed.ncbi.nlm.nih.gov/22043449 doi:10.3945/an.110.1008

Wu, M. Y., Chen, C. S., Yiang, G. T., Cheng, P. W., Chen, Y. L., Chiu, H. C., Liu, K. H., Lee, W. C., & Li, C. J. (2018). The Emerging Role of Pathogenesis of IgA Nephropathy. *J Clin Med, 7*(8). doi:10.3390/jcm7080225

Xu, Y-H., Barnes, S., Sun, Y., Grabowsi, G.A., (2010). Multi-system disorders of glycosphingolipid and ganglioside metabolism. *Journal of Lipid Research*, 5i. doi: 10.1194/jlr.R003996

Yallowitz, A. R., Hrycaj, S. M., Short, K. M., Smyth, I. M., & Wellik, D. M. (2011). Hox10 Genes Function in Kidney Development in the Differentiation and Integration of the Cortical Stroma. *PLOS ONE, 6*(8), e23410. Retrieved from https://doi.org/10.1371/journal.pone.0023410. doi:10.1371/journal.pone.0023410

You, A., Tong, J. K., Grozinger, C. M., & Schreiber, S. L. (2001). CoREST is an integral component of the CoREST- human histone deacetylase complex. *Proc Natl Acad Sci U S A, 98*(4), 1454-1458. Retrieved from https://pubmed.ncbi.nlm.nih.gov/11171972 doi:10.1073/pnas.98.4.1454

Yu, X., Ma, R., Wu, Y., Zhai, Y., & Li, S. (2018). Reciprocal Regulation of Metabolic Reprogramming and Epigenetic Modifications in Cancer. *Frontiers in Genetics, 9*, 394-394. Retrieved from https://pubmed.ncbi.nlm.nih.gov/30283496 doi:10.3389/fgene.2018.00394

Yuan, H. T., Tipping, P. G., Li, X. Z., Long, D. A., & Woolf, A. S. (2002). Angiopoietin correlates with glomerular capillary loss in anti-glomerular basement membrane glomerulonephritis. *Kidney Int, 61*(6), 2078-2089. Retrieved from https://doi.org/10.1046/j.1523-1755.2002.00381.x. doi:10.1046/j.1523-1755.2002.00381.x

Zhu, X., Lee, H. G., Perry, G., & Smith, M. A. (2007). Alzheimer disease, the two-hit hypothesis: an update. *Biochim Biophys Acta, 1772*(4), 494-502. doi:10.1016/j.bbadis.2006.10.014

Figures created with BioRender.com

Biography

The author was born June 22, 1990 in Woonsocket, Rhode Island, United States. They attended Montrose Area jr/sr High School in Montrose, PA, United States from 2004 to 2008 before going to Emory University in Atlanta, GA, United States (2008-2012). At Emory they majored in Biology and minored in Global Health, Society, and Culture and studying abroad in London for a summer to explore sociology and compare the clinical and public health systems of the United States and United Kingdom. They worked for three years of undergrad as a lab technician in the Fridovich-Keihl genetics lab. After completing a Bachelor of Science in Biology they attended the Tulane School of Public Health and Tropical Medicine in New Orleans, LA, United States (2012-2014) receiving a Master's in Public Health in Global Environmental Health Sciences specializing in Disaster Management. The author then continued at Tulane in the Tulane School of Medicine doctoral program in Biomedical Sciences starting classes in 2014 and in the Saifudeen lab in 2015. While in the Saifudeen lab the author contributed as second author to one publication, and presented abstracts at the American Society of Nephrology, the Southern Region AFMR/SSCI for Regional Meeting winning a Trainee Travel award and being selected for an oral presentation in 2016, and several abstracts at the Tulane Health Science Research Days poster presentations wining the Michael A. Gerber Prize for Research in Molecular and Cellular Biology award (2017), and winning outstanding morning speaker at the BMS Student Retreat for presentation of their preliminary thesis data. The author has just begun a job as a Regulatory Compliance Specialist at the Tulane HRPO.